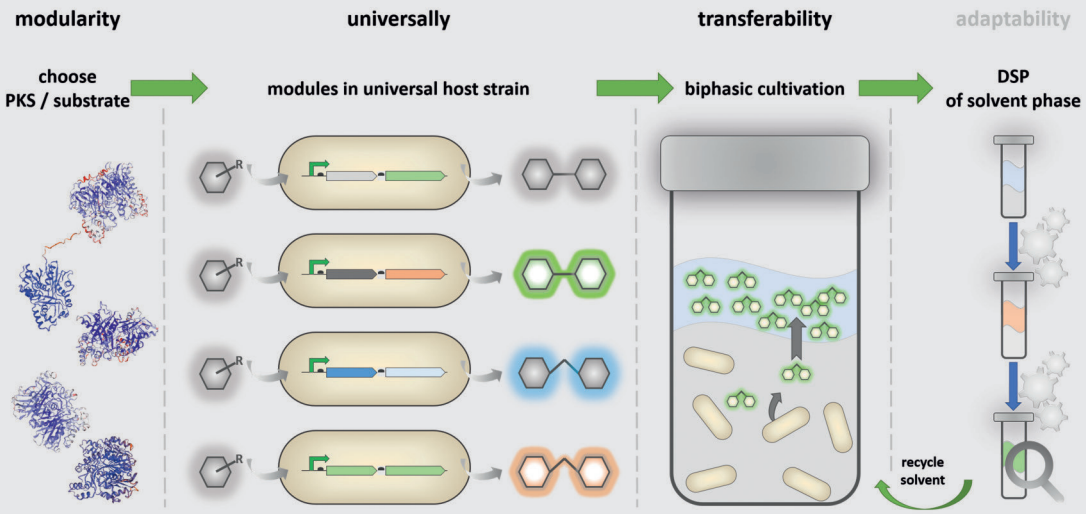

Strain- and process engineering for polyketides production with *Pseudomonas taiwanensis* VLB120 in two-phase cultivations

Tobias Philipp Schwanemann

Schlüsseltechnologien / Key Technologies
Band / Volume 276
ISBN 978-3-95806-726-4

Mitglied der Helmholtz-Gemeinschaft

JÜLICH
Forschungszentrum

Strain- and process engineering for polyketides production with *Pseudomonas taiwanensis* VLB120 in two-phase cultivations

Inaugural Dissertation

for the attainment of the title of doctor in the

Faculty of Mathematics and Natural Sciences at the

Heinrich-Heine-Universität Düsseldorf

presented by

Tobias Philipp Schwanemann

born in

Hannover, Germany

Jülich, July 2023

Forschungszentrum Jülich GmbH
Institut für Bio-und Geowissenschaften
Biotechnologie (IBG-1)

Strain- and process engineering for polyketides production with *Pseudomonas taiwanensis* VLB120 in two-phase cultivations

Tobias Philipp Schwanemann

Schriften des Forschungszentrums Jülich
Reihe Schlüsseltechnologien / Key Technologies Band / Volume 276

ISSN 1866-1807 ISBN 978-3-95806-726-4

Bibliografische Information der Deutschen Nationalbibliothek.
Die Deutsche Nationalbibliothek verzeichnet diese Publikation in der
Deutschen Nationalbibliografie; detaillierte Bibliografische Daten
sind im Internet über http://dnb.d-nb.de abrufbar.

Herausgeber und Vertrieb:	Forschungszentrum Jülich GmbH Zentralbibliothek, Verlag 52425 Jülich Tel.: +49 2461 61-5368 Fax: +49 2461 61-6103 zb-publikation@fz-juelich.de www.fz-juelich.de/zb
Umschlaggestaltung:	Grafische Medien, Forschungszentrum Jülich GmbH
Druck:	Grafische Medien, Forschungszentrum Jülich GmbH
Copyright:	Forschungszentrum Jülich 2023

Schriften des Forschungszentrums Jülich
Reihe Schlüsseltechnologien / Key Technologies, Band / Volume 276

D 61 (Diss. Düsseldorf, Univ., 2023)

ISSN 1866-1807
ISBN 978-3-95806-726-4

Vollständig frei verfügbar über das Publikationsportal des Forschungszentrums Jülich (JuSER)
unter www.fz-juelich.de/zb/openaccess.

The thesis has been conducted at the Institute of Bio- and Geosciences, IBG-1: Biotechnology, Forschungszentrum Jülich GmbH, from February 2020 until October 2023 under the supervision of Prof. Dr. Nick Wierckx.

Published by permission of the
Faculty of Mathematics and Natural Sciences at
Heinrich-Heine-University Düsseldorf

Examiner: **Prof. Dr. Nick Wierckx**
Institute of Bio- and Geosciences, IBG-1: Biotechnology
Forschungszentrum Jülich GmbH
Jülich

Co-examiner: **Prof. Dr. Julia Frunzke**
Institute of Bio- and Geosciences, IBG-1: Biotechnology
Forschungszentrum Jülich GmbH
Jülich

Date of oral examination: 26th of October 2023

„[…] Der Mensch wird nur glücklich, wenn er alle seine Fähigkeiten und Möglichkeiten entfalten und benutzen kann.
Aristoteles glaubte an drei Formen des Glücks: Die erste Form des Glücks ist ein Leben der Lust und der Vergnügungen. Die zweite Form des Glücks ist ein Leben als freier, verantwortlicher Bürger. Die dritte Form des Glücks ist das Leben als Forscher und Philosoph."

Jostein Gaarder, 1991.
Sophies Welt – Roman über die Geschichte der Philosophie

Publications

The scientific work of this thesis have been published in the following original publications or are summarized in manuscripts that will be submitted soon:

Schwanemann, T., Otto, M., Wierckx, N., & Wynands, B. (2020). *Pseudomonas* as Versatile Aromatics Cell Factory. *Biotechnology Journal*, *1900569*, 1900569. https://doi.org/10.1002/biot.201900569

Schwanemann, T., Otto, M., Wynands, B., Marienhagen, J., & Wierckx, N. (2023). A *Pseudomonas taiwanensis* malonyl-CoA platform strain for polyketide synthesis. *Metabolic Engineering*, *77*(February), 219–230. https://doi.org/10.1016/j.ymben.2023.04.001

Schwanemann, T., Krink, N., Nikel, P.I., Wynands, B., & Wierckx, N. (2023). Engineered passive glucose uptake in *Pseudomonas taiwanensis* VLB120 for increased resource efficiency in bioproduction. – to be submitted

Schwanemann, T., Urban, E., Eberlein, C., Gätgens, J., Rago, D., Krink, N., Nikel, P.I., Heipieper, H.J., Wynands, B., & Wierckx, N. (2023). Production of (hydroxy)benzoate-derived polyketides by engineered *Pseudomonas* with *in situ* extraction. *Bioresource Technology*, *388*(129741), 0–11. https://doi.org/10.1016/j.biortech.2023.129741

Funding

This work was funded by the German Federal Environmental Foundation (Deutsche Bundesstiftung Umwelt - DBU) through the PhD scholarship 20019/638-32 and German Academic Exchange Service (DAAD) by scholarship 57556281.

List of abbreviations

The list includes no generic metabolites, organisms or names of genes.
For common abbreviations not included in this section, see, for example, the Journal of Cell Biology Author Guidelines. (https://rupress.org/jcb/pages/standard-abbreviations; no warranty of completeness)

ACC	Acetyl-CoA carboxylase
ACP	Acyl carrier protein
ACS	Acridone synthases
antiSMASH	antibiotics and secondary metabolite analysis shell (genome mining tool)
BAS	Benzaldehyde synthase
BC	Before Christ
BCD	Bicistronic design element
BIS	Biphenyl synthase
BMBF	Bundesministerium für Bildung und Forschung (German Federal Ministry of Education and Research)
BPS	Benzophenone synthase
CDW	Cell dry weight
CHI	Chalcone isomerase
CHIL	Chalcone isomerase-like
CHS	Chalcone synthase
4CL	4-Coumaroyl:CoA ligase
CoA	Coenzyme A
CRediT	Contributor Roles Taxonomy
Cti	*cis-trans* Isomerase
CURS	Curcumin synthase
CUS	Bismethoxycurcumin synthase
DAPG	2,4 Diacetylphloroglucinol
DBU	Deutsche Bundesstiftung Umwelt (German Federal Environmental Foundation)
DCS	Diketide synthases
DMAPP	Dimethylallyl pyrophosphate
DSP	Downstream process
EC_{50}	Effective concentration
ED	Entner-Doudoroff pathway
EDEMP cycle	Cyclic operating Entner-Doudoroff-Embden- Meyerhof-Parnas-pentose phosphate pathway
e.g.	*Exempli gratia*
EMP	Embden-Meyerhof-Parnas pathway
ERC	European research council
FAME	Fatty acid methyl esters
FAS	Fatty acid synthesis
FID	Flame ionization detector
GC	Gas chromatography
GRC	Genome-reduced *chassis* strain
HESI	Heated electrospray ionization
HPLC	High performance liquid chromatography
IPP	Isopentenyl pyrophosphate
ISPR	*In situ* product removal
JuPoD	In-house database for compound m/z (FZ Jülich, Germany)
k_La	Oxygen mass transfer coefficient

K_M	Michaelis constant
LECA	Last eukaryotic common ancestor
$logK_{O/W}$	Logarithmic distribution coefficient
$logP_{M/B}$	Logarithmic partition coefficient in biological membranes
$logP_{O/W}$	Logarithmic partition coefficient
Ma	Megaannum (million years ago)
MMC	Maximum membrane concentration
MS	Mass spectrometry
MSM	Mineral salt medium
m/z	Mass-to-charge ratio
NIST	a commercial database for compound m/z (National Institute of Standards and Technology, USA)
NRPS	Non-ribosomal peptide synthase
OKS	Octaketide synthase
PAL	phenylalanine ammonia-lyase
PCS	Pentaketide synthase
PEG	Polyethylene glycol
pH	Logarithmic inverse activity of hydrogen ions in solution
PHA	Polyhydroxyalkanoate
PPP	Pentose phosphate pathways
PPTase	Phosphopantetheinyl transferase
4'-PP	4'-phosphopanthetheine
PKS	Polyketide synthase
PQQ	Pyrroloquinoline quinone
PTFE	Polytetrafluoroethylene
QNS	Quinolone synthases
RI	Retention time index
S_{aq}	Solubility in aqueous phase
STS	Stilbene synthase
TAL	tyrosine ammonia-lyase
TCA cycle	Tricarboxylic acid cycle (citrate cycle)
2,4,6-TriHBP,	2,4,6-Trihydroxybenzophenone (phlorobenzophenone)
2,3',4,6-TetraHBP	2,3',4,6-Tetrahydroxybenzophenone
ToF	Time of flight

List of figures

Figures of the appendices are not included.

Table of contents

Summary

Polyketides are a highly diverse group of secondary metabolites with great potential for lead compounds for applications in multiple industries. Biotechnological hosts are frequently used for their heterologous production. For polyketide synthesis, identical precursors are assembled to complex compounds with highly different properties while using the same cellular resources. Consequently, the choice of polyketide synthase (PKS) determines the final product and the interchangeable nature of PKS allows the production of various compounds by minimal modifications of the host organism. In particular, PKS III represent an interesting group of catalysts due to their simplicity compared to other PKS. In this work, an alternative bacterial production host, *Pseudomonas taiwanensis* VLB120, was developed for the production of various polyketide products in two-phase cultivations for *in situ* product removal.

Malonyl-CoA is often the limiting precursor for polyketide synthesis by PKS III in bacterial hosts. To increase its availability, different metabolic engineering strategies were applied for rational development of a *Pseudomonas* malonyl-CoA platform strain. Initially, a strain with removed catabolic pathways for aromatics served as the basis. Native periplasmic glucose oxidation was also deleted to force glucose utilization via intracellular NADPH-producing reaction steps. Additionally, the acetyl-CoA node in central metabolism was modified by altered citrate synthase activity and additional expression of an acetyl-CoA carboxylase. Inference of fatty acid biosynthesis was achieved by the implementation of an alternative β-ketoacyl-ACP synthase II (FabF-2) with subsequent deletion and exchange of the native enzyme by a unique identifier sequence. All these modifications resulted in the malonyl-CoA platform strain No. 3 which was able to produce up to several milligrams of pinosylvin, up to 84 mg L^{-1} resveratrol and flaviolin titers which were more than doubled compared to parental strains.

The titers of the products made of malonyl-CoA was further enhanced by the use of an alternative glucose transporter since the native glucose transport of Pseudomonads requires energy. The replacement or additional expression of the passive transporter Glf_{Zm} (originally from *Zymomonas mobilis*) enabled the production of up to 98 mg L^{-1} resveratrol. Additionally, an increase of up to 10% in cinnamate production in a phenylalanine platform strain was achieved.

To go one step further, the previously developed platform strains were used to produce various polyketides using alternative precursor molecules, including first-time heterologous *in vivo* biosyntheses and new-to-nature fluorinated aromatics. For this purpose, screening of suitable enzyme combinations was performed and product properties as well as the interaction with the host were investigated. The observed product instability was counteracted by the application of 2-undecanone as a second phase for *in situ* product removal which emerged from a solvent screening. This eventually led to the *de novo* synthesis of 2,4,6-trihydroxybenzophenone, 3,5-dihydroxybiphenyl, 2,3',4,6-tetrahydroxybenzophenone and 4-hydroxycoumarin in two-phase cultivations.

Zusammenfassung

Polyketide sind eine äußerst vielfältige Gruppe von Sekundärmetaboliten mit einem hohem Potenzial in zahlreichen Branchen und werden häufig biotechnologisch hergestellt. Bei Polyketiden werden gleiche Vorläufermoleküle zu komplexen Verbindungen mit sehr unterschiedlichen Eigenschaften zusammengesetzt; hierbei wird auf die gleichen zellulären Ressourcen zurückgegriffen. Folglich bestimmen die verwendeten Polyketidsynthasen (PKS) das finale Produkt, und der austauschbare Charakter der PKS ermöglicht die Herstellung verschiedener Verbindungen durch minimale Veränderungen des Wirtsorganismus. Insbesondere PKS III stellen aufgrund ihres simplen Aufbaus im Vergleich zu anderen PKS eine interessante Gruppe von Katalysatoren dar. In dieser Arbeit wurde ein alternativer bakterieller Produktionswirt, *Pseudomonas taiwanensis* VLB120, für die Produktion verschiedener Polyketidprodukte in Zweiphasenkulturen zur *in situ* Produktentfernung entwickelt.

Die Bereitstellung von Malonyl-CoA ist oft der limitierende Schritt für die Polyketidsynthese durch PKS III in bakteriellen Wirten. Um die Verfügbarkeit zu erhöhen, wurden verschiedene Strategien des *metabolic engineering* zur rationalen Entwicklung eines *Pseudomonas*-Malonyl-CoA-Plattformstammes verwendet. Zunächst diente ein Stamm mit entfernten Aromatenabbauwegen als Grundlage. Die native periplasmatische Glukoseoxidation wurde ebenfalls entfernt, um die Glukoseverwertung über intrazelluläre NADPH-produzierende Reaktionsschritte zu erzwingen. Zusätzlich wurde der Acetyl-CoA-Knotenpunkt im zentralen Stoffwechsel durch veränderte Citrat-Synthase-Aktivität und zusätzliche Expression einer Acetyl-CoA-Carboxylase modifiziert. Eine Beschränkung der Fettsäurebiosynthese wurde durch die Implementierung einer alternativen β-Ketoacyl-ACP-Synthase II (FabF-2) mit anschließender Deletion und Austausch des nativen Enzyms durch eine einzigartige Identifizierungssequenz erreicht. All diese Modifikationen führten zu dem Malonyl-CoA-Plattform-Stamm Nr. 3, der in der Lage war, bis zu mehrere Milligramm Pinosylvin oder bis zu 84 mg L^{-1} Resveratrol zu produzieren. Der Titer von Flaviolin konnte zudem mehr als verdoppelt werden.

Die Produktkonzentrationen der aus Malonyl-CoA hergestellten Produkte wurde durch die Verwendung eines alternativen Glukosetransporters weiter gesteigert, da der native Glukosetransport in Pseudomonaden Energie erfordert. Der Austausch oder die zusätzliche Expression des passiven Transporters Glf_{Zm} (ursprünglich aus *Zymomonas mobilis*) ermöglichte die Produktion von bis zu 98 mg L^{-1} Resveratrol. Darüber hinaus wurde in einem Phenylalanin-Plattformstamm eine Steigerung der Zimtsäureproduktion um bis zu 10 % erreicht.

Aufbauend auf diesen Arbeiten wurden im nächsten Schritt mit den zuvor entwickelten Plattformstämmen mittels alternativer Vorläufermoleküle verschiedene Polyketide hergestellt, darunter erstmalige heterologe *in vivo* Biosynthesen und neuartige fluorierte Aromaten. Dazu wurde ein Screening geeigneter Enzymkombinationen durchgeführt und die Produkteigenschaften sowie die Wechselwirkung mit dem Wirt untersucht. Der festgestellten Produktinstabilität wurde durch die Anwendung von 2-Undecanon als zweite Phase zur *in situ* Produktaufarbeitung entgegengewirkt, welches aus einem Lösungsmittel-Screening hervorging. Dies führte schließlich zur *de novo* Synthese von 2,4,6-Trihydroxybenzophenon, 3,5-Dihydroxybiphenyl, 2,3',4,6-Tetrahydroxybenzophenon und 4-Hydroxycumarin in Zweiphasenkulturen.

1. General introduction

1.1 Microbiology and secondary metabolites - A story of success in human history and culture

The oldest preserved history of humankind is the “Epic of Gilgamesh” and “Gilgamesh, Enkidu, and the Netherworld” from 2400 – 1800 BC in cuneiform on twelve clay tablets written in verses from the region of ancient Mesopotamia (Wieland, 2020). It is a story about the adventures of King Gilgamesh with his friend Enkidu about their life and death and Gilgamesh’s search for immortality, which remained reserved for the gods. Even in this ancient tale, there are indications of the use of biotechnological processes. Enkidu, who previously symbolized the embodiment of the "wild man", becomes a part of the community through the consumption of bread and wine which were seen as cultural achievements. The exact mechanisms that made the production of alcohol and fermented food possible were completely unknown to people at that time. Though, it is a good example of how products of microbial origin have accompanied humanity at least for multiple millennia. However, microbes as the “magical ingredient” were not known back in the days of Gilgamesh. In modern times “classical biotechnology” aims to use the native capabilities of microorganisms for food and beverage production (Maurya et al., 2021). From the ancient Mesopotamian perspective, the use of biotechnological products, as they are called today, was a kind of cultural progress. Even today the increased use of biotechnological products is frequently associated with cultural and/or technical progress in humankind (Verma et al., 2011). In traditional medicine fermented plant broths or lotions served as treatment against infections, likely due to the incidental formation of antimicrobials or even antibiotics (Pan et al., 2014). Additionally, psychoactive plants and fungi were used for certain religious traditions and ceremonies to connect to other mystical or non-physical worlds which defy rational scientific concepts.

Transferring knowledge, gained by observations, to common or written knowledge was limited in those days. During antiquity, early natural philosophy often relied on individual observations with limited equipment and interpretation of observed phenomena was aggravated by a lack of methods and diversity in nature’s classification. Despite this, several ancient postulations are still valid today. For example, the formulation of the atomic hypothesis of indestructible moving particles by Leucippus and Democritus in the fifth century BC is still valid today in chemistry and biochemistry. According to Aristotle, the task of natural philosophy is the consideration of substances with your own sense, insomuch as they can be moved and can be grasped conceptually. Classical rationalism, starting from the 16th century, served as profound basis for subsequent reliable and reproducible research which is still an important foundation in today’s research. Nevertheless, empirical experiments still represent the foundation for the falsification (or validation) of hypotheses and theories. Modern science is

characterized by the systematic search for new insights which rely on questions or theories followed by the experiment and respective control experiments, interpretation and discussion. A starting point for modern biology as an independent research field could be taken as the publication of "*On the Origin of Species"* by Charles Darwin in 1859 (Darwin, 1859) which described the diversity of life in a strict rational context. However, Darwin himself was by training a theologian and the work was in conflict with the biblical Book of Genesis, which brought him into conflict with his own self-understanding.

The discovery of bacteria, the first microorganisms identified, is usually attributed to the year 1676 and the work of Antoni van Leeuwenhoek, a pioneer in microscopy (van Leeuwenhoek, 1676). Since then, bacteria were frequently found to be responsible for diseases and the shortened shelf life of many food products. The discovery of bacterial species and experiments about their vitality under specific conditions was the predominant biological research of the past centuries by Louis Pasteur (Bordenave, 2003) and Robert Koch (Münch, 2003). Milestones, like industrial acetone-butanol-ethanol fermentation by Chaim Weizmann in the early 20th century (Sauer, 2016) enabling the production of explosives or the discovery of antibiotic penicillin by Alexander Fleming in 1929 (Fleming, 1929) mark a change in microbial research and societal demand. The discovery of DNA as the "code of life" and increasing capabilities for sequencing and synthesis are central achievements in humankind's scientific understanding of founding synthetic biology, metabolic engineering (García-Granados et al., 2019) and modern genetics.

1.1.1. Future pursuit: sustainable bioeconomy

Under the proverbial "sword of Damocles" that is the destruction of the environment, for example by the exploitation of fossil resources and the resulting anthropogenic climate change, the pursuit of a bioeconomy with sustainable use of resources is the goal of the modern era especially in biotechnological research in order to achieve sustainability (Aguilar et al., 2019; S. Y. Lee et al., 2019; Perišić et al., 2022; Wei et al., 2022; L. P. Yu et al., 2019). Industrial biotechnology aims to economically reduce waste formation in chemical synthesis, replace environmentally polluting processes and reduce the emission of carbon (Straathof et al., 2019). In the research field of organic chemistry and industrial biotechnology, for instance, alternative feedstocks for ethanol fermentation and biodiesel production (Cabrera-Jiménez et al., 2023) have been in focus for decades. Thus, energy delivery and transport could incrementally phase out the use of fossil resources (Winter & Meys, 2022). Unfortunately, rising energy demands and financially beneficial but environmentally unfriendly substitutions over the last few decades, mean that a switch to bio-based fuels cannot compensate for the increased use of mineral oil and other fossil resources (United Nations Environment Programme, 2022). The first generation of biofuels was based on fermentable crops and sugars whose usage was in competition

with agricultural food production (de Almeida & Colombo, 2021; Morone et al., 2023). Next, lignocellulose biomass feedstocks such as straw along with agricultural waste streams were used for biofuel production (Singh et al., 2022), followed by biomass from wood industry waste to funnel multi-substrate mixtures to a value-added circular economy (Okolie et al., 2021). The overall aim is not only to replace fuels and other mineral oil-derived products such as most plastics but to provide alternative materials for everyday use (Eversberg et al., 2022) and to make alternative carbon stocks like mixed plastic waste accessible for establishing circular economies (S. Lee et al., 2023; Merchan et al., 2022; N. Wierckx et al., 2015; Zimmerman et al., 2020).

Sustainability is not only related to the reduction of carbon emissions (Winter & Meys, 2022) but also to the preservation of biodiversity. Techno-economic assessments of new sustainable products have to be competitive regarding titer, rate, yield and energy consumption (Moutinho et al., 2021). The development of new production processes should consider the use of sustainable resources and the end-of-life of the respective product to integrate the idea of a circular economy already at the beginning of a process (Carus & Dammer, 2018; Talwar & Holden, 2022). Besides bulk commodities and chemicals, this should also apply to small-volume products such as specialty chemicals from nature, like plant extracts for the recovery of secondary metabolites for human use (Khattab & Farag, 2020).

Transforming established chemical processes into processes with lower energy demands and valorizing waste streams is of economic and ecological interest. On account of this, enzymes and whole-cell catalysts are frequently used for biomanufacturing, stereoselective chemistry, and to reduce the number of required synthesis steps (Sheldon et al., 2020; Woodley, 2019). For the use of enzymes in biotechnological environments in harsh conditions, they were engineered and evolved for temperature stability, solvent tolerance, alternative substrates and further purposes. Screening of metagenomics libraries from various environments displays the start of the development of an industrial enzymatic catalyst. Subsequent laboratory directed evolution (Arnold & Volkov, 1999) and untargeted or targeted mutagenesis and iteration of these steps finally result in usable biocatalysts. For the development of directed evolution as an engineering strategy, the Nobel Prize was awarded to Frances Hamilton Arnold in 2018 highlighting how society benefits from and has become dependent on biomanufacturing and related biocatalyst development.

As enzyme function is derived from its structure, structural biology has always been of concern in targeted protein engineering. The breakthrough development of computationally predicted protein structures by AlphaFold2 (Jumper et al., 2021) is having a positive impact on researchers' opportunities in experiment design and evaluation. As AlphaFold2 is a frequently used tool now, not only by protein engineers but also for metabolic engineering purposes, it has become clear that the restriction to

metagenomics libraries and mutants thereof is a natural limit for the application and exploration of new enzymatic reactions. Therefore, a technology that could invent new enzymes from scratch would broaden the field of biotechnology enormously because it would in principle allow the development of catalysts for reactions that have no biological blueprint. Recently developed artificial intelligence-based programs like ProtGPT2 (Ferruz et al., 2022) or RFdiffusion (J. L. Watson et al., 2023) may already show glimpses of that future which may well be accompanied by machine learning programs for multiple purposes like retrosynthesis (T. Yu et al., 2023) and more. By doing so, promising metabolites could find their way to marvelous new applications for the advancing needs of humankind.

1.2. Secondary metabolites - From occasional by-product to omnipresence

The need for biocatalysts is not just limited to the previously mentioned proteins or funneling various feedstock into bioprocesses but also to produce required metabolites. Metabolites are the intermediate products of chemical reactions in living organisms and the sum of all these chemical reactions within an organism is called metabolism (Nielsen & Keasling, 2016). Metabolism is often categorized as primary or secondary metabolism. Primary metabolism includes the reaction patterns, also called pathways, that are essential for life and are present in a plethora of organisms. Those pathways that occur only in specific species and are not necessarily essential are referred to as secondary metabolic pathways. These classifications are not strict and essentiality is highly dependent on the organisms' natural habitat which might not be accurately mimicked in a laboratory environment. Secondary metabolites are typically of low molecular weight like alcohols or organic acids but rather large and more complex structures are also known like polyketides or some antibiotics. Secondary metabolites are made by many organisms but do not directly contribute to growth, reproduction or cellular development. They are defined as: "[Metabolites that] do not play an explicit role in the internal economy of the organism that produces it „[sic]" and stands „[sic]" in direct contrast to primary metabolites, which maintain fundamental cellular life processes." (Delgoda & Murray, 2017). Usually, these secondary metabolites provide tolerance to stress conditions or improves competition and thus possess benefits for the respective organisms in their ecological niches (Williams et al., 1989) and as such have been key factors in the spreading of life throughout the world and the development of ecological diversity.

The basis of ecological diversity is described by the abiogenesis theory of life. According to this theory, life started during the Hadean about four billion years ago (Świezyński, 2016) (Figure 1-1). Since then, prokaryotes like cyanobacteria and archaea dominated life during the Precambrian (4 billion – 541 million years ago) (Cohen et al., 2013) and caused stromatolite sediments. Early metabolic traits like biological redox chemistry can be assigned to the time before and around the Great Oxidation Event

(Mateos et al., 2022). Additionally, during the Paleoproterozoic era (2500 – 1600 million years ago) the first eukaryote, also called the last eukaryotic common ancestor (LECA) (Brocks et al., 2023), arose by an endosymbiotic event resulting in the creation of algae (De Clerck et al., 2012). Early eukaryotes from 1600 to 800 million years ago were still missing characteristic cholesterol but used the precursors protosteroids instead and are therefore called “protosterol biota” (Brocks et al., 2023). Even though timescales for the origin of different phyla are relatively poor and error-prone (X. Zhang & Shu, 2021), about 500 million years ago around the Cambrian explosion, algae living exclusively in aqueous environments developed which contained the metabolic processes of photosynthesis, glycolysis, and the citric acid cycle. About 50 million years later, liverwort-like organisms started to settle on land, marking the appearance of early terrestrial plants. With that occurrence, new secondary metabolite pathways emerged (Davies et al., 2020). Newly developed molecular characteristics and strategies allowed these pioneers to cope with aridity, temperature changes, adhesion on soil and direct sunlight. Some of these new capabilities included the synthesis of compounds or polymers that are considered unremarkable from today’s perspective because of their omnipresence. As an example, one of the game-changing new capabilities was the formation of lignin which allowed vertical growth and transportation of water and nutrients. Key to this new capability were gene duplication events that allowed parallel evolution towards new biosynthesis pathways with products that protected organisms for instance from ultraviolet light (Delgoda & Murray, 2017; X. Zhang & Shu, 2021). The promiscuous use of primary metabolism catalysts for new metabolites shows how secondary metabolism evolution can lead to new essential capabilities in new ecological niches (Cavalier-Smith, 1992). Similar use of formerly primary metabolic catalysts paved the way for invertebrate (e.g. the arthropods) invasion of land 480 million years ago and the vertebrate land invasion 416 million to 359 million years ago (Janvier & Clément, 2010).

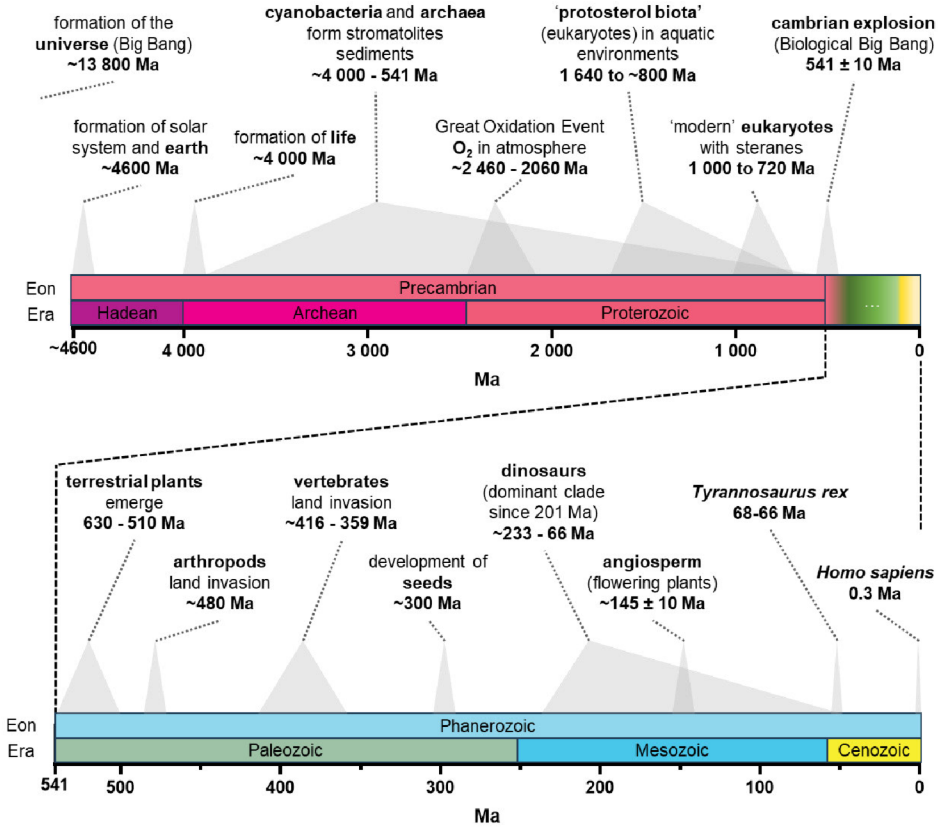

Figure 1-1 Selected events during the development of life in million years (Ma) with Eon and Era from Cohen et al. (2013).

The development of new secondary products has typically resulted in ecological benefits. Such as tolerance mechanisms or competition benefits from the production of antibiotics, for instance. Other metabolic pathways co-evolved with species. Therefore, colors and pheromones for attraction or repulsion of organisms, cellular- and inter species-communication (Krespach et al., 2023) or cross-activities with an organism's microbiome appeared. The opportunities of the biosynthetic capacity are enormous and still allow new findings. In the present day most dominant plants are angiosperms (flowering plants) which make up approximately 85% and evolved at least 145 million years ago (Delgoda & Murray, 2017). Alongside their development and co-evolution with e.g. insects, the number of secondary metabolites increased enormously due to flowering, fertilizing symbiosis, fragrance development and attraction to nectar by volatile chemicals. Additionally, carotenoids, terpenes, polyketides like chalcones, anthocyanins, anthocyanidins, stilbenoids, as well as non-ribosomal peptides and many more derivatives originating from the shikimate pathway appeared (Erb & Kliebenstein, 2020). Molecular precursors of secondary metabolites are generally derived either from acetyl-CoA/malonyl-CoA, amino acids, purine nucleotides, the shikimate pathway intermediates or

from isopentenyl pyrophosphate (IPP) and dimethylallyl pyrophosphate (DMAPP) (Desmet et al., 2021). In this way, diverse secondary metabolism pathways branch from the same nodes in primary metabolism. Many ancient enzyme lineages appeared in parallel with new species. For example starch-degrading enzymes appeared alongside with the development of seeds and the germination process about 300 million years ago (Weng, 2014). In addition to plants as a secondary metabolic resource, bacteria have been in competitive environments for an even longer period from an evolutionary perspective. Although most of today's known (and commercialized) antibiotics were found in filamentous Gram-positive bacteria, it is believed that only about 1-3% of *Streptomyces'* antibiotics have been found (Traxler & Kolter, 2015). This highlights how limited our knowledge and unexploited potential of the molecular repertoire in nature's diversity is.

The evolutionary trajectory of species can also be examined by molecular trajectories of different secondary metabolite pathways. This includes the emergence or evaluation of speciation by enzyme homologies to cast light on Darwinian evolution from a molecular perspective (Wen et al., 2020; Weng, 2014). In addition to revealing the history, molecular evolution also serves as an opportunity to reveal microbial interaction with plants via the analysis of the metabolome (Pang et al., 2021). Additionally, these relations can also reveal beneficial traits of some secondary metabolites like trihydroxychalcone-derived isoflavonoids which induce nodulation by rhizobia in legumes (Weng, 2014). Based on the gene homologies, computational screening and prediction of secondary metabolite clusters serve as a leading discovery tool in molecular research like the *antibiotics and secondary metabolite analysis shell* - antiSMASH 7.0 (Blin et al., 2023).

1.2.1. Usefulness of secondary metabolites for humankind

The ingredients of drugs in medicine like antibiotics, antivirals or anti-tumor agents originally derive from natural isolation (Atanasov et al., 2021; Bisht et al., 2021; Miller et al., 2020; Newman & Cragg, 2020). In food and beverages, some secondary metabolites were used as sweeteners, colorants and flavors. Others are used as crop protectants in agriculture (Kallscheuer, Classen, et al., 2019). Chemical modifications increase the compound's persistence to cope with natural degradation and allow long-term effectiveness in the respective application (Reed & Alper, 2018; Sanyuan Shi et al., 2022). Actually, some can be found as a precursor for plastics or other special polymer materials. Production and extraction of these secondary metabolites have ever since been of biotechnological interest (Alara et al., 2021; W. Schmid, 1849). Therefore, the breeding of natural producers (Fu et al., 2018) and heterologous production were investigated for many compounds (Yadav et al., 2019). One group of secondary metabolites of particular interest for humankind are polyketides (Weissman & Leadlay, 2005).

1.3. Biosynthesis of polyketides - A kaleidoscope of chemistry by nature

Polyketides are a structurally very versatile group of secondary metabolites (Figure 1-2) produced by bacteria, fungi, plants and symbionts such as lichens (Masters & Bräse, 2012; Morita et al., 2019). Their extraordinary richness of facets resembles that of a kaleidoscope, where new compounds are constantly being discovered (Helfrich et al., 2014; Nivina et al., 2019). In spite of their structural diversity, they are made by condensation of the same coenzyme A (CoA)-bound acyl chains (Y. A. Chan et al., 2009) that are condensed for elongation. Finally, the intermediate products condense with themselves forming aromatic groups or cyclic compounds. The ketone reaction intermediates with multiple carbonyl groups give polyketides their name. The well-characterized group of flavonoids arose simultaneously with the colonization of terrestrial areas around 550 - 470 million years ago by bryophytes, such as liverworts, likely displaying the origin of plant polyketide synthesis (Davies et al., 2020; Wen et al., 2020; Yonekura-Sakakibara et al., 2019).

Enzymes that form polyketides are called polyketide synthases (PKS). They are categorized into three different types (Figure 1-2). PKS type I consist of one large amino acid sequence folding to several catalytic domains for distinct functions during the non-iterative elongation process, including acyl carrier domains (Grininger, 2023). PKS type II consist of multiple separate proteins that allow iterative cycles for product formation (Jia Wang et al., 2020). PKS type III are rather small enzymes compared to type I. They condense single or multiple malonyl-CoA extensions to final aromatic compounds (Morita et al., 2010). In contrast to PKS I and II systems, these lack the ability to perform additional reactions besides the polymerization. PKS I and II also perform reduction of intermediates or use different CoA extender units beside malonyl-CoA (Y. A. Chan et al., 2009). For example, propionyl-CoA or methylmalonyl-CoA are accepted by PKS I variants (Englund et al., 2022) or 2-isopropylmalonyl-CoA by PKS II during 3,5-dihydroxy-4-isopropylstilbene (tapinarof/benvitimod) synthesis in *Photorhabdus luminescens* (Maglangit et al., 2020; H. B. Park et al., 2020) or aryl polyene synthesis in *Xenorhabdus doucetiae* (Grammbitter et al., 2019; Schöner et al., 2016) (Figure 1-2). The first discovered PKS III was a chalcone synthase (CHS) forming the naringenin chalcone from *p*-coumaryl-CoA and three malonyl-CoA (Ikuro Abe & Morita, 2010).

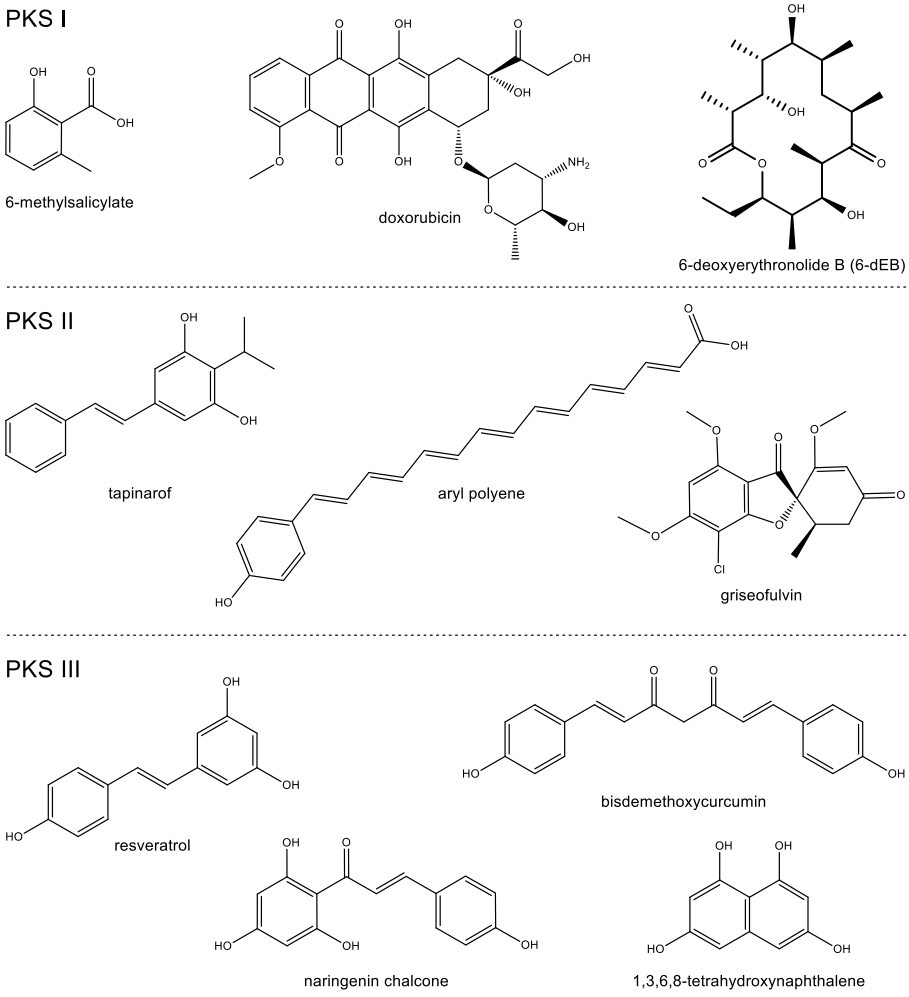

Figure 1-2 Structural diverse polyketide examples of PKS type I, II & III with their respective name.

In nature, polyketides are usually modified with different functional groups which keep them water-soluble or specify their physiological function. This includes hydroxylation, glycosylation, prenylation and many more (Masters & Bräse, 2012). For this functionalization also intermediates from non-related secondary metabolite pathways are used as in the case of cannabinoids, which are prenylated compounds with a core made by orcinol synthase or olivetol synthase (Gülck & Møller, 2020). This example intertwines the independent secondary metabolite pathways of terpenes and polyketides.

1.3.1. PKS and fatty acid biosynthesis in close evolutionary relationship

For modern biotechnological use and production of polyketides by metabolic engineering strategies, the relation and evolutionary origin of PKS are of interest. The reaction mechanism of PKS is highly

similar to that in fatty acid synthesis (FAS) (Cronan & Thomas, 2009; Staunton & Weissman, 2001). FAS is an essential part of primary metabolism to provide necessary building blocks for phospholipids used in cell membrane synthesis, carbon storage, and much more. Pace-making enzymes of bacterial type II FAS are the β-ketoacyl-ACP synthase I and II (FabB, FabF) whose reactions are highly comparable to PKS elongation reactions (Figure 1-3 A) (H. Dong et al., 2021). The close relationship between mitochondrial FAS II and bacterial FAS II supports the endosymbiotic event theory (D. I. Chan & Vogel, 2010). Type I FAS and PKS I megasynthases are also more closely related to each other than to PKS III or FAS II (Shimizu et al., 2017). Some special lipids from mycobacteria are even made by collaborative synthesis by PKS and FAS (Gokhale et al., 2007) Overall PKS and FAS systems display a shared phylogeny in evolution (Cronan & Thomas, 2009).

Both FAS and PKS use substrates bound via a thioester bond. An acyl chain covalently bound to CoA allows further chemical reactions like ester formation and reduction, or Claisen and Aldol condensation reactions (Morita et al., 2019). The linkage to CoA increases the activity of the carbonyl group, resulting from the increased polarity of the carbon atom covalently bound to the sulfur ($\Delta G^{0\prime}$ -31.5 kJ mol^{-1} for acetyl-CoA hydrolysis (Wünschiers et al., 2013)). Thus, thioester-linked metabolites allow specific elongation reactions in biochemical processes. CoA is a product of 4'-phosphopantetheine (4'-PP) from the pantothenate pathway and two adenosine triphosphates (ATP) (Beld et al., 2014). 4'-PP is frequently used as a prosthetic group and is ubiquitously present in organisms (Beld et al., 2014). Therefore, pantothenate is proposed to have existed in the primordial soup according to the Oparin-Haldane hypothesis of the origin of life (Holliday et al., 2007) (Figure 1-1).

For FAS, acetyl-CoA is carboxylated to malonyl-CoA by a biotin-dependent acetyl-CoA carboxylase (ACC) (Cronan, 2021). In eukaryotes, this enzyme is a single large protein with multiple subunits (Xiaoxu Chen et al., 2018). In prokaryotes, ACC consists of two (Jäger et al., 1996) to four distinct subunits (Cronan, 2021). For use in FAS, the C3 unit of malonyl-CoA is transferred to an acyl carrier protein (ACP) which has to be activated by a phosphopantetheinyl transferase (PPTase) (Beld et al., 2014) with 4'-PP, leading to the same linkage like in CoA-bound metabolites. The holo-ACP (active form) specifically interacts with the subsequent enzymes in fatty acid elongation to shift the respective substrate from one reaction cavity to the next (Cronan, 2014b) (Figure 1-3 B) and is the third most abundant protein in certain prokaryotes (Cronan & Thomas, 2009). PKS I and II use their own ACP homologs encoded within the megasynthase in PKS I systems or as separate proteins for interaction with PKS II. The substrate, e.g. malonyl-CoA, is either loaded onto the respective ACP of the PKS system or used directly as substrate like in the case of type III PKSs. Even hybrids of PKS III and PKS I where PKS III provides the starter substrate for PKS I were discovered (B. Zhang et al., 2023). In all described cases, and also in non-ribosomal polypeptide synthesis, 4'-PP serves as a flexible connection between different catalytic centers.

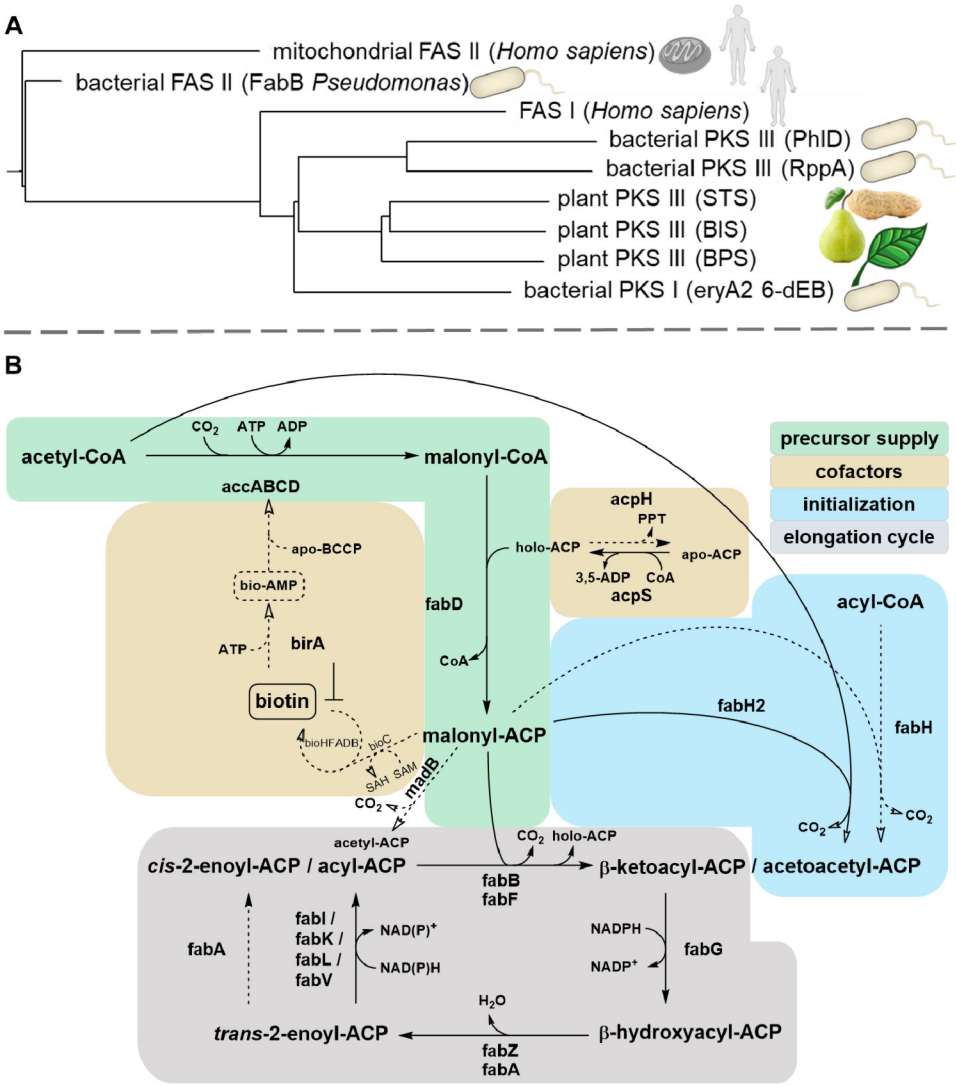

Figure 1-3 Relationship of FAS and PKS and FAS in species of Pseudomonas.

A) *Phylogenetic relationship of different FAS proteins and PKS of diverse origin by "Multi-Way exhaustive pairwise alignment" by BLOSUM 62 matrix. PhlD, phloroglucinol synthase; RppA, 1,3,6,8-tetrahydroxynaphthalene synthase; STS, stilbene synthase; BIS, biphenylsynthase; BPS, benzophenone synthase; eryA2, 6-deoxyerythronolide-B synthase.* ***B)*** *Scheme of fatty acid biosynthesis (FAS) in prokaryotes. Different "sections" during FAS which are also homologous present in PKS I & II* (Cronan & Thomas, 2009) *are indicated by colors (green, precursor supply; orange, cofactor synthesis; blue, FAS initialization; grey, FAS elongation cycle). Abbreviations: accA, acetyl-CoA carboxylase subunit alpha; accB, acetyl-CoA carboxylase biotin carboxyl carrier protein (BCCP); accC, acetyl-CoA carboxylase biotin carboxylase; accD, acetyl-CoA carboxylase subunit beta; fabD, malonyl-CoA:ACP transacylase; fabB, ß-ketoacyl-ACP synthase I; fabF, ß-ketoacyl-ACP synthase II; fabH and fabH2, ß-ketoacyl-ACP synthase III; madB, malonyl-ACP decarboxylase; fabG, ß-ketoacyl-ACP reductase; fabZ, 3-hydroxyacyl-ACP dehydratase; fabA, 3-hydroxyacyl-ACP dehydratase and trans-2-decenoyl-ACP isomerase (bifunctional); fabI/fabK/fabL/fabV, trans-2-*

enoyl-ACP reductase I, II, III & IV; bioC-bioHFADB, biotin pathway (Cronan, 2014a); birA, biotin protein ligase; acpP, acyl carrier protein; acpS, 4'phosphopantetheinyl transferase (PPTase); acpH, ACP hydrolase.

For the synthesis of saturated acyl chains during FAS, the β-ketoacyl-ACP product from ketoacyl synthases (KS), sometimes called acyltransferase (AT), is further processed by β-ketoacyl reduction (KR), hydroxyacyl dehydration (DH) and enoyl reduction (ER). PKS I and II have homologous KS/AT, KR, DH and ER modules (Grininger, 2023). By domain variations or lacking domains, PKS products can be tailored towards new products or enantiomer pure products (Miyazawa et al., 2021) and also new-to-nature products (Klaus & Grininger, 2018; Miyazawa et al., 2020; Sanyuan Shi et al., 2022).

In contrast to type I and II, PKS III uses CoA-activated substrates exclusively. Multiple extender units can be condensed by one synthase and modifications of the respective product, if any, occur after PKS action, independently. That simplicity compared to other PKSs makes PKS III attractive enzymes for biotechnological production purposes.

1.3.2. Biosynthesis of PKS III natural products

PKS III represent the simplest PKS type and PKS III are broadly spread in various forms of life. CHS, the archetype of PKS III, served as a basis for the elucidation of the reaction mechanism (Ikuro Abe & Morita, 2010; Pandith et al., 2020; Tropf et al., 1995), distribution and diversity in organisms (D. Guo et al., 2022; Morita et al., 2019; Waki et al., 2021) and was therefore extensively reviewed under different aspects (Ikuro Abe, 2020; Austin & Noel, 2003; Bisht et al., 2021; Delmulle et al., 2018; C. Liu & Li, 2022; Morita et al., 2010; Palmer & Alper, 2019; D. Yu et al., 2012).

Physiologically, PKS III function as homodimers and are of moderate size (390-400 amino acids, 40–45 kDa) (Ikuro Abe & Morita, 2010). The plant and bacterial origins display different superfamilies and sequence homologies do not necessarily correlate with the respective product formation due to multiple independent evolution lines of different plant PKS III from CHS. This means, that a sequence alignment does not directly allow a distinction between e.g. a CHS, a stilbene synthase (STS) or benzophenone synthase (BPS) (Beerhues & Liu, 2009). Plant PKS III often use aromatic CoA esters from the phenylpropanoid pathway (like *p*-coumaroyl-CoA, cinnamoyl-CoA, benzoyl-CoA, etc.) as a starter unit for subsequent elongation, but other acyl-CoA starters are reported as well (Morita et al., 2019). CHS and STS form the identical polyketide intermediate from the same substrates but catalyze a different intra-molecular carbon-carbon cyclization reaction by either C6 → C1 Claisen or C2 → C7 aldol condensation (Figure 1-4). In a previous study, it was even possible to engineer a CHS towards an STS, highlighting their close relationship (Austin et al., 2004). The common catalytic center is characterized by Cys^{164} for binding starter residues and intermediates, as well as His^{303} and Asn^{336} for catalysis. Additionally, Phe^{215} is important for the size of the cavity (numbering of CHS from Alfalfa,

Medicago sativa). The growing polyketide chain is guided by adjacent amino acids and the cavity's size. Further conserved amino acids in $CHS_{alfalfa}$ are Thr^{132}, Ser^{133}, Thr^{194}, Thr^{197}, Gly^{256}, Phe^{265}, and Ser^{338}. Elongation stops due to the restricted space of the intermediate molecules (Austin et al., 2004; Pandith et al., 2020). Ring-closing reactions of polyketide intermediates with e.g., O5→C1 result in lactone products (Figure 1-4).

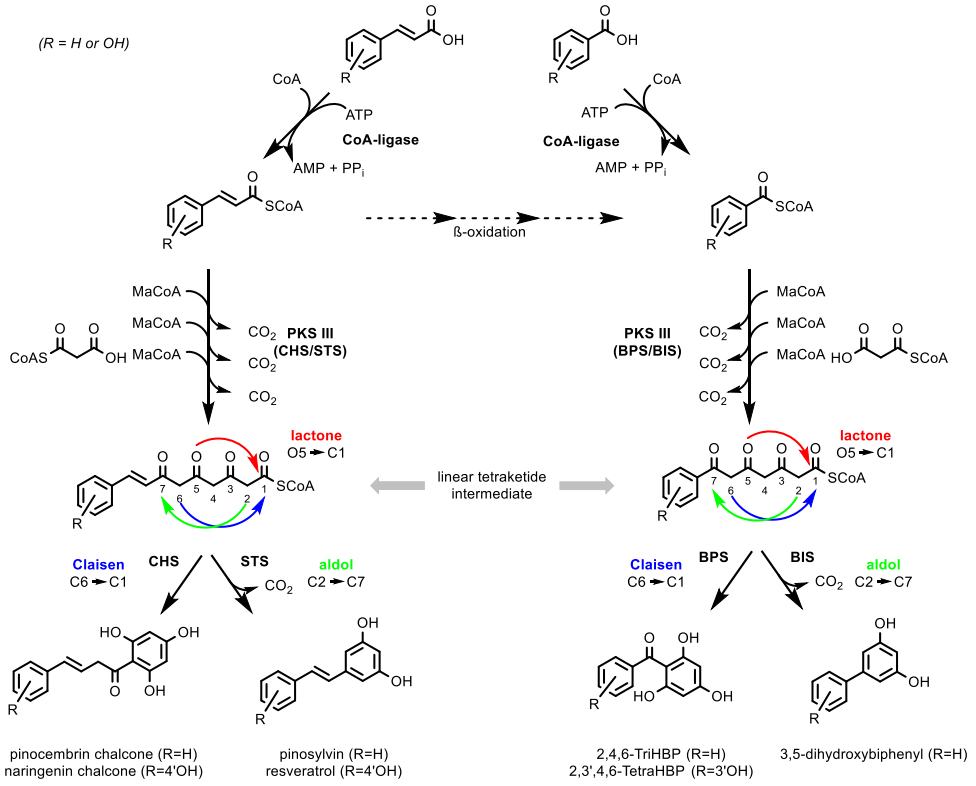

Figure 1-4 Reaction scheme of different plant PKS III and their substrates.
Different ring-closing reactions are indicated by colored arrows (blue, Claisen condensation; green, aldol condensation; red, laconization). Dashed arrows indicate multiple reaction steps, the release of coenzyme A is not illustrated. Abbreviations: CHS, chalcone synthase; STS, stilbene synthase; BPS, benzophenone synthase; BIS, biphenyl synthase, 2,4,6-TriHBP, 2,4,6-trihydroxybenzophenone; 2,3',4,6-TetraHBP, 2,3',4,6-tetrahydroxybenzophenone.

CHS are associated with other enzymes of the flavonoid pathway like chalcone isomerases (CHI) and type IV CHI-like (CHIL) proteins, which lack catalytic activity but arrange close proximities of enzyme cascades *in vivo* to counteract enzyme promiscuity and improved flavonoid synthesis (Waki et al., 2021). Ancient forms of flavonoid metabolism, like in mosses, lack CHI and CHIL proteins but are still capable to produce flavonoids (Davies et al., 2020). STS as a sub-functionalized group of CHS are not associated with CHIL-like proteins (Waki et al., 2020).

The diversity of PKS III is enormous and besides CHS, STS, BPS and BIS it includes further groups like 2-pyrone synthase (2-PS) for 2-methyltriacetic acid lactone, pentaketide synthase (PCS) for 5,7-dihydroxy-2-methylchromone and octaketide synthase (OKS) for emodin biosynthesis (Y. Guo et al., 2021). Additionally, benzalacetone synthase (BAS), acridone synthases (ACS), quinolone synthases (QNS), and multiple different enzymes for curcuminoid synthesis like bismethoxycurcumin synthase (CUS) or diketide synthases (DCS) in combination with curcumin synthase (CURS), and many more are also functioning as PKS III (Morita et al., 2019; Shimizu et al., 2017). More variants are still discovered today, which produce a broad plethora of compounds (B. Zhang et al., 2023; W. Zhang et al., 2023) and mutants thereof allow an even broader product spectrum (S. P. Shi et al., 2009). Although promiscuous use of alternative substrates is possible, the affinity (K_M) for starter and elongation unit is affected. K_M of malonyl-CoA can range from ~1 µM in bacterial flaviolin synthesis (Shengying Li et al., 2007) to ~9-14 µM in plants' native conversion products like stilbenes (C. G. Lim et al., 2011) or biphenyls (Chizzali et al., 2016) and up to ~300-400 µM for alternative substrates like salicyl-CoA (Chizzali et al., 2016). Access to multiple PKS products is requested due to their broad applicability. However the variations in affinity plus seasonal variations by natural producers are considerations when it comes to polyketide's biotechnological production. The different affinities require a well-considered choice of a production platform, be it natural producers or engineered biotechnological hosts.

1.3.3. Metabolic engineering strategies for heterologous polyketide synthesis

Polyketides have potential benefits for human health and application in the pharmaceutic-, cosmetics-food and beverages industries (Atanasov et al., 2021; Isogai et al., 2022; Hongbiao Li et al., 2022). Laborious purification (Alara et al., 2021) and consequently high costs of polyketides from natural resources has led to their heterologous production in different biotechnological hosts to allow economic production (Braga & Faria, 2022; X. Liu et al., 2017; Palmer & Alper, 2019; Wolf et al., 2021; D. Yang et al., 2020). Often multiple products were made per study due to the products' uniform synthesis from identical precursors. The interchangeable product spectrum results from the used PKS III which determines the product in the same strain background. For the synthesis of core structures like resveratrol, naringenin and others, multiple candidate genes were usually tested in hosts to elucidate the best functional heterologous genes in the respective host. Simple polyketides are made with bacterial hosts and further functionalized products are usually made with eukaryotic production platforms (Naseri, 2023) due to the limited applicability of e.g. plant- or fungi-derived polyketide modifying enzymes like monooxygenases, methyltransferases, prenyltransferases, glycosylases or reductases in biotechnological bacterial workhorses (D. Yang et al., 2023).

In order to increase product titers of these specialty chemicals, different metabolic engineering strategies were applied, leading to remarkable product titers. Frequently, *Escherichia coli* is used as an established host and expression is driven by a strong and inducible T7 expression system (Jeong et al., 2015; Kallscheuer et al., 2016; C. G. Lim et al., 2011; J. Wu et al., 2021). Expression strength is often a limiting factor for product titers. In yeasts (Ibrahim et al., 2021; Rainha et al., 2020), like *S. cerevisiae* (M. Li et al., 2015; Meng et al., 2023; Q. Zhang et al., 2021) or *Yarrowia lipolytica* (Sáez-Sáez et al., 2020), the respective production genes were integrated multiple times and subsequent screening of the best producer is done (Naseri, 2023; Sáez-Sáez et al., 2020). With yeast production platforms, the highest polyketide titers have been reached by combining metabolic and process optimization. Up to 12.4 g L^{-1} (Sáez-Sáez et al., 2020) and more recently up to 22.5 g L^{-1} resveratrol (M. Liu et al., 2022) were made in this way.

For some products the respective PKS III are not stable in the applied conditions like temperature or power input. Therefore, co-expression with chaperones (Zhao et al., 2018) or enzyme engineering (Zha et al., 2008) led to improved PKS III mutant variants (Meyer et al., 2019; Rao et al., 2013; P. V. van Summeren-Wesenhagen & Marienhagen, 2015). Additionally, fusion proteins with solubilizing tags (Kallscheuer, Kage, et al., 2019), or fusion proteins to set up a scaffold of precursor-delivering enzyme and PKS III (M. Liu et al., 2022; J. Zhang et al., 2022) are made. Unfortunately, the rather complex product synthesis requires some effort in the development of advanced screening assays functioning *in vivo*, expression-coupled transcriptional biosensors (De Paepe et al., 2018; Hwang et al., 2023; Heng Li et al., 2017; H. Sun et al., 2020; Terán et al., 2006; Xu et al., 2014) or colorants for detection (D. Yang et al., 2018).

Despite targeting the expression strength or use of enzyme variants for higher product titers, the supply of malonyl-CoA precursors was also revealed as a bottleneck in heterologous production (Milke & Marienhagen, 2020). Physiological concentrations can vary enormously between different species and engineered variants (Gläser et al., 2020). Therefore, the expression of ACC was either increased by additional expression (Leonard et al., 2007; P. V. van Summeren-Wesenhagen & Marienhagen, 2015; J. Wu et al., 2021; Zha et al., 2009), deregulation from native repressors (Milke, Kallscheuer, et al., 2019) or feedback-insensitive variants were developed (J. W. Choi & Da Silva, 2014; Shuobo Shi et al., 2014), which allow increased malonyl-CoA supply for both, essential FAS and heterologous polyketide synthesis. Alternatively, external supplementation of malonate and subsequent coupling to CoA represents also another established strategy (Jeschek et al., 2017; Leonard et al., 2008; B. Liang et al., 2019; Santos et al., 2011; Sui et al., 2020). To enable this coupling reaction, a part of a malonate degradation pathway has to be implemented (Crosby et al., 2012; Y. S. Kim, 2002; Stoudenmire et al., 2017; Suvorova et al., 2012; Z. Wang et al., 2020).

Besides increasing the supply reaction for malonyl-CoA, its downstream consumption in FAS displays the major drain of precursor (Milke & Marienhagen, 2020). Modifying FAS in a production host is rather challenging because of its essentiality and the resulting crucial tradeoff between sufficient carbon flux into FAS and inference to elevate intracellular malonyl-CoA concentrations to allow effective use of PKS with higher K_M. FAS is either decreased by permanent modification regarding promoter of single genes (Salas-Navarrete et al., 2018), or replacements by weaker enzyme variants (Bergler et al., 1994; Koppisch & Khosla, 2003; Mains & Fox, 2023; Srinivas & Cronan, 2017) or by temporary knockdowns that separate growth and production phases by silencing and anti-sense RNA (Y. Yang et al., 2015) or CRISPRi (J. long Liang et al., 2016; Tao et al., 2018). In combination with a suitable screening method, FAS interference can be rather effective (D. Yang et al., 2018). Furthermore, engineering of FAS for a variable chain length of fatty acids might also be applicable for malonyl-CoA availability (Mains & Fox, 2023).

1.4. *Pseudomonas* as biotechnological production host

The selection of a suitable biotechnological production host is limited by its genetic accessibility (Martin-Pascual et al., 2021) to allow the implementation of heterologous biochemical pathways (Bitzenhofer et al., 2021) and depends on the biosynthetic capabilities that are connected to the product of interest and safe handling (Blombach et al., 2022). Different hosts have variable inherent limitations in their metabolic engineering opportunities and subsequent applicability (López et al., 2022). Pseudomonads are upcoming hosts for biotechnological purposes (Weimer et al., 2020) due to their exceptional endurance of xenobiotics and solvents that allow alternative production approaches, such as two-phasic bioprocesses, that would not be feasible for other host organisms such as yeasts and *E. coli* (Hermann J. Heipieper et al., 2007). Originally derived from soil isolates, multiple laboratory platform strains are available, including those with reduced genomes for improved handling and applicability for biotechnological purposes (Leprince et al., 2012; P. Liang et al., 2020; Martinez-García et al., 2020; Martínez-García et al., 2014; Daniel C. Volke et al., 2020; Wynands et al., 2019). Pseudomonads are capable of shifting more or less carbon from substrate into biomass formation or adapting the substrate uptake rate. This can lead to an up to eight-fold increase in NAD(P)H generation in responds to solvent stress (Blank et al., 2008). This enables Pseudomonads to thrive in fuel and xenobiotic-contaminated environments.

The characteristic ability to withstand harsh conditions and increase substrate uptake rate for energy generation allows the use of energy-depending tolerance mechanisms (H. J. Heipieper & Martínez, 2010; Kusumawardhani et al., 2018; Ramos et al., 2015). Pseudomonads are equipped with several outstanding tolerance mechanisms that allow anti-microbial metabolite production and also the usage

of potentially toxic solvents for *in situ* product removal (ISPR). The tolerance mechanisms include e.g. *cis-trans* isomerase (Cti) (Hermann J. Heipieper et al., 1995) in the periplasm for modifying inner membrane fluidity when membrane-incorporating compounds accumulate (Eberlein et al., 2018). Another characteristic is the presence of multiple efflux pumps that extrude organic solvents or other toxic compounds. A large degree of freedom in the choice of solvent for ISPR is a clear benefit (Schwanemann et al., 2020) (section 1.5.1.).

Various glucose utilizing catabolic pathways emerged during evolution. The classical linear Enter-Doudoroff (ED) pathway requires nine reaction steps and consequently fewer enzymes than the textbook example glycolysis (Embden-Meyerhof-Parnas pathway - EMP) with ten steps to catabolize glucose to pyruvate and glyderaldehyde-3-phosphate (GAP). ED is broadly spread in Archaea and Gram-negative bacteria but not too much in Gram-positives (Kopp & Sunna, 2020). It key enzyme 2-keto-3-deoxygluconate-6-phosphate aldolase is actually broader spread between different species than phosphofructokinase from EMP (Xi Chen et al., 2016). However, the ED yields less ATP per glucose molecule than classical EMP (netto output per mol glucose: 1 ATP+2 NAD(P)H in ED vs 2 ATP + 2 NAD(P)H in EMP) (Kopp & Sunna, 2020). According to their ecological niche, species either rely on higher energy yield and higher investment in protein synthesis like *E. coli*, which uses the EMP pathway. Alternatively, using the ED pathway for glucose utilization requires less resources and allows fast conversion (Schada Von Borzyskowski et al., 2020). All types of glucose-utilizing catabolic pathways exist in diverse variations depending on the host's native environment. A characteristic difference between ED to EMP in the upper glucose utilization is the oxidation of glucose-6-phosphate (G6P) in ED instead of a next phosphorylation step like in EMP (Kopp & Sunna, 2020).

The glycolytic metabolism of Pseudomonads relies on a combination of the Entner-Doudoroff, the Embden-Meyerhof-Parnas, and pentose phosphate pathways (PPP) that partially operates in a cyclic manner. The merged variant of ED, EMP, and PPP is called the EDEMP cycle (Figure 1-5) (Kopp & Sunna, 2020; Nikel et al., 2015). Per round of the EDEMP cycle, pyruvate is formed and a glyceraldehyde-3-phosphate. The glyceraldehyde-3-phosphate is either converted further to pyruvate via the EMP pathway as well or two of these molecules can, via dihydroxyacetone-phosphate, reform fructose-1,6-bisphosphate in gluconeogenic direction. Due to the lack of the EMP characteristic enzyme phosphofructokinase, the triosephosphate can only be used in gluconeogenesis fashion. The newly formed hexose can again form ATP and NADPH and provide precursors for various pathways during the reuse during the EDEMP cycle (Figure 1-5). In consequence, this specific utilization of carbohydrates provides fructose-6-phosphate under various environmental conditions and allows additional balancing between ATP formation from glyceraldehyde-3-phosphate oxidation by EMP or increased supply of biomass building blocks from gluconeogenic intermediates. In response to increased NADPH demands, more carbon can be shifted into the PPP from gluconate-6-phosphate. The

resulting fructose-6-phosphate and glyceraldehyde-3-phosphate can be recycled to gluconate-6-phosphate. This recycling of PPP products provides increased availability of redox equivalents and ATP by the loss of only one CO_2 (Nikel et al., 2021). Although ED is required for biomass formation, this shift into PPP enables the unique energy-dependent tolerance mechanisms of *Pseudomonas* species because it increases the supply of protons for the respiratory chain (NAD(P)H = 10 H^+; $PQQH_2$ = 8 H^+; 4 H^+ = 1 ATP (Silverstein, 2014)).

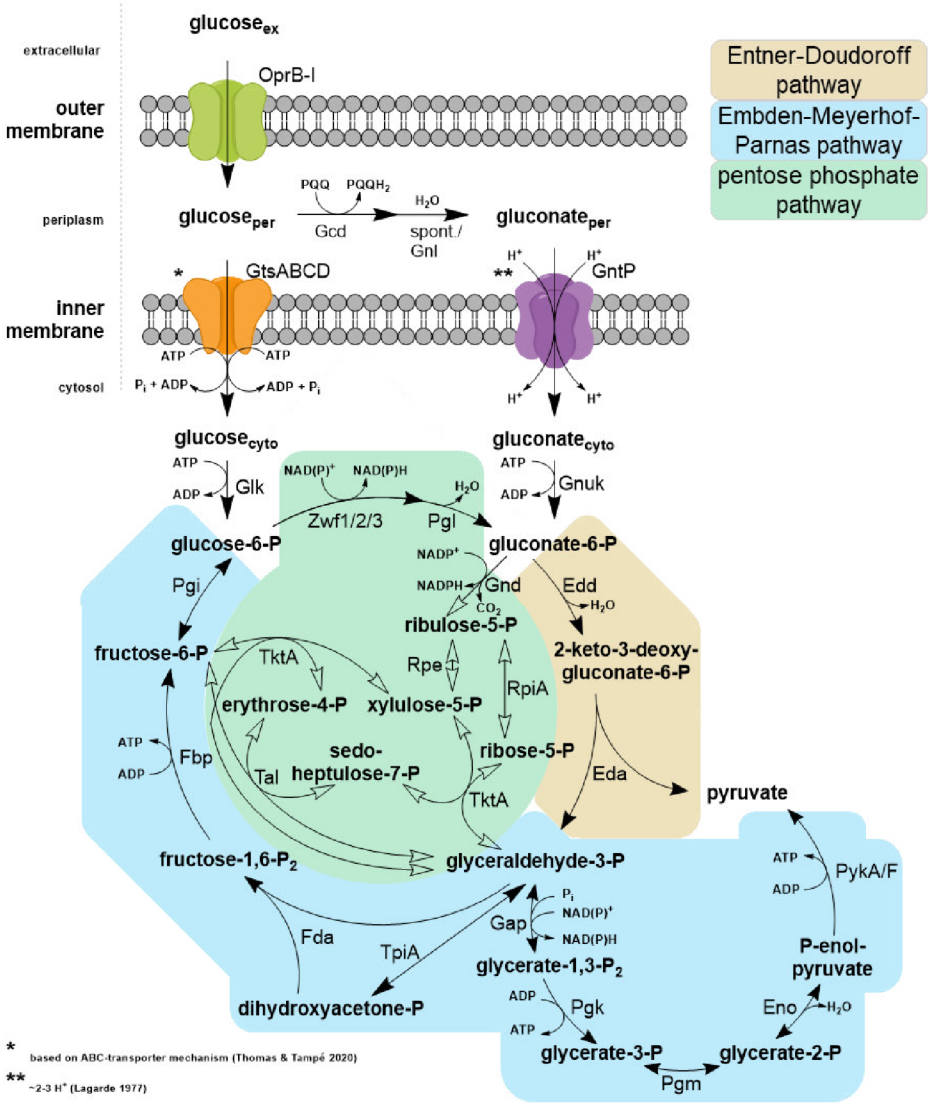

Figure 1-5 Glucose transport and catabolism by the EDEMP cycle in P. taiwanensis VLB120.
The EDEMP consists of reactions that are usually assigned to the Entner-Doudoroff pathway (orange), the Embden-Meyerhof-Parnas pathway (blue) and pentose phosphate pathway (green). Solid arrows indicate major reactions in Pseudomonas, hollow arrows represent schematic reactions of the pentose phosphate pathway without enzyme names. Transporters are color coded according to their transport mechanism (green, passive transport; orange, ATP-binding-cassette-type transporter (Thomas & Tampé, 2020)*; purple, proton symporter transporter requiring 2-3 H^+ according to* Lagarde (1977)*). Metabolites*

are shown in bold letters with phosphate indicated by P, enzymes are indicated by established abbreviations. The figure is partly adapted from the manuscript Schwanemann et al.2023 (in preparation). Abbreviations: suffix -ex, extracellular; suffix -per, periplasmic; suffix -cyto, cytosolic; OprB-I, carbohydrate-selective porin; GtsABCD, glucose ABC transporter; GntP, D-gluconate transporter; PQQ, pyrroloquinoline quinone; Gcd, PQQ-dependent glucose dehydrogenase; Gnl, gluconolactonase; Glk, glucokinase; GnuK, D-gluconate kinase; Zwf1/2/3, Glucose-6-phosphate dehydrogenase; Pgl, 6-phosphogluconolactonase; Gnd, 6-phosphogluconate dehydrogenase; Rpe, ribulose-5-phosphate 3-epimerase; RpiA, ribose-5-phosphat isomerase; TktA, transketolase; Tal, transaldolase B; Edd, 6-phosphogluconate dehydratase; Eda, 2-keto-3-deoxy-gluconate-6-phosphate aldolase; TpiA, triose phosphate isomerase; Fda, fructose-1,6-bisphosphat aldolase; Fbp, fructose-1,6-bisphosphatase; Pgi, glucose-6-P isomerase; Gap, glyceraldehyde-3-P dehydrogenase; Pgk, phosphoglycerate kinase; Pgm, phosphoglycerate mutase; Eno, phosphoenolpyruvate hydratase; PykA/F, pyruvate kinase.

Species of the genus *Pseudomonas* are often classified in biosafety level 2, with the notorious *Pseudomonas aeruginosa* as archetypical pathogenic species. However, other non-pathogenic environmental isolates of *Pseudomonas* species include exceptions to the S2 classification. These exceptions include *Pseudomonas putida* KT2440, a descendant of *P. putida* mt-2 lacking the pWW0 plasmid (Bagdasarian et al., 1981) and solvent-tolerant *Pseudomonas* spp. VLB120, also known as *P. taiwanensis* VLB120 (Panke et al., 1998). *P. putida* KT2440 is classified as HV1 by the US Food and Drug Regulation Administration (FDA). This refers to a host-vector level of 1 describing its safe use in laboratory environments and not an implementation in food products such as the GRAS-status (Generally Regarded as Safe) (Kampers et al., 2019). *P. taiwanensis* VLB120 is natively capable to utilize xylose and can tolerate second phase of organic solvents (Köhler et al., 2015), making it applicable for various processes due to the broader substrate spectrum and robustness. The legal status as S1 organism and metabolic capabilities make certain strains of pseudomonads, and especially *P. taiwanensis* VLB120, suitable hosts for biotechnological processes. Their use for the biosynthesis of various products including heterologous secondary metabolites has already been proven and will be summarized in the following section.

The following section 1.4.1 was written by me as a contribution to the review article "Pseudomonas as Versatile Aromatics Cell Factory" from Tobias Schwanemann, Maike Otto, Nick Wierckx, and Benedikt Wynands (2020), which is also indicated in the Publications section of this thesis.*

1.4.1. Use of *Pseudomonas* for (aromatic) secondary metabolites synthesis

Besides rather simple aromatic commodity and bulk chemicals, the synthesis of high-value aromatic fine chemicals is an expanding field (Mark et al., 2019; Shrestha et al., 2019; Trantas et al., 2015). Pseudomonads are used as natural and heterologous secondary metabolite producers (H. Gross & Loper, 2009; Loeschcke & Thies, 2015, 2020) and are treasure troves of enzymes involved in their biosynthesis (Masuo et al., 2016; Shahid et al., 2018). Multiple gene clusters, coding for non-ribosomal peptide synthase (NRPS) or polyketide synthase (PKS) pathways reveal versatility for mining of new promising molecules (Blin et al., 2019) like dialkylresorcinols, carotinoids, acyl-polyenes (Schöner et al., 2016) and many more. Aromatic fine chemicals can derive from the shikimate pathway exclusively

by condensations of respective aromatic precursors (e.g. phenazines), degradation or conversion of intermediates (e.g. pyrrolnitrin) or by incorporation with other precursors by NRPS (e.g. pyoverdines/siderophores, pyoluteorin). Alternatively, they can be formed by PKS, which catalyze a ring closure after condensation of acyl-extender units by Claisen- or aldol condensation (e.g., phloroglucinol, chalcones, stilbenes) (P. V. van Summeren-Wesenhagen & Marienhagen, 2013). Thus, the formation of aromatics can be completely independent from the shikimate pathway, although the enzymes responsible are considered to be slower and more cumbersome.

1.4.1.1. Non-polyketide aromatic secondary metabolites

Pseudomonas spp. produce about 100 different phenazines from chorismate as a central metabolic intermediate (Bilal et al., 2017). Many of these have antibiotic properties (X. J. Jin et al., 2016), but they can also function as redox mediators that enable interaction with electrodes for a reduced oxygen demand (Bosire & Rosenbaum, 2017; Schmitz et al., 2015). Phenazines production is regulated in a complex, quorum sensing-dependent manner (Bilal et al., 2017; S. Sun et al., 2016). Heterologous biosynthesis in *P. putida* KT2440 is highly dependent on the origin of the respective synthesis operon (Askitosari et al., 2019). The highest titer with a rationally engineered natural producer for phenazine-1-carboxylic acid was achieved with *P. aeruginosa* PA1201 by elevating DAHP synthases expression, promoter exchange of two phenazine clusters and the transporter MexGHI, and by blocking 21 competing secondary metabolite clusters and limiting essential chorismate-consuming reactions. The resulting rationally engineered strain produced up to 9.9 g L^{-1} phenazine-1-carboxylate in a fed-batch fermentation (K. Jin et al., 2015). In contrast, strain *P. chlororaphis* P3 obtained by mutagenesis and screening of *P. chlororaphis* HT66 reached a titer of 1.7 g L^{-1} phenazine-1-carboxamide (X. J. Jin et al., 2016). Further optimization of the culture conditions enabled production of 9.2 g L^{-1} phenazine-1-carboxamide with *P. chlororaphis* P3 Δ*lon* in shake flasks (Peng et al., 2018). Disrupting the phenazine pathway enabled the synthesis of 1.2 g L^{-1} 2-acetamidophenol in *P. chlororaphis* P3 Δ*phzB* due to a native arylamine N-acetyltransferase (S. Guo et al., 2020). The hydroquinone glycoside arbutin is frequently produced by cell-free enzymatic conversion or in biotransformation processes (Zhu et al., 2018). The ability to perform glycosylation is a major advantage of eukaryotic hosts compared to prokaryotic hosts. Nevertheless, functional glycosylation for the synthesis of plant-derived metabolites by *P. chlororaphis* P3 was accomplished for arbutin. The respective genes of the pathway, starting from supplemented 4-hydroxybenzoate, were expressed including a glycosidase from the native promoter P_{phz} (S. Wang et al., 2018).

Violacein is a vesicle-secreted antibiotic from various Gram-negative bacteria like *Chromobacterium violaceum*. It is a violet bisindole derived from tryptophan (S. Y. Choi et al., 2020) and has been

synthesized by *P. putida* strains by inserting the 7.4 kb operon from *C. violaceum* into random genomic loci by the yTREX system reaching up to 105 mg L^{-1} (Domröse et al., 2017). Pyrrolnitrin, another compound derived from tryptophan but natively occurring in *Pseudomonas* species, is an agricultural fungicide (H. Gross & Loper, 2009; Kilani & Fillinger, 2016; Mishra & Arora, 2018). Production strains were traditionally generated by screening for analogue-resistant mutants (Elander et al., 1971). Pyrrolnitrin is produced by various species with co-occurring ability of phloroglucinol biosynthesis (Mavrodi et al., 2001) at various concentrations depending on the applied low cost fermentation substrate (Pawar et al., 2019).

Pseudomonads contain innate NRPS for the formation of siderophores, like pyoverdines and azotobactin (Scholz et al., 2018). Pyoverdines are made in the cytoplasm in response to iron-limiting conditions (Ringel & Brüser, 2018). The formation of functional NRPS require the activation of an acyl carrier protein and peptidyl carrier protein domain by phosphopantetheinyl transferase (PPTase) which in case of *P. putida* KT2440 has a broad substrate spectrum. It thus allows activation without additional heterologous PPTase expression in contrast to other prokaryotes (F. Gross et al., 2005; Owen et al., 2011). This allows functional expression of large NRPS of foreign origin (Gemperlein et al., 2016; F. Gross, Ring, et al., 2006), enabling the production of, among others, 150 mg L^{-1} prodigiosin (Domröse et al., 2017), about 3 mg L^{-1} docosahexaenoic acid (Gemperlein et al., 2016) and 0.6 mg L^{-1} myxothiazol A (F. Gross, Ring, et al., 2006).

1.4.1.2. Aromatic polyketides

There are also shikimate-independent sources of aromatic secondary metabolites like resorcinols and polyketides. Pyoluteorin is a native chlorinated antibiotic with comparable ring-formation like 2,5-dialkylresorcinol deriving from a NRPS/PKS hybrid pathway (Nowak-Thompson et al., 1999, 2003). Significant improvement concerning pyoluteorin production was achieved by deleting transcriptional and translational repressors, Lon protease and regulatory sequences, as well as overexpression of the respective transport operon (H. Shi et al., 2019).

Phloroglucinol, and its derivatives monoacetylphloroglucinol and 2,4-diacetylphloroglucinol (DAPG) are naturally occurring polyketides from diverse *Pseudomonas* spp. (Qing Yan et al., 2017; F. Yang & Cao, 2012). Their application as precursor of rocket fuels (Meyer et al., 2019) and as an antibiotic raised early attention (Birch & Donovan, 1953). PhlD is a bacterial type III PKS, catalyzing the condensation of three malonyl-CoA to phloroglucinol (Bangera & Thomashow, 1999). PhlACB is an acetyltransferase, able to form C-C bonds on aromatics (Pavkov-Keller et al., 2019) and PhlE is an exporter (Abbas et al., 2004). Nakata et al. (1999) produced about 1.2 g L^{-1} DAPG with the natural producer *P. fluorescens* S272 after stress induction with a heat shock. Previously the use of ethanol as carbon source, high C/N

ratios or applying high salt concentrations also increased titers (Yuan et al., 1998). PhlD from *P. fluorescens* Pf-5 was engineered for higher turnover numbers and decreased K_M (Zha et al., 2008), as well as for higher thermostability to facilitate its use in different microorganisms (Rao et al., 2013). Promising variants are $PhlD^{Y256R,A289R}$, $PhlD^{23D9}$ and $PhlD^{M21T,L54V,A82T,A181S}$ with improved properties, as well as PaP79 from Meyer et al. (2019).

Flaviolin (2,5,7-trihydroxy-1,4-naphthoquinone) is a red compound derived from 1,3,6,8-tetrahydroxynaphthalene, a polyketide made from five malonyl-CoA by a type III PKS of bacterial origin (RppA from *Streptomyces* spp., SoceCHS1 from *Sorangium* sp.) (Ueda et al., 1995). It has been used to determine the malonyl-CoA availability in a heterologous host to assess the potential for polyketide synthesis (Incha et al., 2020; D. Yang et al., 2018). In early attempts to produce flaviolin in Pseudomonads, ~6 mg L^{-1} were achieved in *P. putida* KT2440 (F. Gross, Luniak, et al., 2006). In recent attempts, testing RppA variants and different concentrations of supplemented glucose to complex medium, 65 mg L^{-1} were produced with a truncated enzyme variant (Incha et al., 2020). D. Yang et al. (2018) produced 44.7 mg L^{-1} while addition of up to 100 µM cerulenin roughly doubled the titer in a dose-dependent manner.

Plant-derived polyketides can also partly be derived from an aromatic CoA-ester like cinnamoyl-CoA, benzoyl-CoA, or 4-coumaroyl-CoA as starter unit in combination with acyl-CoA extenders, which form a second phenyl group (Chouhan et al., 2017; Morita et al., 2019; Pandith et al., 2020). Synthesis of the plant metabolite bisdemethoxycurcumin (~2 mg L^{-1}) was achieved by combining an incomplete natural phenylpropanoid degradation pathway with a heterologously expressed curcuminoid synthase (Incha et al., 2020). Examples of chalcone or stilbene synthesis with *Pseudomonas* spp. as heterologous host are lacking thus far. However, export of polyphenols like naringenin and other compounds by RND-type efflux pump TtgABC from *P. putida* DOT-T1E, has been identified (Terán et al., 2006) indicating an interesting potential for this class of compounds. Moreover, malonyl-CoA precursor supply was increased by deletion of *fabF* in *P. denitrificans* (Zhou et al., 2020). The previously mentioned *Pseudomonas* strains that efficiently synthesize precursors like *trans*-cinnamate (Otto et al., 2019) and benzoate (Otto et al., 2020), would make ideal chassis for such polyketides.

1.5. Two-phase cultivations - Vision of a transferable modular production process

To design an economically viable bioprocess for polyketide production, it is essential to bring the aspects of the product of interest and suitable production host into a broader scope. Such a process must be competitive to the isolation of polyketides from natural resources (Abubakar & Haque, 2020; Alara et al., 2021; Uwineza & Waśkiewicz, 2020) and chemical synthesis. Chemical synthesis (Orsini et

al., 1997) and isolation from natural resources (Alara et al., 2021) may go in hand with environmental pollution and exploitation of specific species if rare substances are the goal.

Biotechnological production processes can range from million tons per year scale for some products like lysine (Jie Liu et al., 2022), glutamate (Kumar et al., 2014), and ethanol, to rather small production volumes with high-value products in the medical sector like the factor VIII production (G. Ling & Tuddenham, 2020; Mannully et al., 2018). The cost for the development of a production process must be justified by its economic parameters profit margin, yield, and sales value. High costs for an extensive process development may only be justified for low-volume and high-value products because small improvements in the yield will result in a large added economic value. On the other hand, for high-volume and low-value products, a costly process development may not be economically feasible. Products with intermediate margins like enzymes are usually produced by similar upstream fermentations and an altered subsequent downstream purification according to the enzyme's properties and required purity. In these production processes a few established microbial hosts are equipped with the respective coding sequence of the gene of interest in a standard expression system like orthogonal T7 promoter-driven pET expression vector systems (Miroux & Walker, 1996) or methanol-inducible yeast promoters (Karbalaei et al., 2020). Intensification of individual production conditions affects either the fermentation or downstream steps for the individual proteins of interest (Asani et al., 2023; Baradia et al., 2023; Da et al., 2018).

To produce secondary metabolites as specialty chemicals, intensive development of the upstream process would be required, despite small quantity demands. Such products are either made by very different species, which might be challenging in handling, or require intensive metabolic engineering of established biotechnological hosts to produce a single product of interest. Polyketides, with their modular biosynthesis, represent an exception. Here, the exchange of a single gene can result in a different product, using the same cellular resources. Hence, the development of new production strains for new products can be fast. However, low product concentrations, product toxicity, or product instability may hinder commercial production. Despite the molecular differences and diversity of natural polyketides, many of them accumulate in biological membranes due to their similar hydrophobicity (Schönsee & Bucheli, 2020). This property has naturally a toxic effect on the host, but can also be used for product purification by applying a second organic phase layer during the production cultivation (Tharmasothirajan et al., 2021).

All in all, the modularity of the products of interest with shared biophysical properties and the resulting fast generation of new production strains allow the use of an integrated strain and process design with ISPR by organic solvents (Pedraza de la Cuesta et al., 2019). In principle, the idea follows a holistic "Plug&Play" concept like in computing (both on software level, like DNA, and hardware level, like

strains). Similar to generic enzyme production fermentations, a reproducible fermentation setup is used. An additional water-immiscible layer is added to the cultivation broth which extracts the product during microbial production and consequently integrates the first purification step within the upstream process as outlines in the manuscript section of this thesis (Figure 1-6) (Hermann J. Heipieper et al., 2007). Subsequently, only a smaller volume containing the product must be treated during the downstream process (DSP). Due to the comparable extraction properties of many polyketides (Alara et al., 2021), this represents a modular and transferable production approach.

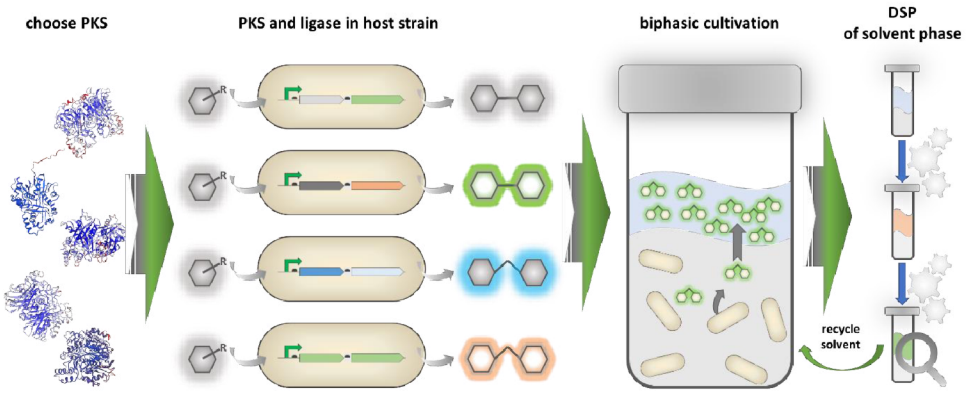

Figure 1-6 Process concept for modular production of PKS products by biphasic/two-phase fermentation.
First, a functional PKS is chosen for the product of interest. Then, the coding sequences of the PKS and an appropriate CoA-ligase, if required, are implemented into a broadly applicable host strain. The selected production strain is cultivated in the presence of a solvent for ISPR. The solvent is subsequently separated and used in the purification steps toward the pure product. Abbreviations: polyketide synthase, PKS; downstream process, DSP.

The choice of solvent and host are economically crucial; plus, to establish a sustainable process, the recyclable solvent should originate from non-fossil resources. In addition to the transferable process design, the choice of solvent can lead to a (semi-) auto-sterile cultivation if a solvent is exclusively tolerated by highly specialized species. To have a broad degree of freedom regarding the choice of solvent, the use of solvent-tolerant species like Pseudomonads is an advantage. They are established for aromatics production and demonstrated proof of principles for ISPR multiple times (Schwanemann et al., 2020). To demonstrate the principle, cultivation in shaken cultures represents a reasonable basis for following developments towards a transferable polyketide production process by pseudomonads.

The following section 1.5.1 was written by me as a contribution to the review article "Pseudomonas as Versatile Aromatics Cell Factory" from Tobias Schwanemann, Maike Otto, Nick Wierckx, and Benedikt Wynands (2020), which is also indicated in the Publications section of this thesis.*

1.5.1. Aromatics production with Pseudomonas in solvent two-phase fermentations: featured and empowered by solvent-tolerance

1.5.1.1. *Solvent tolerance and toxicity*

One unique feature of certain *Pseudomonas* spp. is their solvent tolerance. The mechanisms of solvent tolerance have been extensively reviewed (H. J. Heipieper & Martínez, 2010; Ramos et al., 2015), as has the potential of solvent tolerance in biotransformation (De Bont, 1998; Hermann J. Heipieper et al., 2007; Kusumawardhani et al., 2018; Ramos et al., 2015; Sardessai & Bhosle, 2004). The main determining factors of solvent tolerance is extrusion of the toxic solvent by diverse energy-dependent efflux pumps (Kieboom & de Bont, 1998; Rojas et al., 2001). The extrusion mediated by resistance-nodulation-division (RND) family transporters is driven by the proton motive force. Energy requirements of this and other tolerance mechanisms are provided by an increased catabolic capacity including an increased substrate uptake rate and elevated TCA cycle flux with a simultaneously reduced biomass formation according to the "driven by demand" concept in response to solvent stress (Blank et al., 2008; Isken et al., 1999; Molina-Santiago et al., 2017). Other stress response genes are induced for protein refolding and scavenging of reactive oxygen species (Domínguez-Cuevas et al., 2006). Additionally, *cis-trans*-isomerization of lipids in the cell membrane by Cti increases the membrane rigidity to counteract its destabilization caused by the accumulation of solvent in the membrane. This short-term mechanism is supported by an increased embedment of *de novo*-synthesized saturated fatty acids into the phospholipid bilayer as a longer-term response (Hermann J. Heipieper et al., 1995).

The application of biphasic liquid-liquid fermentations with a hydrophobic 2nd phase serving as extractant integrates downstream processing into the production process (Hermann J. Heipieper et al., 2007). The use of solvent-tolerant strains offers a wider degree of freedom regarding the application of suitable solvents with desired product extraction qualities and phase separation characteristics to simplify product recovery and purification. Such systems provide *in situ* extraction of toxic products to reach high product concentrations, and they can also contain a reservoir of toxic substrate, negating the need for complex fed-batch strategies. The latter strategy is applied in several studies with *Pseudomonas* spp. in production processes of aromatic compounds […]. Besides classical organic solvents, ionic liquids can also be used for *in situ* recovery of aromatics (Van Den Berg et al., 2008), although their high price is often a major hurdle. The specific selection of solvents for their intended application (Sprakel & Schuur, 2019) or the use of solvents in pertraction processes with membranes are used (Heerema, Roelands, et al., 2011; Leonie E. Hüsken et al., 2002). The determination of a suitable biocompatible solvent is a major task for the application of two-phase

bioconversions and -transformations (Dafoe & Daugulis, 2014; Grundtvig et al., 2018). Here, we focus on hydrophobic, highly toxic products and substrates in bioconversion and biotransformation using whole cells of *Pseudomonas* in combination with organic solvents.

The choice of organic solvent and microbial host is a decisive for the overall production process (Priebe & Daugulis, 2018). The range of biocompatible solvents strongly depends on the selected host organism. Many organic solvents are toxic to cells due to their solubility in cell membranes. There, they change membrane fluidity (Neumann et al., 2006), lead to permeabilization or swelling, and affect membrane proteins (H. J. Heipieper & Martínez, 2010). The $logP_{O/W}$, the logarithmic partitioning coefficient of water and octanol, is used as a reference for the hydrophobicity of a solvent (Laane et al., 1987). It is also directly correlated to the partitioning of a solvent between a buffer solution and biological membranes ($logP_{M/B}$) by an equation from Sikkema et al. (1994).

$$logP_{M/B} = 0.97 \times logP_{O/W} - 0.64$$

Because of this, the physical parameter $logP_{O/W}$ allows estimation of the level of toxicity of a solvent (H. J. Heipieper & Martínez, 2010). Values of $logP_{O/W}$ between 1 and 4 are generally considered as toxic for microorganisms (D. Liu et al., 1982) since they exceed a critical concentration in membranes in the range of 400 mM (Neumann et al., 2005). The determination of the maximum membrane concentration (MMC), which considers $logP_{M/B}$ and solubility of compound in the aqueous phase (S_{aq}), is an accurate predictor of solvent cytotoxicity (De Bont, 1998; H. J. Heipieper & Martínez, 2010; Neumann et al., 2005).

$$MMC = S_{aq} \times 10^{logP_{M/B}}$$

Besides MMC the determination of a respective $logP_{crit}$ for various strains and solvents also offers a rational base for the selection of a suitable microbial host-solvent system (Inoue & Horikoshi, 1989; Prpich & Daugulis, 2006; Vrionis et al., 2002). Despite the use of monomeric solvents it is likely that this is also valid for low molecular weight polymers (Harris & Daugulis, 2015).

1.5.1.2. *Process design of biphasic fermentations: Issues to be considered*

Although biphasic fermentations can provide several advantages, the use of solvents or the production of such also comes with specific process-oriented considerations. Particular attention regarding safety requirements in aerated fermentation processes may be needed due to flammability and risk of explosion. Multiple tools simplify the selection of adequate and safe extraction solvents although they are intended mainly for purification processes rather than *in situ* product recovery in highly aerated biological processes (Piccione et al., 2019). The oxygen mass transfer coefficient (k_La) is positively influenced by a hydrophobic phase, allowing facilitated oxygen supply for aerobic processes (Amaral

et al., 2007). Solvents with low vapor pressure, auto-ignition temperature, and boiling temperature are recommended and processes with elevated pressure, low temperatures, and small amounts of solvent and oxygen concentration outside of the explosive range are desirable. Octane for instance, should be applicable when the fermentation process is run at 30°C and at least 4.9 bar (A. Schmid et al., 1999) which is possible in high-pressure, explosion-proof bioreactors (Andrew Schmid et al., 1998). The reduction of flammability and explosion is in contradiction to elevated risks from a pressurized process which has different safety concerns and effects on the biological system (Follonier et al., 2012), requiring special equipment depending on the applied solvent and process parameters. Other advantages of pressurized fermentations are increased biomass formation due to elevated oxygen solubility (Knoll et al., 2005, 2007). However, considerations about health concerns, corrosion of the equipment due to the applied chemicals and waste disposal should be made. Subsequent downstream processes rely on centrifugal separation, de-emulsifiers, temperature shifts or catastrophic phase inversion (Glonke et al., 2016). Lastly, care should also be taken that the applied extractant is not inadvertently degraded by *Pseudomonas* (N. J. P. Wierckx et al., 2005), as solvent losses have a major impact on process economy and environmental impact.

The following section 1.5.2 was written by me as a contribution to the review article "Pseudomonas as Versatile Aromatics Cell Factory" from Tobias Schwanemann, Maike Otto, Nick Wierckx, and Benedikt Wynands (2020), which is also indicated in the Publications section of this thesis.*

1.5.2. Biphasic fermentation processes with *Pseudomonas*

Biphasic reaction systems with organic solvents are often described as an option to facilitate the degradation of toxic water-insoluble xenobiotics (Daugulis, 2001; Déziel et al., 1999; Janikowski et al., 2002; Quijano et al., 2009) like α-pinene by *Pseudomonas fluorescens* NCIMB 11671 (Muñoz et al., 2008), benzene, toluene, 1,4-xylene degradation by *Pseudomonas* sp. ATCC 55595 (Collins & Daugulis, 1999) or phenol by *P. putida* ATCC 11172 (Collins & Daugulis, 1997). Pseudomonads have been applied in two-phase fermentations production processes for decades, ever since Schwartz & McCoy (1977) performed transformations with *P. oleovorans* in presence of cyclohexane. The use of linear alkanes as 2nd phase and substrate for production of the respective oxidation products was applied regularly (M. J. de Smet et al., 1981; Marie Jose de Smet et al., 1983) and was assessed for its economic potential 30 years ago (Witholt et al., 1990).

In the context of aromatics, the oxidation of styrene to (*S*)-styrene oxide with *Pseudomonas* has also been an ongoing research field ever since the 1990's. During this time, the discovery of *P. putida* S12 growing on styrene in a styrene-water system was made (Weber et al., 1993), and usage of styrene degradation genes from e.g. *P. taiwanensis* VLB120 in traditional hosts (Panke et al., 1998; Panke,

Meyer, et al., 1999; Wubbolts et al., 1994) has shifted towards the direct application of the solvent-tolerant Pseudomonads themselves (Table 2). *P. putida* KT2440 carrying a xylene monooxygenase was successfully incubated over 350 h, corresponding to 100 generations, in presence of a mixture of alkanes in a 2nd phase (Panke, De Lorenzo, et al., 1999). Bae et al. (2006) used the styrene degrader *P. putida* SN1 with a disrupted degradation pathway for the oxidation of styrene to (*S*)-styrene oxide for enantiopure biotransformation without the native expression of the styrene monooxygenase being rate-limiting. While a constitutive solvent-tolerant *P. taiwanensis* VLB120 as a host outperformed a heterologous *E. coli* host overexpressing the styrene monooxygenase genes, oxidation is limited by the applicable styrene concentration in the organic phase of bis(2-ethylhexyl)phthalate (BEHP) (J.-B. Park et al., 2007). The influence of the solvent on maintenance and NADPH availability for redox catalysis with whole cells was elucidated in *P. putida* DOT-T1E (Blank et al., 2008). The construction of a constitutive solvent-tolerant strain of *P. taiwanensis* VLB120 (Volmer et al., 2014) and subsequent reduction of required organic solvent (Volmer et al., 2017) yielded an oxidation process with moderate specific activity and volumetric productivity with simultaneously reducing the environmental impact. Analysis of the respective substrate kinetics revealed that excess of glucose results in increased specific activity of the oxidation up to 180 U g_{CDW}^{-1} (Volmer et al., 2019).

Another frequently applied oxidation process is the transformation of toluene to 3-methylcatechol with operon *todC1C2BAD* encoding toluene dioxygenase and *cis*-toluene dihydrodiol dehydrogenase from *P. putida* F1 or DOT-T1E. Wery et al. (2000) introduced the operon into *P. putida* S12 and revealed a reverse correlation between the concentration of added toluene and the 3-methylcatechol yield. Here, the second organic phase had an additional beneficial effect of preventing polymerization of 3-methylcatechol to a brownish precipitate, thereby avoiding a loss of product. Strain improvement of *P. putida* F1 to mutant F107 and subsequent chromosomal multicopy insertion of *todC1C2BAD* enabled a 3-methylcatechol titer of 14 mM with a rate of 105 µmol min^{-1} g_{CDW}^{-1} in strain MC2 without requiring supplementation of antibiotics (L. E. Hüsken et al., 2001). Application of a 2nd phase of octanol elevated the titer further to 25 mM, with the ratio of the liquids plays an important role (Leonie E. Hüsken et al., 2001). Keeping the organic phase separate of the fermentation broth appeared beneficial under the selected conditions (Leonie E. Hüsken et al., 2002). An important step towards the rational design of fermentations with *Pseudomonas* in biphasic partitioning bioreactors was demonstrated by Prpich & Daugulis (2006), who initially determined $logP_{crit}$ of the respective host MC2 and the partitioning coefficient K of 3-methylcatechol with a respective library of solvents. Based on these evaluations a selection of an organic solvent increased the volumetric productivity of 3-methylcatechol by about four-fold to 440 mg L^{-1} h^{-1} and reduced substrate loss of toluene by about four-fold as well. The overall maximal product titer of 5.5 g L^{-1} was limited by applicable volume and capacity of the solvent (the partitioning coefficient), which is better for aliphatic alcohols (Prpich & Daugulis, 2006). Usage of 1,3-

xylene by an incomplete degradation pathway in *P. putida* DOT-T1E offers on opportunity to yield different alkylcatechols. Due to the fact that 3 mM 3-methylcatechol fully inhibited growth, cultivation with 50% (v/v) octanol or decanol was performed and allowed the biosynthesis of 17 mM (2.6 g L^{-1}) or 70 mM (10.7 g L^{-1}), respectively (Rojas et al., 2004). Octanol had a five-fold higher negative impact on cell viability of the applied strain than decanol, explaining the higher overall titer despite a putative smaller partitioning coefficient (Rojas et al., 2004). The *tod* operon of *P. putida* T-57 is controlled by catabolite repression in the presence of glucose. Co-substrates like butanol as an alternative carbon source allowed toluene transformation under non-repressive conditions reaching titers of up to 107 mM 3-methylcatechol in the oleyl alcohol phase (Faizal et al., 2007). Similar strategies to circumvent product toxicities and reach higher titers were applied to multiple other production processes […] of aromatics like *o*-cresol (Faizal et al., 2005), 4-hydroxybenzoate (Ramos-González et al., 2003), 1-naphtol (Janardhan Garikipati & Peeples, 2015) and aliphatic products.

Most examples of biphasic fermentations are whole-cell biotransformations, consisting of one or two enzymatic steps, often relying on cellular metabolism to regenerate redox cofactors. This is mainly because in many cases the substrate is (also) hydrophobic, and the 2nd phase acts as a substrate reservoir which keeps the aqueous concentrations below toxic levels. The application of *de novo* biosynthesis of aromatics in combination with an organic phase is relatively rare. One example was the abovementioned bio-based production of phenol with *P. putida* S12TPL3. Octanol was used as a 2nd phase to extract phenol from the fermentation broth, almost doubling the phenol titer to 9.20 mM compared to 5.01 mM in a monophasic fermentation (N. J. P. Wierckx et al., 2005). The strain was also used with solvent-impregnated resins (Van Den Berg et al., 2008), aqueous poloxamer solutions (Heerema et al., 2010) and membrane separation (Heerema, Roelands, et al., 2011; Heerema, Wierckx, et al., 2011) for phenol recovery. Application of decanol as 2nd phase in a 4-vinylphenol producing derivative of this strain reduced the effect of product toxicity, elevating the titer to 21 mM and doubling volumetric productivity (Verhoef et al., 2009). It should be noted that these totals concentrations are calculated for the combined liquid volumes of water and extractant, and that the concentrations in the organic phase reached much higher values of 58 mM phenol (N. J. P. Wierckx et al., 2005) and 147 mM 4-vinylphenol (Verhoef et al., 2009).

An economic evaluation of a continuous *in situ* pertraction process for phenol production using a *Pseudomonas* resulted in costs of 18 € kg^{-1}, which is at least 20-fold higher than those of the chemical process, with the pertraction unit being the major cost-driving factor which is highly dependent on the mass transfer and thus on the selected extractant (Heerema, Roelands, et al., 2011). An integrated pertraction also requires large distillation columns and a high energy input for solvent regeneration due to constantly low product concentrations. A non-integrated in-stream product recovery approach from a fed-batch cultivation resulted in three-fold increased costs (~57 € kg^{-1}) mainly due to higher

investment costs of the larger reactor due to lower space-time yield, highlighting the advantage of *in situ* product removal (Heerema, Roelands, et al., 2011). Beside the opportunity for different sales strategies to obtain higher prices for products of biological origin, it should be noted that products of higher value or the upcycling of waste streams could potentially enable a profitable bio-based process at lower productivities.

1.6. Aim, significance and outline of this thesis

In this thesis, a combination of metabolic engineering, investigation of physio-chemical properties of polyketides and ISPR in solvent two-phase cultivation is used for the heterologous production of different polyketides. *Pseudomonas taiwanensis* VLB120 serves as a host for the heterologous synthesis of pinosylvin, resveratrol, flaviolin, 2,4,6-trihydroxybenzophenone, 2,3',4,6-tetrahydroxybenzophenone, 3,5-dihydroxybiphenyl, and 4-hydroxycoumarin. All these products are made by transformation of supplemented precursors as well as *de novo* from glucose in a minimal medium. Additionally, the production of phenylpropanoids and fluoro-phenylpropanoids was achieved by a revealed overlapping activity of native metabolism and implemented production genes. The principal objective of this thesis is the establishment of *P. taiwanensis* VLB120 as a biotechnological host for polyketide formation. The presented approach demonstrates an alternative to laborious conventional polyketide production and established heterologous biotechnological production. Additionally, this work reveals new opportunities for future process designs, new products, and it improves the understanding of Pseudomonads' physiology and metabolism of malonyl-CoA.

In the first manuscript genome-reduced and phenylalanine production strains of *P. taiwanensis* VLB120 are extensively engineered to increase the intracellular malonyl-CoA availability for increased product formation. Availability of malonyl-CoA is deduced from pinosylvin, flaviolin and resveratrol titers. Species-specific variations and genes in fatty acid biosynthesis are proposed. Thus, that work possess the first malonyl-CoA platform strain and provided a first insight on Pseudomonads complex intertwined CoA metabolism what is essentially required for *Pseudomonas'* establishment as host for secondary metabolites.

Adapting a biotechnological host to artificial biotechnological production conditions provides valuable insights to increase the titer, rate and yield of productions. To further increase the productivity of the malonyl-CoA platform strains, a passive glucose transporter is tested in various platform strains to reduce energy demand associated with substrate uptake by an ABC-type importer in the second manuscript. The heterologous passive transporter is either additionally implemented or the native glucose transporter is replaced. The conversion yields for resveratrol from *p*-coumarate and cinnamate

production are investigated with considerations of biomass-altering effects. Therefore, this can serve as a blueprint for other production approaches using Pseudomonads as host and glucose as substrate.

In the pursuit of synthesizing polyketides from benzoate derivatives, the experimental determination of molecular properties of 2,4,6-trihydroxybenzophenone towards the accumulation in bacterial membranes and extraction properties are investigated. Experimental evidence for unexpected by-product formation by the host's ability to convert intermediates with its native metabolism and product instabilities led subsequently to two-phase cultivations that allowed ISPR and pure *de novo* synthesis of PKS III products. This work introduces several PKS III products that were not produced in heterologous hosts so far; it thus serves as an initial benchmark and paves the way for further engineering and production approaches towards industrial production processes of polyketides.

Finally, the results are mutually discussed and further considerations regarding strain and cultivation developments are presented while the achievements are placed into a broader context to elucidate future perspectives.

2. Publications and manuscripts

Contributions of the authors to the respective manuscripts were described using the 'Contributor Roles Taxonomy (CRediT) (Allen et al., 2019).

Term	Definition
Conceptualization	Ideas; formulation or evolution of overarching research goals and aims
Methodology	Development or design of methodology; creation of models
Software	Programming, software development; designing computer programs; implementation of the computer code and supporting algorithms; testing of existing code components
Validation	Verification, whether as a part of the activity or separate, of the overall replication/ reproducibility of results/experiments and other research outputs
Formal analysis	Application of statistical, mathematical, computational, or other formal techniques to analyze or synthesize study data
Investigation	Conducting a research and investigation process, specifically performing the experiments, or data/evidence collection
Resources	Provision of study materials, reagents, materials, patients, laboratory samples, animals, instrumentation, computing resources, or other analysis tools
Data Curation	Management activities to annotate (produce metadata), scrub data and maintain research data (including software code, where it is necessary for interpreting the data itself) for initial use and later reuse
Writing - Original Draft	Preparation, creation and/or presentation of the published work, specifically writing the initial draft (including substantive translation)
Writing - Review & Editing	Preparation, creation and/or presentation of the published work by those from the original research group, specifically critical review, commentary or revision – including pre-or postpublication stages
Visualization	Preparation, creation and/or presentation of the published work, specifically visualization/ data presentation
Supervision	Oversight and leadership responsibility for the research activity planning and execution, including mentorship external to the core team
Project administration	Management and coordination responsibility for the research activity planning and execution
Funding acquisition	Acquisition of the financial support for the project leading to this publication

2.1. A *Pseudomonas taiwanensis* malonyl-CoA platform strain for polyketide synthesis

Published as:

Schwanemann, T., Otto, M., Wynands, B., Marienhagen, J., & Wierckx, N. (2023). A *Pseudomonas taiwanensis* malonyl-CoA platform strain for polyketide synthesis. *Metabolic Engineering*, *77*(February), 219–230. https://doi.org/10.1016/j.ymben.2023.04.001

CRediT authorship contribution statement

Tobias Schwanemann: Conceptualization, Methodology, Validation, Formal analysis, Investigation, Writing - Original Draft, Visualization, Funding acquisition

Maike Otto: Methodology, Formal analysis, Investigation

Benedikt Wynands: Validation, Writing - Review & Editing, Supervision

Jan Marienhagen: Resources, Writing - Review & Editing, Supervision

Nick Wierckx: Conceptualization, Validation, Resources, Writing - Review & Editing, Supervision, Funding acquisition, Project administration

Overall contribution: 80%

The presented experimental work was conducted by TS and partly by MO. Validation was done by MO, BW and NW. Visualization of all data was performed by TS. The writing of the original draft was mainly done by TS, which was reviewed and edited by BW, JM and NW. Funding for the project was acquired by TS and NW.

Tobias Schwanemann[a], Maike Otto[a], Benedikt Wynands[a], Jan Marienhagen[a,b] and Nick Wierckx[a‡]

[a] Institute of Bio- and Geosciences, IBG-1: Biotechnology, Forschungszentrum Jülich GmbH, 52425 Jülich, Germany
[b] Institute of Biotechnology, RWTH Aachen University, Worringer Weg 3, D-52074 Aachen, Germany

‡ corresponding author:

Nick Wierckx, Institute of Bio- and Geosciences, IBG-1: Biotechnology, Forschungszentrum Jülich, Wilhelm-Johnen-Straße, 52425 Jülich, Germany. e-mail: n.wierckx@fz-juelich.de

Abstract

Malonyl-CoA is a central precursor for biosynthesis of a wide range of complex secondary metabolites, in native fatty acid biosynthesis and thus of its products. The development of platform strains with increased malonyl-CoA supply can contribute to the efficient production of secondary metabolites, especially if such strains exhibit high tolerance towards these chemicals. In this study, *Pseudomonas taiwanensis* VLB120 was engineered for increased malonyl-CoA availability to produce bacterial and plant-derived polyketides. A multi-target metabolic engineering strategy focusing on decreasing the malonyl-CoA drain and increasing malonyl-CoA precursor availability, led to an increased production of various malonyl-CoA-derived products, including pinosylvin, resveratrol and flaviolin. The production of flaviolin, a molecule deriving from five malonyl-CoA molecules, was doubled compared to the parental strain by this malonyl-CoA increasing strategy. Additionally, the engineered platform strain enabled production of up to 84 mg L^{-1} resveratrol from supplemented *p*-coumarate. One key finding of this study was that acetyl-CoA carboxylase overexpression majorly contributed to an increased malonyl-CoA availability for polyketide production in dependence on the used strain-background and whether downstream fatty acid synthesis was impaired, reflecting its complexity in metabolism. Hence, malonyl-CoA availability is primarily determined by competition of the production pathway with downstream fatty acid synthesis, while supply reactions are of secondary importance for compounds that derive directly from malonyl-CoA in *Pseudomonas*.

Keywords: Polyketide; Malonyl-CoA; *Pseudomonas*; Stilbene; Flaviolin; fatty acid biosynthesis

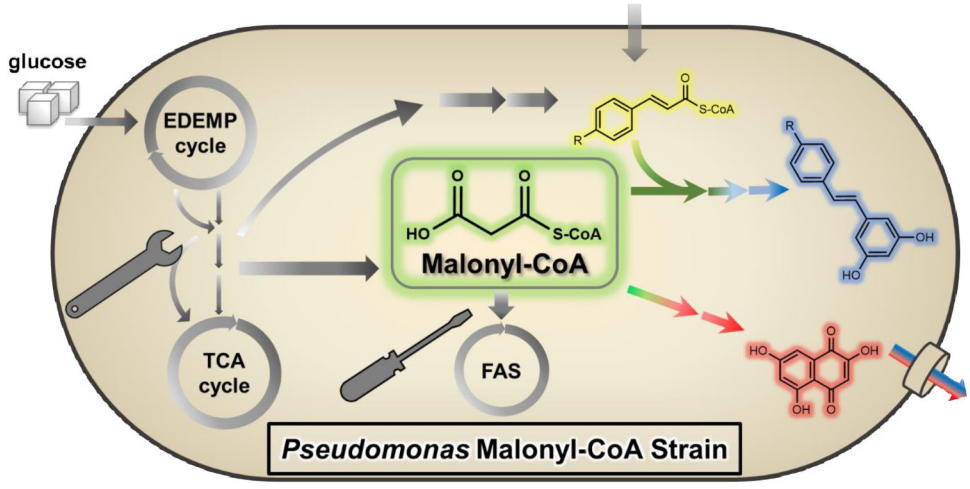

Introduction

Chemical synthesis of plant polyketides is often laborious or unfeasible for very complex products. Currently, the main source of such chemicals are often the natural producers, which accumulate only low amounts of product embedded in a complex biomass matrix. Their production thus requires extensive and costly extraction methods. This can be avoided by the transfer of the natural biosynthesis pathway to industrially established microbial hosts (Braga & Faria, 2022; Wolf et al., 2021; Yang et al., 2020, 2022; Palmer & Alper, 2019), which is often essential for the development of a cost-efficient production process (Liu et al., 2017). Such microbial processes can increase product concentrations, enable better scale-up of production, and facilitate downstream processing (Tharmasothirajan et al., 2021; Jian Wang et al., 2016).

When designing a novel biotechnological production process, it is important to choose a host whose properties best match the expected conditions encountered in the envisioned process applications (Blombach et al., 2022). In this respect, bacteria of the genus *Pseudomonas* are well-known for their resistance towards xenobiotics and solvent tolerance (Bitzenhofer et al., 2021; Ramos et al., 2015). This tolerance is of interest for polyketide products displaying antimicrobial properties. Some Pseudomonads are even natural producers of polyketide antibiotics, such as 2,4-diacetylphloroglucinol (Yang & Cao, 2012) or mupirocin (Gurney & Thomas, 2011). Pseudomonads may also facilitate functional expression of secondary metabolite gene clusters including e.g. polyketide synthases (PKS) and polyketide modifying enzymes from organisms with varying GC-content due to agnostic acceptance of AT-rich regions (Ackermann et al., 2021) whilst having a naturally high GC-content (F. Gross, Luniak, et al., 2006). Additionally they possess a native phosphopantetheinyl transferase with broad substrate spectrum (Beld et al., 2014; Owen et al., 2011). These traits, *inter alia*, make Pseudomonads very suitable hosts for heterologous pathway implementations (Blombach et al., 2022; Loeschcke & Thies, 2015; Nikel & de Lorenzo, 2018). However, *Pseudomonas* is so far rarely used for heterologous polyketide synthesis approaches (Incha et al., 2020). Albeit, they allow fermentation process designs that are not feasible for other organisms such as two-phase cultivations with toxic solvents (e.g. toluene (Ramos-González et al., 2003), decanol, methyl decanoate and more (Demling et al., 2020)) for *in situ* product extraction (Hermann J. Heipieper et al., 2007). Hence, development of a *Pseudomonas* platform for secondary metabolite production, especially polyketides, is highly desirable.

Aromatics production via the shikimate pathway is well established in Pseudomonads and many different molecules derived from aromatic amino acids can be synthesized efficiently such as phenol (Wynands et al., 2018), *trans*-cinnamate (Otto et al., 2019), or *cis*,*cis*-muconate (Kuatsjah et al., 2022; C. Ling et al., 2022) among many more (Schwanemann et al., 2020). Alternatively, aromatics are produced from condensation of coenzyme A (CoA) esters by type III PKS (Bisht et al., 2021; Morita et

al., 2010). High-value polyketides like stilbenoids are synthesized by stilbene synthases (STS) with CoA-bound phenylpropanoids as starter units, which are extended by three malonyl-CoA (also called MaCoA) molecules to form a tetraketide intermediate, followed by a C2→C7 aldol condensation reaction for aromatic ring formation. Pinosylvin (*trans*-3,5-dihydroxystilbene) and resveratrol (*trans*-3,5,4'-trihydroxystilbene) are made from cinnamoyl-CoA or *p*-coumaroyl-CoA as starter molecules, respectively (Jeandet et al., 2021). Other polyketides are exclusively synthesized from malonyl-CoA like the colorant flaviolin which is made by 1,3,6,8-tetrahydroxynaphthalene synthase (THNS) and subsequent spontaneous oxidation (Funa et al., 1999; D. Yang et al., 2018). Synthesis of these secondary metabolites is often limited by product toxicity and intracellular malonyl-CoA content of the host (Milke et al., 2018; P. V. van Summeren-Wesenhagen & Marienhagen, 2015). The limiting malonyl-CoA supply is likely especially relevant for *Pseudomonas* due to the lower native CoA ester content compared to other species (Gläser et al., 2020).

Malonyl-CoA is a central metabolite for fatty acid *de novo* synthesis (FAS) and it serves as precursor for a plethora of secondary metabolites in diverse organisms (Cronan & Thomas, 2009). Especially in polyketide biosynthesis, malonyl-CoA is a frequent extender unit. Due to its universal use as precursor in different biosynthetic pathways, several microbial hosts have been engineered for increased availability of malonyl-CoA for heterologous secondary metabolite production (Jiaqi Liu et al., 2022; Milke & Marienhagen, 2020; Palmer & Alper, 2019). These include *Escherichia coli* (Yang et al., 2018), *Corynebacterium glutamicum* (Milke, Ferreira, et al., 2019; Milke, Kallscheuer, et al., 2019), *Streptomyces* spp. (Liao et al., 2022), *Saccharomyces cerevisiae* (Shiyun Li et al., 2021), and *Yarrowia lipolytica* (Sáez-Sáez et al., 2020).

In this work, a robust genome-reduced *Pseudomonas taiwanensis* VLB120 is engineered as a platform strain for the synthesis of polyketides by increasing intracellular malonyl-CoA availability and reducing the drain into FAS (Figure 2-1).

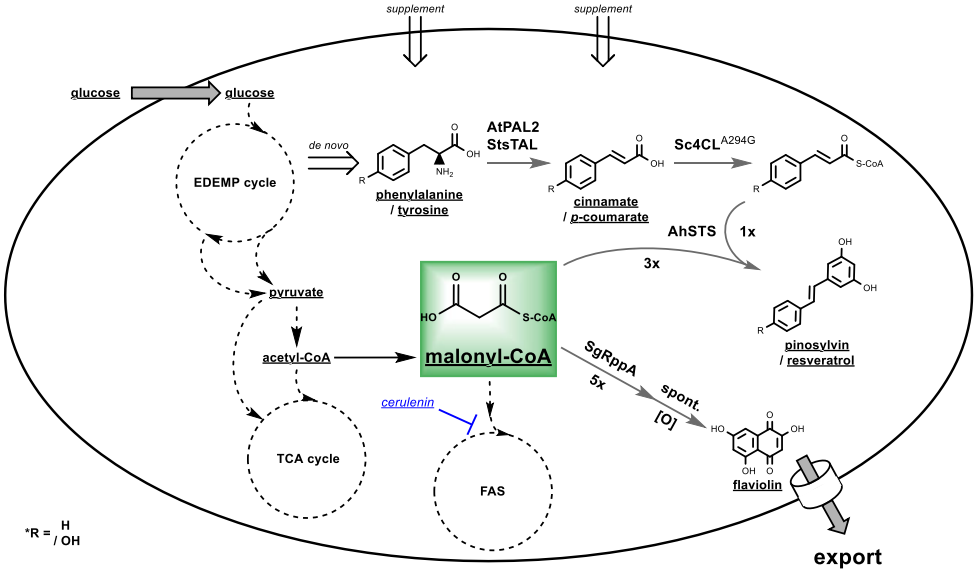

Figure 2-1 Schematic representation of heterologous stilbene and flaviolin synthesis from malonyl-CoA. Target of inhibition by cerulenin and the respective heterologous enzymes for product synthesis are indicated. R represents H or OH group. Abbreviations: EDEMP cycle, Entner-Doudoroff Embden-Meyerhof-Parnas cycle (Nikel et al., 2015); TCA cycle, tricarboxylic acid cycle; FAS, fatty acid biosynthesis; PAL, phenylalanine ammonia-lyase; TAL, tyrosine ammonia-lyase; 4CL, 4-coumaroyl:CoA ligase; STS, stilbene synthase; RppA, 1,3,6,8 tetrahydroxynaphthalene synthase

Materials and Methods

Bacterial Strains, Plasmids, and Cultivation Conditions

In this study, *Escherichia coli* and *Pseudomonas taiwanensis* VLB120 strains were cultured in LB medium at 37°C and 30°C, respectively, with antibiotics if required (50 mg L^{-1} kanamycin sulfate; 20 mg L^{-1} gentamycin disulfate G418; 100 mg L^{-1} ampicillin sodium salt; 50 mg L^{-1} apramycin sulfate; tetracycline hydrochlorid 30 mg L^{-1}). LB medium contained 10 g L^{-1} peptone, 5 g L^{-1} sodium chloride, and 5 g L^{-1} yeast extract. Solid agar plates contained 1.5% (w/v) agar. For selection of *P. taiwanensis* after conjugational matings, cetrimide agar (Sigma-Aldrich) with 10 mL L^{-1} glycerol or LB with 25 mg L^{-1} irgasan (triclosan) were used. Strains and plasmids used or generated in this study are shown in Supplementary Table S1 and Supplementary Table S2, respectively. The strains are available upon request.

Growth and production experiments started with a liquid LB seed culture inoculated from cryo-conserved stock, followed by an adaptation and main culture in mineral salt medium (MSM) adapted from Hartmans *et al.* (1989) at pH 7 with varying carbon sources and antibiotics if necessary. The medium buffer components (22.3 mM K_2HPO_4 and 13.6 mM NaH_2PO_4) were added 1- to 3-fold. Cerulenin (Sigma-Aldrich) (freshly dissolved in ethanol or methanol when indicated) was added to a final concentration of 180 µM in indicated experiments. Glucose was applied at 30 mM in production cultures and 20 mM in adaptation precultures. The nitrogen concentration of 2 g L^{-1} $(NH_4)_2SO_4$ (≈30 mM NH_4^+) was reduced for nitrogen-limiting conditions to 0.333 g L^{-1} (≈5.05 mM NH_4^+), which corresponds to a C/N ratio of 6:1 under normal conditions and 36:1 when 30 mM glucose was used. MSM adaptation cultures were inoculated from LB seed cultures to an initial OD_{600} of 0.2. In biotransformation experiments a higher initial OD_{600} was used in main cultures as indicated for the respective experiment. Production experiments were performed in 100 mL Erlenmeyer flasks with 10 mL filling volume or in 24 square well System Duetz plates (EnzyScreen, Leiden, Netherlands) with 1.5 mL filling volume. Cultures were shaken at a frequency of 200 rpm (shake flasks) or 300 rpm (System Duetz well plates) in rotary shakers with a throw of 50 mm. Growth and toxicity experiments were performed in MSM with 20 mM glucose in the Growth Profiler (EnzyScreen, Leiden, Netherlands) in 96 square well microtiter plates with 200 µL filling volume at 30°C, 225 rpm and a throw of 50 mm.

Plasmid construction and genetic modifications – DNA Techniques

Plasmids were cloned applying the Gibson assembly methodology using the NEBuilder HiFi DNA Assembly Master Mix (New England Biolabs, New Ipswich, USA). DNA oligonucleotides for PCR and sequencing were purchased from Eurofins Genomics (Ebersberg, Germany) (Supplementary Table S3). DNA fragments used for cloning were amplified using the Q5 High-Fidelity Polymerase Master Mix or purchase synthetically (Supplementary Table S4). Colony PCRs and other diagnostic PCRs were

performed with OneTaq 2x Master Mix (New England Biolabs, New Ipswich, USA) after pre-lysis with alkaline PEG 200 pH 12.75 (Chomczynski & Rymaszewski, 2006). The deletion procedure is based on two successive homologous recombination events. The second homologous recombination is selected through the induction of DNA double strand breaks introduced through I-SceI at its recognition sites introduced by pEMG (Martínez-García & de Lorenzo, 2011), pGNW2 (Wirth et al., 2020) or pSNW2 plasmids (Volke et al., 2020). In short, 400-800 bp of flanking regions of the target gene were amplified from the genome and cloned into a suicide plasmid which integrates into the genome by homologous recombination (HR). Sequences between the flanking sequences result in exchanges instead of full deletions. Subsequent, I-SceI expression induces double strand break and HR results in either wild-type or modified mutant. Lastly, positive strains were cured from the I-SceI expression plasmid (Wynands et al., 2018). Genes for pinosylvin synthesis or flaviolin synthesis were integrated at the Tn7-site and expressed using synthetic constitutive promoters (Zobel et al., 2015). For the recycling of antibiotic resistance marker, constructs with FRT sites flanking the antibiotic resistance gene were used and followed by transformation with pBBFLP for marker excision (Ackermann et al., 2021).

The genes *AtPAL2 and Sc4CL*^{A294G} were codon-optimized for *P. taiwanensis* VLB120 and obtained from a previous study by Otto *et al*. (2019; 2020). The sequence for AhSTS was equipped with a N-terminal his_6-tag and additionally a codon-optimized version (his.$AhSTS_{opt}$) for *P. taiwanensis* VLB120, using the online tool OPTIMIZER (Puigbò et al., 2007) with manual curation of restriction sites according to the SEVA standard, was purchased (Damalas et al., 2020; Martínez-García et al., 2022). Genes were ordered as synthetic DNA fragments from Thermo Fisher Scientific *GeneArt* (Regensburg, Germany). Stilbene synthases AhSTS, PsSTS, and HisPsSTS^{T248A} were provided by van Summeren-Wesenhagen and Marienhagen (2015). Template for acetyl-CoA carboxylase from *C. glutamicum* (CgACC) was pEKEx3_*accBC*_*accD1* (Milke, Ferreira, et al., 2019); SgRppA was codon-optimized as described before for his.$AhSTS_{opt}$. Sequences of ordered synthetic DNA fragments can be seen in Table S4.

Sampling and analysis

Manual measurements of the optical density were performed at 600 nm with GE Healthcare Ultrospec™ 10 device from Fischer Scientific GmbH (Schwerte, Germany).

The online analysis of culture growth by the Growth Profiler device is based on read out of the green pixels of a taken photo. Measured green values by Growth Profiler from photographs' pixels were converted into OD_{600} equivalent values based on a calibration with *P. taiwanensis* VLB120 wild-type strain (Supplementary S5).

Compounds of interest were analyzed by high performance liquid chromatography (HPLC). Samples of stilbenoids were made from 1 mL culture broth mixed with an equal amount of ethyl acetate for

extraction. The mixture was shaken for at least 15 minutes at 1500 rpm in an IKA VIBRAX VXR basic at room temperature. This was followed by a 10-15 minutes centrifugation step in Centrifuge 5425 from Eppendorf AG (Wesseling-Berzdorf/Germany). Eight hundred microliter of the top layer were transferred into an amber glass vial for evaporation at room temperature. After full evaporation, acetonitrile was added to reach a one- to eight-fold concentration of extracted compounds being in the linear correlation of HPLC analysis. HPLC vials were closed with a solvent resistant PTFE lined cap. Cinnamate was not quantified from extracts but from filtered aqueous supernatants of a culture. Authentic reference solutions of pinosylvin were made in acetonitrile. Cinnamate stock solutions were dissolved in water titrated with NaOH. HPLC analysis was performed in a 1260 Infinity II HPLC equipped with a 1260 DAD WR (Agilent Technologies) using an ISAspher 100-5 C18 BDS column (Isera, Düren, Germany) at a temperature of 40°C and a flow of 0.8 mL min^{-1}. Quantification was done with a DAD detector at 245 nm for cinnamate and 300 nm for pinosylvin. The injection volume was 10 µL and the flow profile of the solvents for the first 2 minutes was initially 10% acetonitrile (ACN) and 90% H_2O with 0.1% trifluoroacetic acid (TFA). Afterwards a gradient from 2-6 min from 10% to 100% ACN was performed. From 6-8 min the conditions were hold at 100% ACN. From 8-10 min ACN decreased back to 10% and 90% H_2O with 0.1% TFA. Finally, from 10-12 min the conditions were hold at these conditions. Samples were stored at 14°C during analysis. Retention time of cinnamate is at 7.75 min (245 nm) and pinosylvin elutes after 8.01 min (300 nm).

Flaviolin was measured from culture supernatant when cell pellets appeared colorless, indicating full secretion of flaviolin. HPLC method for flaviolin used the same equipment and 0.8 mL min^{-1} flow rate but at 30°C for the column and an injection volume of 5 µL. Initial flow was 5% ACN and 95% water with 0.1% TFA for 1 min, then from 1-2 min to 30% ACN, 2-11 min gradient to 60% ACN, 11-13 min up to 95% ACN. ACN 95% was hold for 2 min then from 15-17 min ACN decreased back to 5% and hold for 2 min. Detection of flaviolin was done at 310 nm after 8.93 min, after 10.76 another unknown compound eluted in flaviolin supernatants. Flaviolin was identified by reported UV spectrum from Gross et al. (2006) (Supplementary Fig. S6 and Fig. S7). Using the same acquisition method, *p*-coumarate was detected at 280 nm after 7.13 min, resveratrol after 9.08 min at 310 nm, cinnamate at 245 nm after 11.54 min and pinosylvin after 14.35 min at 300 nm.

Significance analysis was performed by determination of the standard deviation or standard error of the mean when indicated, followed by an ordinary one-way or two-way ANOVA using the software GraphPad Prism 9 with assumed Gaussian distribution, minimum $p<0.05$.

Results and Discussion

Pseudomonas as tolerant host towards the stilbenoid pinosylvin

Besides specific cytotoxic properties of stilbenoids, their physical properties also likely pose a general stress on the cell due to their hydrophobicity that can be described as the logarithmic distribution of a compound in an *n*-octanol-water two-phase system (log $P_{O/W}$). In this work, the log $P_{O/W}$ of pinosylvin was determined to be 3.65 ± 0.19 (initial concentration of 35 mg L^{-1}, pH=6.2). The log $P_{O/W}$ of a hydrophobic chemical correlates linearly with its partitioning between bacterial membranes and an aqueous buffer (Sikkema et al., 1994) and is therefore an indicator for a compounds toxicity. Solvent-tolerant Pseudomonads are considered especially resistant to chemicals with a log $P_{O/W}$ value between 2.5 and 4 (Rojas et al., 2004; Sardessai & Bhosle, 2004) making them promising hosts for stilbene synthesis. *P. taiwanensis* VLB120 was chosen over other Pseudomonads due to its solvent-tolerance and classification as biosafety level 1 organism in Germany. Furthermore, there are genome-reduced chassis strains available for this species with greatly improved bioprocess features (Wynands et al., 2019). To assess the tolerance of *P. taiwanensis* VLB120 wild-type, genome-reduced *chassis* strains GRC1, GRC2, GRC3 (Wynands et al., 2019) and *E. coli* BL21 (DE3), these strains (Supplementary Table S1) were cultured in mineral salt medium (MSM) with 0, 50, 100, and 150 mg L^{-1} pinosylvin (Figure 2-2). The growth of *E. coli* BL21 (DE3) was greatly reduced, reaching only 63% of the final biomass in the presence of 50 mg L^{-1} (0.24 mM) pinosylvin compared to the unstressed control and completely inhibited by 100 and 150 mg L^{-1} (0.47 mM and 0.71 mM). In contrast, all *P. taiwanensis* strains were able to grow at all applied concentrations with a reduction of final biomass by about 72% for the highest pinosylvin concentration. With increasing pinosylvin concentration the biomass density decreased, indicating an energy-demanding tolerance mechanism (Isken et al., 1999). Compared to wild-type *P. taiwanensis* VLB120, the genome-reduced *chassis* strains all grew better in the presence of pinosylvin. Strains GRC1 and GRC3 reached the highest final biomass, while GRC2 which constitutively expresses the TtgGHI solvent efflux pump performed slightly worse, indicating that this efflux pump does not significantly contribute to pinosylvin tolerance. However, this efflux pump might be beneficial for later bioprocess development employing biphasic cultivations, and therefore GRC3 with an inducible solvent efflux pump was used as a base strain for polyketide synthesis in this study.

Pinosylvin concentrations decreased during the toxicity assessment experiment with only approximately 30-70% remaining after four days in the sterile medium control and in culture supernatants (Supplementary Fig. S8). This abiotic loss of pinosylvin is consistent with previous reports of resveratrol instability under aerobic conditions (Braga et al., 2018). It is strongly affected by a variety of experimental parameters, thus highlighting the importance of reference cultivations in each experiment in the following sections because varying cultivation times and applied biomasses will

affect the final pinosylvin concentration. Prospectively, stabilization of the product by e.g. *in situ* extraction might be an option.

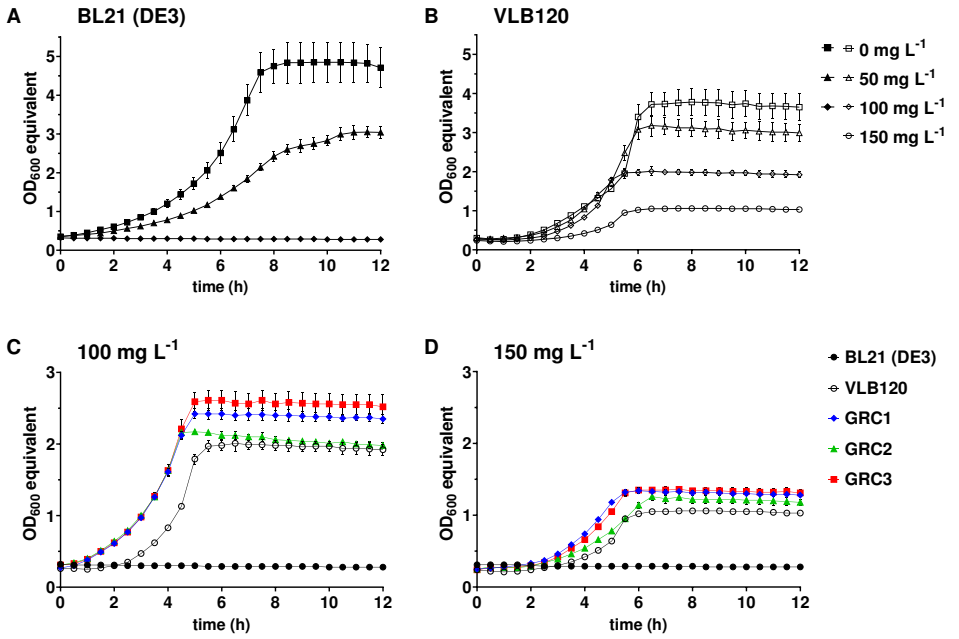

Figure 2-2 Growth of E. coli BL21 (DE3) (A) and P. taiwanensis VLB120 (B) in presence of increasing concentrations of pinosylvin; and genome-reduced chassis strains GRC1, GRC2 and GRC3 in presence of 100 mg L^{-1} (C) and 150 mg L^{-1} pinosylvin (D) in MSM with 20 mM glucose in 96-square half deepwell plates in the Growth Profiler. The corresponding cultures of E. coli BL21, P. taiwanensis VLB120 wild-type are included in C and D for comparison. Error bars indicate the standard deviation (n=3).

Conversion of a phenylalanine platform strain into a pinosylvin producer

We previously engineered a *P. taiwanensis* phenylalanine platform strain (GRC3 Δ8Δ*pykA*-tap; here called GRC3 PHE) with multiple modifications of the shikimate pathway, producing 2.6 mM phenylalanine from 20 mM glucose or 3.3 ± 0.07 mM cinnamate (22.8% Cmol $Cmol^{-1}$) when equipped with phenylalanine ammonia-lyase from *Arabidopsis thaliana* (AtPAL2) (Otto et al., 2019). Pinosylvin synthesis from phenylalanine requires deamination to cinnamate and subsequent CoA activation. Finally, an STS converts the resulting cinnamoyl-CoA and three malonyl-CoA into pinosylvin and four CO_2 (Figure 2-1). Genomic integration of pinosylvin synthesis module *AhSTS-Sc4CL^{A294G}-AtPAL2*, consisting of his-tagged stilbene synthase AhSTS from *Arachis hypogaea* (Schöppner & Kindl, 1984), cinnamate:coenzyme A ligase mutant Sc4CL^{A294G} from *Streptomyces coelicolor* A3 (Kaneko et al., 2003) and AtPAL2 (Cochrane et al., 2004) were made to enable *de novo* cinnamate and pinosylvin synthesis. High initial biomass and addition of 180 µM of FAS inhibiting cerulenin was used to elevate malonyl-

CoA availability (Supplementary S9). Cerulenin addition resulted in strong growth inhibition of the host, leading to only one further doubling of the OD_{600} after its addition. It should be noted that the applied cerulenin concentration was very high compared to concentrations typically used in other hosts such as *E. coli* (≤100 µM (Hu et al., 2022; Yang et al., 2018)) or *C. glutamicum* (25 µM (Kallscheuer et al., 2016)) or pathogenic *Mycobacterium avium* (22 µM (McCarthy, 1988)), likely reflecting the high tolerance of *P. taiwanensis* to chemical stress. Different carbon sources in presence of cerulenin were tested since these can greatly affect product yields due to the entry point into the central carbon metabolism and consequential metabolic rearrangements (Otto et al., 2019). Indeed, final pinosylvin titers were highly dependent on the used carbon source (Figure 2-3 A). The use of glycolytic substrates like glucose and glycerol enabled higher pinosylvin titers of 43.8 ± 0.4 mg L^{-1} (0.21 mM) and 34.4 ± 1.6 mg L^{-1} (0.16 mM), respectively, compared to gluconeogenic substrates like succinate (13.2 ± 0.3 mg L^{-1}, 0.06 mM) and xylose (14.1 ± 0.3 mg L^{-1}, 0.07 mM) (Figure 2-3) which enter central metabolism in the TCA cycle (Köhler et al., 2015). Glucose enabled higher pinosylvin titers than glycerol under the tested conditions. Interestingly, not just pinosylvin, but also cinnamate titers were lower on glycerol than on glucose in the cerulenin-inhibited bioconversion tested here (Figure 2-3 B). This is contrary to cinnamate yields of the parent strain, which were higher on glycerol (Otto et al., 2019). Titers reached on succinate and xylose differ in their cinnamate formation but not in pinosylvin production. An excess of cinnamate was produced under all tested conditions, indicating that malonyl-CoA availability, rather than aromatics production, is the main limiting factor. Addition of formic acid as an auxiliary energy-yielding substrate to glucose increased the titer significantly by 22% although only 5.6% additional carbon was added as formic acid. The formic acid alters the NADH supply (Zobel et al., 2017), which influences enzyme kinetics of central metabolism (Chittori et al., 2011; Ebert et al., 2011), likely reducing flux into the TCA cycle and thus making more acetyl-CoA available as direct precursor of malonyl-CoA. Octanoate is known to counteract cerulenin inhibition (McCarthy, 1988) thereby explaining the low titer of approximately 4 mg L^{-1} (0.02 mM) with this carbon source.

In summary, the tested glycolytic substrates enabled the highest pinosylvin yields, cinnamate accumulated in all cases, and without the effect of cerulenin, pinosylvin titers were low as can be seen for octanoate. The results of this proof-of-principle experiment indicate that malonyl-CoA availability is the main limitation in pinosylvin production and that FAS inhibition with cerulenin increases this availability by enabling STS to compete with native metabolism.

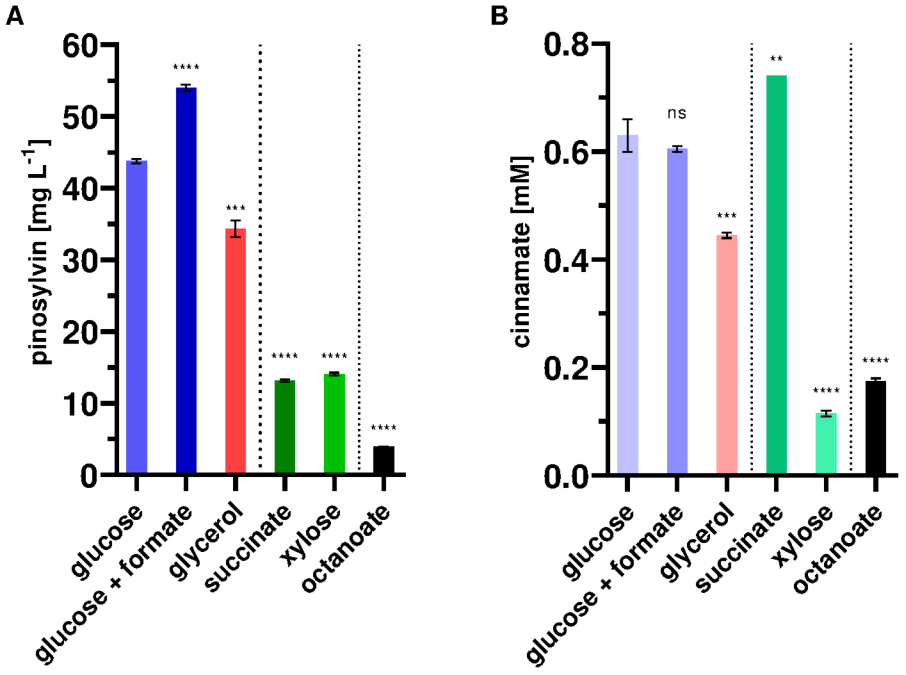

*Figure 2-3 Pinosylvin (A) and cinnamate (B) titers from high biomass de novo synthesis bioconversions using P. taiwanensis GRC3 PHE attTn7::P_{14g}-his.AhSTS-Sc4CL^{A294G}-AtPAL2 with addition of 180 µM cerulenin. Different carbon sources were applied in equal amounts of carbon (180 mM carbon atoms) or plus 10 mM formate. Cultivation in MSM with 1x buffer in 1.5 mL square-well System Duetz with inoculation to initial OD_{600} of 2 (n=2), sampled after 21.3 h. Error bars represent the standard error of the mean. Significance (p<0.05) is indicated by * (**, p≤0.01; ***, p≤0.001; ****, p≤0.0001) from one-way ANOVA. Abbreviation: ns, not significant.*

Genomic deletions to increase pinosylvin titers

The addition of cerulenin is often more costly than the actual product of interest, and the addition of a toxic antibiotic complicates downstream processing of products meant for human use. Also the reached titers with growth-inhibiting cerulenin are highly influenced by the applied initial biomass and this increases complexity due to separate biomass and production formation. Because of this, the use of cerulenin needs to be avoided. To this end, rational targeted gene deletions were performed to increase the supply of malonyl-CoA. Natively, a significant proportion of glucose is oxidized in the periplasm to gluconate by pyrroloquinoline quinone (PQQ)-dependent glucose dehydrogenase (Gcd). Deletion of the encoding gene (*gcd*; PVLB_05240) was reported to have a positive impact on polyhydroxyalkanoate (PHA) production (Poblete-Castro et al., 2013). It also slightly elevated intracellular malonyl-CoA in *P. putida* while simultaneously reducing the level of free CoA (Gläser et al., 2020).

Deletion of *gcd* in the *P. taiwanensis* phenylalanine platform strain GRC3 PHE had a positive effect on pinosylvin titers (Figure 2-4). In contrast, the deletion of PHA synthesis cluster *phaCZC2* (PVLB_02155-02165) and a type II thioesterase (encoded by *tesB*; PVLB_03305) had no beneficial effect or were even detrimental in the GRC3 PHE strain background, even though these were key modifications for increasing the formation of methyl ketones deriving from full procession of FAS in *P. taiwanensis* VLB120 (Nies et al., 2020).

The deletion of *gcd* was shown to have an influence on primary metabolic fluxes and the regulation of various genes of the central metabolism, thereby positively affecting PHA synthesis in *P. putida* (Poblete-Castro et al., 2013). Here, the deletion nearly doubled the pinosylvin titer compared to the parental strain revealing that products using malonyl-CoA as direct precursor also benefit from the deletion of *gcd* and not only peripheral products like PHA, which gain their precursors from full procession of FAS which in turn consumes malonyl-CoA.

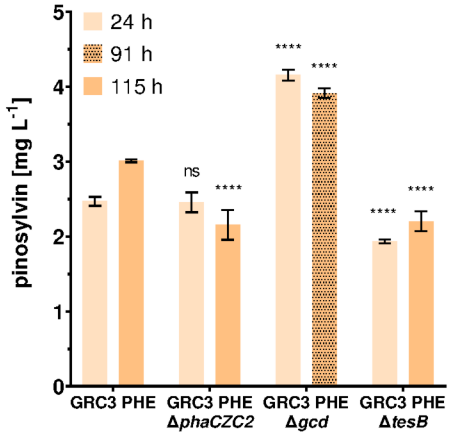

*Figure 2-4 Pinosylvin titers from de novo synthesis based on P. taiwanensis GRC3 PHE attTn7::P_{14g}-his.AhSTS-Sc4CL^{A294G}-AtPAL2 with deletions of PHA production cluster phaCZC2, glucose dehydrogenase gcd or type II thioesterase tesB. Cultivation in MSM 30 mM glucose with 1x buffer in 1.5 mL square-well System Duetz plate, initial OD_{600} was 2. Error bars represent the standard deviation (n=3) and significance (p<0.05) is indicated by * (****, p≤0.0001) from two-way ANOVA. Abbreviation: ns, not significant.*

Engineering the acetyl-CoA node by modulation of citrate synthase activity, ACC expression and deletion of the pyruvate shunt

In previous studies, downregulation of the citrate synthase, the pace-making enzyme of the TCA cycle, increased acetyl-CoA availability in *P. putida* (Kozaeva et al., 2021). It also increased malonyl-CoA availability in *C. glutamicum*, if combined with deregulated expression of the gene for acetyl-CoA carboxylase (ACC) (Milke, Ferreira, et al., 2019; Milke, Kallscheuer, et al., 2019). The fact that formate supplementation increased pinosylvin production in our *P. taiwanensis* GRC3 PHE platform also

indicates that a reduced TCA cycle flux increases malonyl-CoA availability. Thus, we sought to decrease the flux into the TCA cycle by rational strain engineering in the phenylalanine platform.

Attempts to delete the *gltA* gene encoding citrate synthase (PVLB_16320) were unsuccessful in our hands, likely because this gene is considered essential for growth (Molina-Henares *et al.* 2010). We therefore sought to reduce GltA activity with two complementary approaches.

The promoter region upstream of *gltA* (P_{gltA}) was predicted by BPROM (Solovyev & Salamov, 2011) and exchanged by the weak synthetic promoter P_{14a} together with a bicistronic design element (BCD2) (Mutalik et al., 2013; Zobel et al., 2015) (Figure 2-5). Analysis of the promoter exchange variant with SAPPHIRE (Coppens & Lavigne, 2020) revealed a potential -35 region with appropriate distance upstream of the P_{14a} promoter (Supplementary Fig. S10). Originally P_{14a} has a truncated spacer between its -10 and -35 region (Zobel et al., 2015). Due to the potential -35 region upstream of P_{14a} expression might be altered. Therefore, the inserted promoter fused to the potential -35 box is referred to as P_{14a}* (Supplementary Fig. S10).

Besides this transcriptional modulation by promoter exchange, an enzymatic modulation was achieved by replacing *gltA* (PVLB_16320) with *prpC* (PVLB_08385), in the native locus of *gltA*. PrpC is a methylcitrate synthase used in propionate metabolism (Dolan et al., 2022; Ewering et al., 2006). The putative PrpC of *P. taiwanensis* VLB120 is uncharacterized, but for PrpC from *P. aeruginosa* (87.5% aa identity) there are indications that it has a citrate synthase side activity (Dolan et al., 2022; Mitchell et al., 1995; D. Watson et al., 1983). This has also been shown for other methylcitrate synthases, which have a side activity for acetyl-CoA with higher K_M (Chittori et al., 2011). Thus, a replacement of *gltA* with the PrpC-encoding gene likely reduces citrate synthase activity. To achieve this, *prpC* was first deleted, followed by replacement of *gltA* by *prpC* through homologous recombination, leaving the first 99 bp of *gltA* intact followed by a stop codon and 24 bp upstream sequence of the native *prpC* to avoid major changes in regulation and ribosome binding. This gene replacement strategy ensures expression of *prpC* in the absence of its native inducer propionate (Dolan et al., 2022; D. Watson et al., 1983). The successful generation of a strain with replacement of *gltA* by *prpC* showed that citrate synthase function can also be attributed to PrpC. This revealed citrate synthase exchangeability with the native methylcitrate synthase in *P. taiwanensis* VLB120, confirming published results obtained from *P. aeruginosa* (Dolan et al., 2022). Conditional essentiality of *gltA* in *P. taiwanensis* VLB120 must therefore result from *prpC* expression profile which might vary from that of *P. aeruginosa* or other pseudomonads during the used deletion procedure.

In addition, the two strategies were combined by replacing the native promoter of *gltA* with P_{14a}* in the Δ*gltA*::*prpC* strain, resulting in a ΔP_{gltA}::P_{14a}* Δ*gltA*::*prpC* genotype.

Lastly, in order to shift carbon fluxes further towards acetyl-CoA, the pyruvate shunt into the TCA cycle was blocked by deletion of the pyruvate carboxylase-encoding *pycAB*.

Beside the accumulation of the central intermediate acetyl-CoA by reducing the activity of acetyl-CoA-consuming reactions or metabolic bypasses, the conversion of acetyl-CoA to malonyl-CoA by ACC is a known bottleneck in polyketide synthesis (Leonard et al., 2007). In *E. coli*, a significant improvement of malonyl-CoA availability was achieved using balanced expression of the four-subunit ACC from *Photorhabdus luminescens* (Leonard et al., 2007). The ACC of *P. taiwanensis* VLB120 also consists of four subunits *accA*, *accB*, *accC*, and *accD*, coding for carboxyltransferase α, biotin carboxyl carrier protein (BCCP), biotin carboxylase, and carboxyltransferase β, respectively. In *C. glutamicum*, the overexpression of ACC alone had no effect on malonyl-CoA availability, but it was beneficial in combination with further modifications causing increased acetyl-CoA supply (Milke, Ferreira, et al., 2019). To test the effect of an additional heterologous ACC on malonyl-CoA availability in *P. taiwanensis*, the dimeric ACC from *C. glutamicum* (*Cg_accBC-accD1*; CgACC) was episomally expressed using plasmid pBT'T in pinosylvin-producing strains with modified acetyl-CoA node to identify possible synergistic effects.

Pinosylvin production with *P. taiwanensis* GRC3 PHE strains modified around their acetyl-CoA node resulted in varying growth (Supplementary Fig. S11) and titers when compared to the respective control (Figure 2-5). Without the heterologous expression of CgACC, none of the modifications resulted in increased titers compared to the GRC3 PHE control (Figure 2-5 A). Sometimes contrary tendencies in titers were observed between those strains with and without pBT'T-*CgACC*, as for the strain with P_{gltA} promoter exchange (Figure 2-5 A, B). This is likely related to the complex (and partly unknown) regulation of acetyl-CoA and malonyl-CoA homeostasis in primary metabolism of *P. taiwanensis*. We hypothesize that it might also be influenced by the drain of erytrose-4-phosphate and phosphoenolpyruvate into the shikimate pathway in the used phenylalanine platform strain in these experiments. Here, availability of malonyl-CoA, and not cinnamate, is the major bottleneck.

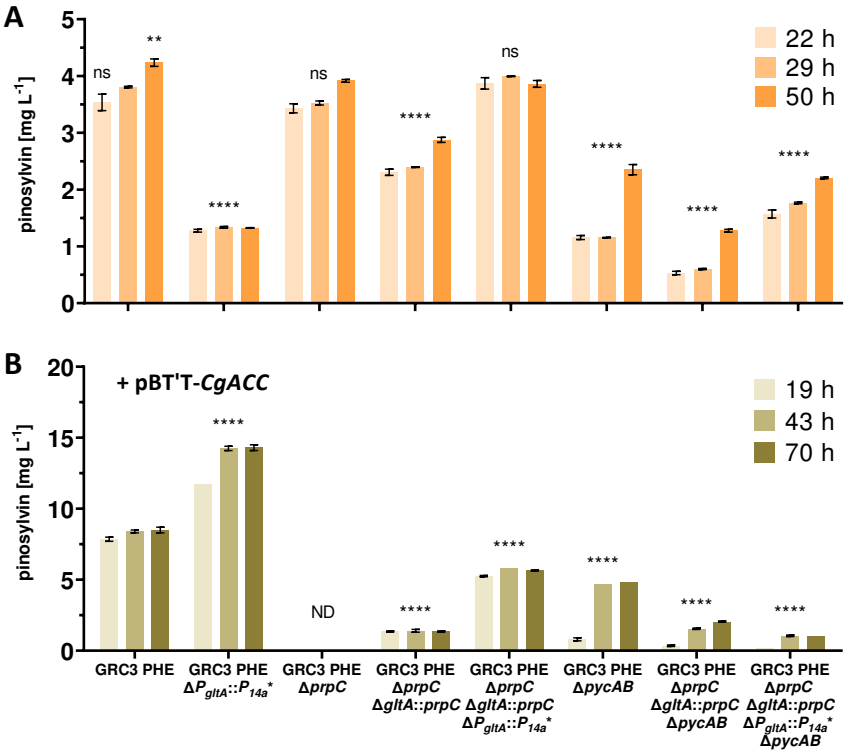

*Figure 2-5 Pinosylvin titers of P. taiwanensis GRC3 PHE attTn7::P_{14g}-his.AhSTS-Sc4CL^{A294G}-AtPAL2 with modifications concerning the acetyl-CoA node (A) and with additional plasmid pBT'T-CgACC (B). Cultivation in MSM 30 mM glucose with 1x buffer in 1.5 mL square-well System Duetz plate, initial OD_{600} was 2 in A and 0.4 in B. Error bars represent the standard error of the mean (n=2) and significance (p<0.05) is indicated by * (**, p≤0.01; ****, p≤0.0001) from two-way ANOVA of t2. Abbreviation: ns, not significant; ND, not determined.*

The main improvements in pinosylvin production were achieved by plasmid-based overexpression of ACC from *C. glutamicum* as it was the case in previous studies (Miyahisa et al., 2005; Zha et al., 2009; Zhao et al., 2018). Overexpression of CgACC increased pinosylvin formation compared to the control strain *P. taiwanensis* GRC3 PHE *chassis* without the pBT'T-*CgACC* plasmid. The combination of a P_{gtlA} promoter exchange with CgACC overexpression led to a further increase of the pinosylvin titer to 14 mg L^{-1} (0.07 mM), which was more than a three-fold increase compared to the *P. taiwanensis* GRC3 PHE starting strain under similar conditions. We reasoned that the modifications and gained knowledge should be applied in a metabolic context lacking an increased flux into the shikimate pathway.

Transfer to a platform strain without enhanced aromatics production

Many polyketides do not necessarily require an aromatic CoA ester precursor. Instead, they can be formed from malonyl-CoA exclusively, like the colorant flaviolin. Hence, we aimed to have a strain purely engineered for malonyl-CoA availability without interference of cinnamate formation. Deletion of *gcd* and altered citrate synthase expression in combination with heterologous CgACC expression enabled higher pinosylvin titers in a phenylalanine platform strain. Yet, cinnamate *de novo* supply was higher than its conversion to pinosylvin in these strains which were based on an aromatic production strain and so the shikimate pathway competes with carbon flux towards malonyl-CoA. Therefore, to reduce complexity of the production system and enable a better evaluation of engineering strategies around malonyl-CoA, beneficial modifications were transferred to a strain without an enhanced flux into the shikimate pathway and thus limited aromatics production. The chosen strain, GRC3Δ6 (Δ*pobA*, Δ*hpd*, Δ*quiC*, Δ*quiC1*, Δ*quiC2*, Δ*benABCD*), is a GRC3 derivative lacking several degradation pathways of aromatics to prevent precursor depletion. A codon-optimized version of *SgRppA* from *Streptomyces griseus*, encoding THNS, was integrated into the genome of this strain at the Tn7 attachment site (*attTn7*) followed by kanamycin resistance marker recycling (Ackermann et al., 2021) to yield a constitutive flaviolin producer. Thereby, a product formed exclusively from 5 units of malonyl-CoA serves as reporter for malonyl-CoA availability to reduce probable additional complexity from precursor supplementation. Experiments were conducted in 3-fold buffered MSM to avoid pH shifts and ensure flaviolin secretion during cultivation because if buffered insufficiently, cell pellets appeared dark and flaviolin accumulation in the supernatant was distinctly reduced (Supplementary Fig. S12).

Flaviolin was quantified from culture supernatant by comparing absorbance peak area in HPLC due to the unavailability of an authentic standard (Figure 2-6 A). HPLC analysis confirmed the previously identified positive effect of Δ*gcd* on polyketide production from glucose with an increased flaviolin titer by about 25% compared to the parental GRC3Δ6 flaviolin producer. Addition of formate also significantly increased the flaviolin titer, but this effect was abolished upon deletion of *gcd*. Notably, both, deletion of Gcd and supplementation of formate changes formation of reducing equivalents (NADPH and NADH), either by forcing the use of glucose-6-phosphate dehydrogenase (Volke et al., 2021) or through formate dehydrogenases (Zobel et al., 2017). This could be a reason why these two approaches do not cumulatively increase flaviolin titers.

The promoter exchange of P_{gltA}::P_{14a}* caused a significant additional increase of the flaviolin titer by 7% compared to the Gcd deletion, while constitutive genomic expression from P_{14f} of CgACC at integration site PVLB_23545-40 had no additional positive effect here (Figure 2-6 A). 3-oxoacyl-ACP synthase III (FabH) is required for initiation of fatty acid biosynthesis (McNaught et al., 2023). Deletion of a FabH homologue-encoding PVLB_18090 (84.7% aa identity to fabH_1 (PFL_1532) from *P. protegens* Pf-5; 74.6% aa identity to fabH1 (PA3286) from *P. aeruginosa* PAO1) (Kondakova et al., 2015)

had no effect on the flaviolin titer either. FabH2 (PVLB_17265) (85.9% aa identity to fabH_2 (PFL_1626) from *P. protegens* Pf-5; 84.9% aa identity to fabH (Pp_4379) from *P. putida* KT2440) seems to be essential for FAS initiation because multiple deletion attempts failed. A malonyl-CoA platform strain of the first generation (GRC3Δ6MC-I) was made by removal of the *attTn7*-based flaviolin production module though pEMG-mediated repair of the Tn7-site to wild-type sequence (Figure 2-6 A). When using ethanol as sole carbon and energy source or nitrogen limitation, none of the implemented modifications of GRC3Δ6MC-I-based flaviolin producer showed a positive effect on production (Supplementary Fig. S13), but GRC3Δ6MC-I may be beneficial for synthesis of products further downstream deriving from FAS. Deletion of the pyruvate carboxylase (PycAB) resulted in decreased titers in all tested approaches as observed previously for the GRC3 PHE. This anaplerotic bypass of acetyl-CoA through the pyruvate shunt into the TCA cycle highlights that malonyl-CoA supply requires more than just streamlining central carbon metabolism flux to acetyl-CoA in *Pseudomonas*.

While the previously described modifications were made with the intention to increase the formation of malonyl-CoA, the drain of malonyl-CoA into FAS is known to heavily influence malonyl-CoA availability and should thus be addressed. Expression of FabF-2, a FabF (3-ketoacyl-ACP synthase II) homologue identified in *P. putida* F1, allowed deletion of 3-ketoacyl-ACP synthases in *E. coli*, the essential and pace-making reaction of FAS (H. Dong et al., 2021). Here, the FabF-2 homologue from *P. putida* KT2440 (PP_3303) was chromosomally integrated at PVLB_02480/85 and expressed by the constitutive promoter P_{EM7} in the flaviolin producer GRC3Δ6Δ*gcd*ΔP_{gltA}::P_{14a}*. Deletion of natively essential FabF (PVLB_07185) and exchange by a unique barcoding sequence was subsequently achieved (Figure 2-6 B). However, 55 bp of *fabF* remained after deletion due to promoter-like regions within *fabF* coding sequence and partly overlapping coding sequence of 4-amino-4-deoxychorismate lyase gene (Supplementary Table S2). This new flaviolin producer reached the highest flaviolin titers, exceeding previous production by 2-fold compared to its predecessor GRC3Δ6Δ*gcd*ΔP_{gltA}::P_{14a}*. The second-generation platform strain GRC3Δ6MC-II was made from this FAS-modified flaviolin producer. Integration of FabF-2 alone reduced flaviolin titers by about 10% indicating a slightly increased precursor drain into FAS, which might be of interest for products deriving from acyl-ACPs. Modifications that did not lead to increased polyketide product titers were listed in Supplementary S14. Based on homologies (Kondakova et al., 2015; McNaught et al., 2023; Whaley et al., 2021) and deletions, we depicted the fatty acid biosynthesis pathway in *P. taiwanensis* (Supplementary Fig. S15).

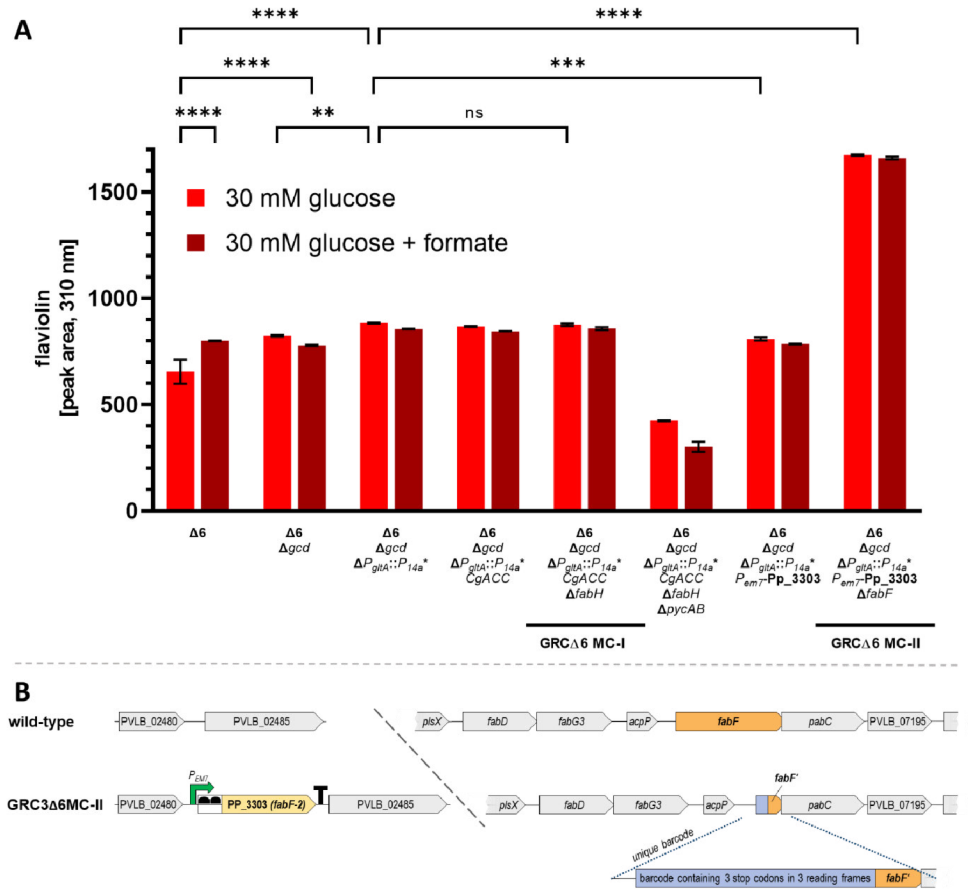

*Figure 2-6 Flaviolin titers in supernatants of different flaviolin producer strains based on aromatics catabolism deficient GRC3Δ6 with additional indicated modifications (A). Cultivation in MSM with 3x buffer, 30 mM glucose or with additional 10 mM formate in 1.5 mL square-well System Duetz plate, inoculation with 1% of adaption culture. Samples were taken after 91 h and 92.5 h, respectively to ensure full growth and THN to flaviolin oxidation. Error bars represent the standard deviation (n=3) and significance (p<0.05) is indicated by * (**, p≤0.01; ***, p≤0.001; ****, p≤0.0001) from two-way ANOVA. Abbreviation: ns, not significant; GRC3Δ6 MC-I, genotype of malonyl-CoA platform strain 1; GRC3Δ6 MC-II, genotype of malonyl-CoA platform strain 2. An illustration of the genetic design of fabF-2 integration and deletion of native fabF in the genomic context of the wild-type sequence and GRC3Δ6MC-II is shown in (B). PVLB_02480, hypothetical protein; PVLB_02485, carbamoyltransferase; plsX, phosphate acyltransferase; fabD, malonyl CoA-acyl carrier protein transacylase; fabG3, 3-ketoacyl-(acyl-carrier-protein) reductase; acpP, acyl carrier protein; fabF, 3-oxoacyl-(acyl carrier protein) synthase II; pabC, 4-amino-4-deoxychorismate lyase; PVLB_07195, hypothetical protein*

Overexpression of CgACC enhances stilbenoid production

After increasing flaviolin titers by reducing FAS, additional expression of CgACC did not further increase flaviolin titers (Figure 2-6, Supplementary S12). The modifications likely increased the net flux towards malonyl-CoA, but they also likely increased the intracellular malonyl-CoA concentration, affecting enzyme kinetics. This effect is not apparent with RppA due to its low K_M (Supplementary S12), but

other synthases for more complex molecules often have a much higher K_M, thus highlighting a limitation of flaviolin as reporter.

To test this hypothesis, and to determine whether the overexpression of acetyl-CoA synthase provides a benefit for other polyketide synthases, the pinosylvin production module was inserted into *P. taiwanensis* strains GRC3Δ6MC-II with and without genomic *CgACC* expression. The resulting strains were tested using high initial biomass concentrations for a biotransformation with phenylalanine, cerulenin, or both as supplements. Under all of the tested conditions, overexpression of *CgACC* significantly increased pinosylvin titers (Figure 2-7, Supplementary Fig. S16). The effect was most prominent with phenylalanine supplementation without cerulenin, in which case the strain with *CgACC* produced 3.5-fold more pinosylvin than the control. With phenylalanine and cerulenin, a titer of 71 ± 1 mg L^{-1} (0.35 mM) was reached by GRC3Δ6MC-II *CgACC*. Hence, GRC3Δ6MC-II *CgACC* without any production module was named GRC3Δ6MC-III in following experiments due to its superior performance compared to GRC3Δ6MC-II in all plant polyketide synthesis approaches with supplements. Interestingly, the newly obtained GRC3Δ6MC-III-based strains with Δ*fabF* and additional ACC acidify batch culture medium if not buffered sufficiently (Supplementary Fig. S12). Under cerulenin inhibition, biotransformations of the GRC3 PHE strain (Figure 2-3) produce only slightly less pinosylvin titers compared to GRC3Δ6MC-III with cerulenin (Figure 2-7), although conditions vary somewhat making a direct comparison difficult. In contrast, the impact of the malonyl-CoA modifications becomes apparent in the absence of cerulenin, where MC-III produces 3-fold more than the PHE chassis in the absence of phenylalanine supplementation, and nearly 8-fold more when phenylalanine was supplemented to MC-III (comp. Fig 4 & 7).

Titers from supplemented phenylalanine were about 33.3 mg L^{-1} (0.16 mM) for the new GRC3Δ6MC-III from only 30 mM (5.4 g L^{-1}) glucose as source for biomass and thus for malonyl-CoA. In other studies with a pinosylvin forming *E. coli* titers of 53 mg L^{-1} (0.25 mM) were reached from LB medium with additional 10 g L^{-1} glycerol and supplemented cinnamate (Salas-Navarrete et al., 2018). Pinosylvin titers of *C. glutamicum* DelAro^3 from supplemented cinnamate, 40 g L^{-1} glucose and 25 µM cerulenin were 121 ± 2 mg L^{-1} (0.57 mM) and thus about twice the titer obtained by GRC3Δ6MC-III in biotransformation with all supplements while DelAro^3 used approximately 7-fold glucose concentration (Kallscheuer et al., 2016).

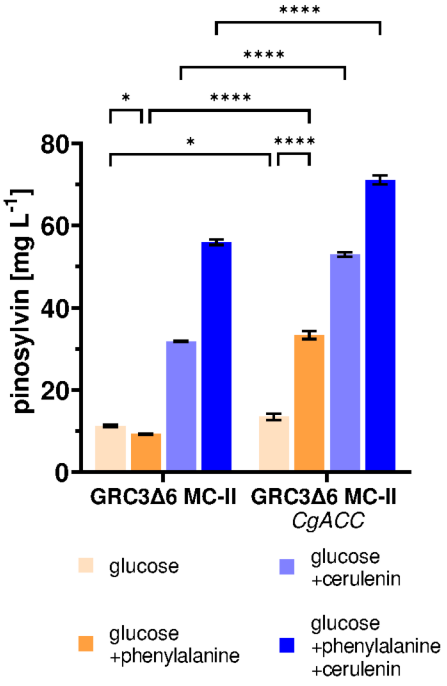

*Figure 2-7 Biotransformation approach of GRC3Δ6MC II and GRC3Δ6MC II CgACC with pinosylvin production module for pinosylvin synthesis. Cultivation in MSM 30 mM glucose with 3x buffer and different supplements (2 mM phenylalanine, 180 µM cerulenin) in 1.5 mL square-well System Duetz plate, initial OD_{600} was 3.4 and 2.7 (Supplementary S16), sampled after 21 h. Error bars represent the standard deviation (n=3) and significance ($p<0.05$) is indicated by * (****, $p\leq0.0001$) from two-way ANOVA.*

Evaluation of platform strain GRC3Δ6MC-III by stilbenoid synthesis

In order to elucidate probable effects by more than one reporter molecule deriving from phenylalanine, resveratrol as a product of tyrosine and *p*-coumarate conversion (Feng et al., 2022) was produced (Figure 2-8). The inclusion of this additional product has two main advantages: (1) it broadens the applicable product-spectrum of the new platform strain GRC3Δ6MC-III, and (2) it makes optimal use of the CoA-substrate preference of AhSTS which may reflect in malonyl-CoA consumption. The respective strains were equipped with the pinosylvin production module (Supplementary S17), or with a resveratrol production module (Figure 2-8) in which phenylalanine-specific AtPAL2 was replaced by tyrosine-specific ammonia-lyase StsTAL (Cui et al., 2020). In order to assess the possibility of *de novo* synthesis of phenylpropanoid precursors with a lower metabolic burden, a point mutation was introduced in *aroF-1* (P148L) (Wynands et al., 2018) leading to a more moderate increase of metabolic flux into the shikimate pathway compared to the GRC3 PHE strain used in section 3.3 (Figure 2-8). However, when supplemented with *p*-coumarate, resveratrol concentrations were 84 ± 2.2 mg L^{-1} (0.37 mM) and 62.5 ± 2.6 mg L^{-1} (0.27 mM) for GRC3Δ6MC-III and GRC3Δ6MC-III aroF-1^{P148L}, respectively

(Figure 2-8). These results indicate that even a moderate increase in aromatics production caused a negative effect likely due to the metabolic burden of aromatics production (Fig. S17, Figure 2-8). Approximately 72% of the supplemented *p*-coumarate (0.5 mM) was converted to the product resveratrol with 30 mM glucose in medium for growth and CoA-esters supply (Supplementary Fig. S18). In previous studies using *C. glutamicum* about 169 ± 11.8 mg L^{-1} (0.8 mM) resveratrol were reached in shake flasks from 220 mM glucose and 5 mM *p*-coumarate which corresponds to a 7-fold higher glucose supply but only 2-fold higher product titer than in this study. However, 1.71 g L^{-1} (7.5 mM) were reached in biphasic fed-batch cultivation with that strain (Tharmasothirajan et al., 2021). Highest titers so far were reached by yeast *Y. lipolytica* production systems reaching 12.4 g L^{-1} (54.4 mM) (Sáez-Sáez et al., 2020) and up to 22.5 g L^{-1} (98.7 mM) resveratrol (Liu et al., 2022).

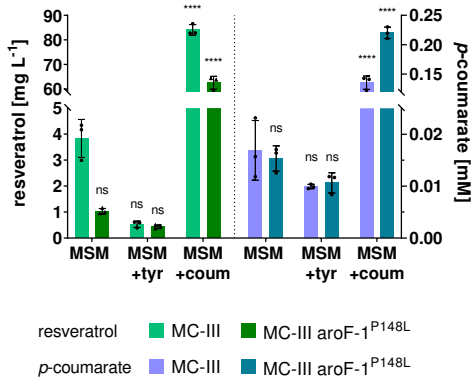

*Figure 2-8 Titers of resveratrol and p-coumarate in de novo production experiments and with supplementation of tyrosine (0.5 mM) or p-coumarate (0.5 mM). Cultivation was performed in MSM 30 mM glucose with 3x buffer in 1.5 mL square-well System Duetz plate, initial OD_{600} was 0.2, sampled after 24 h. Triangular symbols indicate individual resveratrol titers of the replicates. Error bars represent the standard deviation (n=3) and * indicates p<0.05 confidence interval (***, p≤0.001; ****, p≤0.0001) of two-way ANOVA analysis. Abbreviation: ns, not significant, MSM, mineral salt medium; tyr, tyrosine; coum, p-coumarate.*

Overall, this experiment highlights three aspects. First, even a relatively moderate shift of carbon into the shikimate pathway by introduction of AroF-1^{P148L} results in reduced stilbenoid production. Second, using non-preferred CoA substrates by the used PKS III influences overall achievable product titers (Supplementary Fig. S17). Given the difference in price and availability of the phenylpropanoids precursors and the stilbenes, a biotransformation approach is therefore likely the most economic option. Third, the new malonyl-CoA platform strain GRC3Δ6MC-III can easily be equipped with different production modules to produce different polyketide products (Supplementary S19).

Conclusion

In this study, a genome-reduced *P. taiwanensis* VLB120 strain with high tolerance towards pinosylvin was engineered for stilbenoid synthesis. Elimination of the metabolic burden of *de novo* synthesis of aromatic precursors was beneficial to achieving efficient production. Malonyl-CoA platform strains were developed using flaviolin as reporter and stilbenes as demonstrator products. Replacement of 3-ketoacyl-ACP synthase II (FabF) in native fatty acid metabolism by the heterologous isoenzyme FabF-2 from *P. putida* KT2440 significantly increased flaviolin titers up to the point where malonyl-CoA availability was no longer limiting for flaviolin synthesis, likely by reducing the drain on malonyl-CoA imposed by fatty acid biosynthesis. The benefit of additional CgACC expression only became apparent for pinosylvin production, likely due to the higher K_M value of AhSTS compared to RppA. In general, this study confirms that the malonyl-CoA node is highly complex, and that engineering of increased malonyl-CoA availably requires a cumulative, multi-factorial approach. This was achieved in the engineered *P. taiwanensis* GRC3Δ6MC-III malonyl-CoA platform, which enabled efficient synthesis of both pinosylvin and resveratrol. The strategies for increasing malonyl-CoA supply in *Pseudomonas* will be valuable for future metabolic engineering approaches in related species, and the *P. taiwanensis* GRC3Δ6MC-III platform has a broad applicability for production of malonyl-CoA-derived secondary metabolites.

Declaration of competing interest

The authors declare no competing interest.

Funding

This work was supported by the German Federal Environmental Foundation (DBU) [PhD Scholarship 20019/638-32], and the German Federal Ministry of Education and Research (BMBF) with the project NO-STRESS [FKZ 031B0852A].

2.2. Engineered passive glucose uptake in *Pseudomonas taiwanensis* VLB120 for increased resource efficiency in bioproduction

To be submitted:

Schwanemann, T., Krink, N., Nikel, P.I., Wynands, B., & Wierckx, N. (2023). Engineered passive glucose uptake in *Pseudomonas taiwanensis* VLB120 for increased resource efficiency in bioproduction. – to be submitted

CRediT authorship contribution statement

Tobias Schwanemann: Conceptualization, Methodology, Validation, Formal analysis, Investigation, Writing - Original Draft, Visualization, Funding acquisition

Nicolas Krink: Conceptualization, Writing - Review & Editing, Supervision

Pablo I. Nikel: Conceptualization, Resources

Benedikt Wynands: Validation, Writing - Review & Editing, Supervision

Nick Wierckx: Conceptualization, Validation, Resources, Writing - Review & Editing, Supervision, Funding acquisition, Project administration

Overall contribution: 80%

The presented experimental work was conducted by TS. Validation was done by NK, BW and NW. Visualization of all data was performed by TS. The writing of the original draft was mainly done by TS, which was reviewed and edited by NK, BW, and NW. Funding for the project was acquired by TS and NW.

Tobias Schwanemann[a], Nicolas Krink[b], Pablo I. Nikel[b], Benedikt Wynands[a] and Nick Wierckx[a‡]

[a] Institute of Bio- and Geosciences, IBG-1: Biotechnology, Forschungszentrum Jülich GmbH, 52425 Jülich, Germany

[b] *The Novo Nordisk Foundation Center for Biosustainability, Technical University of Denmark, Kongens Lyngby, Denmark*

‡ corresponding author:

Nick Wierckx, Institute of Bio- and Geosciences, IBG-1: Biotechnology, Forschungszentrum Jülich, Wilhelm-Johnen-Straße, 52425 Jülich, Germany. e-mail: n.wierckx@fz-juelich.de

Abstract
Glucose is the main substrate in biotechnological production process. In *Pseudomonas*, this sugar is either taken up directly or first oxidized to gluconate in the periplasm. While gluconate is taken up via a proton-driven symporter, the import of glucose is mediated by an ABC-type transporter, and hence both require energy. In this study, we heterologously expressed the energy-independent glucose facilitator protein (Glf) from *Zymomonas mobilis* to replace the native energy-demanding glucose transport systems thereby increasing the metabolic energy efficiency. Implementation of passive glucose uptake increased product titers and yields of cinnamate and resveratrol by >10% and 26% in engineered production strains.

Keywords

Pseudomonas, glucose transport, metabolic engineering, strain optimization, ATP consumption

Introduction

The uptake of carbohydrates is a fundamental process of microbial life. Especially, for the uptake of sugars across biological membranes, a plethora of different sugar utilization and transport systems have evolved in bacteria (Jeckelmann & Erni, 2020) in high dependency on the respective ecological niche. Biotechnological processes usually differ significantly from the microorganism's natural habitats, e.g. by high concentrations of carbon sources and a lack of microbial competition. It is thus not surprising that the native sugar uptake and metabolism are not necessarily ideal for the applied bioprocess. In *Pseudomonas*, glucose enters the periplasm from the extracellular space via porin OprB-I (Wylie & Worobec, 1995). It is subsequently taken up into the cytosol via ATP-binding cassette (ABC) transporter GtsABCD at the expense of ATP (del Castillo et al., 2007) or oxidized to gluconate by periplasmic glucose dehydrogenase (GDH, Gcd). Periplasmic oxidation of glucose allows Pseudomonads to shunt electrons via the pyrroloquinoline quinone (PQQ) cofactor directly into the respiratory chain (An & Moe, 2016). Periplasmic gluconate can further be oxidized to 2-keto-gluconate by the gluconate 2-dehydrogenase complex (Gad; PP_3382-3384) in some Pseudomonads (Kohlstedt & Wittmann, 2019). However, *Pseudomonas taiwanensis* VLB120 lacks this second periplasmic oxidation. In contrast to GtsABCD, the gluconate transporter GntP/GntT or 2-ketogluconate transporters KguT both belong to the major facilitator superfamily (MFS) proton symporters (del Castillo et al., 2007) and are thus also energy-dependent.

After translocation into the cytosol, glucose is phosphorylated by glucokinase (Glk) and subsequently converted by one of the glucose 6-phosphate dehydrogenase (Zwf) isoenzymes (Volke et al., 2021) and 6-phosphogluconolactonase (Pgl) to yield 6-phosphogluconate which is an intermediate of the EDEMP cycle (Nikel et al., 2015) (Figure 2-9). Regulation of glucose uptake and sugar catabolism is controlled *inter alia* by the two-component system response regulator GltR-II (PP_1012 in *Pseudomonas putida* KT2440/ PVLB_20105 in *P. taiwanensis* VLB120) and repressor HexR (PP_1021 / PVLB_20065) (del Castillo et al., 2008; H. G. Lim et al., 2022; Udaondo et al., 2018). 2-Keto-3-deoxy-6-phosphogluconate (KDPG) is one the effectors of HexR (J. Kim et al., 2008) whose deletion has been shown to be beneficial for the production of *cis*,*cis*-muconate production in strains lacking Gcd due to the derepression of the intracellular catabolic genes (Bentley et al., 2020; Rorrer et al., 2022). In certain bioprocesses, excessive periplasmic oxidation of glucose to gluconate via gluconolactone is disadvantageous due to the acidification of the culture broth as this can inhibit microbial growth or require titration of base in pH-controlled cultivations. To avoid massive pH fluctuations or the need of excessive base titration while simultaneously enabling the application of higher glucose concentration in batch cultivations, the respective *gcd* gene can be deleted and may even lead to improved production (Bentley et al., 2020; Poblete-Castro et al., 2013; Schwanemann, Otto, et al., 2023). However, this deletion may cause detrimental effects because gluconate formation is involved in a wide regulatory network (Volke et al.,

2023). A metabolic engineering strategy that implements an alternative uptake system may further improve production in strains with deleted *gcd.* This would be widely applicable in many different cultivation approaches that use glucose as substrate.

An altered glucose uptake system influences production and the cells' energy status if a passive transporter is used for the uptake of glucose from the periplasm into the cytosol in a biotechnological environment. Native energy-driven glucose transport systems are often beneficial in environments with low carbohydrate concentration because they allow uptake with high affinity against concentration gradients into the cell (Jeckelmann & Erni, 2020). This can be a distinct advantage under competitive conditions with limited glucose availability. In an artificial laboratory environment, substrates are usually supplied in concentrations exceeding the physiological K_M values of the respective uptake systems by several orders of magnitude. Therefore, the native sugar transport is usually not adapted to bioprocess requirements (Jeckelmann & Erni, 2020) and in the case of some Pseudomonads leads to excessive acidification by gluconate as carbon sequestration strategy (del Castillo et al., 2007).

An alternative glucose uptake system, specifically interesting for biotechnological applications, can be found in *Zymomonas mobilis*. This bacterium naturally occurs in carbohydrate-rich environments and is an established facultative anaerobic host for ethanol fermentation with higher ethanol yields than yeasts due to its use of the Entner-Doudoroff pathway and low biomass formation (Rogers et al., 1976; X. Wang et al., 2018; S. Yang et al., 2016). In *Z. mobilis*, glucose is taken up along the concentration gradient through a glucose facilitator (Glf) protein without the expense of energy (Snoep et al., 1994) unlike the glucose phosphotransferase system of *Escherichia coli* and the ABC glucose transporter of Pseudomonads. The facilitated diffusion mediated by Glf_{Zm} enables natively the uptake of glucose at very high specific uptake rate (Fuhrer et al., 2005) but with low reported affinity of K_M 1-4 mM (Parker et al., 1995; Weisser et al., 1995) as well as xylose and fructose, however, with much lower affinities compared to glucose (Kurgan et al., 2021; Weisser et al., 1995). Glf_{Zm} appears as a promising transporter for sugars in an energy-independent manner that might be favorable in bioprocesses with increased energy demands. In *E. coli*, replacing the PEP-consuming phosphotransferase system with Glf_{Zm} increased shikimate production (Yi et al., 2003), while expression of Glf_{Zm} in *P. putida* enabled the use of alternative carbohydrates (Bujdoš et al., 2023).

In this study, Glf_{Zm} was introduced into several genome-reduced *chassis* strains (GRC3) of *P. taiwanensis* VLB120. These strains were previously tailored for improved efficiency in bioprocesses by removal of dispensable or disadvantageous cellular features (Wynands et al., 2019), which is expanded in this study by the engineering of glucose uptake. Its impact on production strains was

investigated for the biosynthesis of resveratrol and cinnamate showcasing the applicability of Glf_{Zm} and its benefits in *Pseudomonas* for the production of different molecules from glucose.

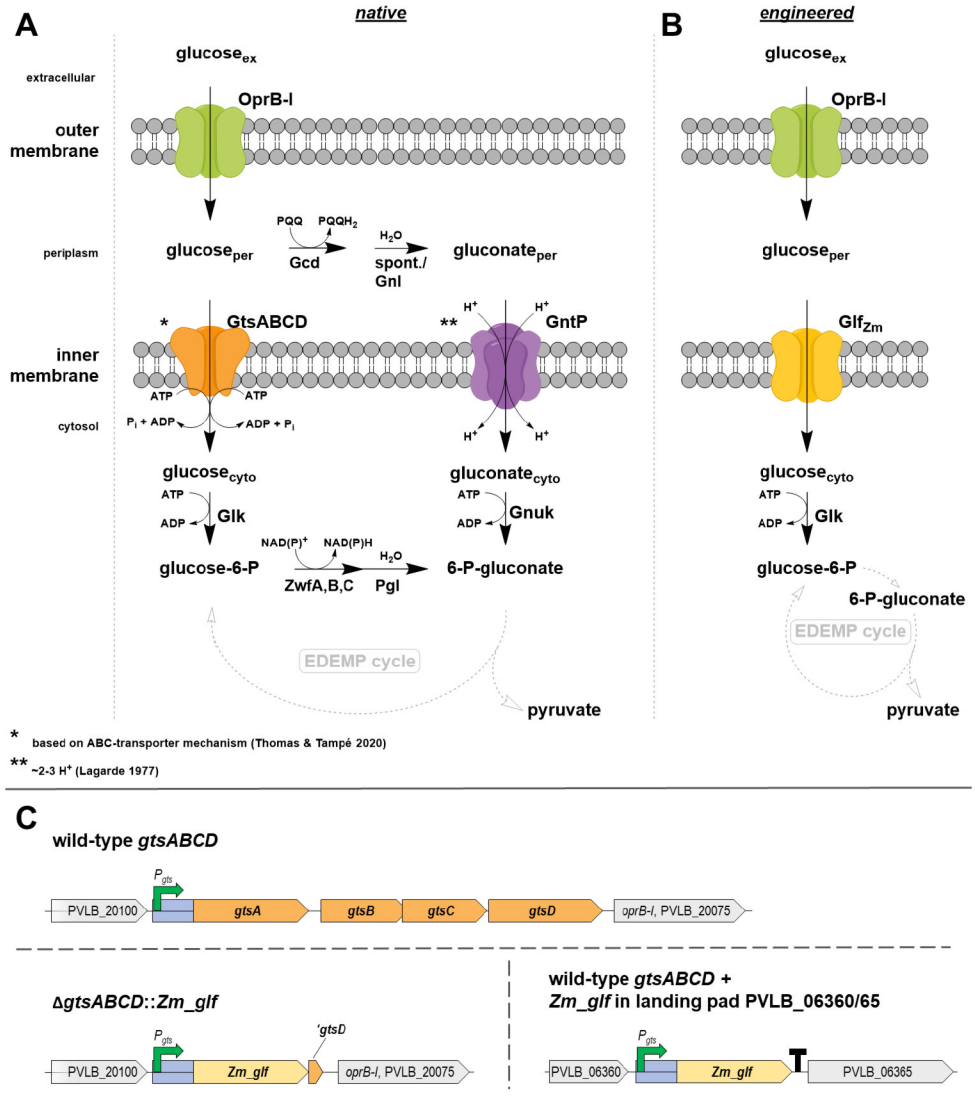

Figure 2-9 Upper glucose metabolism in P. taiwanensis and gene synteny of transporters.
(A) Overview of native and (B) engineered glucose uptake in P. taiwanensis VLB120. (C) Genetic organization of glucose uptake-encoding genes in wild-type and engineered P. taiwanensis VLB120. Abbreviations: OprB-I, carbohydrate-selective porin; GtsABCD, glucose ABC transporter; P_{gts}, presumed promoter region (200 bp upstream of the start codon of gtsABCD (PVLB_20095-80)); GntP, D-gluconate transporter; Glf_{Zm}, glucose facilitator protein from Zymomonas mobilis; PQQ, pyrroloquinoline quinone; Gcd, PQQ-dependent glucose dehydrogenase; Gnl, gluconolactonase; Glk, glucokinase; GnuK, D-gluconate kinase; Zwf, Glucose-6-phosphate dehydrogenase; Pgl, 6-phosphogluconolactonase; EDEMP cycle, Entner-Doudoroff Embden-Meyerhof-Parnas cycle (Nikel et al., 2015).

Materials and Methods

Cultivation Conditions, Media, DNA techniques

Escherichia coli and *Pseudomonas taiwanensis* VLB120 strains were cultured on agar plates (15 g L^{-1}) or in LB medium (10 g L^{-1} peptone, 5 g L^{-1} sodium chloride, and 5 g L^{-1} yeast extract) or modified (3 * 22.3 mM K_2HPO_4 and 3 * 13.6 mM NaH_2PO_4) mineral salts medium (MSM) (Hartmans et al., 1989) at 37°C and 30°C, respectively. Antibiotics were added if required (50 mg L^{-1} kanamycin sulfate; 20 mg L^{-1} gentamicin sulfate solution; 100 mg L^{-1} ampicillin sodium salt; tetracycline hydrochloride 30 mg L^{-1}). For biotransformation experiments for the production of resveratrol 1mM *p*-coumarate was supplemented to the medium. Plasmids were constructed applying the NEBuilder HiFi DNA Assembly methodology and knockout procedures were performed applying the I-SceI system that is based on two consecutive homologous recombination events as described previously (Schwanemann, Otto, et al., 2023; Wynands et al., 2018). All strains, plasmids and DNA oligonucleotides used in this study are shown in Supplementary Table S1, Table S2 and Table S3, respectively. The amino acid sequence of the glucose facilitator protein from *Zymomonas mobilis* (Glf_{Zm}) used for codon optimization corresponds to UniProt entry P21906 (Supplementary Table S4). The 200 bp upstream of *gtsABCD* (PVLB_20095-80) serve as promoter region of heterologous Glf_{Zm} expression constructs.

Cultivations for the production of cinnamate (Otto et al., 2019) or resveratrol were performed in 24-square well plate system Duetz as described previously by Schwanemann et al. (2023).

Analysis

Growth characterization experiments were performed in 96-square well plates in Growth Profiler with respective calibration for conversion of “green-value” from pixels of a picture into OD_{600} equivalent.

Determination of the optical density were performed at 600 nm with GE Healthcare Ultrospec™ 10 device from Fischer Scientific GmbH (Schwerte, Germany).

To determine biomass concentration by cell dry weight (CDW) and OD_{600}, experiments were executed in 100 mL shake flasks with 11% filling volume and samples of 10 mL were collected in dried and pre-weighted glass centrifuge tubes from Glaswarenfabrik Karl Hecht GmbH & Co KG (Sondheim, Germany) that were centrifuged for 20 min at 4000 g and washed with 5 mL 0.9% NaCl. After discarding the supernatant, the pellets were dried at 65 °C. A respective medium control was processed in parallel.

For the analysis of resveratrol 1 mL culture broth was extracted with ethyl acetate and processed further in amber glass vials as described in detail previously (Schwanemann, Otto, et al., 2023). Cinnamate and *p*-coumarate were quantified from filtered culture supernatant and all supplements and products were analyzed by HPLC.

For the detection and quantification of cinnamate, *p*-coumarate and resveratrol, a 1260 Infinity II HPLC with a 1260 DAD WR (Agilent Technologies) and an ISAspher 100-5 C18 BDS column (Isera, Düren,

Germany) was used, using the identical settings as previously for resveratrol analysis (Schwanemann, Otto, et al., 2023). Cinnamate, *p*-coumarate and resveratrol were measured at 245, 280, and 310 nm, and eluted after 11.54, 7.13, and 9.08 min, respectively.

All experiments were executed in replicates and significance analysis was performed using 1-way ANOVA with a confidence interval of $p < 0.05$.

Results and Discussion

Effect of Glf_{Zm} on biomass formation in different P. taiwanensis strains

The expression of Glf from *Z. mobilis* in different *P. taiwanensis* GRC3 strains included either the exchange of glucose transporter *gtsABCD* by *Zm_glf* or the additional expression of *Zm_glf* from a neutral expression site (PVLB_06360-65) (Figure 2-9 B, Figure 2-10). The same modifications were introduced in GRC3Δ*gcd* and a malonyl-CoA platform strain (GRC3Δ6 MC-III) (Schwanemann, Otto, et al., 2023) which are incapable of periplasmic glucose oxidation to gluconate. To elucidate the effect, final biomass concentrations were determined by CDW to calculate biomass yields (Figure 2-10 A) and growth rates (Figure 2-10 B) by OD_{600} equivalent from Growth Profiler experiments. The transporter exchange did not alter biomass yields in the GRC3 background. The additional expression of *Zm_glf* even reduced the biomass yield compared to the GRC3 control and the GRC3 strain with the replaced transporter. However, the difference was only significant when compared to the latter. In GRC3Δ*gcd* strain background a similar trend of final biomass yields was observed for additional Glf_{Zm} expression. The reduced biomass yield might be an effect of limited membrane space and increased maintenance when *Zm_glf* is additionally expressed from the same promoter as native *gtsABCD*.

Application of the expression strategies in strain GRC3Δ6 MC-III, which was metabolically engineered for increased malonyl-CoA supply, including a *gcd* deficiency (Schwanemann, Otto, et al., 2023), no significant changes were determined regarding biomass yield but a reduced growth rate was observed. A trend to yield a high final biomass for the exchanged transporter strain was noted, albeit the respective control reached a slightly lower final biomass than the other GRC3 control strains. That might be not surprising given that this strain was engineered for bioproduction.

When comparing growth rates of the respective strains (Figure 2-10 B, Supplementary S5) the deletion of Gcd alone did not decrease maximal growth rate but the malonyl-CoA platform strain, GRC3Δ6 MC-III has a 24% decreased growth rate of 0.36 h^{-1} compared to the GRC3 with 0.47 h^{-1}. Strains undergoing periplasmic gluconate formation showed no impact on their growth rate. However, strains with deleted Gcd with GtsABCD replaced by Glf_{Zm} showed a severe growth rate reduction by approximately half. This was because these strains relied solely on glucose uptake via the heterologous Glf_{Zm}. The additional expression of Glf_{Zm} decreased the rate by 23% or 19% for strains lacking Gcd (GRC3Δ*gcd*) or the malonyl-CoA platform strain (GRC3Δ6 MC-III), respectively.

In general, it can be concluded that the glucose uptake systems in *P. taiwanensis* VLB120 can be replaced by Glf_{Zm} with little effect on biomass yield, although growth is affected. Exponentially growing *Pseudomonas*, especially GRC3 with higher energy efficiency, is not energy-limited (Zobel et al., 2017). Growth rates were impaired in those strains without periplasmic glucose oxidation and exchanged transporter GtsABCD by Glf_{Zm}. When relying on glucose import of a heterologous transporter exclusively, which evolved in a different host and different environmental conditions, it is likely

unbalanced due to the hosts' cell envelope and expression capabilities, which could be addressed and optimized by an adaptive laboratory evolution (ALE) set up. However, the effects of glucose uptake modifications on growth were here only tested on non-producing strains. Deep engineering for the conversion of glucose to products typically causes growth rate reductions and higher energy demands, and here the use of Glf_{Zm} might be more beneficial.

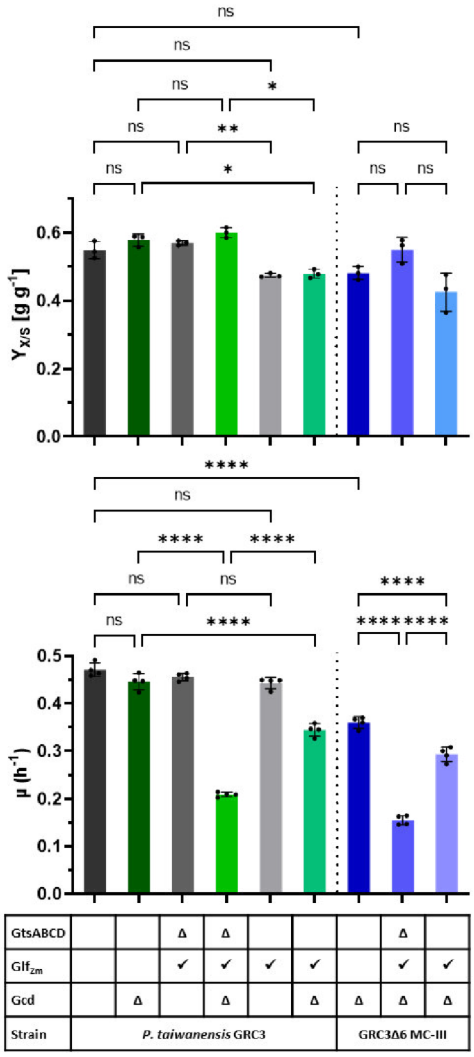

Figure 2-10 Biomass yields and kinetics of different Glf_{Zm} strains.
*A) Final biomass yields ($g_{biomass}/g_{glucose}$) resulting from the determined cell dry weight of P. taiwanensis VLB120 GRC3, GRC3Δgcd and GRC3Δ6MC-III with either replaced glucose transporter gene gtsABCD by Zm_glf or with Zm_glf expression from landing pad PVLB_06360/65. Grown in shake flasks with 30 mM (5.4 g L^{-1}) glucose and 3-fold buffered MSM for 24 h with inoculation of 1% from the adaption culture. B) Growth rate of the same strains determined in Growth Profiler experiment from 'OD_{600} equivalent' values obtained from 3-fold buffered MSM with 20 mM glucose (Supplementary S5). Error bars represent the standard deviation (n=3 in A or n=4 in B). Statistical analysis was made by 1-way ANOVA with p<0.05 with p=0.05 (**, p<0.01; ****, p<0.0001). Abbreviations: ns, not significant; $Y_{X/S}$, biomass yield; μ, growth rate.*

Effect of Glf_{Zm} on cinnamate formation by P. taiwanensis

To test the effect of Glf_{Zm} in established *P. taiwanensis* VLB120 aromatics production strains, a high-yield cinnamate producer was equipped with the alternative glucose uptake system. Strain *P. taiwanensis* GRC3Δ8ΔpykA-tap (Otto et al., 2019) (here called GRC3 PHE) was the basis as phenylalanine platform strain. When equipped with a phenylalanine ammonia-lyase (AtPAL2) from *Arabidopsis thaliana* at the genomic Tn7 integration site (*attTn7*::P_{14f}-*AtPAL2*), this strain produces cinnamate from glucose with a yield of 23% Cmol Cmol^{-1}.

Cinnamate synthesis was evaluated in engineered strains featuring either native or modified glucose transport, as well as with and without periplasmic oxidation of glucose to gluconate (Figure 2-11). In strains with exchange of the glucose uptake titers were significantly improved to 4.3 mM. In backgrounds with additional Glf_{Zm}, the expression driven by the P_{gts} promoter may compete with native GtsABCD expression and gluconate uptake. In the shown experiment, GRC3 PHE PVLB_06360/65::P_{gts}-*Zm_glf attTn7*::P_{14f}-*AtPAL2* outperformed the respective control strain GRC3 PHE *attTn7*::P_{14f}-*AtPAL2* in cinnamate titers (4.1 mM GRC3 PHE vs 4.7 mM for landing-pad::P_{gts}-*Zm_glf*). To obtain results from modifications with Glf_{Zm} expression with changed glucose utilization Δ*gcd*-strains were obtained. Deletion of *gcd* did slightly reduce final OD_{600} and had minor negative effect on cinnamate titers (4.1 ± 0.04 mM for GRC3 PHE, 4.0 ± 0.03 mM GRC3 PHE Δ*gcd*). This relatively minor effect on production would likely be offset in scaled-up batch cultures through the avoidance of transient acid formation. Without periplasmic Gcd, both expression strategies for Glf_{Zm} improved cinnamate titers to approximately 4.4 mM from 30 mM glucose compared to strain GRC3 PHE Δ*gcd,* which constitutes a significant 10% improvement of the production.

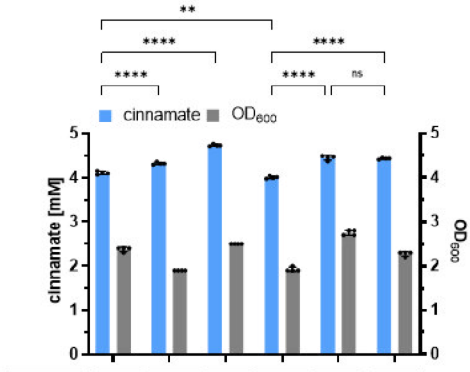

GtsABCD		Δ			Δ	
Glf_{Zm}		✓	✓		✓	✓
Gcd				Δ	Δ	Δ
Strain	GRC3 PHE *attTn7*::*FRT*-P_{14f}-*AtPAL2*					

Figure 2-11 Cinnamate production by different Glf_{Zm} strains.
*Cinnamate titer and OD_{600} of GRC3 PHE and GRC3 PHE Δgcd with markerless cinnamate module (attTn7::P_{14f}-AtPAL2) with either replaced glucose transporter gene gtsABCD by Zm_glf or with Zm_glf expression from landing pad PVLB_06360/65. Grown in 24-square deep well plate with 30 mM (5.4 g L^{-1}) glucose, 3-fold buffered MSM, sampled after 115 h in stationary phase. Error bars represent the standard deviation (n=4). Statistical analysis made by 2-way ANOVA with p=0.05 (**, p<0.01; ****, p<0.0001).*

Effect of Glf_{Zm} on resveratrol formation in P. taiwanensis

A malonyl-CoA platform strain (GRC3Δ6 MC-III) was evaluated for its ability to produce resveratrol from glucose and *p*-coumarate (Figure 2-12) with implemented *Zm_glf*. Resveratrol production was enabled by equipping the strain with the corresponding stilbene production module (*attTn7*::*FRT-P_{14f}-his.AhSTS-Sc4CL^{A294G}*). The GRC3Δ6 MC-III control with the stilbene module produced 77.6 mg L^{-1} (0.34 mM) resveratrol from 1 mM *p*-coumarate with 0.717 mM remaining precursor. This resveratrol production is in a similar range compared those previously reported (Schwanemann, Otto, et al., 2023). By exchanging the GtsABCD glucose transporter with Glf_{Zm}, 97.7 mg L^{-1} (0.43 mM) resveratrol was produced, which represents a 26% improvement. Since this strain background already features a *gcd* knockout, this constitutes a complete replacement of glucose uptake by Glf_{Zm}. In contrast to previous reports (Braga et al., 2018), no product loss was observed (Supplementary S6), with only 0.54 mM *p*-coumarate remaining. The additional expression of *Zm_glf* in a GtsABCD^{+} background reduced overall biomass and resveratrol titer (Figure 2-12).

Consequently, GRC3Δ6 MC-III Δ*gtsABCD*::*Zm_glf* with stilbene production module was identified as a better platform for resveratrol production from *p*-coumarate than GRC3Δ6 MC-III and thus *P. taiwanensis* GRC3Δ6MC-III Δ*gtsABCD*::*Zm_glf* is hereafter called GRC3Δ6MC-IV (generation No. 4 of the malonyl-CoA platform strain).

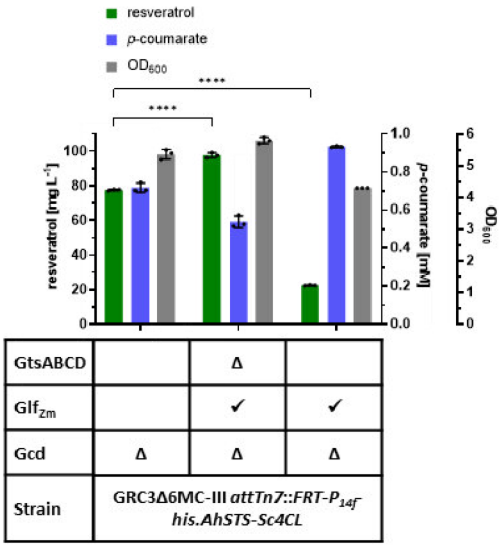

Figure 2-12 Resveratrol production by different Glf_{Zm} strains.
*Resveratrol and p-coumarate titer of GRC3Δ6MC-III with stilbene module (attTn7::FRT-P_{14f}-his.AhSTS-AtPAL2) with either replaced glucose transporter gene gtsABCD by Zm_glf or with Zm_glf expression from landing pad PVLB_06360/65. Grown in 24-square deep well plate with 30 mM (5.4 g L^{-1}) glucose, 3-fold buffered MSM and 1 mM p-coumarate for 24 h. Error bars represent the standard deviation (n=3). Statistical analysis made by 2-way ANOVA with p=0.05 (****, p<0.0001).*

Conclusion

In this study we investigated the impact of modified glucose uptake in *P. taiwanensis* VLB120 GRC3 and derivatives thereof by a passive facilitator. Final biomass yields of GRC3 and Gcd-deficient variants were not affected significantly when *gtsABCD* was replaced by Glf_{Zm}. Additional expression of Glf_{Zm} generally didn't lead to improved growth or production, indicating that glucose uptake is not limited by transport *per se* or that membrane stress from the additional transport protein outweighed any potential benefit. In the absence of production, the resource-efficient passive glucose uptake came at the cost of reduced growth rates when both native glucose uptake systems were eliminated. However, this replacement boosted bioproduction of value-added aromatic molecules from different primary pathways, highlighting the strategy's broad applicability. The enhancement was observed not only in the synthesis of cinnamate (10% increase), a shikimate pathway-derived product, but also in resveratrol production (26% increase), which is derived from malonyl-CoA and supplemented *p*-coumarate. Hereby, Glf_{Zm} can demonstrate its benefits in the absence of Gcd when the used host relies on cytosolic glucose metabolism, which is used in several bioprocess setups to ensure pH stability. However, the implementation of Glf_{Zm} in production strains with native glucose oxidation can be improved as well, as demonstrated for cinnamate formation. This straightforward engineering of the strain could boost future efforts in optimizing *Pseudomonas* for production applications.

Declaration of competing interest
The authors declare no competing interest.

Funding
This work was supported by the German Federal Environmental Foundation (DBU) [PhD Scholarship 20019/638-32], the German Academic Exchange Service [DAAD Scholarship 57556281], and the German Federal Ministry of Education and Research (BMBF) with the project NO-STRESS [FKZ 031B0852A].

2.3. Production of (hydroxy)benzoate-derived polyketides by engineered *Pseudomonas* with *in situ* extraction

Published as:

Schwanemann, T., Urban, E., Eberlein, C., Gätgens, J., Rago, D., Krink, N., Nikel, P.I., Heipieper, H.J., Wynands, B., & Wierckx, N. (2023). Production of (hydroxy)benzoate-derived polyketides by engineered *Pseudomonas* with *in situ* extraction. *Bioresource Technology*, *388*(129741), 0–11. https://doi.org/10.1016/j.biortech.2023.129741

CRediT authorship contribution statement

Tobias Schwanemann: Conceptualization, Methodology, Validation, Formal analysis, Investigation, Writing - Original Draft, Visualization, Funding acquisition

Esther A. Urban: Methodology, Formal analysis, Investigation

Christian Eberlein: Methodology, Formal analysis

Jochem Gätgens: Methodology, Formal analysis

Daniela Rago: Methodology, Formal analysis

Nicolas Krink: Supervision, Writing - Review & Editing

Pablo I. Nikel: Conceptualization, Resources, Writing - Review & Editing

Hermann J. Heipieper: Resources

Benedikt Wynands: Validation, Writing - Review & Editing, Supervision

Nick Wierckx: Conceptualization, Validation, Resources, Writing - Review & Editing, Supervision, Funding acquisition, Project administration

Overall contribution: 60%

The presented experimental work was conducted by TS and partly by EU. Special analysis methodologies of some experiments were performed by CE, JG and DR. Validation was done by TS, BW and NW. Visualization of all data was performed by TS. The writing of the original draft was mainly done by TS, which was reviewed and edited by BW, NW and all co-authors. Funding for the project was acquired by TS and NW.

Tobias Schwanemann[a], Esther A. Urban[a], Christian Eberlein[b], Jochem Gätgens[a], Daniela Rago[c], Nicolas Krink[c], Pablo I. Nikel[c], Hermann J. Heipieper[b], Benedikt Wynands[a] and Nick Wierckx[a]‡

[a] Institute of Bio- and Geosciences, IBG-1: Biotechnology, Forschungszentrum Jülich GmbH, Germany
[b] Department of Environmental Biotechnology, Helmholtz-Centre for Environmental Research - UFZ, 04318 Leipzig, Germany
[c] The Novo Nordisk Foundation Center for Biosustainability, Technical University of Denmark, Kongens Lyngby, Denmark

‡ corresponding author**:**

Nick Wierckx, Institute of Bio- and Geosciences, IBG-1: Biotechnology, Forschungszentrum Jülich, Wilhelm-Johnen-Straße, 52425 Jülich, Germany. e-mail: n.wierckx@fz-juelich.de

Abstract

Polyketides from (hydroxy)benzoates are an interesting group of plant polyphenolic compounds, whose biotechnological production is so-far underrepresented due to their challenging heterologous biosynthesis. Efficient heterologous production of 2,4,6-tri- and 2,3',4,6-tetrahydroxybenzophenone, 3,5-dihydroxybiphenyl, and 4-hydroxycoumarin by whole-cell biocatalysis in combination with *in situ* product extraction with an organic solvent was demonstrated. Production was highly dependent on the used CoA ligase and polyketide synthase type III. Therefore, different combinations of polyketide synthases and benzoate-CoA ligases were evaluated for their biosynthesis performance in the solvent-tolerant *Pseudomonas taiwanensis* VLB120. A solvent screening yielded 2-undecanone as biocompatible, extraction-efficient solvent with good phase separation. In aqueous-organic two-phase cultivations, this solvent extraction circumvents product instability in the aqueous cultivation medium, and it increases yields by reducing inhibitory effects. Complete *de novo* synthesis from glucose of all (hydroxy)benzoate-derived polyketides was achieved in two-phase cultivations with metabolically engineered strains. Additionally, mutasynthesis was applied to obtain fluorinated benzophenone derivatives.

Keywords: Benzophenones, Polyketide synthesis, mutasynthesis, *Pseudomonas taiwanensis*, ISPR by extraction

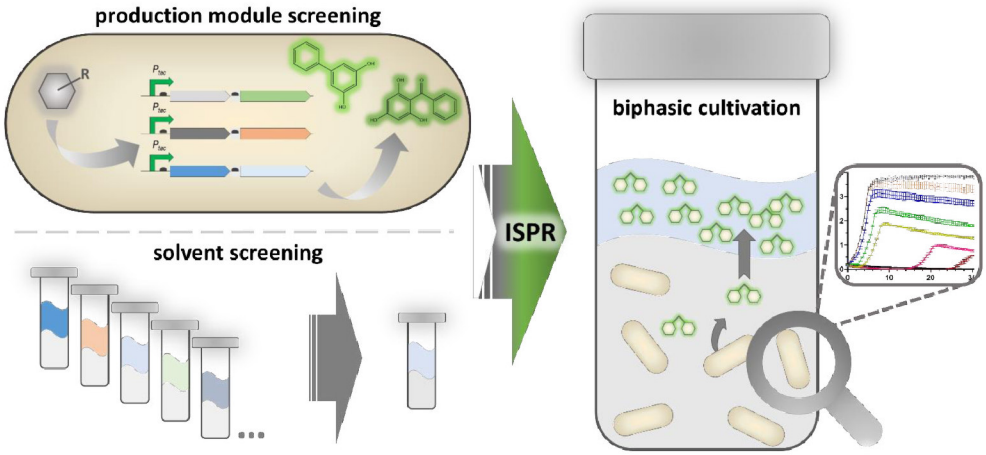

Introduction

Plant secondary metabolites made by polyketide synthases type III (PKS III) (Morita et al., 2019) are a versatile group of compounds with diverse biosynthesis pathways and a high exploration potential for new compounds. Polyphenols made from coenzyme A (CoA)-activated phenylpropanoids, like stilbenes or chalcones, are frequent targets of heterologous production in industrial biotechnology hosts (Isogai et al., 2022; Hongbiao Li et al., 2022) due to their applications as dietary and food supplements, as well as cosmetic ingredients (Kallscheuer, Classen, et al., 2019). In contrast, polyketides synthesized by PKS III from smaller precursors like CoA-bound (hydroxy)benzoates are underrepresented in terms of their heterologous production. Ever since the first isolation of α-mangostin in 1849 (W. Schmid, 1849), plant-derived benzophenones and xanthones (Remali et al., 2022) have been an important source for dyes and phytoalexins with potential applications in the pharmaceutical sector and health-promoting effects (Bisht et al., 2021). In plants, biosynthesis of xanthones is achieved via the benzophenone synthesis pathway by benzophenone synthase (BPS), a PKS III. 2,4,6-Trihydroxybenzophenone (2,4,6-TriHBP), also known as phlorobenzophenone, is the C6 → C1 Claisen condensation product of the tetraketide intermediate, made from benzoyl-CoA and three malonyl-CoA by BPS. Benzophenones are themselves diverse secondary metabolites with large variety in glycosylation, prenylation, hydroxylation and other modifications (Beerhues & Liu, 2009; S. B. Wu et al., 2014). Access to these metabolites is so far limited to complex extraction from natural resources (Miller et al., 2020) or chemical synthesis (Ehianeta et al., 2016).

Due to these costly production processes and thus limited availability, the exploration of potential applications of these compounds is hindered. In order to circumvent laborious extraction processes of natural plant producers, underlying yield variation and seasonal variability, heterologous biosynthesis with microorganisms is a preferred approach to reliably provide the respective products in a sustainable manner (Kallscheuer, Classen, et al., 2019; Prabowo et al., 2022). Additionally, the use of xenobiotic precursors allows the synthesis of synthetic analogues in mutasynthesis approaches (Reed & Alper, 2018). Halogenation with fluorine as substitute is often of interest during the development of pharmaceutical molecules because of altered persistence and accessibility while maintaining the desired biological activity (Cros et al., 2022). Conversion towards new-to-nature methyl- or fluoro-benzophenones is not possible in the natural plant producer, but can be enabled through heterologous production in microbial hosts.

Heterologous microbial biosynthesis of polyketides can thus provide more efficient production and new-to-nature derivatives, but the product's antimicrobial activity and instability poses a major challenge (Virklund et al., 2022). Thus, an *ab initio* choice of a biotechnological production host with suitable native tolerance to the envisioned products and associated process conditions is essential to achieve efficient production (Blombach et al., 2022). Considering product-host-process interactions

upfront, the genome-reduced solvent-tolerant *Pseudomonas taiwanensis* GRC3 (Wynands et al., 2019) was considered to be a suitable choice for investigating the heterologous biosynthesis benzophenones and related compounds. This species has also been extensively engineered for the production of polyketide precursors including malonyl-CoA (Schwanemann, Otto, et al., 2023), benzoate (Otto et al., 2020), *p*-coumarate (Wynands et al., 2023) and other aromatics (Schwanemann et al., 2020).

In this study, *P. taiwanensis* GRC3 was engineered for the production of 2,4,6-trihydroxybenzophenone, 2,3',4,6-tetrahydroxybenzophenone, 3,5-dihydroxybiphenyl, 4-hydroxycoumarin, and new-to-nature derivatives thereof. This is achieved in an integrated approach including the selection and expression of efficient synthetic biosynthesis pathways, metabolic engineering for completely *de novo* production, feeding of precursor analogs in a mutasynthesis approach, and solvent selection for *in situ* product removal (ISPR) and stabilization. Through this approach the *P. taiwanensis* GRC3 platform was harnessed to facilitate production of highly interesting polyketides derived from benzoates and their derivatives.

Materials and Methods

Strains and cultivation conditions

All used strains in this study can be seen in Supplementary Table S1. *Escherichia coli* DH5α and PIR2 were used as cloning hosts. Production experiments were performed with different strains of a genome-reduced *Pseudomonas taiwanensis* GRC3 (Wynands et al., 2019). *P. taiwanensis* VLB120, *Pseudomonas putida* KT2440, *E. coli* BL21 (DE3), *Bacillus subtilis* substrain 168, *Streptomyces venezuelae* NRRL B-65442 (DSM 112328), *Corynebacterium glutamicum* ATCC 13032 (DSM 20300), and *Saccharomyces cerevisiae* S288C (DSM 1333) were used in biocompatibility experiments. LB complex medium was routinely used during cloning and genetic engineering workflows and for seed cultures to inoculate minimal medium pre-cultures. Adaption cultures and production experiments were performed in Hartmans' mineral salt medium (MSM) (Hartmans et al., 1989) with three-fold buffer concentration (3 * 22.3 mM K_2HPO_4 and 3 * 13.6 mM NaH_2PO_4) and 20 or 30 mM glucose, respectively (Schwanemann, Otto, et al., 2023). Aromatic precursors or 180 µM cerulenin (resolved in methanol or ethanol) (Sigma-Aldrich) were supplemented from stock solutions. In biocompatibility experiments, other complex media, namely BHI medium (BD Difco™, United Kingdom), liquid GYM medium (glucose 4 g L^{-1}; yeast extract 4 g L^{-1}, malt extract 10 g L^{-1}) and YEPS medium (1% (w/v) yeast extract, 2% (w/v) peptone, 2% (w/v) sucrose) were used as indicated in the respective experiment for the respective species. If needed antibiotics were added (50 mg L^{-1} kanamycin sulfate; 20 mg L^{-1} gentamicin sulfate; 100 mg L^{-1} ampicillin sodium salt).

Cultivation in the presence of a second water-immiscible phase was performed in 4 mL ROTILABO glass sample vials in the Growth Profiler 960 (EnzyScreen, Heemstede, the Netherlands) with a white 3D-printed rack (Rönitz et al., unpublished). The filling volume was 500 µL MSM with three-fold buffer and 30 mM glucose with respective antibiotics, if needed. Use of different media is indicated in the respective experiments. Up to 20% (v/v) (i.e., 100 µL) solvents were added if solvents were used in subsequent HPLC analysis. In other solvent screening experiments (biocompatibility, carbon source, different organisms in the presence of 2-undecanone) 540 µL MSM and 60 µL solvent were used. Growth profiler settings were 30°C, 225 rpm with 50 mm amplitude and pictures were taken each 30 min and green values were obtained from the pixels by the corresponding software.

Plasmid and strain construction

New production strains of *P. taiwanensis* were either obtained by electroporation of replicating plasmids into twice with 10% (v/v) glycerol washed cell pellets (voltage 2500 V, capacitance 25 µF, resistance 200 Ω, cuvette 2 mm) (K. H. Choi et al., 2006) or by site-specific genomic integration of mini-Tn7 transposons into the respective attachment site in a work flow described by Ackermann et al. (2021) and Zobel et al. (2015). Plasmids were cloned applying the Gibson assembly methodology using

the NEBuilder HiFi DNA Assembly Master Mix (New England Biolabs, New Ipswich, USA). All used plasmids, oligonucleotides and DNA fragments in this study can be seen in Supplementary Table S2, S3 and S4. PCRs and colony PCR were made using either Q5 polymerase or OneTaq polymerase with prior alkaline PEG lysis as described previously (Schwanemann, Otto, et al., 2023).

Solvent screening, extraction and emulsification experiments

For the determination of extraction coefficients of 2,4,6-TriHBP, benzoate, cinnamate and flaviolin with different solvents, a solution of three-fold-buffered ultra-pure water was prepared to mimic the medium conditions with a concentration of approximately 1 mM of the respective compound. A flaviolin solution was obtained from culture supernatant in three-fold buffered MSM of strain GRC3Δ6MC-II *attTn7*::*FRT-*P_{14f}*-SgRppA* (Schwanemann, Otto, et al., 2023). Extraction was assessed at pH ~7 and 6.5. The pH was adjusted from 7.02 to 6.50 for 2,4,6-TriHBP, from 7.00 to 6.49 for benzoate, from 7.00 to 6.50 for cinnamate and from 7.02 to 6.50 for flaviolin solution using a 5 M hydrochloric acid solution. Extraction was performed in 2-mL reaction tubes in triplicates with different organic solvents and as a control without any solvent. Five-hundred microliter of the respective solvent and 500 µL of the respective aqueous solution were shaken at 1400 rpm for 10 min, centrifuged at 16,000 g for 10 min and finally the separate phases were analyzed for the compounds' concentration by HPLC.

For the extraction of 2,4,6-TriHBP with 1-octanol, a solution of ultra-pure water with ~1 mM 2,4,6-TriHBP was prepared. The pH value was set between 4.1 and 10.1 with sodium hydroxide and hydrochloric acid solutions. Extraction was performed in 2-mL reaction tubes in triplicates. Except for the controls, 1 mL 1-octanol was added to 1 mL sample. The pH of the aqueous phase for each sample was measured in equilibrium. Phases were separately analyzed for 2,4,6-TriHBP concentrations by HPLC. Back-extraction experiments using 2-undecanone were performed analogously.

To investigate interphase formation of solvents with MSM and cells, strain GRC3Δ6MC-II was inoculated at higher cell density to OD_{600} 10.8. One milliliter of culture was transferred to a 2-mL reaction tube, as well as 500 µL of the respective solvent. The tubes were shaken at 1400 rpm for 13 h at room temperature. For visual comparison of phase separation and interphase formation, images were taken after shaking, centrifugation at 4000 g at 25°C for 1.5 min, and after centrifugation for 6.5 min (Supplementary S12). Variations of cell density and centrifugations are indicated in the respective experiments (Supplementary S12).

Sampling from production experiments and analytical methods

Determination of the optical density were performed at 600 nm with GE Healthcare UltrospecTM 10 device from Fischer Scientific GmbH (Schwerte, Germany).

For regular cultivations in the Growth Profiler using 96-square-well plates with a filling volume of 200 µL, the obtained green value were converted to OD_{600} equivalents using the following calibration:

$$OD_{600}\ \text{equivalent} = a * (gValue - gBlank)^b + c * (gValue - gBlank)^d + e * (gValue - gBlank)^f$$

with a = 0.0328, b = 1.08, c = $5.6 * 10^{-7}$, d = 3.13, e = $1.47 * 10^{-13}$, f = 6.64 and gBlank = 17.330. Abbreviations: gValue, green value; gBlank, green value of reference medium. The calibration was performed for the *P. taiwanensis* VLB120 wild type in half-deepwell microtiter plates (CR1496dg, EnzyScreen) sealed with sandwich covers (CR1296c, EnzyScreen).

GC-FID analysis of fatty acid composition

Extraction of membrane lipids was performed according to (Bligh & Dyer, 1959; Morrison & Smith, 1964). The resulting fatty acid methyl esters (FAME) were analyzed by gas chromatography (GC) with flame ionization detector (FID) (Agilent Technologies 6890N Network GC Systems; Model: HP5890, Hewlett-Packard, Palo Alto, USA). The used column was a 50 m CP-Sil 88 (Agilent Technologies) with 0.25 mm inner diameter and 0.25 µm film thickness. Helium flow was set to 1 mL min^{-1}. The GC temperature program started at 40°C for 2 min, followed by a temperature ramp of +8 °C min^{-1} up to 220°C, which was hold for 5 min. The pressure program started at 27.7 psi (186.15 kPa) for 2 min, followed by a gradient of 0.82 psi min^{-1} (5.65 kPa min^{-1}) to final 45.7 psi (310.26 kPa) which was hold for 15.55 min. Injection temperature was 240°C with split-less injection volume of 1 µL by Agilent Technologies 7683B Series Injector, the FID detector temperature was 270°C. FAME were identified by co-injection of authentic reference compounds obtained from Supelco (Bellefonte, PA). *Trans/cis* ratio of unsaturated membrane fatty acids was calculated taking the sum of the FAME of palmitoleic acid (C16:1Δ9*cis*) and *cis*-vaccenic acid (C18:1Δ11*cis*) as divisor and the sum of their corresponding *trans* configuration as dividend (Heipieper et al., 1992).

Sample preparation from production experiments

Supernatant samples were made by centrifugation and subsequent filtration. To obtain extracts for polyketide analysis, 950 µL culture broth were transferred in a reaction tube with 50 µL 1 M hydrochloric acid. Then 950 µL ethyl acetate were added and vortexed for 15 min, followed by centrifugation and transfer to amber HPLC vials for evaporation as published previously by Schwanemann et al., (2023). Dried samples were resolved in acetonitrile for analysis in amber vials

with PTFE-lined caps. From two-phasic cultivations, the cultivation tubes were centrifuged for 1 min at 4000 g and 50 µL of the organic layer were transferred into amber vials with an inlet for small volumes and measured in HPLC. Aqueous supernatants were obtained from filtered aqueous phase.

HPLC analysis

HPLC analysis was done as previously reported by Schwanemann et al., (2023) for the flaviolin acquisition method in 1260 Infinity II HPLC equipped with a 1260 DAD WR (Agilent Technologies) using an ISAspher 100-5 C18 BDS column (Isera, Düren, Germany) at a temperature of 30°C and a flow of 0.8 mL min^{-1}. Benzoate was detected at 232 nm after 9.47 min; 2,4,6-trihydroxybenzophenone at 330 nm after 11.43 min; cinnamate at 270 nm after 11.72 min; 3,5-dihydroxybiphenyl at 250 nm after 12.06 min. 3-hydroxybenzoate was detected after 6.75 at 300 nm, 3-hydroxycinnamate after 7.85 min at 270 nm and 2,3',4,6-TetraHBP after 8.26 min at 330 nm. 2-Hydroxybenzoate (salicylate) was detected at 300 nm after 10.84 min and 4-hydroxycoumarin after 9.14 at 280 nm. 3-Methyl benzoate was detectable after 11.72 min at 232 nm.

Authentic standards were prepared in acetonitrile for 2,4,6-TriHBP, 2,3',4,6-TetraHBP, 2,3-dihydroxybiphenyl and 4-hydroxycoumarin. Benzoic acids and phenylpropanoids were solved in water titrated with a sodium hydroxide solution if needed to obtain reference solutions.

GC-ToF MS analysis

Verification of sample composition was made for selected extraction samples by GC-ToF MS analysis according to a standard method published by (Hummel et al., 2010). Extract samples obtained from production experiments were resolved in acetonitrile which were previously used in HPLC analysis. The samples were lyophilized overnight in a Christ LT-105 freeze drier (Martin Christ Gefriertrocknungsanlagen, Osterode am Harz, Germany) and then stored at -20°C. Samples were consecutively derivatized with 50 µL MeOX (20 mg mL^{-1} O-methylhydroxylamine in pyridine) for 90 min at 30°C and 600 rpm in a thermomixer followed by an incubation with 80 µL of added MSTFA (N-acetyl-N-(trimethylsilyl)-trifuoroacetamide) for 90 min at 40°C and 600 rpm. For the determination of the derivatized metabolites an Agilent 6890N gas chromatograph (Agilent, Waldbronn, Germany) was used coupled to a Waters Micromass GCT Premier high resolution time of flight mass spectrometer (Waters, Eschborn, Germany). The system was controlled by Waters MassLynx 4.1 software. Injections were performed by a Gerstel MPS 2 (Gerstel, Mülheim ad Ruhr, Germany) controlled by Maestro software. One microliter sample was injected into a split/splitless injector at 280°C at varying split modes.

The GC was equipped with a 30 m Agilent EZ-Guard VF-5ms + 10 m guard column (Agilent, Waldbronn, Germany). The constant helium flow was set to 1 mL min^{-1}. The GC temperature program started at 60°C with a hold time of 2 min, followed by a temperature ramp of +12 °C min^{-1} up to the final temperature of 300°C, hold time of 8 min. The ToF MS was operated in positive electron impact $[EI]^+$ mode at an electron energy of 70 eV. Ion source temperature was set to 180°C. The MS was tuned and calibrated with the mass fragmentation pattern of Heptacosa (heptacosafluoro-tributylamine).

For the annotation of known metabolites a baseline noise corrected fragmentation pattern together with the corresponding current RI value (Retention time Index) was compared to the in house accurate m/z database JuPoD, and the commercial nominal m/z database NIST (National Institute of Standards and Technology, USA).

Unknown peaks were identified by a virtual reconstruction of the derivatized metabolite structure via the measured baseline noise corrected accurate mass m/z fragment pattern in comparison to an accurate m/z fragment register inside the JuPoD main library and were subsequent verified by virtual derivatization and fragmentation of the predicted structure.

LC-UV-MS/MS analysis

The analysis of mutasynthesis was done by LC-(UV)-MS/MS of culture supernatant and ethyl acetate extracts (prepared, as previously described for HPLC analysis).

The sample analysis was performed on a Vanquish Duo UHPLC binary system (Thermo Fisher Scientific, USA) coupled to a DAD-(ESI)IDX Orbitrap Mass Spectrometer (Thermo Fisher Scientific, USA), according to a previously published method (Kildegaard et al., 2021). Briefly, the chromatographic separation was achieved using a Waters ACQUITY BEH C18 (10 cm × 2.1 mm, 1.7 µm) equipped with an ACQUITY BEH C18 guard column kept at 40°C and mobile phase consisting of MilliQ water + 0.1% formic acid (A) and acetonitrile + 0.1% formic acid (B) using a flow rate of 0.35 mL min^{-1}. Sample injection was 1 µL. The DAD settings were 10 Hz for data collection rate and the wavelength range was 190-600 nm with a bandwidth of 2 nm.

The MS acquisition was set in positive and negative-heated electrospray ionization (HESI) mode with a voltage of 3500 V and 2500 V respectively, acquiring in full MS/MS spectra (Data dependent acquisition-driven MS/MS) in the mass range of 70-1000 Da. The data dependent acquisition settings were the following: automatic gain control (AGC) target value set at 4e5 for the full MS and 5e4 for the MS/MS spectral acquisition, the mass resolution was set to 120,000 for full scan MS and 30,000 for MS/MS events. Precursor ions were fragmented by stepped High-energy collision dissociation (HCD) using collision energies of 20, 40, and 60.

Statistical analysis

Analysis was performed by determination of the standard deviation (SD) or standard error of the mean (SEM) when indicated. In case of biological and technical replicates, the biological replicates were used for mean determinations. Additionally, ordinary one-way or two-way ANOVA with post-hoc tukey test using the software GraphPad Prism 9 with assumed Gaussian distribution, minimum $p<0.05$ were applied when needed to determine significance.

Results and Discussion

Toxicity and properties of 2,4,6-trihydroxybenzophenone and cellular response

Properties of benzoate-derived polyketides and physiological effects on biotechnological production hosts are still a mostly unexplored field. In order to gain a solid basis for heterologous natural product formation, the toxicity of 2,4,6-TriHBP on an aromatics catabolism-deficient *Pseudomonas taiwanensis* GRC3Δ6 (Δ*pobA*, Δ*hpd*, Δ*quiC*, Δ*quiC1*, Δ*quiC2*, Δ*benABCD*) was investigated using different concentrations of 2,4,6-TriHBP (Figure 2-13A). With increasing concentrations of 2,4,6-TriHBP the biomass formation decreased with a correlating prolonged lag phase. The decreasing biomass in dependency to the applied 2,4,6-TriHBP concentration is an indication of 2,4,6-TriHBP uncoupling the proton motive force or of an energy-demanding tolerance mechanism of the microorganism (Isken et al., 1999). Interestingly, the biomass signal of the control culture with no 2,4,6-TriHBP stayed nearly constant over the whole period of cultivation, while biomass values decreased over time in the stationary phase of cultures supplemented with 2,4,6-TriHBP. In addition, a red colorization of the cultures and the medium controls was observed, which could also influence the green pixel counts (green value) of the Growth Profiler which were converted into OD_{600} equivalents. Thus, the decrease in the stationary phase could either result from cell lysis and/or counteracting pixel readouts from ongoing color change. The 2,4,6-TriHBP concentration was strongly reduced at the end of cultivation in both medium controls and culture supernatants (Supplementary S5). Therefore, toxicity might be exacerbated by as yet unknown degradation products of 2,4,6-TriHBP.

In order to examine toxicity effects of 2,4,6-TriHBP itself, 2,4,6-TriHBP was spiked directly into exponentially growing cultures of *P. taiwanensis* VLB120 wild type and GRC3 on succinate. The toxicity given as the effective concentration (EC_{50}) causing 50% growth inhibition was determined and, additionally, cellular phospholipids were extracted and analyzed (Bligh & Dyer, 1959; Morrison & Smith, 1964) for their *trans*/*cis* fatty acids composition. This composition allows to draw conclusions of the activity of the periplasmic *cis*-*trans*-isomerase (Cti) (Eberlein et al., 2018) and thus the mode of toxicity of 2,4,6-TriHBP. The graphically determined EC_{50} of *P. taiwanensis* GRC3 was approximately 2 mM (Figure 2-13B) and 2.3 mM for the wild type (Supplementary S5). This is in a similar range compared to other compounds with a similar $LogP_{O/W}$ like toluene and 4-chlorophenol (Mauger et al., 2021). The *trans*/*cis* ratio of unsaturated fatty acids shifted from 0.31 to 0.37, 0.57 and up to 0.71 with the increasing applied 2,4,6-TriHBP concentrations in strain GRC3. This indicates activity of the short-term stress response deriving from Cti which has only access to its substrates when the inner membrane stability is impaired due to changes in its fluidity and rigidity, and thus its permeability (Eberlein et al., 2018). Thus, 2,4,6-TriHBP is directly affecting the bacterial inner cell membrane rigidity which likely contributes to its cytotoxicity. In contrast to the prior toxicity experiment (Figure 2-13A),

the later supplementation and quantification of the effects in growth and fatty acid composition allows to subscribe the observed effects directly to 2,4,6-TriHBP.

The partitioning of small uncharged compounds into biological membranes correlates with their partitioning coefficient of water and octanol ($logP_{O/W}$) (Heipieper et al., 2007; Sikkema et al., 1994). Therefore, partitioning of 2,4,6-TriHBP was tested at different pH values in an octanol-water system. Due to the definition of $logP_{O/W}$ as pure water-octanol mixture, the values obtained here are given as $logK_{O/W}$ due to the presence of salts in the aqueous phase (Figure 2-13C). 2,4,6-TriHBP partitioning into octanol decreased with increasing pH due to its deprotonation. At acidic conditions up to a pH of approximately 6.5, the $logK_{O/W}$ remains constant at ~2.6 and the solution remains transparent. From pH 6.5 to 9 distribution shifted towards equal partitioning ($logK_{O/W}\approx0$) until it is predominantly present in the aqueous phase at pH>9 and yellow colored in the aqueous phase. This pH-dependent partitioning may result in interference of the proton motive force and thus contribute to the toxic properties of 2,4,6-TriHBP because compounds with a $logP_{O/W}$ of 1-5 are generally considered as toxic due lethal accumulation in bacterial membranes if their water solubility is sufficient (Neumann et al., 2005; Schwanemann et al., 2020). Many natural small-size products are within this toxic range (Schönsee & Bucheli, 2020) contributing to their challenging high titer production in biotechnological hosts.

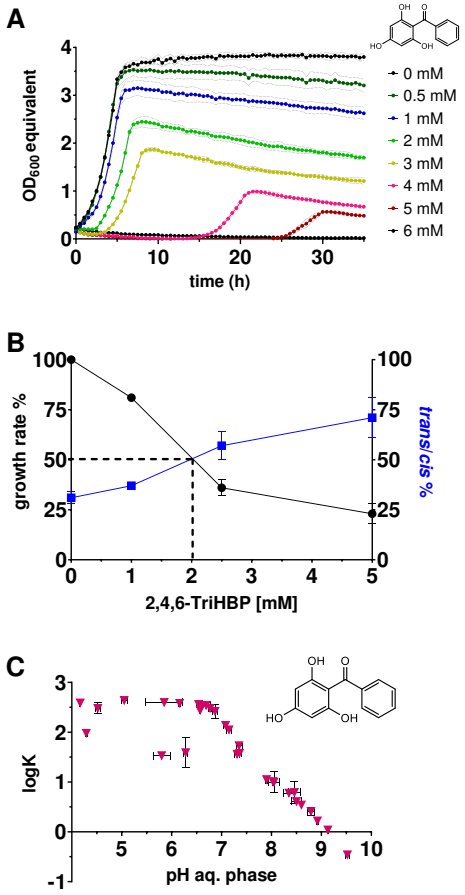

Figure 2-13 Characterization of 2,4,6-TriHBP effects on host organism and partitioning in buffer:1-octanol system. A) Growth of P. taiwanensis GRC3Δ6 in mineral salt medium (MSM) with 20 mM glucose and 2,4,6-TriHBP (0-6 mM) in 96-square-well plate Growth Profiler cultivations (green value converted to OD_{600} equivalent) with initial OD_{600} 0.2. ***B)*** *Relative growth rate from OD_{560} and trans/cis ratio of membrane phospholipids of P. taiwanensis GRC3 grown in MSM with 10 mM succinate in dependence to added 2,4,6-TriHBP. Error bars represent the standard deviation of the mean (n_{bio}=2, n_{tech}=3). The dashed line represents the IC_{50} concentration.* ***C)*** *Logarithmic plot of the partitioning coefficient of an aqueous 2,4,6-TriHBP solution (170 mg L^{-1}) containing 36 mM phosphate buffer with 1-octanol in 1:1 mixtures in dependence of the pH in equilibrium (pH 4.17 to 9.52). The pH was adjusted with 0.1 M HCl_{aq} and $NaOH_{aq}$ at 25°C. Error bars represent the standard deviations of the pH and $logK_{O/W}$ (n=3, if not indicated differently).*

Identification of suitable enzyme combinations for benzoate polyketide synthesis

For biosynthesis of benzophenones and related polyketides, a respective aromatic precursor has to be CoA-activated by a ligase and subsequently converted by a BPS or biphenyl synthase (BIS). In order to identify suitable combinations of these two activities, pBT'T plasmid-based expression of different benzoate-CoA ligases and BPS or BIS were screened in *P. taiwanensis* GRC3Δ6. This screening was done in biotransformation experiments with high initial biomass and cerulenin as fatty acid biosynthesis inhibitor to artificially increase malonyl-CoA supply, which revealed a production dependence on the used ligase and BPS (Figure 2-14). The combination of BPS from *Hypericum sampsonii* (HsBPS) and benzoate-CoA ligase from *Rhodopseudomonas palustris* (RpBZL) performed significantly the best for 2,4,6-TriHBP formation, achieving a titer of 270 ± 3 mg L^{-1} (Figure 2-14A). Biosynthesis of 2,4,6-TriHBP was previously demonstrated in *Escherichia coli* without providing quantitative data (Klamrak et al., 2021). Another study using *Saccharomyces cerevisiae* achieved approximately 450 µg L^{-1} of 2,4,6-TriHBP from glucose and supplemented benzoate (Liu et al., 2020). In both cases, heterologous biosynthesis was likely limited by product stability and toxicity, precursor supply, as well as enzyme expression and activity (Virklund et al., 2022). Therefore, the here shown combinatorial pathway screening in a tolerant host demonstrated its potential.

In plants, 2,3',4,6-TetraHBP serves as universal precursor for xanthone biosynthesis (Beerhues & Liu, 2009; Remali et al., 2022) and is made either from 2,4,6-TriHBP by selective oxidation (El-Awaad et al., 2016), or from 3-hydroxybenzoate as ligation substrate (Schmidt & Beerhues, 1997). For the formation of 2,3',4,6-TetraHBP from 3-hydroxybenzoate combinations of HaBPS or HsBPS with ligases RpBZL or $PxBCL_M$ performed similarly well in our experimental setup without significant difference (Figure 2-14B). This exploitation of substrate promiscuity led to much lower titers of 26-27 mg L^{-1}, but this first heterologous 2,3',4,6-TetraHBP synthesis was confirmed by GC-ToF MS (Supplementary S6) and by an authentic reference standard in HPLC.

Benzoate-derived polyketide aromatic ring formation can also be achieved by an aldol condensation reaction, catalyzed by BIS resulting in formation of 3,5-dihydroxybiphenyl, a precursor of the phytoalexin aucuparin (Beerhues & Liu, 2009; B. Liu et al., 2007). GC-TOF was applied (Supplementary S6) to confirm the formation of 3,5-dihydroxybiphenyl from benzoate with ligase RpBZL in combination with BIS1 from *Malus domestica* (MdBIS1) at low titers (Figure 2-14C). This indicates a lower activity of BIS compared to BPS in heterologous application.

Interestingly, in all these biotransformation cinnamate or 3-hydroxycinnamate were identified as by-product, in accordance with the applied precursor benzoate or 3-hydroxybenzoate. These by-products did not occur when a PKS III was used that does not accept benzoyl-CoA as substrate like ScCHS, indicating that *in vivo* synthase activity was involved in their formation.

Some PKS III were reported to have a promiscuous activity for 4-hydroxycoumarin synthesis from salicyl-CoA (2-hydroxybenzoyl-CoA) and one malonyl-CoA (Liu et al., 2010). 4-Hydroxycoumarin is a natural precursor of anticoagulants and was thus of interest in previous metabolic engineering studies but not by exploiting BIS side-activity (Choo & Ahn, 2019; Y. Lin et al., 2013). In the conversion approach of 2-hydroxybenzoate (salicylate) 4-hydroxycoumarin could be detected in small amounts in all approaches, revealing the applicability of BIS for its *in vivo* formation (Figure 2-14D). The most suitable enzyme combination for that was BIS1 from pear *Pyrus communis* (PcBIS1) with CoA ligase SdgA from *Streptomyces sp*. WA46. In conclusion, each product was successfully biosynthesized and its identity confirmed. Additionally, a suitable combination for each product was identified by a biotransformation approach with cerulenin.

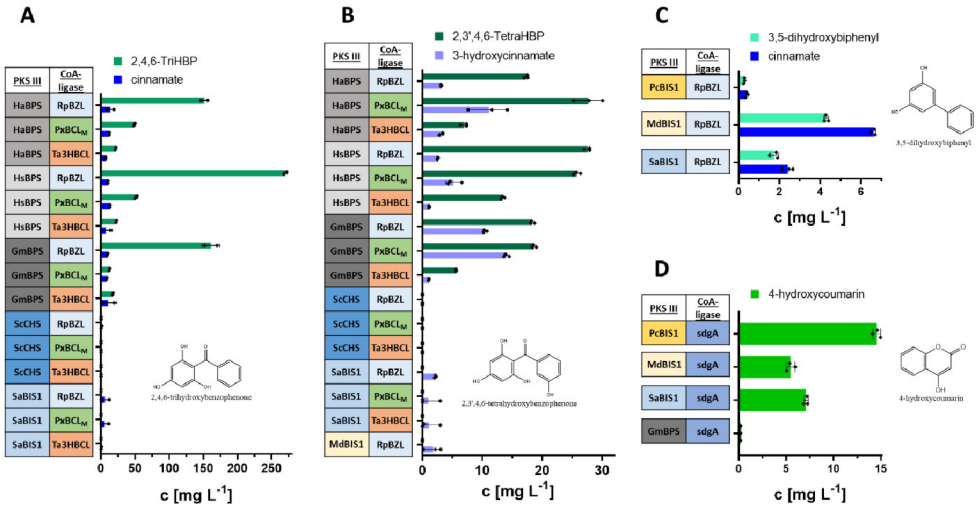

Figure 2-14 Tested enzyme combinations for product synthesis by cerulenin supplemented transformations.
A) *Titers from biotransformation of benzoate to 2,4,6-TriHBP and cinnamate by different gene combinations expressed from pBT'T plasmid in P. taiwanensis GRC3Δ6 cultured with an initial* OD_{600} *of 4. Error bars indicate standard deviation of the mean (n=2).* ***B)*** *Titers from biotransformation of 3-hydroxybenzoate to 2,3',4,6-TetraHBP and 3-hdroxycinnamate.* ***C)*** *Titers of 3,5-dihydroxybiphenyl and cinnamate from benzoate.* ***D)*** *4-Hydroxycoumarin from 2-hydroxybenzoate biotransformation by different gene combinations. All biotransformations were performed in MSM with 30 mM glucose, 2 mM supplemented benzoate, 3-hydroxybenzoate or 2-hydroxybenzoate, 154.2 mM ethanol (from cerulenin stock) and 180 µM cerulenin with initial* OD_{600} *1 if not indicated differently. Samples were 2-fold concentrated for HPLC analysis. Error bars represent the standard deviation (n=3) if not indicated differently. Significance was determined by two-way ANOVA with tukey test. Abbreviations: HaBPS, benzophenone synthase from Hypericum androsaemum; HsBPS, benzophenone synthase from Hypericum sampsonii; GmBPS, benzophenone synthase from Garcinia mangostana; ScCHS, chalcone synthase from Swertia chirayita; SaBIS1, biphenyl synthase 1 from Sorbus aucuparia; MdBIS1, biphenyl synthase 1 from Malus domestica;, PcBIS1, biphenyl synthase 1 from Pyrus communis; RpBZL, benzoate-CoA ligase from Rhodopseudomonas palustris; PxBCL*$_M$*, benzoate-CoA ligase from Paraburkholderia xenovorans LB400; Ta3HBCL, 4-hydroxy/ 3-hydroxy benzoate CoA ligase from Thaurea aromatica K172; sdgA, 2-hydroxybenzoate-CoA ligase from Streptomyces sp. WA46*

Characterization of selected polyketide production strains

After identification of suitable combinations of BPS/BIS with respective CoA ligases the conversion of the precursor towards the polyketide was done without the use of heavily interfering cerulenin in fatty acid biosynthesis to provide artificially high malonyl-CoA availability. Therefore, *P. taiwanensis* GRC3Δ6MC-II with increased malonyl-CoA availability and without benzoate degradation pathway was used for synthesis of benzoate-derived polyketides to allow direct comparison of the different production pathways.

Highest titers of about 59 ± 9 mg L^{-1} were achieved for 2,4,6-TriHBP from benzoate (Figure 2-15A), while conversion with MdBIS1 resulted in about 1 mg L^{-1} 3,5-dihydroxybiphenyl (Figure 2-15A). The relatively low production of 3,5-dihydroxybiphenyl is in line with reported *in vitro* enzyme kinetics for HsBPS (Huang et al., 2012) and MdBIS1 (Stewart et al., 2017). As above, cinnamate was detectable in small amounts in both conversions. The produced 2,4,6-TriHBP and cinnamate only cumulate to half of the consumed concentration of benzoate (Figure 2-15B), indicating that product instability plays a significant role here.

Promiscuity-based synthesis of 2,3',4,6-TetraHBP from 3-hydroxybenzoate achieved titers of approximately 18 mg L^{-1} (Fig 3 A), with no clear preference for the three tested enzyme combinations as observed previously in the presence of cerulenin (Fig 2B). Synthesis of 4-hydroxycoumarin with PcBIS1-sdgA yielded a titer of about 3.7 ± 2.3 mg L^{-1}, which is orders of magnitude lower compared to previous studies using PqsD as synthase (Choo & Ahn, 2019; Lin et al., 2013). Nevertheless, this demonstrates BIS usability for 4-hydroxycoumarin synthesis, especially because using PqsD as alternative promiscuous synthase in our *Pseudomonas* host resulted in low titers close to the limit of detection. In total, these approaches demonstrate production dependence on malonyl-CoA availability in cultures without cerulenin, enzyme activity of used BPS compared to BIS and *Pseudomonas* as superior host in this application compared to previous studies (Klamrak et al., 2021; Liu et al., 2020).

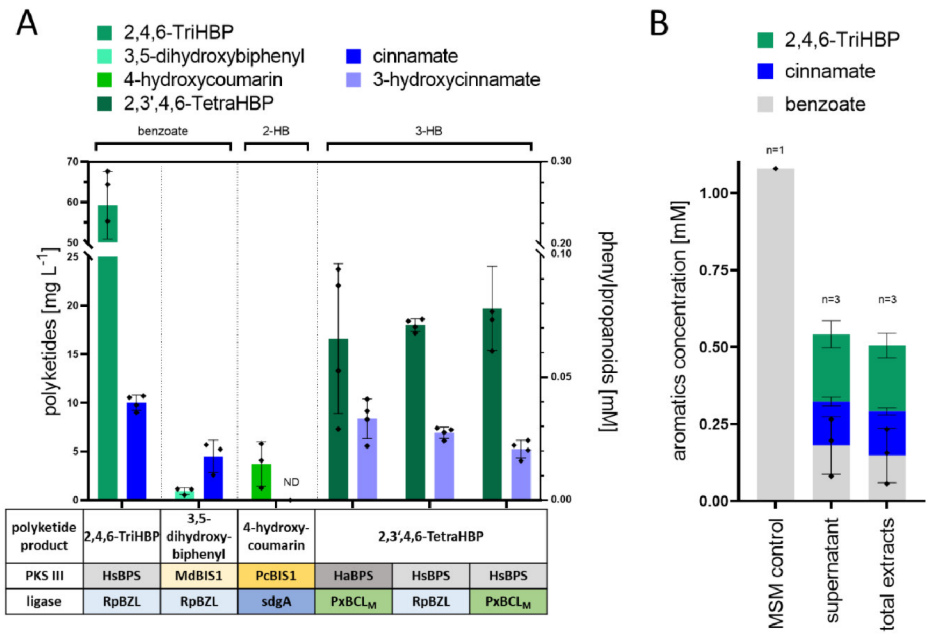

Figure 2-15 Transformation and product stability with selected production strains.
A) Titers of benzoate- and hydroxybenzoate-derived polyketides (green) and phenylpropanoid (blue) from respective supplemented precursors using platform strain GRC3Δ6MC-II with respective pBT'T plasmids. Inoculation OD_{600} was 0.2 in MSM three-fold buffered and 30 mM glucose and 1 mM supplemented precursor benzoate, salicylate or 3-hydroxybenzoate. ***B****) Mass balance of benzoate, cinnamate and 2,4,6-TriHBP in medium control, supernatant and total culture extract. Error bars represent standard deviation (n=4 and n=3). Abbreviation ND, not detected.*

Phenylpropanoids as by-products

In experiments containing benzoate or 3-hydroxybenzoate as precursor, cinnamate and 3-hydroxycinnamate, respectively, were detected by HPLC and GC-ToF MS analysis (Supplementary S6). Cinnamate was not identified as by-product of published BPS *in vitro* characterizations (Nualkaew et al., 2012) or in our experiments using a chalcone synthase which does not accept benzoyl-CoA as substrate (ScCHS, Figure 2-14A). These two aspects indicate that the by-products result from the interaction of the applied PKS III or its catalyzed reaction with the native metabolism of *P. taiwanensis*. Here we propose the formation of phenylpropanoids by an interplay of incomplete tetraketide intermediate formation by PKS III and subsequent conversion in *P. taiwanensis* VLB120 in a partly reversed β-oxidation from overlapping activities (Figure 2-16A). A CoA-activated benzoate or derivative serves as starter unit for benzophenone or biphenyl synthesis. Malonyl-CoA units are subsequently condensed to elongate the carbon chain by two C atoms at a time. In order to yield cinnamic acid it is necessary to reduce the first keto group of the polyketide intermediate by a redox equivalent to a hydroxy group (reaction A), requiring a 3-hydroxyacyl-CoA dehydrogenase activity,

followed by a double bond formation by releasing H_2O (reaction B) by an enoyl-CoA hydratase activity. Lastly, the phenylpropanoyl-CoA is hydrolyzed (reaction C) to obtain free phenylpropanoic acid and CoA. Alternatively, the last reaction could by catalyzed by a CoA-transferase or it could occur through spontaneous hydrolysis. A similar reversed β-oxidation has been described in different hosts (Kallscheuer et al., 2017). Interestingly, 4-hydroxycoumarin synthesis does not result in detectable 2-hydroxycinnamate formation but it is reported that this molecule can spontaneously form coumarin instead. The here observed phenomenon reveals the capability of *Pseudomonas* to utilize PKS III catalytic intermediates through one of its many complex β-oxidation pathways (Thompson et al., 2020). These findings open opportunities for promiscuous application of Pseudomonads' versatile metabolic capabilities for phenylpropanoid synthesis.

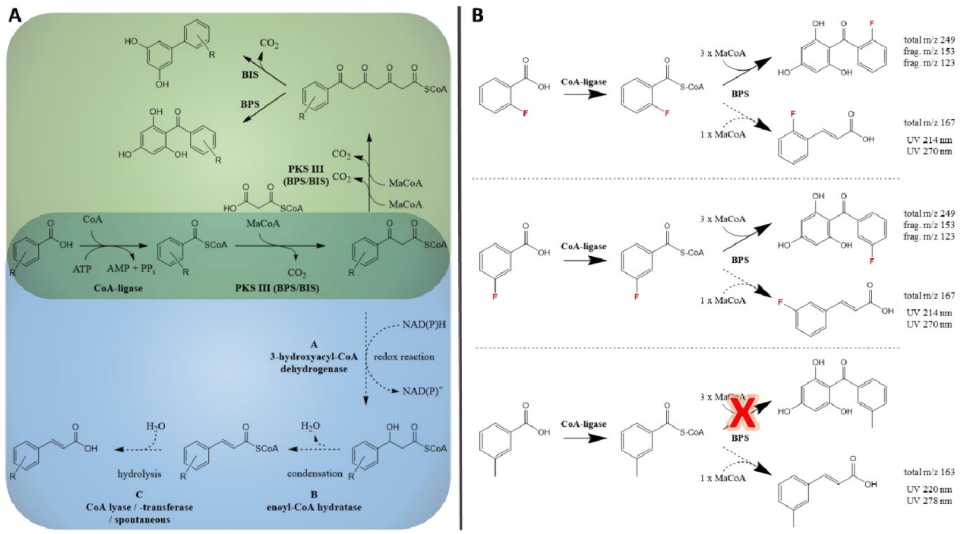

Figure 2-16 By-product formation and mutasynthesis.
A) Schematic reaction of the proposed pathway for phenylpropanoid side-product formation by PKS type III in a heterologous host like P. taiwanensis VLB120. Solid arrows indicate polyketide formation reactions (green region). Dashed arrows indicate putative reactions towards phenylpropanoids (blue region) with indications of required reactions A, B and C. CoA release is not indicated in the illustration. ***B)*** *Schematic conversion products from fluorinated or methylated benzoate precursors in mutasynthesis experiments by CoA ligases and BPS. UV spectra maxima and m/z in H^+ mode of the molecule and respective signature fragments are given (Supplementary S7). Abbreviations: CoA, coenzyme A; MaCoA, malonyl coenzyme A; PKS III, polyketide synthase type III; BPS/BIS, benzophenone synthase / biphenyl synthase; NAD(P)H, nicotinamide adenine dinucleotide (phosphate); frag, signature fragment; UV, ultraviolet*

Mutasynthesis with fluoro-benzoates and methyl-benzoate

The artificial incorporation of fluorine can tune physiochemical features of organic molecules and halogenation also modifies persistence of drugs (Reed & Alper, 2018; Shi et al., 2022). Incorporation of fluorine by PKS III was already demonstrated for flavanones (Abe et al., 2000) and stilbenes (Morita et al., 2001). In order to test weather fluorine can also be incorporated into benzophenones, different

fluoro-benzoate derivatives were used for polyketide formation (Figure 2-16B). Conversion by *P. taiwanensis* GRC3Δ6MC-III with pBT'T plasmids containing different combinations of ligases and BPS or BIS (Figure 2-14, Figure 2-16B) resulted in 2-F-cinnamate and 2,4,6-trihydroxy-2'-F-benzophenone from 2-F-benzoic acid (Supplementary S7). From 3-F-benzoic acid the respective products 3-F-cinnamate and 2,4,6-trihydroxy-3'-F-benzophenone were synthesized (Supplementary S7). However, for the fluoro-benzophenone products several signals were observed in LC-MS/MS analysis relating to the expected m/z and characteristic fragmentation pattern for identification. This also reveals that several products beside the expected main product were formed which might be related to the previously observed product instability in medium. The fluorinated products had a slightly retarded retention time when compared to their natural pendant likely due to weaker van-der-Waals interaction (Dalvi & Rossky, 2010). Semi-quantitative tendencies (Supplementary S7, raw data) reveal RpBZL was the preferred ligase compared to $PxBCL_M$ for 2- and 3-F-benzoate derived products. Use of HaBPS resulted in higher 2- or 3-F-cinnamate signals and HsBPS in higher fluorinated polyketide signals respectively which may reflect the BPS promiscuity and binding affinities towards the respective intermediate products during elongation synthesis.

When using 3-methyl benzoate as supplement the respective conversion product 3-methyl cinnamate was detected but not the corresponding methyl trihydroxybenzophenone (Figure 2-16B, Supplementary S7) which would result from full conversion by a respective BPS. The highest signals for 3-methyl cinnamate were reached when $PxBCL_M$ was used as ligase in conversions. As a control, samples from cultivations without any supplemented precursor resulted in no product formation and addition of benzoate resulted in cinnamate and 2,4,6-TriHBP formation, as expected.

These qualitative detections of fluorinated products indicate that the used ligases and BPSs can accept fluorinated precursors to some extend and that 3-methyl benzoyl-CoA extension by BPSs and BISs are only incomplete. These findings support the understanding of PKS III promiscuity towards starter units and pave the way for future benzophenone derivatization in bioconversions. Additionally, promiscuity opens new opportunities for fluoro-phenylpropanoid synthesis which might be further improved by engineering enzymatic activity towards their synthesis in future which was already in focus for type I PKS systems (Rittner et al., 2022; Sirirungruang et al., 2022). The biggest challenge of protein engineering of PKS III will likely be the lack of high throughput screening assays.

In situ product removal of 2,4,6-TriHBP in two-phase cultivation

Instability of 2,4,6-TriHBP heterologous (hydroxy)benzophenone biosynthesis was previously suggested by Klamrak et al. (2021). A red precipitate was observed when the colored culture supernatant of the toxicity experiment was treated with hydrochloric acid while the liquid remained

yellow (Figure 2-17A). A pure 2,4,6-TriHBP solution remains clear at low pH. Abiotic 2,4,6-TriHBP degradation experiments in medium with different trace element solutions at low pH (Figure 2-17A) led to the assumption that under aerobic conditions, 2,4,6-TriHBP polymerizes to a 'benzoyl-phlorotannin'-like product at moderate pH (>6) and in the presence of iron ions (Wang et al., 2017). According to this hypothesis, iron is either directly reduced from an electron of 2,4,6-TriHBP or from formed radical oxygen species (ROS), subsequently resulting in a phenol coupling reaction (Phang et al., 2023) (Supplementary S8), leading to product loss and potential toxic conversion products.

Given that this product instability is a result of deprotonation and metal ions in medium, ISPR with a water-immiscible organic solvent was considered to avoid this effect by sequestering the instable product (Figure 2-17B). Such *in situ* liquid-liquid extraction can increase overall product titer and facilitate downstream purification. The concept of two-phase partitioning bioreactors is used in environmental biotechnology for treatment of toxic and/or volatile compounds (Malinowski, 2001) but it can also be used as reservoir strategy for the product (Heipieper et al., 2007). Many natural products including polyketides exhibit similar physical properties regarding solubility and partitioning into organic solvents from aqueous solutions (Schönsee & Bucheli, 2020). The used biotechnological host organism defines the degree of freedom in the choice of solvents, and the solvent-tolerant *P. taiwanensis* VLB120 used here allows a wide degree of freedom due its native solvent resistance to saturated solutions of 1-octanol, styrene and others (Blombach et al., 2022).

A solvent screening was performed to identify a suitable extractant for *in situ* product removal. An initial pre-selection was done based on physicochemical properties which were: density ≤ 900 g L^{-1}; boiling point ≥ 120°C; solubility in water ≤ 0.3 g L^{-1}; logP ≥ 3.1; toxicity health score ≤2 (if available) (Grundtvig et al., 2018) and flash point ≥ 95°C. Solvents fulfilling these criteria allow facilitated separation, safe handling, and reduced solvent loss in future applications. Additionally, the low $logP_{O/W}$ boundary takes account of the host's solvent tolerance. This led to the selection of methyl decanoate, ethyl decanoate, dioctyl ether, ethyl oleate, hexadecane, butyl octanoate, isobutyl octanoate, 2-butyl-octanoic acid (CAS 27610-92-0) and 2-hexyldecanoic acid (CAS 25354-97-6) (Supplementary Table S9). Nevertheless, some solvents outside these strict boundaries have a lower flashpoint but a history of previous applications, namely 1-octanol, 1-nonanol, 1-decanol and 2-undecanone (Demling et al., 2020) and were therefore considered as well. These 13 solvents were experimentally tested for their extraction efficiency regarding the product 2,4,6-TriHBP, the by-product cinnamate, the substrate benzoate and the hydrophilic polyketide product flaviolin to evaluate transferability of these results to other applications (Supplementary S10 and Table S11). Additional factors such as liquid-liquid phase separation, (Supplementary S12), biocompatibility (Supplementary S13), and use as sole carbon source by *P. taiwanensis* VLB120 (Supplementary S14) were examined.

The five most suitable solvents are shown in Figure 2-17C. Partitioning of 2,4,6-TriHBP, benzoate, and cinnamate was best for long chain alcohols (Supplementary S10), 2-undecanone and medium-chain-length ester solvents. To consider purification of 2,4,6-TriHBP from benzoate or cinnamate by-products present in culture broth, the separation factor was determined from their respective partitioning coefficients. Phase separation and formation of an undesired interphase was the poorest for the alcohols and the solvents were ranked accordingly (rank 1, poor to rank 5, good) (Supplementary S12). Solvents serving as sole carbon source by *P. taiwanensis* VLB120 were also expressed in a ranking from undesired 'good growth' (rank 1) to 'no growth' (rank 5) (Supplementary S14). As expected all alcohols were consumed as well as isobutyl octanoate which may indicate some promiscuity of native esterases (Lu et al., 2021).

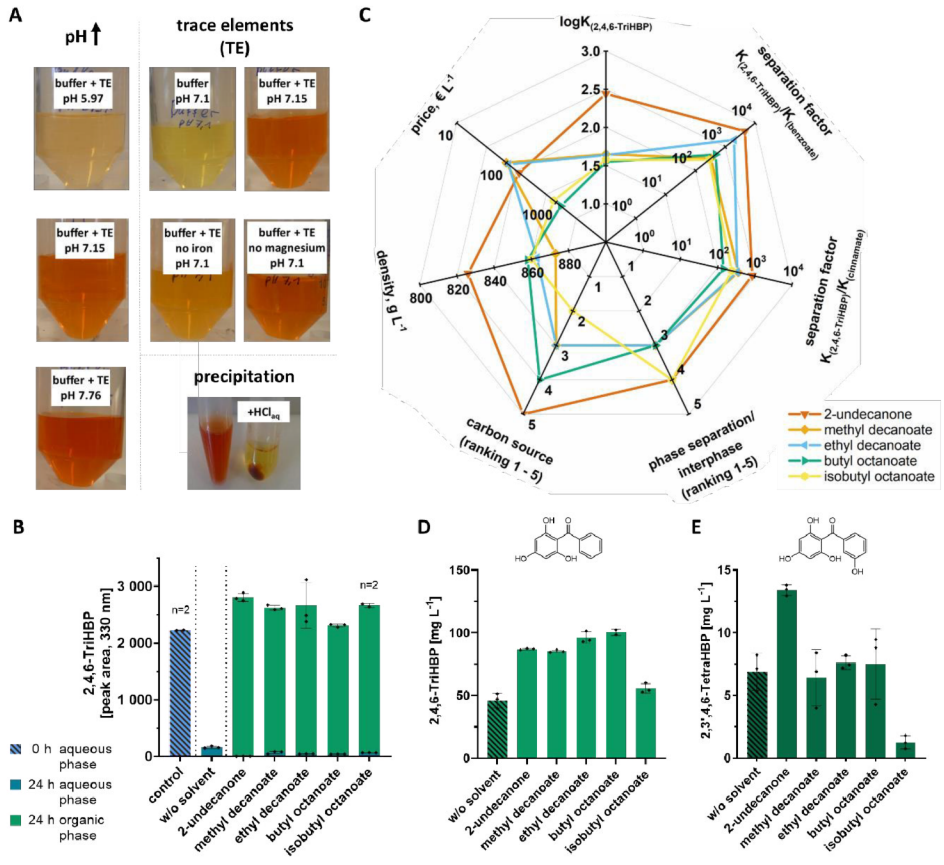

Figure 2-17 Polyketide 2,4,6-TriHBP conversion, solvent screening and application.
A) Images of 2,4,6-TriHBP solutions after 24 hours in phosphate buffer (36 mM) with trace elements (TE) at pH 6, 7.2 and 7.8 (left) and with variations of trace element solution with and without Fe and Mg. Precipitation of conversion product in 2,4,6-TriHBP solution in P_i-buffer before and after addition of HCl_{aq} (bottom). ***B)*** *Remaining 2,4,6-TriHBP (from 1 mM) in MSM with and without a 2:1 ratio of solvent after 24 h.* ***C)*** *Radar chart of selected solvent screening parameters and selected solvents (supplementary S10 to S14 for all considered parameters and solvents in experimental screening procedure).* ***D)*** *Titer of 2,4,6-TriHBP and* ***E)*** *2,3',4,6-TetraHBP in two-phase cultivations from bioconversion by strain GRC3Δ6MC-II pBT'T-HsBPS-RpBZL in*

three-fold buffered MSM (+Km) 30 mM glucose and 2 mM supplemented benzoate or 3-hydroxybenzoate and 20% solvent, respectively. Inoculation occurred with calculated OD_{600} of 0.2. Error bars represent the standard deviations after 24 h (n=3, if not indicated differently). Abbreviation: w/o, without

Considering all criteria, 2-undecanone and medium-chain-length esters were the most promising solvents and increasing the stability of externally added 2,4,6-TriHBP (Figure 2-17B). Thus, these five candidates were tested in biotransformation approaches using 20% (v/v) of the respective solvent as *in situ* extractant (Figure 2-17D, Supplementary S15, S16). These cultures were performed with 30 mM glucose and 1 mM of the respective aromatic precursor, with a starting OD_{600} of 0.2 which is expected to increase to approximately 4 based on online growth measurement. Total 2,4,6-TriHBP titers were approximately doubled from 45 mg·L^{-1} (0.2 mM) to 86.9 mg·L^{-1} (0.378 mM) with 2-undecanone or even 100.4 mg L^{-1} (0.436 mM) with butyl octanoate as solvent phase. However, this was not the case for isobutyl octanoate, in spite of the fact that the latter served as potential additional carbon source. Hence, product concentration within the organic solvent were approximately 2 mM in 2-undecanone. In principle, back-extraction of 2,4,6-TriHBP from 2-undecanone solution can be achieved by an alkaline solution at pH 12 with about 71% efficiency (Supplementary S17).

When using 3-hydroxybenzoate for the 2,3',4,6-TetraHBP production only 2-undecanone increased total product titers from 6.9 ± 1.5 mg L^{-1} (0.028 mM) to 13.4 ± 0.4 mg L^{-1} (0.054 mM) (Figure 2-17E). According to these results, 2-undecanone was the most suitable solvent for *in situ* polyketide extraction. The benefit of using a solvent-tolerant *Pseudomonas* is apparent in direct comparison to different microbes in two-phase cultivations with 2-undecanone, especially compared to yeast or Gram-positive bacteria (Supplementary S19), which was expected due to 2-undecanone's $logP_{O/W}$ of 4.1.

In order to test whether the addition of solvents *per se* can affect polyketide formation, flaviolin as a highly hydrophilic product deriving from malonyl-CoA condensation was produced. Here, no effect was observed for most solvents as expected except for 2-undecanone which even reduced flaviolin titers (Supplement S18). This may be due to structural similarities of the solvent with intermediate condensation products leading to enzyme inhibition by competition. Overall, these results demonstrate the benefit of ISPR for reducing product instability and inhibition. Additionally, it highlights the need to tailor solvent screenings to product, substrate, and microbes accordingly.

Heterologous de novo polyketide synthesis in solvent two-phase cultivation

The supplementation of aromatic precursors for polyketide starter units represents an additional production parameter that increases cost and process complexity and may hinder commercialization as "natural-origin" product. To circumvent this, production modules for benzoate (*attTn7*::*FRT-*P_{14f}*-phdBCDE-Sc4CL-AtPAL2*) (Otto et al., 2020), 3-hydroxybenzoate (*attTn7*::P_{14f}*-LaCH-II*), and

2-hydroxybenzoate (*attTn7*::P_{14g}-*menF-pchB*) were constructed and genomically integrated into the malonyl-CoA platform strain GRC3Δ6MC-III with increased malonyl-CoA availability (Schwanemann, Otto, et al., 2023). The resulting strains were subsequently transformed with pBT'T-based plasmids for the *de novo* synthesis of 2,4,6-TriHBP, 3,5-dihydroxybiphenyl, 2,3',4,6-TetraHBP or 4-hydroxycoumarin. These strains were able to produce the target polyketide fully *de novo*, i.e., in a mineral glucose medium with 2-undecanone for ISPR without supplementation of aromatic precursors. Thus, it is in principle possible to produce them from sustainable resources including the solvent 2-undecanone (Nies et al., 2020). For 2,4,6-TriHBP, 3,5-dihydroxybiphenyl and 2,3',4,6-TetraHBP this represents their first heterologous *de novo* biosynthesis.

As before, the highest titers were achieved with 2,4,6-TriHBP, indicating that in this *de novo* biosynthesis the polyketide production module is the limiting factor. The best producing strains of GRC3Δ6MC-III *attTn7*::*FRT-*P_{14f}*-phdBCDE-sc4CL-atPAL2* pBT'T-*HsBPS-RpBZL* produced 17.9 ± 0.14 mg L^{-1} 2,4,6-TriHBP from 30 mM glucose (Figure 2-18A) which is about a third of what was produced in previous biotransformation approaches (Figure 2-15). The challenging competition for carbon between malonyl-CoA and products of the shikimate pathway needed in polyketide formation were already revealed during construction of the GRC3Δ6MC-III strain (Schwanemann, Otto, et al., 2023). Clonal variation from different transformants was observed for two out of six 2,4,6-TriHBP production strains, as well as for other producers which indicates genetic instability of the combined production modules. However, error margins between replicates of single transformants were small and not significant, enabling reliable production from selected clones. Benzoate formation is a result of the incorporated phenylalanine ammonia-lyase together with the phenylpropanoid degradation pathway that converts cinnamate to benzoate. The well-performing clones produced no cinnamate, while this intermediate was detected in cultures with low 2,4,6-TriHBP titers, suggesting a bottleneck at the level of *phdBCDE* in the latter strains.

Titers of 3,5-dihydroxybiphenyl by strain GRC3Δ6MC-III *attTn7*::*FRT-*P_{14f}*-phdBCDE-sc4CL-atPAL2* pBT'T-*MdBIS1-RpBZL* were around 0.75 mg L^{-1} (Figure 2-18B). Concentrations of benzoate were about three-fold higher (0.15 mM) than in the 2,4,6-TriHBP cultures and no cinnamate was detected. This represents the first heterologous *de novo* 3,5-dihydroxybiphenyl biosynthesis, while the relatively low titers highlight the potential of engineering BIS kinetics applicable in biotechnological productions.

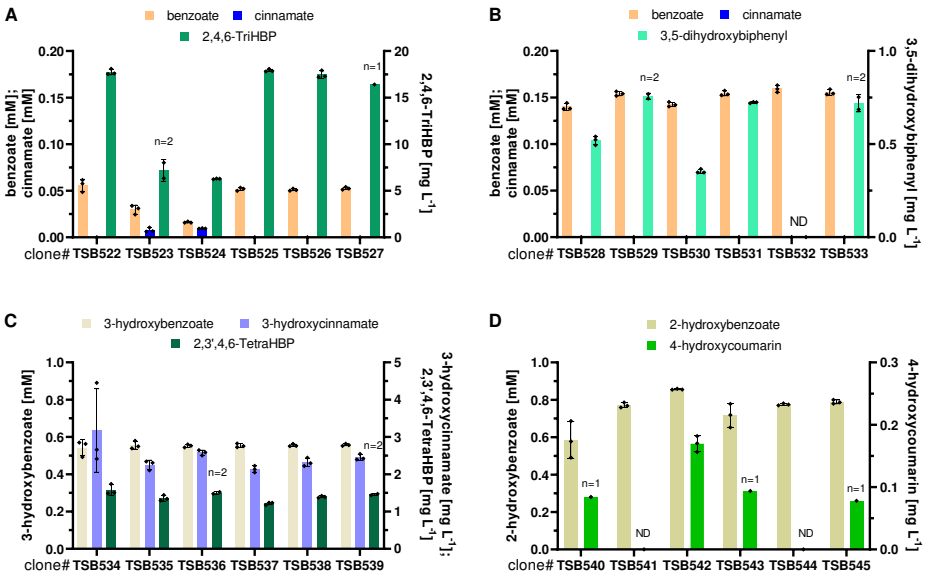

Figure 2-18 Two-phase cultivation for de novo product biosynthesis.
A) Titers of benzoate, cinnamate and 2,4,6-TriHBP from strain GRC3Δ6MC-III attTn7::FRT-P14f-phdBCDE-sc4CL-atPAL2 pBT'T-HsBPS-RpBZL; ***B)*** *titers of benzoate, cinnamate and 3,5-dihydroxybiphenyl from strain GRC3Δ6MC-III* attTn7::FRT-P_{14f}-phdBCDE-sc4CL-atPAL2 *pBT'T*-MdBIS1-RpBZL*;* ***C)*** *titers of 3-hydroxybenzoate, 3-hydroxycinnamate and 2,3',4,6-TetraHBP from strain GRC3Δ6MC-III* attTn7::P_{14f}-LaCH-II *pBT'T*-HsBPS-RpBZL*;* ***D)*** *titers of 2-hydroxycinnamate and 4-hydroxycoumarin from strain GRC3Δ6MC-III* attTn7::P_{14g}-menF-pchB *pBT'T*-PcBIS1-sdgA *from 30 mM glucose in* de novo *biosynthesis in two-phase cultivation with 20% (v/v) solvent. Error bars represent standard deviation of three replicates (n=3) if not indicated differently. Abbreviation: ND, not detected; TSB522-545, individual strain number. Significance was determined by two-way ANOVA with tukey test.*

With the 2,3',4,6-TetraHBP production strain, titers of approximately 1.6 mg L^{-1} were achieved without significant differences between tested clones (Figure 2-18C). In this strain, the 3-hydroxybenzoate precursor is synthesized via a chorismatase type II enzyme from *Lentzea aerocolonigenes* (LaCH-II, Supplementary Table S4) (Grüninger et al., 2019). This one-step synthesis of 3-hydroxybenzoate from chorismate resulted in much higher precursor titers up to 0.55 mM, even though this strain is not engineered in its shikimate pathway. Interestingly, the concentration of this PKS-synthesized by-product 3-hydroxycinnamate (2.5 mg L^{-1}) was higher than that of the main product 2,3',4,6-TetraHBP, again highlighting the *in vivo* drain of polyketide intermediates as described above in the biotransformation experiments. This is likely a result of disadvantageous BPS kinetics to alternative starting substrates in combination with increased Km for malonyl-CoA extender units for alternative starters (Chizzali et al., 2016; Huang et al., 2012). Identification of a specific BPS sequence for 3-hydroxybenzoyl-CoA, plus deletion of β-oxidation genes responsible for PKS-intermediate conversion may thus improve heterologous 2,3',4,6-TetraHBP synthesis.

4-Hydroxycoumarin synthesis requires 2-hydroxybenzoate formation from chorismate in two-steps by an isochorismate synthase (menF, Supplementary Table S4) and isochorismate pyruvate lyase (pchB, Supplementary Table S4). Up to 0.85 mM 2-hydroxybenzoate were produced by strain GRC3Δ6MC-III *attTn7*::P_{14f}-*menF-pchB* pBT'T-*PcBIS1-sdgA* (Figure 2-18D) revealing dependency on used precursor production modules. Exploiting biphenyl synthase side-activity for salicyl-CoA conversion product was inefficient because product titers, if obtained any, were close to the detection limit to allow characteristic UV spectra and reached up to 0.17 mg L^{-1} 4-hydroxycoumarin. Nevertheless, the successful *de novo* 4-hydroxycoumarin synthesis by biphenyl synthases demonstrates the broad applicability of BIS (Liu et al., 2010) as an alternative to other already established synthesis routes (Lin et al., 2013).

A combination of genetic modules for polyketide and precursor synthesis enabled completely *de novo* production from glucose, but the relatively low product titers compared to cultures with supplementation of benzoate, 3-hydroxybenzoate or 2-hydroxybenzoate will likely make the biotransformation approach more efficient. Further evaluation is needed here with regard to process intensifications including higher substrate and biomass concentrations to boost product titers.

Conclusion

This study achieved microbial synthesis of plant-benzophenones, 3,5-dihydroxybiphenyl, and 4-hydroxycoumarin. *P. taiwanensis* GRC3Δ6 MC-III proved an efficient host, thriving in two-phase cultivations with 2-undecanone for ISPR to enhance product titers and stability. Mutasynthesis approaches enabled the proof-of-principle production of methylated and fluorinated polyketides, which may be further increased if PKS can be tailored to the specific precursors. In summary, this study establishes a versatile *Pseudomonas* production platform in an aqueous-organic two-phase cultivation for the synthesis of polyketides with a broad application range, which can be further enhanced by process intensification, and expanded by the implementation of new precursor-pathway combinations.

Declaration of competing interest

The authors declare no competing interest.

Acknowledgements

The authors are thankful to Prof. Ludger Beerhues and Dr. Benye Liu from the Institute of Pharmaceutical Biology at Technical University of Braunschweig for their kind gifts of plasmids containing RpBZL, HaBPS, HsBPS and SaBIS1 and to provide reference UV spectra of products, as well as for fruitful scientific discussions. Additionally, TS is thankful to Julian Greb for discussions and input about the 2,4,6-TriHBP polymerization hypothesis.

Funding

T.S. gratefully acknowledges the support by the German Federal Environmental Foundation (DBU) [PhD Scholarship 20019/638-32] and German Academic Exchange Service (DAAD) [scholarship 57556281]; C.E., H.H., B.W. and N.W. thank the German Federal Ministry of Education and Research (BMBF) with the project NO-STRESS [FKZ 031B0852A and 031B0852C]. NW further acknowledges funding from the European Union (ERC, PROSPER, 101044949). The financial support from The Novo Nordisk Foundation through grants NNF20CC0035580, LiFe (NNF18OC0034818) and TARGET (NNF21OC0067996), the Danish Council for Independent Research (SWEET, DFF-Research Project 8021-00039B), and the European Union's Horizon 2020 Research and Innovation Programme under grant agreement No. 814418 (SinFonia) to P.I.N. is gratefully acknowledged. N.K. gratefully acknowledges the support of the Novo Nordisk Foundation Postdoctoral Fellowship for research within biotechnology-based synthesis and production: DF2AP2 (NNF20OC0065068).

3. General discussion and perspectives

3.1. Engineering strategies for malonyl-CoA availability and future applications

This thesis compiles and tests multiple genetic engineering approaches of *P. taiwanensis* GRC3 strains for increased availability of malonyl-CoA for the synthesis of polyketide products. The essential use of malonyl-CoA for fatty acid and lipid biosynthesis makes the engineering of increased accumulation a particular complex challenge (Milke & Marienhagen, 2020). Since availability of malonyl-CoA in FAS likely determines the overall cellular concentration, increased conversion of acetyl-CoA to malonyl-CoA by ACC allows only a modest increase in polyketide formation. Consequently, the competing FAS and polyketide formation are tightly regulated in native polyketide producers e.g. in the Streptomycetaceae family (C. Y. Lin et al., 2020; Lyu et al., 2020; Maharjan et al., 2010). As a conclusion, the insertion of malonyl-CoA consuming reaction steps represents a metabolic burden and neither the increase of supply reactions nor streamlining of upstream carbon flux necessarily result in increased productivity of polyketide products.

Here, a key to higher productivity was the use of an alternative β-ketoacyl-ACP synthase FabF-2 with so far uncharacterized substrate profile and kinetic parameters. As one of the two pace-making enzymes during FAS, the exchange of FabF-activity by inserting *fabF-2* represents a genetically stable modification. In contrast, the downregulation of several FAS-related genes frequently occurred by interference of expression strength by nucleotide-based regulation whose long-term genetic stability can be questionable (J. long Liang et al., 2016; Tao et al., 2018; D. Yang et al., 2018; Y. Yang et al., 2015). As FabF-2 was discovered in *P. putida* F1 (H. Dong et al., 2021) and is also encoded by PP_3303 in *P. putida* KT2440, a simple deletion of *fabF* or *fabB* in different species of *Pseudomonas* might be possible, making use of the lower affinity for malonyl-ACP by this homolog enzyme. A similar approach would apply to some malonyl-CoA platform strains of *C. glutamicum* (Kallscheuer et al., 2016; Milke, Ferreira, et al., 2019; Milke, Kallscheuer, et al., 2019), which contain an alternative native *fasB* (Nickel et al., 2010; Radmacher et al., 2005) that could fulfill the function of the native type I FAS enzyme, FasA. Malonyl-CoA availability is dependent on the downstream affinity (K_M) in FAS and cerulenin experiments demonstrated further room for improvement in *P. taiwanensis* GRC3Δ6 MC-III. However, engineered hosts have to stay vital with sufficient growth for reliable handling. Further mutants of either FabF or FabB seem promising targets for improved strain variants of *P. taiwanensis* GRC3Δ6 MC-III if the effects are not too detrimental for subsequent handling.

The benefit of the deletion of the Gcd is a rather *Pseudomonas*-specific effect due to altered redox metabolite formation from intracellular hexose oxidation reactions which eventually lead to an altered CoA metabolism (Gläser et al., 2020). However, the observation that NADPH formation and product synthesis from malonyl-CoA may be dependent on each other is of importance for other approaches

of secondary metabolite formation by Pseudomonads. Additionally, the ability of high NADPH availability due to the carbon catabolism of *Pseudomonas* can transform Pseudomonads into pivotal hosts for challenging-to-produce compounds. The formation of benzoate-based polyketides in this thesis has already demonstrated the potential as a platform organism.

Besides NADPH as a key-feature, increased substrate uptake can lead to a broad applicability of *P. taiwanensis* for multiple purposes. While experiments with the glucose facilitator protein in different strains were performed in this thesis, the actual glucose uptake rate needs further investigation. Variation in substrate uptake rate can lead to major carbon rearrangement within the central carbon metabolism and hence in a changed supply of different side pathways like FAS or the shikimate pathway. Due to its broad applicability, the use of Glf_{Zm} has the potential to increase productivity not only for those products depicted in this thesis but also for other products such as rhamnolipids and other surfactants or compounds with glycosylation.

Previously published microbial hosts for polyketide synthesis were often cultivated in media with higher substrate concentration than the 30 mM glucose used as sole carbon and energy source in this thesis. *C. glutamicum* DelAro^4, an engineered host for the synthesis of naringenin and resveratrol produced only 12 mg L^{-1} from 40 g L^{-1} glucose without any supplements and up to 158 mg L^{-1} with cerulenin and tyrosine (Kallscheuer et al., 2016). Up to 30 mg L^{-1} resveratrol from 80 g L^{-1} glucose was reached in batch fermentation due to product instability in the presence of an elevated oxygen supply. Yield-wise, the here developed *P. taiwanensis* GRC3Δ6 MC-III and MC-IV outperform these early results of *C. glutamicum* DelAro^4. A more recent generation of *C. glutamicum* platform strain, *C. glutamicum* DelAro^4-4cl C7 mufasO_{BCD1} was able to produce up to 1.71 g L^{-1} (0.26 mM h^{-1}; $Y_{mol(RES)/mol(p\text{-coumarate})}$ = 0.92) resveratrol in two-phase fed-batch cultivations with tributyrin as extractant (Tharmasothirajan et al., 2021). This approach highlights the enormous benefit of product separation in production processes of polyketide products. In shaken batch cultures, that strain produced up to 52 ± 2.2 mg L^{-1} resveratrol from 220 mM glucose. However, these achievements were already outperformed by the here presented results, where 84 mg L^{-1} resveratrol was reached from 30 mM glucose with *P. taiwanensis* GRC3Δ6 MC-III (Schwanemann, Otto, et al., 2023) or even up to 98 mg L^{-1} resveratrol by *P. taiwanensis* GRC3Δ6 MC-IV based producers. Biphasic production experiments have already proved the ability to double titers for hydroxybenzophenone synthesis by *P. taiwanensis* GRC3Δ6 MC-II deriving strains in this work (Schwanemann et al., 2023). Consequently, biphasic fed-batch cultivation for resveratrol production with strain *P. taiwanensis* GRC3Δ6 MC-IV containing the stilbene module for *p*-coumarate transformation would be highly promising to obtain high-titer resveratrol production.

The rational construction of malonyl-CoA platform strains showed that malonyl-CoA consumption reactions represent the major target for metabolic engineering in *Pseudomonas*. Although direct

quantification of intracellular malonyl-CoA was not completed (Supplementary IV), the relative increases were observed by altered product concentrations which were synthesized from malonyl-CoA. The product range obtained in this work includes polyketides made exclusively from malonyl-CoA, such as flaviolin, and those obtained from the conversion of aromatic CoA-ester precursors resulting in pinosylvin, resveratrol, 2,4,6-TriHBP, 2,3',4,6-TetraHBP, 3,5-dihydroxybiphenyl, 4-hydroxycoumarin, phenylpropanoids and fluorinated derivatives of some of the products.

In future applications of the obtained platform strains, they could be equipped with diverse production modules for plant-polyketides such as flavonoids by the implementation of a suitable pathway (consisting of 4CL, CHS, CHI and CHIL), or raspberry ketone pathway (consisting of 4CL, BAS and BAR) (Milke et al., 2020). The latter might be promising for *Pseudomonas* as a host due to the required NADPH-dependent reduction step. Other products, like *Pseudomonas protegens*-derived phloroglucinol or diacetyl phloroglucinol (DAPG) represent microbial antibiotics (F. Yang & Cao, 2012) that might contribute to solving the antibiotics crisis. Although natural producers are available (Nakata et al., 1999), heterologous synthesis in a related species that is malonyl-CoA optimized might be of great interest, especially for the antibiotic DAPG. Interestingly, DAPG is formed by enzymatically catalyzed Friedel-Crafts acylation on an aromatic ring (Pavkov-Keller et al., 2019), with substrates structurally closely related to the produced polyketide 2,4,6-TriHBP in this thesis. Promiscuity experiments of the respective enzyme revealed a broad substrate range (Żądło-Dobrowolska et al., 2019) and even allowed the synthesis of alternative acylbenzophenone products with a mutant variant of that enzyme (Żądło-Dobrowolska et al., 2020). Additionally, phloroglucinol can be chlorinated to yield 2,4-dichlorobenzene-1,3,5-triol, which allows mutasynthesis already during the biosynthesis (Qing Yan et al., 2021) and thus highlights the large spectrum of possible further natural modifications of phloroglucinols, including phlorobenzophenones. Alternatively, the here discovered, successful malonyl-CoA engineering strategies can be applied in natural producers to increase their productivity.

The list of possible polyketide products appears endless (Morita et al., 2019), especially when exploring those polyketides that are not exclusively made by PKS III, but also those produced by PKS I and II. Substances with the most pharmacological potential often derive from more complex PKS or NRPS (Weissman & Leadlay, 2005), but also use methylmalonyl-CoA and other CoA-esters as condensation units. Thus, the here obtained malonyl-CoA platform strains pave the way for future polyketide production projects with Pseudomonads.

3.2. Perspective of two-phase cultivations and scale-up

The concept of two-phase cultivation with solvents for ISPR was able to show its high potential for challenging biosynthesis tasks in the presented thesis. Product instability and toxicity were addressed

and circumvented by cultivation with an organic layer of 2-undecanone. However, the characterization of product 2,4,6-TriHBP led to a proposed polymerization at pH>6. An alternative approach to circumvent product loss would be heterologous biosynthesis at low pH and consequently would require an altered host organism with a preference for acidic cultivation conditions. On the other hand, the protonated form of 2,4,6-TriHBP has a higher membrane solubility according to the performed pH-dependent partitioning experiment with 1-octanol. However, product stability and toxicity are opposed and dependent on cultivation pH in which stability might be of higher importance.

The use of organic solvents with high extraction efficiencies is also limited to specialized organisms and not suitable for all tested polyketide products like in the case of flaviolin. Whether the negative effect of 2-undecanone was specific to flaviolin biosynthesis or generally applicable to more hydrophilic polyketides remains unclear. Alternative approaches to overcome these limitations of solvent-water biphasic systems are the use of impregnated resins or aqueous two-phase partitioning cultivations. Due to the larger size of the particles in an impregnated resign approach, solvent toxicity plays a minor role because they cannot accumulate in the host's membrane. Additionally, they have been successfully applied for example for phenol synthesis (Van Den Berg et al., 2008). Alternatively, the aqueous two-phase partitioning reactor concept is usually considered for protein synthesis and ISPR (Soares et al., 2015). PEG-salts and certain ionic liquids are used as extraction phase but phase separation and water solubility are highly inferior to the here-tested organic solvents (Phong et al., 2018).

As the extraction efficiencies of 2-undecanone and long-chain alcohols were outperforming the other tested solvents in the solvent screening, 2-undecanone might be a good alternative to alcohols as extractants and could serve as alternative to previously published approaches which relied on long-chain alcohol solvents like 1-octanol or 1-decanol (Schwanemann et al., 2020). 2-undecanone combines both, the extraction efficiency of the alcohols and good phase separation observed by ester solvents. The fact that methyl ketones are currently of interest for alternative synthetic fuels and are also produced by microbes is promising to obtain 2-undecanone from sustainable resources (J. Dong et al., 2019; Goh et al., 2012; Nies et al., 2020; J. Park et al., 2012; Qiang Yan et al., 2022).

In addition to polyketide synthesis from different benzoic acids, the here presented two-phase cultivation strategy should also be tested for resveratrol synthesis and other phenylpropanoid-derived polyketides because ISPR was already shown to improve titers (Tharmasothirajan et al., 2021). In order to see if the inhibitory effect of 2-undecanone on flaviolin applies to other solely malonyl-CoA-derived polyketide products other type III PKS and also certain PKS I and II should be tested such as 6-methylsalicylate synthesis by PKS I ChlB1 (Kallscheuer, Kage, et al., 2019).

3.3. Conclusion and impact of this thesis

The successfully shown heterologous synthesis of polyketides, especially those obtained from benzoate derivatives, represents the first of its kind for some of the products as an alternative to isolation from natural resources. The mutasynthesis, to obtain products containing fluorine or methyl groups, was successful but limited by poor enzyme kinetics, which may be addressed by modifying the active site/cavity of BPS by directed enzyme evolution. Additionally, the mutasynthesis was used for the synthesis of new-to-nature phenylpropanoids. The latter was possible due to the discovered ability of *P. taiwanensis* VLB120 to convert intermediate polyketide products by native metabolic activity to phenylpropanoids. In this work, a reverse β-oxidation for the observed phenomenon was proposed but the elucidation of the respective genes would require further proof by control experiments with β-oxidation-deficient strains (S. Liu et al., 2023).

The metabolic network and genes of FAS in *P. taiwanensis* VLB120 were proposed in this work but regulation remains unclear due to limited homology to known FAS of other organisms. Nevertheless, the obtained platform strains *P. taiwanensis* GRC3Δ6 MC-III and *P. taiwanensis* GRC3Δ6 MC-IV have shown their potential for resveratrol synthesis and other malonyl-CoA products. As these strains outperform other established hosts in shaken cultures, the most promising next step for increasing production is the fermentation in fed-batch mode and further process development to obtain high-titers.

The selection of 2-undecanone from a solvent screening and subsequent successful increase in the production of benzoate-derived polyketides represents a first proof-of-principle towards a transferable integrated production approach for secondary metabolites. To demonstrate the "Plug&Play" concept (Figure 1-6) in more depth, it should be applied to all obtained production modules from this work (Supplementary V). Thereby, *Pseudomonas* can be challenged and established as a biotechnological host for polyketide synthesis with reduced effort for process intensification for varying products. The use and sharing of the engineered bacterial platform strains and metabolic engineering strategies of this thesis is therefore highly recommended to obtain sustainable polyketide production for a bioeconomy future.

4. References

Abbas, A., McGuire, J. E., Crowley, D., Baysse, C., Dow, M., & O'Gara, F. (2004). The putative permease PhlE of *Pseudomonas fluorescens* F113 has a role in 2,4-diacetylphloroglucinol resistance and in general stress tolerance. *Microbiology*, *150*(7), 2443–2450. https://doi.org/10.1099/mic.0.27033-0

Abe, I., Morita, H., Nomura, A., & Noguchi, H. (2000). Substrate specificity of chalcone synthase: Enzymatic formation of unnatural polyketides from synthetic cinnamoyl-CoA analogues. *Journal of the American Chemical Society*, *122*(45), 11242–11243. https://doi.org/10.1021/ja0027113

Abe, Ikuro. (2020). Biosynthesis of medicinally important plant metabolites by unusual type III polyketide synthases. *Journal of Natural Medicines*, *74*(4), 639–646. https://doi.org/10.1007/s11418-020-01414-9

Abe, Ikuro, & Morita, H. (2010). Structure and function of the chalcone synthase superfamily of plant type III polyketide synthases. *Natural Product Reports*, *27*(6), 809–838. https://doi.org/10.1039/b909988n

Abubakar, A. R., & Haque, M. (2020). Preparation of Medicinal Plants: Basic Extraction and Fractionation Procedures for Experimental Purposes. *Journal of Pharmacy & Bioallied Sciences*, *12*(1), 1. https://doi.org/10.4103/JPBS.JPBS_175_19

Ackermann, Y. S., Li, W.-J., Op de Hipt, L., Niehoff, P.-J., Casey, W., Polen, T., Köbbing, S., Ballerstedt, H., Wynands, B., O'Connor, K., Blank, L. M., & Wierckx, N. (2021). Engineering adipic acid metabolism in *Pseudomonas putida*. *Metabolic Engineering*, *67*(February), 29–40. https://doi.org/10.1016/j.ymben.2021.05.001

Aguilar, A., Twardowski, T., & Wohlgemuth, R. (2019). Bioeconomy for Sustainable Development. In *Biotechnology Journal* (Vol. 14, Issue 8). https://doi.org/10.1002/biot.201800638

Alara, O. R., Abdurahman, N. H., & Ukaegbu, I. (2021). Extraction of phenolic compounds: A review. *Current Research in Food Science*, *4*, 200–214. https://doi.org/10.1016/j.crfs.2021.03.011

Allen, L., O'Connell, A., & Kiermer, V. (2019). How can we ensure visibility and diversity in research contributions? How the Contributor Role Taxonomy (CRediT) is helping the shift from authorship to contributorship. *Learned Publishing*, *32*(1), 71–74. https://doi.org/10.1002/leap.1210

Amaral, P. F. F., Freire, M. G., Rocha-Leão, M. H. M., Marrucho, I. M., Coutinho, A.P., J., & Coelho, M. A. Z. (2007). Optimization of oxygen mass transfer in a multiphase bioreactor with perfluorodecalin as a second liquid phase. *Biotechnology and Bioengineering*, *99*(3), 588–598. https://doi.org/10.1002/bit.21640

An, R., & Moe, L. A. (2016). Regulation of pyrroloquinoline quinone-dependent glucose dehydrogenase activity in the model rhizosphere-dwelling bacterium *Pseudomonas putida* KT2440. *Applied and Environmental Microbiology*, *82*(16), 4955–4964. https://doi.org/10.1128/AEM.00813-16

Arnold, F. H., & Volkov, A. A. (1999). Directed evolution of biocatalysts. *Current Opinion in Chemical Biology*, *3*(1), 54–59. https://doi.org/10.1016/S1367-5931(99)80010-6

Asani, P. C., Baradia, H., Chattopadhyay, S., Kumar, M., & Kumar, S. M. (2023). Process optimization and techno-economic analysis for the production of lipase from *Bacillus* sp. *Journal of Taibah University for Science*, *17*(1), 2198925. https://doi.org/10.1080/16583655.2023.2198925

Askitosari, T. D., Boto, S. T., Blank, L. M., & Rosenbaum, M. A. (2019). Boosting Heterologous Phenazine Production in Pseudomonas putida KT2440 Through the Exploration of the Natural

Sequence Space. *Frontiers in Microbiology*, *10*(AUG). https://doi.org/10.3389/FMICB.2019.01990

Atanasov, A. G., Zotchev, S. B., Dirsch, V. M., the International Natural Product Sciences Taskforce, & Supuran, C. T. (2021). Natural products in drug discovery: advances and opportunities. *Nature Reviews Drug Discovery*, *20*(3), 200–216. https://doi.org/10.1038/s41573-020-00114-z

Austin, M. B., Bowman, M. E., Ferrer, J.-L., Schröder, J., & Noel, J. P. (2004). An Aldol Switch Discovered in Stilbene Synthases Mediates Cyclization Specificity of Type III Polyketide Synthase. *Chemistry and Biology*, *11*, 1179–1194. https://doi.org/10.1016/j.chembiol.2004.05.024

Austin, M. B., & Noel, J. P. (2003). The chalcone synthase superfamily of type III polyketide synthases. *Natural Product Reports*, *20*(1), 79–110. https://doi.org/10.1039/b100917f

Bae, J. W., Han, J. H., Park, M. S., Lee, S.-G., Lee, E. Y., Jeong, Y. J., & Park, S. (2006). Development of recombinant *Pseudomonas putida* containing homologous styrene monooxygenase genes for the production of (*S*)-styrene oxide. *Biotechnology and Bioprocess Engineering*, *11*, 530–537. https://doi.org/10.1007/2FBF02932079

Bagdasarian, M., Lurz, R., Rückert, B., Franklin, F. C., Bagdasarian, M. M., Frey, J., & Timmis, K. N. (1981). Specific-purpose plasmid cloning vectors II. Broad host range, high copy number, RSF 1010-derived vectors, and a host-vector system for gene cloning in *Pseudomonas*. *Gene*, *16*(1–3), 237–247. https://doi.org/10.1016/0378-1119(81)90080-9

Bangera, M. G., & Thomashow, L. S. (1999). Identification and characterization of a gene cluster for synthesis of the polyketide antibiotic 2,4-diacetylphloroglucinol from *Pseudomonas fluorescens* Q2-87. *Journal of Bacteriology*, *181*(10), 3155–3163. https://doi.org/10.1128/jb.181.10.3155-3163.1999

Baradia, H., Kumar, S. M., & Chattopadhyay, S. (2023). Techno-economic analysis of production and purification of lipase from *Bacillus subtilis* (NCIM 2193). *Preparative Biochemistry & Biotechnology*, 1–6. https://doi.org/10.1080/10826068.2023.2185638

Beerhues, L., & Liu, B. (2009). Biosynthesis of biphenyls and benzophenones - Evolution of benzoic acid-specific type III polyketide synthases in plants. *Phytochemistry*, *70*(15–16), 1719–1727. https://doi.org/10.1016/j.phytochem.2009.06.017

Beld, J., Sonnenschein, E. C., Vickery, C. R., Noel, J. P., & Burkart, M. D. (2014). The phosphopantetheinyl transferases: Catalysis of a post-translational modification crucial for life. *Natural Product Reports*, *31*(1), 61–108. https://doi.org/10.1039/c3np70054b

Bentley, G. J., Narayanan, N., Jha, R. K., Salvachúa, D., Elmore, J. R., Peabody, G. L., Black, B. A., Ramirez, K., De Capite, A., Michener, W. E., Werner, A. Z., Klingeman, D. M., Schindel, H. S., Nelson, R., Foust, L., Guss, A. M., Dale, T., Johnson, C. W., & Beckham, G. T. (2020). Engineering glucose metabolism for enhanced muconic acid production in *Pseudomonas putida* KT2440. *Metabolic Engineering*, *59*, 64–75. https://doi.org/10.1016/j.ymben.2020.01.001

Bergler, H., Wallner, P., Ebeling, A., Leitinger, B., Fuchsbichler, S., Aschauer, H., Kollenz, G., Högenauer, G., & Turnowsky, F. (1994). Protein EnvM is the NADH-dependent enoyl-ACP reductase (FabI) of *Escherichia coli*. *Journal of Biological Chemistry*, *269*(8), 5493–5496.

Bilal, M., Guo, S., Iqbal, H. M. N., Hu, H., Wang, W., & Zhang, X. (2017). Engineering *Pseudomonas* for phenazine biosynthesis, regulation, and biotechnological applications: a review. *World Journal of Microbiology and Biotechnology*, *33*(10), 1–11. https://doi.org/10.1007/s11274-017-2356-9

Birch, A. J., & Donovan, F. W. (1953). Studies in relation to Biosynthesis. I. Some possible routes to derivatives of Orcinol and Phloroglucinol. *Australian Journal of Chemistry*, *6*(4), 360–368.

https://doi.org/10.1071/CH9530360

Bisht, R., Bhattacharyya, A., Shrivastava, A., & Saxena, P. (2021). An Overview of the Medicinally Important Plant Type III PKS Derived Polyketides. *Frontiers in Plant Science*, *12*(October), 1–21. https://doi.org/10.3389/fpls.2021.746908

Bitzenhofer, L. N., Kruse, L., Thies, S., Wynands, B., Lechtenberg, T., Kozaeva, E., Thilo Wirth, N., Eberlein, C., Jaeger, K.-E., Iván Nikel, P., Heipieper, H. J., Wierckx, N., & Loeschcke, A. (2021). Towards robust *Pseudomonas* cell factories to harbour novel biosynthetic pathways. *Essays in Biochemistry*, *in press*(May), 1–18. https://doi.org/https://doi.org/10.1042/EBC20200173

Blank, L. M., Ionidis, G., Ebert, B. E., Bühler, B., & Schmid, A. (2008). Metabolic response of *Pseudomonas putida* during redox biocatalysis in the presence of a second octanol phase. *FEBS Journal*, *275*(20), 5173–5190. https://doi.org/10.1111/j.1742-4658.2008.06648.x

Bligh, E. G., & Dyer, W. J. (1959). A rapid method of total lipid extraction and purification. *Canadian Journal of Biochemistry and Physiology*, *37*(8).

Blin, K., Shaw, S., Augustijn, H. E., Reitz, Z. L., Biermann, F., Alanjary, M., Fetter, A., Terlouw, B. R., Metcalf, W. W., Helfrich, E. J. N., van Wezel, G. P., Medema, M. H., & Weber, T. (2023). antiSMASH 7.0: new and improved predictions for detection, regulation, chemical structures and visualisation. *Nucleic Acids Research*, *51*(W1). https://doi.org/10.1093/NAR/GKAD344

Blin, K., Shaw, S., Steinke, K., Villebro, R., Ziemert, N., Lee, S. Y., Medema, M. H., & Weber, T. (2019). antiSMASH 5.0: updates to the secondary metabolite genome mining pipeline. *Nucleic Acids Research*, *47*(W1), W81–W87. https://doi.org/10.1093/nar/gkz310

Blombach, B., Grünberger, A., Centler, F., Wierckx, N., & Schmid, J. (2022). Exploiting unconventional prokaryotic hosts for industrial biotechnology. *Trends in Biotechnology*, *40*(4), 385–397. https://doi.org/10.1016/j.tibtech.2021.08.003

Bordenave, G. (2003). Louis Pasteur (1822–1895). *Microbes and Infection*, *5*(6), 553–560. https://doi.org/10.1016/S1286-4579(03)00075-3

Bosire, E. M., & Rosenbaum, M. A. (2017). Electrochemical potential influences phenazine production, electron transfer and consequently electric current generation by *Pseudomonas aeruginosa*. *Frontiers in Microbiology*, *8*(MAY), 260405. https://doi.org/10.3389/FMICB.2017.00892/BIBTEX

Braga, A., & Faria, N. (2022). Biotechnological production of specialty aromatic and aromatic-derivative compounds. *World Journal of Microbiology and Biotechnology*, *38*(5). https://doi.org/10.1007/s11274-022-03263-y

Braga, A., Oliveira, J., Silva, R., Ferreira, P., Rocha, I., Kallscheuer, N., Marienhagen, J., & Faria, N. (2018). Impact of the cultivation strategy on resveratrol production from glucose in engineered *Corynebacterium glutamicum*. *Journal of Biotechnology*, *265*(July 2017), 70–75. https://doi.org/10.1016/j.jbiotec.2017.11.006

Brocks, J. J., Nettersheim, B. J., Adam, P., Schaeffer, P., Jarrett, A. J. M., Güneli, N., Liyanage, T., van Maldegem, L. M., Hallmann, C., & Hope, J. M. (2023). Lost world of complex life and the late rise of the eukaryotic crown. *Nature*, *618*, 767–773. https://doi.org/10.1038/s41586-023-06170-w

Bujdoš, D., Popelářová, B., Volke, D. C., Nikel, P. I., Sonnenschein, N., & Dvořák, P. (2023). Engineering of *Pseudomonas putida* for accelerated co-utilization of glucose and cellobiose yields aerobic overproduction of pyruvate explained by an upgraded metabolic model. *Metabolic Engineering*, *75*, 29–46. https://doi.org/10.1016/j.ymben.2022.10.011

Cabrera-Jiménez, R., Tulus, V., Gavaldà, J., Jiménez, L., Guillén-Gosálbez, G., & Pozo, C. (2023).

Microalgae Biofuel for a Heavy-Duty Transport Sector within Planetary Boundaries. *ACS Sustainable Chemistry & Engineering*, *11*(25), 9359–9371. https://doi.org/10.1021/ACSSUSCHEMENG.3C00750

Carus, M., & Dammer, L. (2018). The Circular Bioeconomy - Concepts, Opportunities, and Limitations. *Industrial Biotechnology*, *14*(2), 83–91. https://doi.org/10.1089/ind.2018.29121.mca

Cavalier-Smith, T. (1992). Origins of Secondary Metabolism. *Ciba Foundation Symposium*, *171*, 64–87. https://doi.org/10.1002/9780470514344.CH5

Chan, D. I., & Vogel, H. J. (2010). Current understanding of fatty acid biosynthesis and the acyl carrier protein. *Biochemical Journal*, *430*(1), 1–19. https://doi.org/10.1042/BJ20100462

Chan, Y. A., Podevels, A. M., Kevany, B. M., & Thomas, M. G. (2009). Biosynthesis of polyketide synthase extender units. *Natural Product Reports*, *26*(1), 90–114. https://doi.org/10.1039/b801658p

Chen, Xi, Schreiber, K., Appel, J., Makowka, A., Fähnrich, B., Roettger, M., Hajirezaei, M. R., Sönnichsen, F. D., Schönheit, P., Martin, W. F., & Gutekunst, K. (2016). The Entner-Doudoroff pathway is an overlooked glycolytic route in cyanobacteria and plants. *Proceedings of the National Academy of Sciences of the United States of America*, *113*(19), 5441–5446. https://doi.org/10.1073/pnas.1521916113

Chen, Xiaoxu, Yang, X., Shen, Y., Hou, J., & Bao, X. (2018). Screening phosphorylation site mutations in yeast acetyl-CoA carboxylase using malonyl-CoA sensor to improve malonyl-CoA-derived product. *Frontiers in Microbiology*, *9*(JAN), 1–8. https://doi.org/10.3389/fmicb.2018.00047

Chittori, S., Savithri, H. S., & Murthy, M. R. N. (2011). Crystal structure of *Salmonella typhimurium* 2-methylcitrate synthase: Insights on domain movement and substrate specificity. *Journal of Structural Biology*, *174*(1), 58–68. https://doi.org/10.1016/j.jsb.2010.10.008

Chizzali, C., Swiddan, A. K., Abdelaziz, S., Gaid, M., Richter, K., Fischer, T. C., Liu, B., & Beerhues, L. (2016). Expression of biphenyl synthase genes and formation of phytoalexin compounds in three fire blight-infected *Pyrus communis* cultivars. *PLoS ONE*, *11*(7), 1–16. https://doi.org/10.1371/journal.pone.0158713

Choi, J. W., & Da Silva, N. A. (2014). Improving polyketide and fatty acid synthesis by engineering of the yeast acetyl-CoA carboxylase. *Journal of Biotechnology*, *187*, 56–59. https://doi.org/10.1016/j.jbiotec.2014.07.430

Choi, K. H., Gaynor, J. B., White, K. G., Lopez, C., Bosio, C. M., Karkhoff-Schweizer, R. A. R., & Schweizer, H. P. (2005). A Tn7-based broad-range bacterial cloning and expression system. *Nature Methods*, *2*(6), 443–448. https://doi.org/10.1038/nmeth765

Choi, K. H., Kumar, A., & Schweizer, H. P. (2006). A 10-min method for preparation of highly electrocompetent *Pseudomonas aeruginosa* cells: Application for DNA fragment transfer between chromosomes and plasmid transformation. *Journal of Microbiological Methods*, *64*(3), 391–397. https://doi.org/10.1016/j.mimet.2005.06.001

Choi, S. Y., Lim, S., Cho, G., Kwon, J., Mun, W., Im, H., & Mitchell, R. J. (2020). *Chromobacterium violaceum* delivers violacein, a hydrophobic antibiotic, to other microbes in membrane vesicles. *Environmental Microbiology*, *22*(2), 705–713. https://doi.org/10.1111/1462-2920.14888

Chomczynski, P., & Rymaszewski, M. (2006). Alkaline polyethylene glycol-based method for direct PCR from bacteria, eukaryotic tissue samples, and whole blood. *BioTechniques*, *40*(4), 454–458. https://doi.org/10.2144/000112149

Choo, H. J., & Ahn, J. H. (2019). Synthesis of Three Bioactive Aromatic Compounds by Introducing

Polyketide Synthase Genes into Engineered *Escherichia coli*. *Journal of Agricultural and Food Chemistry*, *67*(31), 8581–8589. https://doi.org/10.1021/acs.jafc.9b03439

Chouhan, S., Sharma, K., Zha, J., Guleria, S., & Koffas, M. A. G. (2017). Recent advances in the recombinant biosynthesis of polyphenols. *Frontiers in Microbiology*, *8*(NOV), 1–16. https://doi.org/10.3389/fmicb.2017.02259

Cochrane, F. C., Davin, L. B., & Lewis, N. G. (2004). The *Arabidopsis* phenylalanine ammonia lyase gene family: Kinetic characterization of the four PAL isoforms. *Phytochemistry*, *65*(11), 1557–1564. https://doi.org/10.1016/j.phytochem.2004.05.006

Cohen, K. M., Finney, S. C., Gibbard, P. L., & Fan, J. (2013). The ICS International Chronostratigraphic Chart. *Episodes*, *36*(3), 199–204.

Collins, L. D., & Daugulis, A. J. (1997). Characterization and optimization of a two-phase partitioning bioreactor for the biodegradation of phenol. *Applied Microbiology and Biotechnology*, *48*(1), 18–22. https://doi.org/10.1007/s002530051008

Collins, L. D., & Daugulis, A. J. (1999). Benzene/toluene/p-xylene degradation. Part I. Solvent selection and toluene degradation in a two-phase partitioning bioreactor. *Applied Microbiology and Biotechnology*, *52*(3), 354–359. https://doi.org/10.1007/s002530051531

Coppens, L., & Lavigne, R. (2020). SAPPHIRE: a neural network based classifier for σ70 promoter prediction in *Pseudomonas*. *BMC Bioinformatics*, *21*(1), 415. https://doi.org/10.1186/s12859-020-03730-z

Cronan, J. E. (2014a). Biotin and Lipoic Acid: Synthesis, Attachment and Regulation. *EcoSal Plus*, *6*(1), 139–148. https://doi.org/doi:10.1128/ecosalplus.ESP-0001-2012

Cronan, J. E. (2014b). The chain-flipping mechanism of ACP (acyl carrier protein)-dependent enzymes appears universal. *Biochemical Journal*, *460*(2), 157–163. https://doi.org/10.1042/BJ20140239

Cronan, J. E. (2021). The Classical, Yet Controversial, First Enzyme of Lipid Synthesis: *Escherichia coli* Acetyl-CoA Carboxylase. *Microbiology and Molecular Biology Reviews*. https://doi.org/10.1128/mmbr.00032-21

Cronan, J. E., & Thomas, J. (2009). Bacterial fatty acid synthesis and its relationships with polyketide synthetic pathways. In *Methods in Enzymology* (1st ed., Vol. 459, Issue B). Elsevier Inc. https://doi.org/10.1016/S0076-6879(09)04617-5

Cros, A., Alfaro-Espinoza, G., Maria, A. De, Wirth, N. T., & Nikel, P. I. (2022). Synthetic metabolism for biohalogenation. *Current Opinion in Biotechnology*, *74*, 180–193. https://doi.org/10.1016/j.copbio.2021.11.009

Crosby, H. A., Rank, K. C., Rayment, I., & Escalante-Semerena, J. C. (2012). Structure-guided expansion of the substrate range of methylmalonyl coenzyme a synthetase (MatB) of *Rhodopseudomonas palustris*. *Applied and Environmental Microbiology*, *78*(18), 6619–6629. https://doi.org/10.1128/AEM.01733-12

Cui, P., Zhong, W., Qin, Y., Tao, F., Wang, W., & Zhan, J. (2020). Characterization of two new aromatic amino acid lyases from actinomycetes for highly efficient production of *p*-coumaric acid. *Bioprocess and Biosystems Engineering*, *43*(7), 1287–1298. https://doi.org/10.1007/s00449-020-02325-5

Da, R., Ferreira, G., Rodrigues Azzoni, A., & Freitas, S. (2018). Techno-economic analysis of the industrial production of a low-cost enzyme using *E. coli*: the case of recombinant β-glucosidase. *Biotechnol Biofuels*, *11*, 81. https://doi.org/10.1186/s13068-018-1077-0

Dafoe, J. T., & Daugulis, A. J. (2014). In situ product removal in fermentation systems: Improved

process performance and rational extractant selection. *Biotechnology Letters*, *36*(3), 443–460. https://doi.org/10.1007/s10529-013-1380-6

Dalvi, V. H., & Rossky, P. J. (2010). Molecular origins of fluorocarbon hydrophobicity. *Proceedings of the National Academy of Sciences of the United States of America*, *107*(31), 13603–13607. https://doi.org/10.1073/pnas.0915169107

Damalas, S. G., Batianis, C., Martin-Pascual, M., de Lorenzo, V., & Martins dos Santos, V. A. P. (2020). SEVA 3.1: enabling interoperability of DNA assembly among the SEVA, BioBricks and Type IIS restriction enzyme standards. *Microbial Biotechnology*, *0*, 1–14. https://doi.org/10.1111/1751-7915.13609

Darwin, C. (1859). *On the origin of species by means of natural selection, or, The preservation of favoured races in the struggle for life* (1. edition). John Murray. https://www.nhmshop.co.uk/on-the-origin-of-species.html

Daugulis, A. J. (2001). Two-phase partitioning bioreactors: A new technology platform for destroying xenobiotics. *Trends in Biotechnology*, *19*(11), 457–462. https://doi.org/10.1016/S0167-7799(01)01789-9

Davies, K. M., Jibran, R., Zhou, Y., Albert, N. W., Brummell, D. A., Jordan, B. R., Bowman, J. L., & Schwinn, K. E. (2020). The Evolution of Flavonoid Biosynthesis: A Bryophyte Perspective. *Frontiers in Plant Science*, *11*(February), 1–21. https://doi.org/10.3389/fpls.2020.00007

de Almeida, M. A., & Colombo, R. (2021). Production Chain of First-Generation Sugarcane Bioethanol: Characterization and Value-Added Application of Wastes. *BioEnergy Research*, *16*(2), 924–939. https://doi.org/10.1007/S12155-021-10301-4

De Bont, J. A. m. (1998). Solvent-tolerant bacteria in biocatalysis. *Trends in Biotechnology*, *16*(12), 493–499. https://doi.org/10.1016/S0167-7799(98)01234-7

De Clerck, O., Bogaert, K. A., & Leliaert, F. (2012). Diversity and Evolution of Algae: Primary Endosymbiosis. *Advances in Botanical Research*, *64*, 55–86. https://doi.org/10.1016/B978-0-12-391499-6.00002-5

De Las Heras, A., Carreño, C. A., & De Lorenzo, V. (2008). Stable implantation of orthogonal sensor circuits in Gram-negative bacteria for environmental release. *Environmental Microbiology*, *10*(12), 3305–3316. https://doi.org/10.1111/j.1462-2920.2008.01722.x

De Paepe, B., Maertens, J., Vanholme, B., & De Mey, M. (2018). Modularization and Response Curve Engineering of a Naringenin-Responsive Transcriptional Biosensor. *ACS Synthetic Biology*, *7*(5), 1303–1314. https://doi.org/10.1021/acssynbio.7b00419

de Smet, M. J., Wynberg, H., & Witholt, B. (1981). Synthesis of 1,2-epoxyoctane by *Pseudomonas oleovorans* during growth in a two-phase system containing high concentrations of 1-octene. *Applied and Environmental Microbiology*, *42*(5), 811–816. https://doi.org/10.1128/aem.42.5.811-816.1981

de Smet, Marie Jose, Kingma, J., Wynberg, H., & Witholt, B. (1983). *Pseudomonas oleovorans* as a tool in bioconversions of hydrocarbons: growth, morphology and conversion characteristics in different two-phase systems. *Enzyme and Microbial Technology*, *5*(5), 352–360. https://doi.org/10.1016/0141-0229(83)90007-8

del Castillo, T., Duque, E., & Ramos, J. L. (2008). A set of activators and repressors control peripheral glucose pathways in *Pseudomonas putida* to yield a common central intermediate. *Journal of Bacteriology*, *190*(7), 2331–2339. https://doi.org/10.1128/JB.01726-07

del Castillo, T., Ramos, J. L., Rodríguez-Herva, J. J., Fuhrer, T., Sauer, U., & Duque, E. (2007).

Convergent peripheral pathways catalyze initial glucose catabolism in *Pseudomonas putida*: Genomic and flux analysis. *Journal of Bacteriology*, *189*(14), 5142–5152. https://doi.org/10.1128/JB.00203-07

Delgoda, R., & Murray, J. E. (2017). Evolutionary Perspectives on the Role of Plant Secondary Metabolites. In *Pharmacognosy: Fundamentals, Applications and Strategy* (pp. 93–100). Academic Press. https://doi.org/10.1016/B978-0-12-802104-0.00007-X

Delmulle, T., De Maeseneire, S. L., & De Mey, M. (2018). Challenges in the microbial production of flavonoids. *Phytochemistry Reviews*, *17*(2), 229–247. https://doi.org/10.1007/s11101-017-9515-3

Demling, P., von Campenhausen, M., Grütering, C., Tiso, T., Jupke, A., & Blank, L. M. (2020). Selection of a recyclable *in situ* liquid-liquid extraction solvent for foam-free synthesis of rhamnolipids in a two-phase fermentation. *Green Chemistry*, *22*, 8495–8510. https://doi.org/10.1039/D0GC02885A

Desmet, S., Morreel, K., & Dauwe, R. (2021). Origin and Function of Structural Diversity in the Plant Specialized Metabolome. *Plants*, *10*(11), 2393. https://doi.org/10.3390/PLANTS10112393

Déziel, E., Comeau, Y., & Villemur, R. (1999). Two-liquid-phase bioreactors for enhanced degradation of hydrophobic/toxic compounds. *Biodegradation*, *10*(3), 219–233. https://doi.org/10.1023/A:1008311430525

Ditta, G., Stanfield, S., Corbin, D., & Helinski, D. R. (1980). Broad host range DNA cloning system for Gram-negative bacteria: Construction of a gene bank of *Rhizobium meliloti*. *Proceedings of the National Academy of Sciences of the United States of America*, *77*(12 II), 7347–7351. https://doi.org/10.1073/pnas.77.12.7347

Dolan, S. K., Wijaya, A., Kohlstedt, M., Gläser, L., Brear, P., Silva-Rocha, R., Wittmann, C., & Welch, M. (2022). Systems-wide dissection of organic acid assimilation in *Pseudomonas aeruginosa* reveals a novel path to underground metabolism. *MBio*, *13*(6). https://doi.org/https://doi.org/10.1128/mbio.02541-22

Domínguez-Cuevas, P., González-Pastor, J. E., Marqués, S., Ramos, J. L., & De Lorenzo, V. (2006). Transcriptional tradeoff between metabolic and stress-response programs in *Pseudomonas putida* KT2440 cells exposed to toluene. *Journal of Biological Chemistry*, *281*(17), 11981–11991. https://doi.org/10.1074/jbc.M509848200

Domröse, A., Weihmann, R., Thies, S., Jaeger, K. E., Drepper, T., & Loeschcke, A. (2017). Rapid generation of recombinant *Pseudomonas putida* secondary metabolite producers using yTREX. *Synthetic and Systems Biotechnology*, *2*(4), 310–319. https://doi.org/10.1016/j.synbio.2017.11.001

Dong, H., Ma, J., Chen, Q., Chen, B., Liang, L., Liao, Y., Song, Y., Wang, H., & Cronan, J. E. (2021). A cryptic long-chain 3-ketoacyl-ACP synthase in the *Pseudomonas putida* F1 unsaturated fatty acid synthesis pathway. *Journal of Biological Chemistry*, *297*(2), 100920. https://doi.org/10.1016/j.jbc.2021.100920

Dong, J., Chen, Y., Benites, V. T., Baidoo, E. E. K., Petzold, C. J., Beller, H. R., Eudes, A., Scheller, H. V., Adams, P. D., Mukhopadhyay, A., Simmons, B. A., & Singer, S. W. (2019). Methyl ketone production by *Pseudomonas putida* is enhanced by plant-derived amino acids. *Biotechnology and Bioengineering*, *116*(8), 1909–1922. https://doi.org/10.1002/bit.26995

Eberlein, C., Baumgarten, T., Starke, S., & Heipieper, H. J. (2018). Immediate response mechanisms of Gram-negative solvent-tolerant bacteria to cope with environmental stress: *cis-trans* isomerization of unsaturated fatty acids and outer membrane vesicle secretion. *Applied Microbiology and Biotechnology*, *102*(6), 2583–2593. https://doi.org/10.1007/s00253-018-

8832-9

Ebert, B. E., Kurth, F., Grund, M., Blank, L. M., & Schmid, A. (2011). Response of *Pseudomonas putida* KT2440 to increased NADH and ATP demand. *Applied and Environmental Microbiology*, *77*(18), 6597–6605. https://doi.org/10.1128/AEM.05588-11

Ehianeta, T. S., Laval, S., & Yu, B. (2016). Bio- and chemical syntheses of mangiferin and congeners. *BioFactors*, *42*(5), 445–458. https://doi.org/10.1002/biof.1279

El-Awaad, I., Bocola, M., Beuerle, T., Liu, B., & Beerhues, L. (2016). Bifunctional CYP81AA proteins catalyse identical hydroxylations but alternative regioselective phenol couplings in plant xanthone biosynthesis. *Nature Communications*, *7*(May), 1–12. https://doi.org/10.1038/ncomms11472

Elander, R. P., Mabe, J. A., Hamill, R. L., & Gorman, M. (1971). Biosynthesis of pyrrolnitrins by analogue-resistant mutants of *Pseudomonas fluorescens*. *Folia Microbiologica*, *16*(3), 156–165. https://doi.org/10.1007/BF02884206

Englund, E., Schmidt, M., Nava, A. A., Lechner, A., Deng, K., Jocic, R., Lin, Y., Roberts, J., Benites, V. T., Kakumanu, R., Gin, J. W., Chen, Y., Liu, Y., Petzold, C. J., Baidoo, E. E. K., Northen, T. R., Adams, P. D., Katz, L., Yuzawa, S., & Keasling, J. D. (2022). Expanding Extender Substrate Selection for Unnatural Polyketide Biosynthesis by Acyltransferase Domain Exchange within a Modular Polyketide Synthase. *Journal of the American Chemical Society*. https://doi.org/10.1021/jacs.2c11027

Erb, M., & Kliebenstein, D. J. (2020). Plant Secondary Metabolites as Defenses, Regulators, and Primary Metabolites: The Blurred Functional Trichotomy. *Plant Physiology*, *184*(1), 39–52. https://doi.org/10.1104/PP.20.00433

Eversberg, D., Holz, J., & Pungas, L. (2022). The bioeconomy and its untenable growth promises: reality checks from research. *Sustainability Science*, *18*(2), 569–582. https://link.springer.com/article/10.1007/s11625-022-01237-5

Ewering, C., Heuser, F., Benölken, J. K., Brämer, C. O., & Steinbüchel, A. (2006). Metabolic engineering of strains of *Ralstonia eutropha* and *Pseudomonas putida* for biotechnological production of 2-methylcitric acid. *Metabolic Engineering*, *8*(6), 587–602. https://doi.org/10.1016/j.ymben.2006.05.007

Faizal, I., Dozen, K., Hong, C. S., Kuroda, A., Takiguchi, N., Ohtake, H., Takeda, K., Tsunekawa, H., & Kato, J. (2005). Isolation and characterization of solvent-tolerant *Pseudomonas putida* strain T-57, and its application to biotransformation of toluene to cresol in a two-phase (organic-aqueous) system. *Journal of Industrial Microbiology and Biotechnology*, *32*(11–12), 542–547. https://doi.org/10.1007/s10295-005-0253-y

Faizal, I., Ohba, M., Kuroda, A., Takiguchi, N., Ohtake, H., Honda, K., & Kato, J. (2007). Bioproduction of 3-methylcatechol from toluene in a two-phase (organic-aqueous) aystem by a genetically modified solvent-tolerant *Pseudomonas putida* strain T-57. *Journal of Environmental Biotechnology*, *7*(1), 39–44.

Feng, C., Chen, J., Ye, W., Liao, K., Wang, Z., Song, X., & Qiao, M. (2022). Synthetic Biology-Driven Microbial Production of Resveratrol: Advances and Perspectives. *Frontiers in Bioengineering and Biotechnology*, *10*(January), 1–10. https://doi.org/10.3389/fbioe.2022.833920

Ferruz, N., Schmidt, S., & Höcker, B. (2022). ProtGPT2 is a deep unsupervised language model for protein design. *Nature Communications*, *13*(1). https://doi.org/10.1038/s41467-022-32007-7

Fleming, A. (1929). On the Antibacterial Action of Cultures of a Penicillium, with Special Reference to their Use in the Isolation of *B. influenzæ*. *British Journal of Experimental Pathology*, *10*(3), 226.

Follonier, S., Panke, S., & Zinn, M. (2012). Pressure to kill or pressure to boost: A review on the various effects and applications of hydrostatic pressure in bacterial biotechnology. *Applied Microbiology and Biotechnology*, *93*(5), 1805–1815. https://doi.org/10.1007/s00253-011-3854-6

Fu, R., Martin, C., & Zhang, Y. (2018). *Next-Generation Plant Metabolic Engineering, Inspired by an Ancient Chinese Irrigation System*. https://doi.org/10.1016/j.molp.2017.09.002

Fuhrer, T., Fischer, E., & Sauer, U. (2005). Experimental identification and quantification of glucose metabolism in seven bacterial species. *Journal of Bacteriology*, *187*(5), 1581–1590. https://doi.org/10.1128/JB.187.5.1581-1590.2005

Funa, N., Ohnishi, Y., Fujli, I., Shibuya, M., Ebizuka, Y., & Horinouchi, S. (1999). A new pathway for polyketide synthesis in microorganisms. *Nature*, *400*(6747), 897–899. https://doi.org/10.1038/23748

García-Granados, R., Lerma-Escalera, J. A., & Morones-Ramírez, J. R. (2019). Metabolic engineering and synthetic biology: Synergies, future, and challenges. *Frontiers in Bioengineering and Biotechnology*, *7*(MAR), 1–4. https://doi.org/10.3389/fbioe.2019.00036

Gemperlein, K., Zipf, G., Bernauer, H. S., Müller, R., & Wenzel, S. C. (2016). Metabolic engineering of *Pseudomonas putida* for production of docosahexaenoic acid based on a myxobacterial PUFA synthase. *Metabolic Engineering*, *33*, 98–108. https://doi.org/10.1016/j.ymben.2015.11.001

Gläser, L., Kuhl, M., Jovanovic, S., Fritz, M., Vögeli, B., Erb, T. J., Becker, J., & Wittmann, C. (2020). A common approach for absolute quantification of short chain CoA thioesters in prokaryotic and eukaryotic microbes. *Microbial Cell Factories*, *19*(1), 1–13. https://doi.org/10.1186/s12934-020-01413-1

Glonke, S., Sadowski, G., & Brandenbusch, C. (2016). Applied catastrophic phase inversion: a continuous non-centrifugal phase separation step in biphasic whole-cell biocatalysis. *Journal of Industrial Microbiology and Biotechnology*, *43*(11), 1527–1535. https://doi.org/10.1007/s10295-016-1837-4

Goh, E. B., Baidoo, E. E. K., Keasling, J. D., & Beller, H. R. (2012). Engineering of bacterial methyl ketone synthesis for biofuels. *Applied and Environmental Microbiology*, *78*(1), 70–80. https://doi.org/10.1128/AEM.06785-11

Gokhale, R. S., Saxena, P., Chopra, T., & Mohanty, D. (2007). Versatile polyketide enzymatic machinery for the biosynthesis of complex mycobacterial lipids. *Natural Product Reports*, *24*(2), 267–277. https://doi.org/10.1039/B616817P

Grammbitter, G. L. C., Schmalhofer, M., Karimi, K., Shi, Y. M., Schöner, T. A., Tobias, N. J., Morgner, N., Groll, M., & Bode, H. B. (2019). An Uncommon Type II PKS Catalyzes Biosynthesis of Aryl Polyene Pigments. *Journal of the American Chemical Society*, *141*(42), 16615–16623. https://doi.org/10.1021/jacs.8b10776

Grininger, M. (2023). Enzymology of assembly line synthesis by modular polyketide synthases. *Nature Chemical Biology*, *19*(4), 401–415. https://doi.org/10.1038/s41589-023-01277-7

Gross, F., Gottschalk, D., & Müller, R. (2005). Posttranslational modification of myxobacterial carrier protein domains in *Pseudomonas* sp. by an intrinsic phosphopantetheinyl transferase. *Applied Microbiology and Biotechnology*, *68*(1), 66–74. https://doi.org/10.1007/s00253-004-1836-7

Gross, F., Luniak, N., Perlova, O., Gaitatzis, N., Jenke-Kodama, H., Gerth, K., Gottschalk, D., Dittmann, E., & Müller, R. (2006). Bacterial type III polyketide synthases: Phylogenetic analysis and potential for the production of novel secondary metabolites by heterologous expression in pseudomonads. *Archives of Microbiology*, *185*(1), 28–38. https://doi.org/10.1007/s00203-005-

0059-3

Gross, F., Ring, M. W., Perlova, O., Fu, J., Schneider, S., Gerth, K., Kuhlmann, S., Stewart, A. F., Zhang, Y., & Müller, R. (2006). Metabolic Engineering of *Pseudomonas putida* for Methylmalonyl-CoA Biosynthesis to Enable Complex Heterologous Secondary Metabolite Formation. *Chemistry and Biology*, *13*(12), 1253–1264. https://doi.org/10.1016/j.chembiol.2006.09.014

Gross, H., & Loper, J. E. (2009). Genomics of secondary metabolite production by *Pseudomonas* spp. *Natural Product Reports*, *26*(11), 1408–1446. https://doi.org/10.1039/b817075b

Grundtvig, I. P. R., Heintz, S., Krühne, U., Gernaey, K. V., Adlercreutz, P., Hayler, J. D., Wells, A. S., & Woodley, J. M. (2018). Screening of organic solvents for bioprocesses using aqueous-organic two-phase systems. *Biotechnology Advances*, *36*(7), 1801–1814. https://doi.org/10.1016/j.biotechadv.2018.05.007

Grüninger, M. J., Buchholz, P. C. F., Mordhorst, S., Strack, P., Müller, M., Hubrich, F., Pleiss, J., & Andexer, J. N. (2019). Chorismatases-the family is growing. *Organic and Biomolecular Chemistry*, *17*(8), 2092–2098. https://doi.org/10.1039/c8ob03038c

Gülck, T., & Møller, B. L. (2020). Phytocannabinoids: Origins and Biosynthesis. *Trends in Plant Science*, *25*(10), 985–1004. https://doi.org/10.1016/J.TPLANTS.2020.05.005

Guo, D., Wang, H., Zhang, S., & Lan, T. (2022). The type III polyketide synthase supergene family in plants: complex evolutionary history and functional divergence. *Plant Journal*, *112*(2), 414–428. https://doi.org/10.1111/tpj.15953

Guo, S., Wang, Y., Wang, W., Hu, H., & Zhang, X. (2020). Identification of new arylamine N-acetyltransferases and enhancing 2-acetamidophenol production in *Pseudomonas chlororaphis* HT66. *Microbial Cell Factories*, 1–10. https://doi.org/10.1186/s12934-020-01364-7

Guo, Y., Nassar, S., Ma, L., Feng, G., Li, X., Chen, M., Chai, T., Abdel-Rahman, I. A. M., Beuerle, T., Beerhues, L., Wang, H., & Liu, B. (2021). Octaketide Synthase from *Polygonum cuspidatum* Implements Emodin Biosynthesis in *Arabidopsis thaliana*. *Plant and Cell Physiology*, *62*(February), 424–435. https://doi.org/10.1093/pcp/pcaa135

Gurney, R., & Thomas, C. M. (2011). Mupirocin: biosynthesis, special features and applications of an antibiotic from a Gram-negative bacterium. *Applied Microbiology and Biotechnology*, *90*(1), 11–21. https://doi.org/10.1007/s00253-011-3128-3

Harris, J., & Daugulis, A. J. (2015). Biocompatibility of low molecular weight polymers for two-phase partitioning bioreactors. *Biotechnology and Bioengineering*, *112*(12), 2450–2458. https://doi.org/10.1002/bit.25664

Hartmans, S., Smits, J. P., Van der Werf, M. J., Volkering, F., & De Bont, J. A. M. (1989). Metabolism of Styrene Oxide and 2-Phenylethanol in the Styrene-Degrading *Xanthobacter* Strain 124X. *Applied and Environmental Microbiology*, *55*(11), 2850–2855. https://doi.org/10.1128/aem.55.11.2850-2855.1989

Heerema, L., Cakali, D., Roelands, M., Goetheer, E., Verdoes, D., & Keurentjes, J. (2010). Micellar solutions of PEO-PPO-PEO block copolymers for *in situ* phenol removal from fermentation broth. *Separation and Purification Technology*, *73*(2), 319–326. https://doi.org/10.1016/j.seppur.2010.04.019

Heerema, L., Roelands, M., Goetheer, E., Verdoes, D., & Keurentjes, J. (2011). In-situ product removal from fermentations by membrane extraction: Conceptual process design and economics. *Industrial and Engineering Chemistry Research*, *50*(15), 9197–9208. https://doi.org/https://doi.org/10.1021/ie102551g

Heerema, L., Wierckx, N., Roelands, M., Hanemaaijer, J. H., Goetheer, E., Verdoes, D., & Keurentjes, J. (2011). In situ phenol removal from fed-batch fermentations of solvent tolerant *Pseudomonas putida* S12 by pertraction. *Biochemical Engineering Journal*, *53*(3), 245–252. https://doi.org/10.1016/j.bej.2010.11.002

Heipieper, H. J., Diefenbach, R., & Keweloh, H. (1992). Conversion of *cis* unsaturated fatty acids to *trans*, a possible mechanism for the protection of phenol-degrading *Pseudomonas putida* P8 from substrate toxicity. *Applied and Environmental Microbiology*, *58*(6), 1847–1852. https://doi.org/10.1128/aem.58.6.1847-1852.1992

Heipieper, H. J., & Martínez, P. M. (2010). Toxicity of Hydrocarbons to Microorganisms. *Handbook of Hydrocarbon and Lipid Microbiology*, 1563–1573. https://doi.org/10.1007/978-3-540-77587-4_108

Heipieper, Hermann J., Loffeld, B., Keweloh, H., & de Bont, J. A. M. (1995). The *cis/trans* isomerisation of unsaturated fatty acids in *Pseudomonas putida* S12: An indicator for environmental stress due to organic compounds. *Chemosphere*, *30*(6), 1041–1051. https://doi.org/10.1016/0045-6535(95)00015-Z

Heipieper, Hermann J., Neumann, G., Cornelissen, S., & Meinhardt, F. (2007). Solvent-tolerant bacteria for biotransformations in two-phase fermentation systems. *Applied Microbiology and Biotechnology*, *74*(5), 961–973. https://doi.org/10.1007/s00253-006-0833-4

Helfrich, E. J. N., Reiter, S., & Piel, J. (2014). Recent advances in genome-based polyketide discovery. *Current Opinion in Biotechnology*, *29*(1), 107–115. https://doi.org/10.1016/j.copbio.2014.03.004

Holliday, G. L., Thornton, J. M., Marquet, A., Smith, A. G., Rébeillé, F., Mendel, R., Schubert, H. L., Lawrence, A. D., & Warren, M. J. (2007). Evolution of enzymes and pathways for the biosynthesis of cofactors. *Natural Product Reports*, *24*, 972–987. https://doi.org/10.1039/b703107f

Hu, Y., Zhang, C., Zou, L., Zheng, Z., & Ouyang, J. (2022). Efficient biosynthesis of pinosylvin from lignin-derived cinnamic acid by metabolic engineering of *Escherichia coli*. *Biotechnology for Biofuels and Bioproducts*, *15*(1), 1–12. https://doi.org/10.1186/s13068-022-02236-5

Huang, L., Wang, H., Ye, H., Du, Z., Zhang, Y., Beerhues, L., & Liu, B. (2012). Differential Expression of Benzophenone Synthase and Chalcone Synthase in *Hypericum sampsonii*. *Natural Product Communications*, *7*(12), 1615–1618. https://doi.org/10.1177/1934578x1200701219

Hummel, J., Strehmel, N., Selbig, J., Walther, D., & Kopka, J. (2010). Decision tree supported substructure prediction of metabolites from GC-MS profiles. *Metabolomics*, *6*(2), 322–333. https://doi.org/10.1007/s11306-010-0198-7

Hüsken, L. E., Beeftink, R., De Bont, J. A. M., & Wery, J. (2001). High-rate 3-methylcatechol production in *Pseudomonas putida* strains by means of a novel expression system. *Applied Microbiology and Biotechnology*, *55*(5), 571–577. https://doi.org/10.1007/s002530000566

Hüsken, Leonie E., Dalm, M. C. F., Tramper, J., Wery, J., De Bont, J. A. M., & Beeftink, R. (2001). Integrated bioproduction and extraction of 3-methylcatechol. *Journal of Biotechnology*, *88*(1), 11–19. https://doi.org/10.1016/S0168-1656(01)00252-8

Hüsken, Leonie E., Oomes, M., Schroën, K., Tramper, J., De Bont, J. A. M., & Beeftink, R. (2002). Membrane-facilitated bioproduction of 3-methylcatechol in an octanol/water two-phase system. *Journal of Biotechnology*, *96*(3), 281–289. https://doi.org/10.1016/S0168-1656(02)00045-7

Hwang, H. G., Milito, A., Yang, J. S., Jang, S., & Jung, G. Y. (2023). Riboswitch-guided chalcone

synthase engineering and metabolic flux optimization for enhanced production of flavonoids. *Metabolic Engineering*, *75*(September 2022), 143–152. https://doi.org/10.1016/j.ymben.2022.12.006

Ibrahim, G. G., Yan, J., Xu, L., Yang, M., & Yan, Y. (2021). Resveratrol production in yeast hosts: Current status and perspectives. *Biomolecules*, *11*(6), 1–17. https://doi.org/10.3390/biom11060830

Incha, M. R., Thompson, M. G., Blake-Hedges, J. M., Liu, Y., Pearson, A. N., Schmidt, M., Gin, J. W., Petzold, C. J., Deutschbauer, A. M., & Keasling, J. D. (2020). Leveraging host metabolism for bisdemethoxycurcumin production in *Pseudomonas putida*. *Metabolic Engineering Communications*, *10*(December 2019), e00119. https://doi.org/10.1016/j.mec.2019.e00119

Inoue, A., & Horikoshi, K. (1989). A Pseudomonas thrives in high concentrations of toluene. In *Nature* (Vol. 338, Issue 6212, pp. 264–266). https://doi.org/10.1038/338264a0

Isken, S., Derks, A., Wolffs, P. F. G., & De Bont, J. A. M. (1999). Effect of organic solvents on the yield of solvent-tolerant *Pseudomonas putida* S12. *Applied and Environmental Microbiology*, *65*(6), 2631–2635. https://doi.org/10.1128/aem.65.6.2631-2635.1999

Isogai, S., Tominaga, M., Kondo, A., & Ishii, J. (2022). Plant Flavonoid Production in Bacteria and Yeasts. *Frontiers in Chemical Engineering*, *4*(July), 1–20. https://doi.org/10.3389/fceng.2022.880694

Jäger, W., Peters-Wendisch, P. G., Kalinowski, J., & Pühler, A. (1996). A *Corynebacterium glutamicum* gene encoding a two-domain protein similar to biotin carboxylases and biotin-carboxyl-carrier proteins. *Archives of Microbiology*, *166*(2), 76–82. https://doi.org/10.1007/s002030050359

Janardhan Garikipati, S. V. B., & Peeples, T. L. (2015). Solvent resistance pumps of *Pseudomonas putida* S12: Applications in 1-naphthol production and biocatalyst engineering. *Journal of Biotechnology*, *210*, 91–99. https://doi.org/10.1016/j.jbiotec.2015.06.419

Janikowski, T., Velicogna, D., Punt, M., & Daugulis, A. (2002). Use of a two-phase partitioning bioreactor for degrading polycyclic aromatic hydrocarbons by a *Sphingomonas* sp. *Applied Microbiology and Biotechnology*, *59*(2–3), 368–376. https://doi.org/10.1007/s00253-002-1011-y

Janvier, P., & Clément, G. (2010). Muddy tetrapod origins. *Nature*, *463*(7277), 40–41. https://doi.org/10.1038/463040a

Jeandet, P., Vannozzi, A., Sobarzo-Sánchez, E., Uddin, M. S., Bru, R., Martínez-Márquez, A., Clément, C., Cordelier, S., Manayi, A., Nabavi, S. F., Rasekhian, M., El-Saber Batiha, G., Khan, H., Morkunas, I., Belwal, T., Jiang, J., Koffas, M., & Nabavi, S. M. (2021). Phytostilbenes as agrochemicals: biosynthesis, bioactivity, metabolic engineering and biotechnology. *Natural Product Reports*, *38*, 1282–1329. https://doi.org/10.1039/d0np00030b

Jeckelmann, J. M., & Erni, B. (2020). Transporters of glucose and other carbohydrates in bacteria. *Pflugers Archiv European Journal of Physiology*, *472*(9), 1129–1153. https://doi.org/10.1007/s00424-020-02379-0

Jeong, Y. J., Woo, S. G., An, C. H., Jeong, H. J., Hong, Y. S., Kim, Y. M., Ryu, Y. B., Rho, M. C., Lee, W. S., & Kim, C. Y. (2015). Metabolic engineering for resveratrol derivative biosynthesis in *Escherichia coli*. *Molecules and Cells*, *38*(4), 318–326. https://doi.org/10.14348/molcells.2015.2188

Jeschek, M., Bahls, M. O., Schneider, V., Marlière, P., Ward, T. R., & Panke, S. (2017). Biotin-independent strains of *Escherichia coli* for enhanced streptavidin production. *Metabolic Engineering*, *40*, 33–40. https://doi.org/10.1016/j.ymben.2016.12.013

Jin, K., Zhou, L., Jiang, H., Sun, S., Fang, Y., Liu, J., Zhang, X., & He, Y. W. (2015). Engineering the central biosynthetic and secondary metabolic pathways of *Pseudomonas aeruginosa* strain PA1201 to improve phenazine-1-carboxylic acid production. *Metabolic Engineering*, *32*, 30–38. https://doi.org/10.1016/j.ymben.2015.09.003

Jin, X. J., Peng, H. S., Hu, H. B., Huang, X. Q., Wang, W., & Zhang, X. H. (2016). ITRAQ-based quantitative proteomic analysis reveals potential factors associated with the enhancement of phenazine-1-carboxamide production in *Pseudomonas chlororaphis* P3. *Scientific Reports*, *6*(May), 1–14. https://doi.org/10.1038/srep27393

Jumper, J., Evans, R., Pritzel, A., Green, T., Figurnov, M., Ronneberger, O., Tunyasuvunakool, K., Bates, R., Žídek, A., Potapenko, A., Bridgland, A., Meyer, C., Kohl, S. A. A., Ballard, A. J., Cowie, A., Romera-Paredes, B., Nikolov, S., Jain, R., Adler, J., … Hassabis, D. (2021). Highly accurate protein structure prediction with AlphaFold. *Nature*, *596*(7873), 583–589. https://doi.org/10.1038/s41586-021-03819-2

Kallscheuer, N., Classen, T., Drepper, T., & Marienhagen, J. (2019). Production of plant metabolites with applications in the food industry using engineered microorganisms. *Current Opinion in Biotechnology*, *56*, 7–17. https://doi.org/10.1016/j.copbio.2018.07.008

Kallscheuer, N., Kage, H., Milke, L., Nett, M., & Marienhagen, J. (2019). Microbial synthesis of the type I polyketide 6-methylsalicylate with *Corynebacterium glutamicum*. *Applied Microbiology and Biotechnology*, *103*(23–24), 9619–9631. https://doi.org/10.1007/s00253-019-10121-9

Kallscheuer, N., Polen, T., Bott, M., & Marienhagen, J. (2017). Reversal of β-oxidative pathways for the microbial production of chemicals and polymer building blocks. *Metabolic Engineering*, *42*(May), 33–42. https://doi.org/10.1016/j.ymben.2017.05.004

Kallscheuer, N., Vogt, M., Stenzel, A., Gätgens, J., Bott, M., & Marienhagen, J. (2016). Construction of a *Corynebacterium glutamicum* platform strain for the production of stilbenes and (2S)-flavanones. *Metabolic Engineering*, *38*, 47–55. https://doi.org/10.1016/j.ymben.2016.06.003

Kampers, L. F. C., Volkers, R. J. M., & Martins dos Santos, V. A. P. (2019). *Pseudomonas putida* KT2440 is HV1 certified, not GRAS. *Microbial Biotechnology*, *12*(5), 845–848. https://doi.org/10.1111/1751-7915.13443

Kaneko, M., Ohnishi, Y., & Horinouchi, S. (2003). Cinnamate:Coenzyme A Ligase from the Filamentous Bacterium *Streptomyces coelicolor* A3(2). *Journal of Bacteriology*, *185*(1), 20–27. https://doi.org/10.1128/JB.185.1.20–27.2003

Karbalaei, M., Rezaee, S. A., & Farsiani, H. (2020). *Pichia pastoris*: A highly successful expression system for optimal synthesis of heterologous proteins. *Journal of Cellular Physiology*, *235*(9), 5867–5881. https://doi.org/10.1002/jcp.29583

Khattab, A. R., & Farag, M. A. (2020). Current status and perspectives of xanthones production using cultured plant biocatalyst models aided by in-silico tools for its optimization. *Critical Reviews in Biotechnology*, *40*(3), 415–431. https://doi.org/10.1080/07388551.2020.1721426

Kieboom, J., & de Bont, J. A. M. (1998). Identification and molecular characterization of an efflux system involved in *Pseudomonas putida* S12 multidrug resistance. *Microbiology*, *273*(1), 85–91. https://doi.org/10.1099/00221287-147-1-43

Kilani, J., & Fillinger, S. (2016). Phenylpyrroles: 30 years, two molecules and (nearly) no resistance. *Frontiers in Microbiology*, *7*(DEC), 1–10. https://doi.org/10.3389/fmicb.2016.02014

Kildegaard, K. R., Arnesen, J. A., Adiego-Pérez, B., Rago, D., Kristensen, M., Klitgaard, A. K., Hansen, E. H., Hansen, J., & Borodina, I. (2021). Tailored biosynthesis of gibberellin plant hormones in yeast. *Metabolic Engineering*, *66*(February), 1–11.

https://doi.org/10.1016/j.ymben.2021.03.010

Kim, J., Jeon, C. O., & Park, W. (2008). Dual regulation of zwf-1 by both 2-keto-3-deoxy-6-phosphogluconate and oxidative stress in *Pseudomonas putida*. *Microbiology*, *154*(12), 3905–3916. https://doi.org/10.1099/mic.0.2008/020362-0

Kim, Y. S. (2002). Malonate metabolism: biochemistry, molecular biology, physiology, and industrial application. *Journal of Biochemistry and Molecular Biology*, *35*(5), 443–451. http://www.ncbi.nlm.nih.gov/pubmed/12359084

Klamrak, A., Nabnueangsap, J., & Nualkaew, N. (2021). Biotransformation of Benzoate to 2,4,6-Trihydroxybenzophenone by Engineered *Escherichia coli*. *Molecules*, *26*(9), 2779. https://doi.org/https://doi.org/10.3390/molecules26092779

Klaus, M., & Grininger, M. (2018). Engineering strategies for rational polyketide synthase design. *Natural Product Reports*, *35*(10), 1070–1081. https://doi.org/10.1039/c8np00030a

Knoll, A., Bartsch, S., Husemann, B., Engel, P., Schroer, K., Ribeiro, B., Stöckmann, C., Seletzky, J., & Büchs, J. (2007). High cell density cultivation of recombinant yeasts and bacteria under non-pressurized and pressurized conditions in stirred tank bioreactors. *Journal of Biotechnology*, *132*(2), 167–179. https://doi.org/10.1016/j.jbiotec.2007.06.010

Knoll, A., Maier, B., Tscherrig, H., & Büchs, J. (2005). The oxygen mass transfer, carbon dioxide inhibition, heat removal, and the energy and cost efficiencies of high pressure fermentation. *Advances in Biochemical Engineering/Biotechnology*, *92*, 77–99. https://doi.org/10.1007/b98918

Köhler, K. A. K., Blank, L. M., Frick, O., & Schmid, A. (2015). D-Xylose assimilation via the Weimberg pathway by solvent-tolerant *Pseudomonas taiwanensis* VLB120. *Environmental Microbiology*, *17*(1), 156–170. https://doi.org/10.1111/1462-2920.12537

Kohlstedt, M., & Wittmann, C. (2019). GC-MS-based 13 C metabolic flux analysis resolves the parallel and cyclic glucose metabolism of *Pseudomonas putida* KT2440 and *Pseudomonas aeruginosa* PAO1. *Metabolic Engineering*, *54*(March), 35–53. https://doi.org/10.1016/j.ymben.2019.01.008

Kondakova, T., D'Heygère, F., Feuilloley, M. J., Orange, N., Heipieper, H. J., & Duclairoir Poc, C. (2015). Glycerophospholipid synthesis and functions in *Pseudomonas*. *Chemistry and Physics of Lipids*, *190*, 27–42. https://doi.org/10.1016/j.chemphyslip.2015.06.006

Koopman, F., Wierckx, N., De Winde, J. H., & Ruijssenaars, H. J. (2010). Identification and characterization of the furfural and 5-(hydroxymethyl)furfural degradation pathways of *Cupriavidus basilensis* HMF14. *Proceedings of the National Academy of Sciences of the United States of America*, *107*(11), 4919–4924. https://doi.org/10.1073/pnas.0913039107

Kopp, D., & Sunna, A. (2020). Alternative carbohydrate pathways–enzymes, functions and engineering. *Critical Reviews in Biotechnology*, *0*(0), 895–912. https://doi.org/10.1080/07388551.2020.1785386

Koppisch, A. T., & Khosla, C. (2003). Structure-based mutagenesis of the malonyl-CoA:acyl carrier protein transacylase from *Streptomyces coelicolor*. *Biochemistry*, *42*(37), 11057–11064. https://doi.org/10.1021/bi0349672

Kozaeva, E., Volkova, S., Matos, M. R. A., Mezzina, M. P., Wulff, T., Volke, D. C., Nielsen, L. K., & Nikel, P. I. (2021). Model-guided dynamic control of essential metabolic nodes boosts acetyl-coenzyme A–dependent bioproduction in rewired *Pseudomonas putida*. *Metabolic Engineering*, *67*, 373–386. https://doi.org/10.1016/j.ymben.2021.07.014

Krespach, M. K. C., Stroe, M. C., Netzker, T., Rosin, M., Zehner, L. M., Komor, A. J., Beilmann, J. M.,

Krüger, T., Scherlach, K., Kniemeyer, O., Schroeckh, V., Hertweck, C., & Brakhage, A. A. (2023). *Streptomyces* polyketides mediate bacteria-fungi interactions across soil environments. *Nature Microbiology*, 1–14. https://doi.org/10.1038/s41564-023-01382-2

Krink-Koutsoubelis, N., Loechner, A. C., Lechner, A., Link, H., Denby, C. M., Vögeli, B., Erb, T. J., Yuzawa, S., Jakociunas, T., Katz, L., Jensen, M. K., Sourjik, V., & Keasling, J. D. (2018). Engineered Production of Short-Chain Acyl-Coenzyme A Esters in *Saccharomyces cerevisiae*. *ACS Synthetic Biology*, *7*(4), 1105–1112. https://doi.org/10.1021/acssynbio.7b00466

Kuatsjah, E., Johnson, C. W., Salvachúa, D., Werner, A. Z., Zahn, M., Szostkiewicz, C. J., Singer, C. A., Dominick, G., Okekeogbu, I., Haugen, S. J., Woodworth, S. P., Ramirez, K. J., Giannone, R. J., Hettich, R. L., McGeehan, J. E., & Beckham, G. T. (2022). Debottlenecking 4-hydroxybenzoate hydroxylation in *Pseudomonas putida* KT2440 improves muconate productivity from *p*-coumarate. *Metabolic Engineering*, *70*, 31–42. https://doi.org/https://doi.org/10.1016/j.ymben.2021.12.010

Kumar, R., Vikramachakravarthi, D., & Pal, P. (2014). Production and purification of glutamic acid: A critical review towards process intensification. *Chemical Engineering and Processing: Process Intensification*, *81*, 59–71. https://doi.org/10.1016/J.CEP.2014.04.012

Kurgan, G., Onyeabor, M., Holland, S. C., Taylor, E., Schneider, A., Kurgan, L., Billings, T., & Wang, X. (2021). Directed evolution of *Zymomonas mobilis* sugar facilitator Glf to overcome glucose inhibition. *Journal of Industrial Microbiology and Biotechnology*, *September*. https://doi.org/10.1093/jimb/kuab066

Kusumawardhani, H., Hosseini, R., & de Winde, J. H. (2018). Solvent Tolerance in Bacteria: Fulfilling the Promise of the Biotech Era? *Trends in Biotechnology*, *36*(10), 1025–1039. https://doi.org/10.1016/j.tibtech.2018.04.007

Laane, C., Boeren, S., Vos, K., & Veeger, C. (1987). Rules for optimization of biocatalysis in organic solvents. *Biotechnology and Bioengineering*, *30*(1), 81–87. https://doi.org/10.1002/bit.260300112

Lagarde, A. (1977). Evidence for an electrogenic 3-deoxy-2-oxo-d-gluconate–proton co-transport driven by the protonmotive force in *Escherichia coli* K12. *Biochemical Journal*, *168*(2), 211–221. https://doi.org/10.1042/BJ1680211

Lee, S., Lee, Y. R., Kim, S. J., Lee, J. S., & Min, K. (2023). Recent advances and challenges in the biotechnological upcycling of plastic wastes for constructing a circular bioeconomy. *Chemical Engineering Journal*, *454*, 140470. https://doi.org/10.1016/J.CEJ.2022.140470

Lee, S. Y., Kim, H. U., Chae, T. U., Cho, J. S., Kim, J. W., Shin, J. H., Kim, D. I., Ko, Y. S., Jang, W. D., & Jang, Y. S. (2019). A comprehensive metabolic map for production of bio-based chemicals. *Nature Catalysis*, *2*(1), 18–33. https://doi.org/10.1038/s41929-018-0212-4

Leonard, E., Lim, K. H., Saw, P. N., & Koffas, M. A. G. (2007). Engineering central metabolic pathways for high-level flavonoid production in *Escherichia coli*. *Applied and Environmental Microbiology*, *73*(12), 3877–3886. https://doi.org/10.1128/AEM.00200-07

Leonard, E., Yan, Y., Fowler, Z. L., Li, Z., Lim, C. G., Lim, K. H., & Koffas, M. A. G. (2008). Strain improvement of recombinant Escherichia coli for efficient production of plant flavonoids. *Molecular Pharmaceutics*, *5*(2), 257–265. https://doi.org/10.1021/mp7001472

Leprince, A., de Lorenzo, V., Völler, P., van Passel, M. W. J., & Martins dos Santos, V. A. P. (2012). Random and cyclical deletion of large DNA segments in the genome of *Pseudomonas putida*. *Environmental Microbiology*, *14*(6), 1444–1453. https://doi.org/10.1111/J.1462-2920.2012.02730.X

Li, Heng, Chen, W., Jin, R., Jin, J. M., & Tang, S. Y. (2017). Biosensor-aided high-throughput screening of hyper-producing cells for malonyl-CoA-derived products. *Microbial Cell Factories*, *16*(1), 1–10. https://doi.org/10.1186/s12934-017-0794-6

Li, Hongbiao, Lyv, Y., Zhou, S., Yu, S., & Zhou, J. (2022). Microbial cell factories for the production of flavonoids–barriers and opportunities. *Bioresource Technology*, *360*, 127538. https://linkinghub.elsevier.com/retrieve/pii/S0960852422008677

Li, M., Kildegaard, K. R., Chen, Y., Rodriguez, A., Borodina, I., & Nielsen, J. (2015). *De novo* production of resveratrol from glucose or ethanol by engineered *Saccharomyces cerevisiae*. *Metabolic Engineering*, *32*, 1–11. https://doi.org/10.1016/j.ymben.2015.08.007

Li, Shengying, Grüschow, S., Dordick, J. S., & Sherman, D. H. (2007). Molecular analysis of the role of tyrosine 224 in the active site of Streptomyces coelicolor RppA, a bacterial type III polyketide synthase. *Journal of Biological Chemistry*, *282*(17), 12765–12772. https://doi.org/10.1074/jbc.M700393200

Li, Shiyun, Zhang, Q., Wang, J., Liu, Y., Zhao, Y., & Deng, Y. (2021). Recent progress in metabolic engineering of *Saccharomyces cerevisiae* for the production of malonyl-CoA derivatives. *Journal of Biotechnology*, *325*(December 2020), 83–90. https://doi.org/10.1016/j.jbiotec.2020.11.014

Liang, B., Sun, G., Wang, Z., Xiao, J., & Yang, J. (2019). Production of 3-hydroxypropionate using a novel malonyl-CoA-mediated biosynthetic pathway in genetically engineered: *E. coli* strain. *Green Chemistry*, *21*(22), 6103–6115. https://doi.org/10.1039/c9gc02286d

Liang, J. long, Guo, L. qiong, Lin, J. fang, He, Z. qi, Cai, F. ji, & Chen, J. fei. (2016). A novel process for obtaining pinosylvin using combinatorial bioengineering in *Escherichia coli*. *World Journal of Microbiology and Biotechnology*, *32*(6). https://doi.org/10.1007/s11274-016-2062-z

Liang, P., Zhang, Y., Xu, B., Zhao, Y., Liu, X., Gao, W., Ma, T., Yang, C., Wang, S., & Liu, R. (2020). Deletion of genomic islands in the *Pseudomonas putida* KT2440 genome can create an optimal chassis for synthetic biology applications. *Microbial Cell Factories*, *19*(70), 1–12. https://doi.org/10.1186/s12934-020-01329-w

Liao, Z., Zhang, J., Shi, Y., Zhang, Y., Ma, Z., Bechthold, A., & Yu, X. (2022). Improvement of Rimocidin Biosynthesis by Increasing Supply of Precursor Malonyl-CoA via Over-expression of Acetyl-CoA Carboxylase in *Streptomyces rimosus* M527. *Current Microbiology*, *79*(6), 1–8. https://doi.org/10.1007/s00284-022-02867-9

Lim, C. G., Fowler, Z. L., Hueller, T., Schaffer, S., & Koffas, M. A. G. (2011). High-yield resveratrol production in engineered *Escherichia coli*. *Applied and Environmental Microbiology*, *77*(10), 3451–3460. https://doi.org/10.1128/AEM.02186-10

Lim, H. G., Rychel, K., Sastry, A. V, Mueller, J., Niu, W., Feist, A. M., & Palsson, B. O. (2022). Machine-learning from *Pseudomonas putida* transcriptomes reveals its transcriptional regulatory network. *Metabolic Engineering*, *72*, 297–310. https://doi.org/10.1016/j.ymben.2022.04.004

Lin, C. Y., Zhang, Y., Wu, J. H., Xie, R. H., Qiao, J., & Zhao, G. R. (2020). Regulatory patterns of crp on monensin biosynthesis in *Streptomyces cinnamonensis*. *Microorganisms*, *8*(2). https://doi.org/10.3390/microorganisms8020271

Lin, Y., Shen, X., Yuan, Q., & Yan, Y. (2013). Microbial biosynthesis of the anticoagulant precursor 4-hydroxycoumarin. *Nature Communications*, *4*(May), 1–8. https://doi.org/10.1038/ncomms3603

Ling, C., Peabody, G. L., Salvachúa, D., Kim, Y., Kneucker, C. M., Calvey, C. H., Monninger, M. A., Munoz, N. M., Poirier, B. C., Ramirez, K. J., John, P. C. St., Woodworth, S. P., Magnuson, J. K., Burnum-Johnson, K. E., Guss, A. M., Johnson, C. W., & Beckham, G. T. (2022). Muconic acid production from glucose and xylose in *Pseudomonas putida* via evolution and metabolic

engineering. *Nature Communications*, *13*(4925). https://doi.org/10.1038/s41467-022-32296-y

Ling, G., & Tuddenham, E. G. D. (2020). Factor VIII: the protein, cloning its gene, synthetic factor and now – 35 years later – gene therapy; what happened in between? *British Journal of Haematology*, *189*(3), 400–407. https://doi.org/10.1111/BJH.16311

Liu, B., Raeth, T., Beuerle, T., & Beerhues, L. (2007). Biphenyl synthase, a novel type III polyketide synthase. *Planta*, *225*(6), 1495–1503. https://doi.org/10.1007/s00425-006-0435-5

Liu, Benye, Kalz, L. F., Jia, Y., Grull, M., Beuerle, T., & Beerhues, L. (2020). Engineering yeast for production of benzophenones and xanthones as precursors of polycyclic polyprenylated acylphloroglucinols. *SPhERe Proceedings: 3rd International Symposium on Pharmaceutical Engineering Research*. https://doi.org/10.24355/dbbs.084-202001221215-0

Liu, Benye, Raeth, T., Beuerle, T., & Beerhues, L. (2010). A novel 4-hydroxycoumarin biosynthetic pathway. *Plant Molecular Biology*, *72*(1–2), 17–25. https://doi.org/10.1007/s11103-009-9548-0

Liu, C., & Li, S. (2022). Engineered biosynthesis of plant polyketides by type III polyketide synthases in microorganisms. *Frontiers in Bioengineering and Biotechnology*, *10*(October), 1–19. https://doi.org/10.3389/fbioe.2022.1017190

Liu, D., Thomson, K., & Kaiser, K. L. E. (1982). Quantitative structure-toxicity relationship of halogenated phenols on bacteria. *Bulletin of Environmental Contamination and Toxicology*, *29*(2), 130–136. https://doi.org/10.1007/BF01606140

Liu, Jiaqi, Wang, X., Dai, G., Zhang, Y., & Bian, X. (2022). Microbial chassis engineering drives heterologous production of complex secondary metabolites. *Biotechnology Advances*, *59*, 107966. https://doi.org/10.1016/j.biotechadv.2022.107966

Liu, Jie, Xu, J. Z., Rao, Z. M., & Zhang, W. G. (2022). Industrial production of L-lysine in *Corynebacterium glutamicum*: Progress and prospects. *Microbiological Research*, *262*, 127101. https://doi.org/10.1016/J.MICRES.2022.127101

Liu, M., Wang, C., Ren, X., Gao, S., Yu, S., & Zhou, J. (2022). Remodelling metabolism for high-level resveratrol production in *Yarrowia lipolytica*. *Bioresource Technology*, *365*(128178). https://doi.org/https://doi.org/10.1016/j.biortech.2022.128178

Liu, S., Narancic, T., Tham, J. L., & O'Connor, K. E. (2023). *β*-oxidation–polyhydroxyalkanoates synthesis relationship in *Pseudomonas putida* KT2440 revisited. *Applied Microbiology and Biotechnology*, *107*(5–6), 1863–1874. https://doi.org/10.1007/s00253-023-12413-7

Liu, X., Ding, W., & Jiang, H. (2017). Engineering microbial cell factories for the production of plant natural products: From design principles to industrial-scale production. *Microbial Cell Factories*, *16*(1), 1–9. https://doi.org/10.1186/s12934-017-0732-7

Loeschcke, A., & Thies, S. (2015). *Pseudomonas putida*—a versatile host for the production of natural products. *Applied Microbiology and Biotechnology*, *99*(15), 6197–6214. https://doi.org/10.1007/s00253-015-6745-4

Loeschcke, A., & Thies, S. (2020). Engineering of natural product biosynthesis in *Pseudomonas putida*. *Current Opinion in Biotechnology*, *in product*(Table 1), 213–224. https://doi.org/10.1016/j.copbio.2020.03.007

López, J. M., Duran, L., & Avalos, J. L. (2022). *Physiological limitations and opportunities in microbial metabolic engineering*. *20*(January). https://doi.org/10.1038/s41579-021-00600-0

Lu, C., Batianis, C., Akwafo, E. O., Wijffels, R. H., Martins, V. A. P., & Weusthuis, R. A. (2021). When metabolic prowess is too much of a good thing: how carbon catabolite repression and metabolic versatility impede production of esterified α,ω-diols in *Pseudomonas putida* KT2440.

Biotechnology for Biofuels, *14*(218), 1–15. https://doi.org/10.1186/s13068-021-02066-x

Lyu, M., Cheng, Y., Han, X., Wen, Y., Song, Y., Li, J., & Chen, Z. (2020). AccR, a TetR Family Transcriptional Repressor, Coordinates Short-Chain Acyl Coenzyme A Homeostasis in *Streptomyces avermitilis*. *Applied and Environmental Microbiology*, *86*(12). https://doi.org/10.1128/AEM.00508-20

Maglangit, F., Yu, Y., & Deng, H. (2020). Bacterial pathogens: threat or treat (a review on bioactive natural products from bacterial pathogens). *Natural Product Reports*. https://doi.org/10.1039/d0np00061b

Maharjan, S., Park, J. W., Yoon, Y. J., Lee, H. C., & Sohng, J. K. (2010). Metabolic engineering of *Streptomyces venezuelae* for malonyl-CoA biosynthesis to enhance heterologous production of polyketides. *Biotechnology Letters*, *32*(2), 277–282. https://doi.org/10.1007/s10529-009-0152-9

Mains, K., & Fox, J. M. (2023). Ketosynthase mutants enable short-chain fatty acid biosynthesis in *E. coli*. *Metabolic Engineering*, *77*, 118–127. https://doi.org/10.1016/j.ymben.2023.03.008

Malinowski, J. J. (2001). Two-phase partitioning bioreactors in fermentation technology. *Biotechnology Advances*, *19*(7), 525–538. https://doi.org/10.1016/S0734-9750(01)00080-5

Mannully, S. T., Ramya, L. N., & Pulicherla, K. K. (2018). Perspectives on progressive strategies and recent trends in the production of recombinant human factor VIII. *International Journal of Biological Macromolecules*, *119*, 496–504. https://doi.org/10.1016/J.IJBIOMAC.2018.07.164

Mark, R., Lyu, X., Lee, J. J. L., Parra-Saldívar, R., & Chen, W. N. (2019). Sustainable production of natural phenolics for functional food applications. *Journal of Functional Foods*, *57*(April), 233–254. https://doi.org/10.1016/j.jff.2019.04.008

Martin-Pascual, M., Batianis, C., Bruinsma, L., Asin-Garcia, E., Garcia-Morales, L., Weusthuis, R. A., Kranenburg, R. van, & Martins dos Santos, V. A. P. (2021). A navigation guide of synthetic biology tools for *Pseudomonas putida*. *Biotechnology Advances*. https://doi.org/10.1016/j.biotechadv.2021.107732

Martínez-García, E., & de Lorenzo, V. (2011). Engineering multiple genomic deletions in Gram-negative bacteria: Analysis of the multi-resistant antibiotic profile of *Pseudomonas putida* KT2440. In *Environmental Microbiology* (Vol. 13, Issue 10, pp. 2702–2716). https://doi.org/10.1111/j.1462-2920.2011.02538.x

Martínez-García, E., Fraile, S., Algar, E., Aparicio, T., Velázquez, E., Calles, B., Tas, H., Blázquez, B., Martín, B., Prieto, C., Sánchez-Sampedro, L., Nørholm, M. H. H., Volke, D. C., Wirth, N. T., Dvořák, P., Alejaldre, L., Grozinger, L., Crowther, M., Goñi-Moreno, A., … de Lorenzo, V. (2022). SEVA 4.0: an update of the Standard European Vector Architecture database for advanced analysis and programming of bacterial phenotypes. *Nucleic Acids Research*, *51*(D1), 1–10. https://doi.org/10.1093/nar/gkac1059

Martinez-García, E., Fraile, S., Rodriguez-Espeso, D., Vecchietti, D., Bertoni, G., & de Lorenzo, V. (2020). The naked bacterium: emerging properties of a surfome-streamlined *Pseudomonas putida* strain. *ACS Synthetic Biology*. https://doi.org/10.1021/acssynbio.0c00272

Martínez-García, E., Nikel, P. I., Aparicio, T., & De Lorenzo, V. (2014). *Pseudomonas* 2.0: genetic upgrading of *P. putida* KT2440 as an enhanced host for heterologous gene expression. *Microbial Cell Factories*, *13*(159), 1–15. https://doi.org/10.1186/s12934-014-0159-3

Masters, K. S., & Bräse, S. (2012). Xanthones from fungi, lichens, and bacteria: The natural products and their synthesis. *Chemical Reviews*, *112*(7), 3717–3776. https://doi.org/10.1021/cr100446h

Masuo, S., Zhou, S., Kaneko, T., & Takaya, N. (2016). Bacterial fermentation platform for producing

artificial aromatic amines. *Scientific Reports*, *6*(1), 1–9. https://doi.org/10.1038/srep25764

Mateos, K., Chappell, G., Klos, A., Le, B., Boden, J., Stüeken, E., & Anderson, R. (2022). The evolution and spread of sulfur cycling enzymes reflect the redox state of the early Earth. *Science Advances*, *9*(27), 1–11. https://doi.org/10.1126/sciadv.ade4847

Mauger, M., Ferreri, C., Chatgilialoglu, C., & Seemann, M. (2021). The bacterial protective armor against stress: The *cis-trans* isomerase of unsaturated fatty acids, a cytochrome-c type enzyme. *Journal of Inorganic Biochemistry*, *224*(November). https://doi.org/10.1016/j.jinorgbio.2021.111564

Maurya, D. K., Kumar, A., Chaurasiya, U., Hussain, T., & Singh, S. K. (2021). Modern era of microbial biotechnology: opportunities and future prospects. *Microbiomes and Plant Health: Panoply and Their Applications*, 317–343. https://doi.org/10.1016/B978-0-12-819715-8.00011-2

Mavrodi, O. V., McSpadden Gardener, B. B., Mavrodi, D. V., Bonsall, R. F., Weller, D. M., & Thomashow, L. S. (2001). Genetic diversity of *phlD* from 2,4-diacetylphloroglucinol-producing fluorescent *Pseudomonas* spp. *Phytopathology*, *91*(1), 35–42. https://doi.org/10.1094/phyto.2001.91.1.35

McCarthy, C. M. (1988). Reversal of cerulenin inhibition of *Mycobacterium avium* by octanoate. *Current Microbiology*, *17*(3), 121–125. https://doi.org/10.1007/BF01573466

McNaught, K. J., Kuatsjah, E., Zahn, M., Prates, É. T., Shao, H., Bentley, G. J., Pickford, A. R., Gruber, J. N., Hestmark, K. V., Jacobson, D. A., Poirier, B. C., Ling, C., Marchi, M. S., Michener, W. E., Nicora, C. D., Sanders, J. N., Szostkiewicz, C. J., Veličković, D., Zhou, M., … Beckham, G. T. (2023). Initiation of fatty acid biosynthesis in *Pseudomonas putida* KT2440. *Metabolic Engineering*, *76*, 193–203. https://doi.org/10.1016/j.ymben.2023.02.006

Meng, L., Diao, M., Wang, Q., Peng, L., Li, J., & Xie, N. (2023). Efficient biosynthesis of resveratrol via combining phenylalanine and tyrosine pathways in *Saccharomyces cerevisiae*. *Microbial Cell Factories*, *22*(1), 46. https://doi.org/10.1186/s12934-023-02055-9

Merchan, A. L., Fischöder, T., Hee, J., Lehnertz, M. S., Osterthun, O., Pielsticker, S., Schleier, J., Tiso, T., Blank, L. M., Klankermayer, J., Kneer, R., Quicker, P., Walther, G., & Palkovits, R. (2022). Chemical recycling of bioplastics: technical opportunities to preserve chemical functionality as path towards a circular economy. *Green Chemistry*, *24*(24), 9428–9449. https://doi.org/10.1039/D2GC02244C

Meyer, A. J., Saaem, I., Silverman, A., Varaljay, V., Mickol, R., Blum, S. M., Tobias, A. V, Schwalm, N. D., Mojadedi, W., Onderko, E., Bristol, C., Liu, S., Casini, A., Eluere, R., Moser, F., Drake, C., Gupta, M., Kelley-Loughnane, N., Lucks, J. B., … Voigt, C. A. (2019). Organism engineering for the bioproduction of the triaminotrinitrobenzene (TATB) precursor phloroglucinol (PG). *ACS Synthetic Biology*, *8*, acssynbio.9b00393. https://doi.org/10.1021/acssynbio.9b00393

Milke, L., Aschenbrenner, J., Marienhagen, J., & Kallscheuer, N. (2018). Production of plant-derived polyphenols in microorganisms: current state and perspectives. *Applied Microbiology and Biotechnology*, *102*(4), 1575–1585. https://doi.org/10.1007/s00253-018-8747-5

Milke, L., Ferreira, P., Kallscheuer, N., Braga, A., Vogt, M., Kappelmann, J., Oliveira, J., Silva, A. R., Rocha, I., Bott, M., Noack, S., Faria, N., & Marienhagen, J. (2019). Modulation of the central carbon metabolism of *Corynebacterium glutamicum* improves malonyl-CoA availability and increases plant polyphenol synthesis. *Biotechnology and Bioengineering*, *116*(6), 1380–1391. https://doi.org/10.1002/bit.26939

Milke, L., Kallscheuer, N., Kappelmann, J., & Marienhagen, J. (2019). Tailoring *Corynebacterium glutamicum* towards increased malonyl-CoA availability for efficient synthesis of the plant pentaketide noreugenin. *Microbial Cell Factories*, *18*(1), 1–12. https://doi.org/10.1186/s12934-

019-1117-x

Milke, L., & Marienhagen, J. (2020). Engineering intracellular malonyl-CoA availability in microbial hosts and its impact on polyketide and fatty acid synthesis. *Applied Microbiology and Biotechnology*, *2017*. https://doi.org/https://doi.org/10.1007/s00253-020-10643-7

Milke, L., Mutz, M., & Marienhagen, J. (2020). Synthesis of the character impact compound raspberry ketone and additional flavoring phenylbutanoids of biotechnological interest with *Corynebacterium glutamicum*. *Microbial Cell Factories*, *19*(92), 1–12. https://doi.org/10.1186/s12934-020-01351-y

Miller, N., Malherbe, C. J., & Joubert, E. (2020). Xanthone- and benzophenone-enriched nutraceutical: Development of a scalable fractionation process and effect of batch-to-batch variation of the raw material (*Cyclopia genistoides*). *Separation and Purification Technology*, *237*, 116465. https://doi.org/10.1016/J.SEPPUR.2019.116465

Miroux, B., & Walker, J. E. (1996). Over-production of Proteins in *Escherichia coli*: Mutant Hosts that Allow Synthesis of some Membrane Proteins and Globular Proteins at High Levels. *J. Mol. Biol*, *260*, 289–298.

Mishra, J., & Arora, N. K. (2018). Secondary metabolites of fluorescent pseudomonads in biocontrol of phytopathogens for sustainable agriculture. *Applied Soil Ecology*, *125*(May), 35–45. https://doi.org/10.1016/j.apsoil.2017.12.004

Mitchell, C. G., Anderson, S. C. K., & El-Mansi, E. M. T. (1995). Purification and characterization of citrate synthase isoenzymes from *Pseudomonas aeruginosa*. *Biochemical Journal*, *309*(2), 507–511. https://doi.org/10.1042/bj3090507

Miyahisa, I., Kaneko, M., Funa, N., Kawasaki, H., Kojima, H., Ohnishi, Y., & Horinouchi, S. (2005). Efficient production of (2*S*)-flavanones by *Escherichia coli* containing an artificial biosynthetic gene cluster. *Applied Microbiology and Biotechnology*, *68*(4), 498–504. https://doi.org/10.1007/s00253-005-1916-3

Miyazawa, T., Fitzgerald, B. J., & Keatinge-Clay, A. T. (2021). Preparative production of an enantiomeric pair by engineered polyketide synthases. *Chemical Communications*, *57*(70), 8762–8765. https://doi.org/10.1039/D1CC03073F

Miyazawa, T., Hirsch, M., Zhang, Z., & Keatinge-Clay, A. T. (2020). An in vitro platform for engineering and harnessing modular polyketide synthases. *Nature Communications*, *11*(1), 1–7. https://doi.org/10.1038/s41467-019-13811-0

Molina-Henares, M. A., de la Torre, J., García-Salamanca, A., Molina-Henares, A. J., Herrera, M. C., Ramos, J. L., & Duque, E. (2010). Identification of conditionally essential genes for growth of *Pseudomonas putida* KT2440 on minimal medium through the screening of a genome-wide mutant library. *Environmental Microbiology*, *12*(6), 1468–1485. https://doi.org/10.1111/j.1462-2920.2010.02166.x

Molina-Santiago, C., Udaondo, Z., Gómez-Lozano, M., Molin, S., & Ramos, J. L. (2017). Global transcriptional response of solvent-sensitive and solvent-tolerant *Pseudomonas putida* strains exposed to toluene. *Environmental Microbiology*, *19*(2), 645–658. https://doi.org/10.1111/1462-2920.13585

Morita, H., Abe, I., & Noguchi, H. (2010). Plant type III PKS. *Comprehensive Natural Products II: Chemistry and Biology*, *1*, 171–225. https://doi.org/10.1016/b978-008045382-8.00022-8

Morita, H., Noguchi, H., Schröder, J., & Abe, I. (2001). Novel polyketides synthesized with a higher plant stilbene synthase. *European Journal of Biochemistry*, *268*(13), 3759–3766. https://doi.org/10.1046/j.1432-1327.2001.02289.x

Morita, H., Wong, C. P., & Abe, I. (2019). How structural subtleties lead to molecular diversity for the type III polyketide synthases. *Journal of Biological Chemistry*, *294*(41), 15121–15136. https://doi.org/10.1074/jbc.REV119.006129

Morone, P., Cottoni, L., & Giudice, F. (2023). Biofuels: Technology, economics, and policy issues. In *Handbook of Biofuels Production* (3rd ed., pp. 55–92). Woodhead Publishing. https://doi.org/10.1016/B978-0-323-91193-1.00012-3

Morrison, W. R., & Smith, L. M. (1964). Preparation of fatty acid methyl esters and dimethylacetals from lipids with boron fluoride-methanol. *Journal of Lipid Research*, *5*(4), 600–608. https://doi.org/10.1016/S0022-2275(20)40190-7

Moutinho, L. F., Moura, F. R., Silvestre, R. C., & Romão-Dumaresq, A. S. (2021). Microbial biosurfactants: A broad analysis of properties, applications, biosynthesis, and techno-economical assessment of rhamnolipid production. *Biotechnology Progress*, *37*(2), e3093. https://doi.org/10.1002/BTPR.3093

Münch, R. (2003). Robert Koch. *Microbes and Infection*, *5*(1), 69–74. https://doi.org/10.1016/S1286-4579(02)00053-9

Muñoz, R., Chambaud, M., Bordel, S., & Villaverde, S. (2008). A systematic selection of the non-aqueous phase in a bacterial two liquid phase bioreactor treating α-pinene. *Applied Microbiology and Biotechnology*, *79*(1), 33–41. https://doi.org/10.1007/s00253-008-1400-y

Mutalik, V. K., Guimaraes, J. C., Cambray, G., Lam, C., Christoffersen, M. J., Mai, Q. A., Tran, A. B., Paull, M., Keasling, J. D., Arkin, A. P., & Endy, D. (2013). Precise and reliable gene expression via standard transcription and translation initiation elements. *Nature Methods*, *10*(4), 354–360. https://doi.org/10.1038/nmeth.2404

Nakata, K., Yoshimoto, A., & Yamada, Y. (1999). Promotion of antibiotic production by high ethanol, high NaCl concentration, or heat shock in *Pseudomonas fluorescens* S272. In *Bioscience, Biotechnology and Biochemistry* (Vol. 63, Issue 2, pp. 293–297). https://doi.org/10.1271/bbb.63.293

Naseri, G. (2023). A roadmap to establish a comprehensive platform for sustainable manufacturing of natural products in yeast. *Nature Communications*, *14*(1916), 1–13. https://doi.org/10.1038/s41467-023-37627-1

Neumann, G., Cornelissen, S., Van Breukelen, F., Hunger, S., Lippold, H., Loffhagen, N., Wick, L. Y., & Heipieper, H. J. (2006). Energetics and surface properties of *Pseudomonas putida* DOT-T1E in a two-phase fermentation system with 1-decanol as second phase. *Applied and Environmental Microbiology*, *72*(6), 4232–4238. https://doi.org/10.1128/AEM.02904-05

Neumann, G., Kabelitz, N., Zehnsdorf, A., Miltner, A., Lippold, H., Meyer, D., Schmid, A., & Heipieper, H. J. (2005). Prediction of the adaptability of *Pseudomonas putida* DOT-T1E to a second phase of a solvent for economically sound two-phase biotransformations. *Applied and Environmental Microbiology*, *71*(11), 6606–6612. https://doi.org/10.1128/AEM.71.11.6606-6612.2005

Newman, D. J., & Cragg, G. M. (2020). Natural Products as Sources of New Drugs over the Nearly Four Decades from 01/1981 to 09/2019. *Journal of Natural Products*, *83*(3), 770–803. https://doi.org/10.1021/acs.jnatprod.9b01285

Nickel, J., Irzik, K., Van Ooyen, J., & Eggeling, L. (2010). The TetR-type transcriptional regulator FasR of *Corynebacterium glutamicum* controls genes of lipid synthesis during growth on acetate. In *Molecular Microbiology* (Vol. 78, Issue 1, pp. 253–265). https://doi.org/10.1111/j.1365-2958.2010.07337.x

Nielsen, J., & Keasling, J. D. (2016). Engineering Cellular Metabolism. *Cell*, *164*(6), 1185–1197.

https://doi.org/10.1016/j.cell.2016.02.004

Nies, S. C., Alter, T. B., Nölting, S., Thiery, S., & Phan, A. N. T. (2020). High titer methyl ketone production with tailored *Pseudomonas taiwanensis* VLB120. *Metabolic Engineering*, *62*, 84–94. https://doi.org/10.1016/j.ymben.2020.08.003

Nikel, P. I., Chavarría, M., Fuhrer, T., Sauer, U., & De Lorenzo, V. (2015). *Pseudomonas putida* KT2440 strain metabolizes glucose through a cycle formed by enzymes of the Entner-Doudoroff, Embden-Meyerhof-Parnas, and pentose phosphate pathways. *Journal of Biological Chemistry*, *290*(43), 25920–25932. https://doi.org/10.1074/jbc.M115.687749

Nikel, P. I., & de Lorenzo, V. (2018). *Pseudomonas putida* as a functional *chassis* for industrial biocatalysis: From native biochemistry to *trans*-metabolism. *Metabolic Engineering*, *50*(April), 142–155. https://doi.org/10.1016/j.ymben.2018.05.005

Nikel, P. I., Fuhrer, T., Lorenzo, V. De, Chavarría, M., & Sánchez-pascuala, A. (2021). Reconfiguration of metabolic fluxes in *Pseudomonas putida* as a response to sub-lethal oxidative stress. *The ISME Journal*, *15*, 1751–1766. https://doi.org/10.1038/s41396-020-00884-9

Nivina, A., Yuet, K. P., Hsu, J., & Khosla, C. (2019). Evolution and Diversity of Assembly-Line Polyketide Synthases. *Chemical Reviews*, *119*(24), 12524–12547. https://doi.org/10.1021/acs.chemrev.9b00525

Nowak-Thompson, B., Chaney, N., Wing, J. S., Gould, S. J., & Loper, J. E. (1999). Characterization of the pyoluteorin biosynthetic gene cluster of *Pseudomonas fluorescens* Pf-5. *Journal of Bacteriology*, *181*(7), 2166–2174. https://doi.org/10.1128/jb.181.7.2166-2174.1999

Nowak-Thompson, B., Hammer, P. E., Hill, D. S., Stafford, J., Torkewitz, N., Gaffney, T. D., Lam, S. T., Molnár, I., & Ligon, J. M. (2003). 2,5-Dialkylresorcinol Biosynthesis in *Pseudomonas aurantiaca*: Novel Head-to-Head Condensation of Two Fatty Acid-Derived Precursors. *Journal of Bacteriolog*, *185*(3), 860–869. https://doi.org/10.1128/JB.185.3.860

Nualkaew, N., Morita, H., Shimokawa, Y., Kinjo, K., Kushiro, T., De-Eknamkul, W., Ebizuka, Y., & Abe, I. (2012). Benzophenone synthase from *Garcinia mangostana* L. pericarps. *Phytochemistry*, *77*, 60–69. https://doi.org/10.1016/j.phytochem.2012.02.002

Okolie, J. A., Mukherjee, A., Nanda, S., Dalai, A. K., & Kozinski, J. A. (2021). Next-generation biofuels and platform biochemicals from lignocellulosic biomass. *International Journal of Energy Research*, *45*(10), 14145–14169. https://doi.org/10.1002/ER.6697

Orsini, F., Pelizzoni, F., Bellini, B., & Miglierini, G. (1997). Synthesis of biologically active polyphenolic glycosides (combretastatin and resveratrol series). *Carbohydrate Research*, *301*(3–4), 95–109. https://doi.org/10.1016/S0008-6215(97)00087-6

Otto, M. (2019). *Microbial catalysis of renewable resources into aromatics via the central metabolic precursor phenylalanine*.

Otto, M., Wynands, B., Lenzen, C., Filbig, M., Blank, L. M., & Wierckx, N. (2019). Rational Engineering of Phenylalanine Accumulation in *Pseudomonas taiwanensis* to Enable High-Yield Production of *Trans*-cinnamate. *Frontiers in Bioengineering and Biotechnology*, *7*(312). https://doi.org/10.3389/fbioe.2019.00312

Otto, M., Wynands, B., Marienhagen, J., Blank, L. M., & Wierckx, N. (2020). Benzoate Synthesis from Glucose Or Glycerol Using Engineered Pseudomonas taiwanensis. *Biotechnology Journal*, *2000211*, 2000211. https://doi.org/10.1002/biot.202000211

Owen, J. G., Copp, J. N., & Ackerley, D. F. (2011). Rapid and flexible biochemical assays for evaluating 4'-phosphopantetheinyl transferase activity. *Biochemical Journal*, *436*(3), 709–717.

https://doi.org/10.1042/BJ20110321

Palmer, C. M., & Alper, H. S. (2019). Expanding the Chemical Palette of Industrial Microbes: Metabolic Engineering for Type III PKS-Derived Polyketides. *Biotechnology Journal*, *14*. https://doi.org/10.1002/biot.201700463

Pan, S. Y., Litscher, G., Gao, S. H., Zhou, S. F., Yu, Z. L., Chen, H. Q., Zhang, S. F., Tang, M. K., Sun, J. N., & Ko, K. M. (2014). Historical perspective of traditional indigenous medical practices: The current renaissance and conservation of herbal resources. *Evidence-Based Complementary and Alternative Medicine*, *2014*. https://doi.org/10.1155/2014/525340

Pandith, S. A., Ramazan, S., Khan, M. I., Reshi, Z. A., & Shah, M. A. (2020). Chalcone synthases (CHSs): the symbolic type III polyketide synthases. *Planta*, *251*(1). https://doi.org/10.1007/s00425-019-03307-y

Pang, Z., Chen, J., Wang, T., Gao, C., Li, Z., Guo, L., Xu, J., & Cheng, Y. (2021). Linking Plant Secondary Metabolites and Plant Microbiomes: A Review. *Frontiers in Plant Science*, *12*, 621276. https://doi.org/10.3389/fpls.2021.621276

Panke, S., De Lorenzo, V., Kaiser, A., Witholt, B., & Wubbolts, M. G. (1999). Engineering of a stable whole-cell biocatalyst capable of (*S*)-styrene oxide formation for continuous two-liquid-phase applications. *Applied and Environmental Microbiology*, *65*(12), 5619–5623. https://doi.org/10.1128/aem.65.12.5619-5623.1999

Panke, S., Meyer, A., Huber, C. M., Witholt, B., & Wubbolts, M. G. (1999). An alkane-responsive expression system for the production of fine chemicals. *Applied and Environmental Microbiology*, *65*(6), 2324–2332. https://doi.org/10.1128/aem.65.6.2324-2332.1999

Panke, S., Witholt, B., & Schmid, A. (1998). Towards a Biocatalyst for (S)-Styrene Oxide Production: Characterization of the Styrene Degradation Pathway of *Pseudomonas* sp. Strain VLB120. *Applied and Environmental Microbiology*, *64*(6), 2032–2043. https://doi.org/https://doi.org/10.1128/AEM.64.6.2032-2043.1998

Park, H. B., Goddard, T. N., Oh, J., Patel, J., Wei, Z., Perez, C. E., Mercado, B. Q., Wang, R., Wyche, T. P., Piizzi, G., Flavell, R. A., & Crawford, J. M. (2020). Bacterial Autoimmune Drug Metabolism Transforms an Immunomodulator into Structurally and Functionally Divergent Antibiotics. *Angewandte Chemie - International Edition*, *59*(20), 7871–7880. https://doi.org/10.1002/anie.201916204

Park, J.-B., Brühler, B., Panke, S., Witholt, B., & Schmid, A. (2007). Carbon Metabolism and Product Inhibition Determine the Epoxidation Efficiency of Solvent-Tolerant *Pseudomonas* sp. Strain VLB120ΔC. *Biotechnology and Bioengineering*, *98*(6). https://doi.org/10.1002/bit.21496

Park, J., Rodríguez-Moyá, M., Li, M., Pichersky, E., San, K. Y., & Gonzalez, R. (2012). Synthesis of methyl ketones by metabolically engineered *Escherichia coli*. *Journal of Industrial Microbiology and Biotechnology*, *39*(11), 1703–1712. https://doi.org/10.1007/s10295-012-1178-x

Parker, C., Barnelp, W. O., Snoep, J. L., Ingram, L. O., & Conway, T. (1995). Characterization of the *Zymomonas mobilis* glucose facilitator gene product (*glf*) in recombinant *Escherichia coli*: examination of transport mechanism , kinetics and the role of glucokinase in glucose transport. *Molecular Microbiology*, *15*(5), 795–802.

Pavkov-Keller, T., Schmidt, N. G., Żądło-Dobrowolska, A., Kroutil, W., & Gruber, K. (2019). Structure and Catalytic Mechanism of a Bacterial Friedel–Crafts Acylase. *ChemBioChem*, *20*(1), 88–95. https://doi.org/10.1002/cbic.201800462

Pawar, S., Chaudhari, A., Prabha, R., Shukla, R., & Singh, D. P. (2019). Microbial pyrrolnitrin: Natural metabolite with immense practical utility. *Biomolecules*, *9*(9).

https://doi.org/10.3390/biom9090443

Pedraza de la Cuesta, S., Knopper, L., van der Wielen, L. A. M., & Cuellar, M. C. (2019). Techno-economic assessment of the use of solvents in the scale-up of microbial sesquiterpene production for fuels and fine chemicals. *Biofuels, Bioproducts and Biorefining*, *13*(1), 140–152. https://doi.org/10.1002/bbb.1949

Peng, H., Tan, J., Bilal, M., Wang, W., Hu, H., & Zhang, X. (2018). Enhanced biosynthesis of phenazine-1-carboxamide by *Pseudomonas chlororaphis* strains using statistical experimental designs. *World Journal of Microbiology and Biotechnology*, *34*(9), 1–10. https://doi.org/10.1007/s11274-018-2501-0

Perišić, M., Barceló, E., Dimic-Misic, K., Imani, M., & Spasojević Brkić, V. (2022). The Role of Bioeconomy in the Future Energy Scenario: A State-of-the-Art Review. *Sustainability*, *14*(1), 560. https://doi.org/10.3390/SU14010560

Peyraud, R., Kiefer, P., Christen, P., Massou, S., Portais, J. C., & Vorholt, J. A. (2009). Demonstration of the ethylmalonyl-CoA pathway by using 13C metabolomics. *Proceedings of the National Academy of Sciences of the United States of America*, *106*(12), 4846–4851. https://doi.org/10.1073/pnas.0810932106

Phang, S. J., Teh, H. X., Looi, M. L., Arumugam, B., Fauzi, M. B., & Kuppusamy, U. R. (2023). Phlorotannins from brown algae: a review on their antioxidant mechanisms and applications in oxidative stress-mediated diseases. *Journal of Applied Phycology*, *0123456789*. https://doi.org/10.1007/s10811-023-02913-4

Phong, W. N., Show, P. L., Chow, Y. H., & Ling, T. C. (2018). Recovery of biotechnological products using aqueous two phase systems. *Journal of Bioscience and Bioengineering*, *126*(3), 273–281. https://doi.org/10.1016/j.jbiosc.2018.03.005

Piccione, P. M., Baumeister, J., Salvesen, T., Grosjean, C., Flores, Y., Groelly, E., Murudi, V., Shyadligeri, A., Lobanova, O., & Lothschütz, C. (2019). Solvent Selection Methods and Tool. *Organic Process Research and Development*, *23*(5), 998–1016. https://doi.org/10.1021/acs.oprd.9b00065

Poblete-Castro, I., Binger, D., Rodrigues, A., Becker, J., Martins Dos Santos, V. A. P., & Wittmann, C. (2013). In-silico-driven metabolic engineering of *Pseudomonas putida* for enhanced production of poly-hydroxyalkanoates. *Metabolic Engineering*, *15*(1), 113–123. https://doi.org/10.1016/j.ymben.2012.10.004

Prabowo, C. P. S., Eun, H., Yang, D., Huccetogullari, D., Jegadeesh, R., Kim, S. J., & Lee, S. Y. (2022). Production of natural colorants by metabolically engineered microorganisms. *Trends in Chemistry*, *4*(7), 608–626. https://doi.org/10.1016/J.TRECHM.2022.04.009

Priebe, X., & Daugulis, A. J. (2018). Thermodynamic affinity-based considerations for the rational selection of biphasic systems for microbial flavor and fragrance production. *Journal of Chemical Technology and Biotechnology*, *93*(3), 656–666. https://doi.org/10.1002/jctb.5524

Prpich, G. P., & Daugulis, A. J. (2006). Solvent Selection For Enhanced Bioproduction of 3-methylcatechol in a Two-Phase Partitioning Bioreactor. *Biotechnology and Bioengineering*, *97*(3), 536–543. https://doi.org/10.1002/bit.21257

Puigbò, P., Guzmán, E., Romeu, A., & Garcia-Vallvé, S. (2007). OPTIMIZER: A web server for optimizing the codon usage of DNA sequences. *Nucleic Acids Research*, *35*(SUPPL.2), W126–W131. https://doi.org/10.1093/nar/gkm219

Quijano, G., Hernandez, M., Thalasso, F., Muñoz, R., & Villaverde, S. (2009). Two-phase partitioning bioreactors in environmental biotechnology. *Applied Microbiology and Biotechnology*, *84*(5),

829–846. https://doi.org/10.1007/s00253-009-2158-6

Radmacher, E., Alderwick, L. J., Besra, G. S., Brown, A. K., Gibson, K. J. C., Sahm, H., & Eggeling, L. (2005). Two functional FAS-I type fatty acid synthases in *Corynebacterium glutamicum*. *Microbiology*, *151*(7), 2421–2427. https://doi.org/10.1099/mic.0.28012-0

Rainha, J., Gomes, D., Rodrigues, L. R., & Rodrigues, J. L. (2020). Synthetic Biology Approaches to Engineer *Saccharomyces cerevisiae* towards the Industrial Production of Valuable Polyphenolic Compounds. *Life*, *10*(56), 1–26. https://doi.org/10.3390/life10050056

Ramos-González, M. I., Ben-Bassat, A., Campos, M. J., & Ramos, J. L. (2003). Genetic engineering of a highly solvent-tolerant *Pseudomonas putida* strain for biotransformation of toluene to *p*-hydroxybenzoate. *Applied and Environmental Microbiology*, *69*(9), 5120–5127. https://doi.org/10.1128/AEM.69.9.5120-5127.2003

Ramos, J. L., Cuenca, M. S., Molina-Santiago, C., Segura, A., Duque, E., Ǵomez-Garciá, M. R., Udaondo, Z., & Roca, A. (2015). Mechanisms of solvent resistance mediated by interplay of cellular factors in *Pseudomonas putida*. *FEMS Microbiology Reviews*, *39*(4), 555–566. https://doi.org/10.1093/femsre/fuv006

Rao, G., Lee, J. K., & Zhao, H. (2013). Directed evolution of phloroglucinol synthase PhlD with increased stability for phloroglucinol production. *Applied Microbiology and Biotechnology*, *97*(13), 5861–5867. https://doi.org/10.1007/s00253-013-4713-4

Reed, K. B., & Alper, H. S. (2018). Expanding beyond canonical metabolism: Interfacing alternative elements, synthetic biology, and metabolic engineering. *Synthetic and Systems Biotechnology*, *3*(1), 20–33. https://doi.org/10.1016/j.synbio.2017.12.002

Remali, J., Sahidin, I., & Aizat, W. M. (2022). Xanthone Biosynthetic Pathway in Plants: A Review. *Frontiers in Plant Science*, *13*(April), 1–15. https://doi.org/10.3389/fpls.2022.809497

Ringel, M. T., & Brüser, T. (2018). The biosynthesis of pyoverdines. *Microbial Cell*, *5*(10), 424–437. https://doi.org/10.15698/mic2018.10.649

Rittner, A., Joppe, M., Schmidt, J. J., Mayer, L. M., Reiners, S., Heid, E., Herzberg, D., Sherman, D. H., & Grininger, M. (2022). Chemoenzymatic synthesis of fluorinated polyketides. *Nature Chemistry*, *14*(9), 1000–1006. https://doi.org/10.1038/s41557-022-00996-z

Rogers, P. L., Lee, K. J., & Tribe, D. E. (1976). Kinetics of alcohol production by *Zymomonas mobilis* at high sugar concentrations. *Biotechnology Letters*, *1*, 165–170.

Rojas, A., Duque, E., Mosqueda, G., Golden, G., Hurtado, A., Ramos, J. L., & Segura, A. (2001). Three Efflux Pumps Are Required To Provide Efficient Tolerance to Toluene in *Pseudomonas putida* DOT-T1E. *Journal of Bacteriology*, *183*(13), 3967–3973. https://doi.org/10.1128/JB.183.13.3967

Rojas, A., Duque, E., Schmid, A., Hurtado, A., Ramos, J. L., & Segura, A. (2004). Biotransformation in double-phase systems: Physiological responses of *Pseudomonas putida* DOT-T1E to a double phase made of aliphatic alcohols and biosynthesis of substituted catechols. *Applied and Environmental Microbiology*, *70*(6), 3637–3643. https://doi.org/10.1128/AEM.70.6.3637-3643.2004

Rorrer, N. A., Sandra, F., Knott, B. C., Beckham, G. T., Rorrer, N. A., Notonier, S. F., Knott, B. C., Black, B. A., Singh, A., Nicholson, S. R., Kinchin, C. P., Schmidt, G. P., Carpenter, A. C., Ramirez, K. J., Johnson, C. W., Salvachu, D., & Crowley, M. F. (2022). Production of β-ketoadipic acid from glucose in *Pseudomonas putida* KT2440 for use in performance-advantaged nylons. *Cell Reports Physical Science*, *3*(4). https://doi.org/10.1016/j.xcrp.2022.100840

Sáez-Sáez, J., Wang, G., Marella, E. R., Sudarsan, S., Cernuda Pastor, M., & Borodina, I. (2020).

Engineering the oleaginous yeast *Yarrowia lipolytica* for high-level resveratrol production. *Metabolic Engineering*, *62*(August), 51–61. https://doi.org/10.1016/j.ymben.2020.08.009

Salas-Navarrete, C., Hernández-Chávez, G., Flores, N., Martínez, L. M., Martinez, A., Bolívar, F., Barona-Gomez, F., & Gosset, G. (2018). Increasing pinosylvin production in *Escherichia coli* by reducing the expression level of the gene *fabI*-encoded enoyl-acyl carrier protein reductase. *Electronic Journal of Biotechnology*, *33*, 11–16. https://doi.org/10.1016/j.ejbt.2018.03.001

Santos, C. N. S., Koffas, M., & Stephanopoulos, G. (2011). Optimization of a heterologous pathway for the production of flavonoids from glucose. *Metabolic Engineering*, *13*(4), 392–400. https://doi.org/10.1016/j.ymben.2011.02.002

Sardessai, Y. N., & Bhosle, S. (2004). Industrial potential of organic solvent tolerant bacteria. *Biotechnology Progress*, *20*(3), 655–660. https://doi.org/10.1021/bp0200595

Sauer, M. (2016). Industrial production of acetone and butanol by fermentation-100 years later. *FEMS Microbiology Letters*, *363*(13), 1–4. https://doi.org/10.1093/femsle/fnw134

Schada Von Borzyskowski, L., Bernhardsgrütter, I., & Erb, T. J. (2020). Biochemical unity revisited: Microbial central carbon metabolism holds new discoveries, multi-tasking pathways, and redundancies with a reason. *Biological Chemistry*, *401*(12), 1429–1441. https://doi.org/10.1515/hsz-2020-0214

Schmid, A., Kollmer, A., Sonnleitner, B., & Witholt, B. (1999). Development of equipment and procedures for the safe operation of aerobic bacterial bioprocesses in the presence of bulk amounts of flammable organic solvents. *Bioprocess Engineering*, *20*(2), 91–100. https://doi.org/10.1007/s004490050565

Schmid, Andrew, Kollmer, A., Mathys, R. G., & Witholt, B. (1998). Developments toward large-scale bacterial bioprocesses in the presence of bulk amounts of organic solvents. *Extremophiles*, *2*(3), 249–256. https://doi.org/10.1007/s007920050067

Schmid, W. (1849). Ueber das Mangostin. *Justus Liebigs Annalen Der Chemie*, *93*(1), 83–88.

Schmidt, W., & Beerhues, L. (1997). Alternative pathways of xanthone biosynthesis in cell cultures of *Hypericum androsaemum* L. *FEBS Letters*, *420*(2–3), 143–146. https://doi.org/10.1016/S0014-5793(97)01507-X

Schmitz, S., Nies, S., Wierckx, N., Blank, L. M., & Rosenbaum, M. A. (2015). Engineering mediator-based electroactivity in the obligate aerobic bacterium *Pseudomonas putida* KT2440. *Frontiers in Microbiology*, *6*(APR), 135742. https://doi.org/10.3389/FMICB.2015.00284/ABSTRACT

Scholz, K., Tiso, T., Blank, L. M., & Hayen, H. (2018). Mass spectrometric characterization of siderophores produced by *Pseudomonas taiwanensis* VLB120 assisted by stable isotope labeling of nitrogen source. *BioMetals*, *31*(5), 785–795. https://doi.org/10.1007/s10534-018-0122-6

Schöner, T. A., Gassel, S., Osawa, A., Tobias, N. J., Okuno, Y., Sakakibara, Y., Shindo, K., Sandmann, G., & Bode, H. B. (2016). Aryl Polyenes, a Highly Abundant Class of Bacterial Natural Products, Are Functionally Related to Antioxidative Carotenoids. *ChemBioChem*, *17*(3), 247–253. https://doi.org/10.1002/cbic.201500474

Schönsee, C. D., & Bucheli, T. D. (2020). Experimental Determination of Octanol-Water Partition Coefficients of Selected Natural Toxins. *Journal of Chemical and Engineering Data*, *65*(4), 1946–1953. https://doi.org/10.1021/acs.jced.9b01129

Schöppner, A., & Kindl, H. (1984). Purification and properties of a stilbene synthase from induced cell suspension cultures of peanut. *Journal of Biological Chemistry*, *259*(11), 6806–6811.

Schwanemann, T., Otto, M., Wierckx, N., & Wynands, B. (2020). *Pseudomonas* as Versatile Aromatics

Cell Factory. *Biotechnology Journal*, *1900569*, 1900569. https://doi.org/10.1002/biot.201900569

Schwanemann, T., Otto, M., Wynands, B., Marienhagen, J., & Wierckx, N. (2023). A *Pseudomonas taiwanensis* malonyl-CoA platform strain for polyketide synthesis. *Metabolic Engineering*, *77*(February), 219–230. https://doi.org/10.1016/j.ymben.2023.04.001

Schwanemann, T., Urban, E. A., Eberlein, C., Jochem, G., Rago, D., Krink, N., Nikel, P. I., Heipieper, H. J., Wynands, B., & Wierckx, N. (2023). Production of (hydroxy)benzoate-derived polyketides by engineered *Pseudomonas* with *in situ* extraction. *Bioresource Technology*, *388*(129741), 0–11. https://doi.org/10.1016/j.biortech.2023.129741

Schwartz, R. D., & McCoy, C. J. (1977). Epoxidation of 1,7 octadiene by *Pseudomonas oleovorans*: fermentation in the presence of cyclohexane. *Applied and Environmental Microbiology*, *34*(1), 47–49. https://doi.org/10.1128/aem.34.1.47-49.1977

Shahid, I., Malik, K. A., & Mehnaz, S. (2018). A decade of understanding secondary metabolism in *Pseudomonas* spp. for sustainable agriculture and pharmaceutical applications. *Environmental Sustainability*, *1*(1), 3–17. https://doi.org/10.1007/s42398-018-0006-2

Sheldon, R. A., Brady, D., & Bode, M. L. (2020). The Hitchhiker's guide to biocatalysis: recent advances in the use of enzymes in organic synthesis. *Chemical Science*, *11*(10), 2587–2605. https://doi.org/10.1039/C9SC05746C

Shi, H., Huang, X., Wang, Z., Guan, Y., & Zhang, X. (2019). Improvement of pyoluteorin production in *Pseudomonas protegens* H78 through engineering its biosynthetic and regulatory pathways. *Applied Microbiology and Biotechnology*, *103*(8), 3465–3476. https://doi.org/10.1007/s00253-019-09732-z

Shi, S. P., Morita, H., Wanibuchi, K., Noguchi, H., & Abe, I. (2009). Enzymatic formation of unnatural novel polyketide scaffolds by plant-specific type III polyketide synthase. *Tetrahedron Letters*, *50*(18), 2150–2153. https://doi.org/10.1016/j.tetlet.2009.02.170

Shi, Sanyuan, Tian, J., & Luo, Y. (2022). Recent advances in fluorinated products biosynthesis. *Bioresource Technology Reports*, *20*, 101288. https://doi.org/10.1016/j.biteb.2022.101288

Shi, Shuobo, Chen, Y., Siewers, V., & Nielsen, J. (2014). Improving production of malonyl coenzyme A-derived metabolites by abolishing Snf1-dependent regulation of Acc1. *MBio*, *5*(3). https://doi.org/10.1128/mbio.01130-14

Shimizu, Y., Ogata, H., & Goto, S. (2017). Type III Polyketide Synthases: Functional Classification and Phylogenomics. *ChemBioChem*, *18*(1), 50–65. https://doi.org/10.1002/cbic.201600522

Shrestha, A., Pandey, R. P., & Sohng, J. K. (2019). Biosynthesis of resveratrol and piceatannol in engineered microbial strains: achievements and perspectives. *Applied Microbiology and Biotechnology*, *103*(7), 2959–2972. https://doi.org/10.1007/s00253-019-09672-8

Sikkema, J., De Bont, J. A. M., & Poolman, B. (1994). Interactions of cyclic hydrocarbons with biological membranes. *Journal of Biological Chemistry*, *269*(11), 8022–8028.

Silverstein, T. P. (2014). An exploration of how the thermodynamic efficiency of bioenergetic membrane systems varies with *c*-subunit stoichiometry of F_1F_0 ATP synthases. *Journal of Bioenergetics and Biomembranes*, *46*(3), 229–241. https://doi.org/10.1007/s10863-014-9547-y

Singh, A., Prajapati, P., Vyas, S., Gaur, V. K., Sindhu, R., Binod, P., Kumar, V., Singhania, R. R., Awasthi, M. K., Zhang, Z., & Varjani, S. (2022). A Comprehensive Review of Feedstocks as Sustainable Substrates for Next-Generation Biofuels. *BioEnergy Research*, *16*(1), 105–122. https://doi.org/10.1007/S12155-022-10440-2

Sirirungruang, S., Ad, O., Privalsky, T. M., Ramesh, S., Sax, J. L., Dong, H., Baidoo, E. E. K., Amer, B., Khosla, C., & Chang, M. C. Y. (2022). Engineering site-selective incorporation of fluorine into polyketides. *Nature Chemical Biology*, *18*(8), 886–893. https://doi.org/10.1038/s41589-022-01070-y

Snoep, J. L., Arfman, N., Yomano, L. P., Fliege, R. K., Conway, T., & Ingram, L. O. (1994). Reconstitution of glucose uptake and phosphorylation in a glucose-negative mutant of *Escherichia coli* by using *Zymomonas mobilis* genes encoding the glucose facilitator protein and glucokinase. *Journal of Bacteriology*, *176*(7), 2133–2135. https://doi.org/10.1128/jb.176.7.2133-2135.1994

Soares, R. R. G., Azevedo, A. M., Van Alstine, J. M., & Raquel Aires-Barros, M. (2015). Partitioning in aqueous two-phase systems: Analysis of strengths, weaknesses, opportunities and threats. *Biotechnology Journal*, *10*(8), 1158–1169. https://doi.org/10.1002/biot.201400532

Solovyev, V., & Salamov, A. (2011). Automatic Annotation of Microbial Genomes and Metagenomic Sequences. In R. W. Li (Ed.), *Metagenomics and its Applications in Agriculture, Biomedicine and Environmental Studies* (pp. 61–78). Nova Science Publishers. https://doi.org/10.5040/9781635577068-0083

Sprakel, L. M. J., & Schuur, B. (2019). Solvent developments for liquid-liquid extraction of carboxylic acids in perspective. *Separation and Purification Technology*, *211*(September 2018), 935–957. https://doi.org/10.1016/j.seppur.2018.10.023

Srinivas, S., & Cronan, J. E. (2017). An Eight-Residue Deletion in *Escherichia coli* FabG Causes Temperature-Sensitive Growth and Lipid Synthesis Plus Resistance to the Calmodulin Inhibitor Trifluoperazin. *Journal of Bacteriology*, *199*(10), 1–14. https://doi.org/https://doi.org/10.1128/JB.00074-17

Staunton, J., & Weissman, K. J. (2001). Polyketide biosynthesis: a millennium review. *Natural Product Reports*, *18*, 380–416. https://doi.org/10.1039/a909079g

Stewart, C., Woods, K., Macias, G., Allan, A. C., Hellens, R. P., & Noel, J. P. (2017). Molecular architectures of benzoic acid-specific type III polyketide synthases. *Acta Crystallographica Section D: Structural Biology*, *73*(12), 1007–1019. https://doi.org/10.1107/S2059798317016618

Stoudenmire, J. L., Schmidt, A. L., Tumen-Velasquez, M. P., Elliott, K. T., Laniohan, N. S., Whitley, S. W., Galloway, N. R., Nune, M., West, M., Momany, C., Neidle, E. L., & Karls, A. C. (2017). Malonate degradation in *Acinetobacter baylyi* ADP1: Operon organization and regulation by MdcR. *Microbiology*, *163*(5), 789–803. https://doi.org/10.1099/mic.0.000462

Straathof, A. J. J., Wahl, S. A., Benjamin, K. R., Takors, R., Wierckx, N., & Noorman, H. J. (2019). Grand Research Challenges for Sustainable Industrial Biotechnology. *Trends in Biotechnology*, *37*(10), 1042–1050. https://doi.org/10.1016/j.tibtech.2019.04.002

Sui, X., Zhao, M., Liu, Y., Wang, J., Li, G., Zhang, X., & Deng, Y. (2020). Enhancing glutaric acid production in *Escherichia coli* by uptake of malonic acid. *Journal of Industrial Microbiology and Biotechnology*, *47*(3), 311–318. https://doi.org/10.1007/s10295-020-02268-6

Sun, H., Zhao, H., & Ang, E. L. (2020). A New Biosensor for Stilbenes and a Cannabinoid Enabled by Genome Mining of a Transcriptional Regulator. *ACS Synthetic Biology*, *9*(4), 698–705. https://doi.org/10.1021/acssynbio.9b00443

Sun, S., Zhou, L., Jin, K., Jiang, H., & He, Y. W. (2016). Quorum sensing systems differentially regulate the production of phenazine-1-carboxylic acid in the rhizobacterium *Pseudomonas aeruginosa* PA1201. *Scientific Reports*, *6*(July), 16–18. https://doi.org/10.1038/srep30352

Suvorova, I. A., Ravcheev, D. A., & Gelfand, M. S. (2012). Regulation and evolution of malonate and propionate catabolism in proteobacteria. *Journal of Bacteriology*, *194*(12), 3234–3240.

https://doi.org/10.1128/JB.00163-12

Świezyński, A. (2016). Where/when/how did life begin? A philosophical key for systematizing theories on the origin of life. *International Journal of Astrobiology*, *15*(4), 291–299. https://doi.org/10.1017/S1473550416000100

Talwar, N., & Holden, N. M. (2022). The limitations of bioeconomy LCA studies for understanding the transition to sustainable bioeconomy. *The International Journal of Life Cycle Assessment*, *27*, 680–703. https://doi.org/10.1007/s11367-022-02053-w

Tao, S., Qian, Y., Wang, X., Cao, W., Ma, W., Chen, K., & Ouyang, P. (2018). Regulation of ATP levels in *Escherichia coli* using CRISPR interference for enhanced pinocembrin production. *Microbial Cell Factories*, *17*(1), 1–13. https://doi.org/10.1186/s12934-018-0995-7

Terán, W., Krell, T., Ramos, J. L., & Gallegos, M. T. (2006). Effector-repressor interactions, binding of a single effector molecule to the operator-bound TtgR homodimer mediates derepression. *Journal of Biological Chemistry*, *281*(11), 7102–7109. https://doi.org/10.1074/jbc.M511095200

Tharmasothirajan, A., Wellfonder, M., & Marienhagen, J. (2021). Microbial Polyphenol Production in a Biphasic Process. *ACS Sustainable Chemistry and Engineering*. https://doi.org/10.1021/acssuschemeng.1c05865

Thomas, C., & Tampé, R. (2020). Structural and Mechanistic Principles of ABC Transporters. *Annual Review of Biochemistry*, *89*, 605–636. https://doi.org/10.1146/annurev-biochem-011520-105201

Thompson, M. G., Incha, M. R., Pearson, A. N., Schmidt, M., Sharpless, W. A., Eiben, C. B., Cruz-Morales, P., Blake-Hedges, J. M., Liu, Y., Adams, C. A., Haushalter, R. W., Krishna, R. N., Lichtner, P., Blank, L. M., Mukhopadhyay, A., Deutschbauer, A. M., Shih, P. M., & Keasling, J. D. (2020). Fatty Acid and Alcohol Metabolism in *Pseudomonas putida*: Functional Analysis Using Random Barcode Transposon Sequencing. *Applied and Environmental Microbiology*, *86*(21), 1–23. https://doi.org/10.1128/AEM.01665-20

Trantas, E. A., Koffas, M. A. G., Xu, P., & Ververidis, F. (2015). When plants produce not enough or at all: Metabolic engineering of flavonoids in microbial hosts. *Frontiers in Plant Science*, *6*(JAN), 1–16. https://doi.org/10.3389/fpls.2015.00007

Traxler, M. F., & Kolter, R. (2015). Natural products in soil microbe interactions and evolution. *Natural Product Reports*, *32*(7), 956–970. https://doi.org/10.1039/C5NP00013K

Tropf, S., Karcher, B., Schroder, G., & Schroder, J. (1995). Reaction mechanisms of homodimeric plant polyketide synthases (stilbene and chalcone synthase). A single active site for the condensing reaction is sufficient for synthesis of stilbenes, chalcones, and 6'-deoxychalcones. *Journal of Biological Chemistry*, *270*(14), 7922–7928. https://doi.org/10.1074/jbc.270.14.7922

Udaondo, Z., Ramos, J. L., Segura, A., Krell, T., & Daddaoua, A. (2018). Regulation of carbohydrate degradation pathways in *Pseudomonas* involves a versatile set of transcriptional regulators. *Microbial Biotechnology*, *11*(3), 442–454. https://doi.org/10.1111/1751-7915.13263

Ueda, K., Kimtf, K., Beppu, T., & Horinouchi, S. (1995). Overexpression of a Gene Cluster Encoding a Chalcone Synthase-like Protein Confers Redbrown Pigment Production in *Streptomyces griseus*. *The Journal of Antibiotics*, *July*, 638–646.

United Nations Environment Programme. (2022). *Emissions Gap Report: The Closing Window - Climate crisis calls for rapid transformation of societies*. https://www.unep.org/emissions-gap-report-2022

Uwineza, P. A., & Waśkiewicz, A. (2020). Recent Advances in Supercritical Fluid Extraction of Natural

Bioactive Compounds from Natural Plant Materials. *Molecules*, *25*(17), 3847. https://doi.org/10.3390/MOLECULES25173847

Van Den Berg, C., Wierckx, N., Vente, J., Bussmann, P., De Bont, J., & Van Der Wielen, L. (2008). Solvent-impregnated resins as an in situ product recovery tool for phenol recovery from *Pseudomonas putida* S12TPL fermentations. *Biotechnology and Bioengineering*, *100*(3), 466–472. https://doi.org/10.1002/bit.21790

van Leeuwenhoek, A. (1676). Observations, communicated to the publisher by Mr. Antony van Leewenhoeck, in a dutch letter of the 9th Octob. 1676. here English'd: concerning little animals by him observed in rain-well-sea- and snow water; as also in water wherein pepper had lain infus. *Philosophical Transactions of the Royal Society of London*, *12*(133), 2821–831. https://doi.org/10.1098/rstl.1677.0003

van Summeren-Wesenhagen, P. V., & Marienhagen, J. (2015). Metabolic engineering of *Escherichia coli* for the synthesis of the plant polyphenol pinosylvin. *Applied and Environmental Microbiology*, *81*(3), 840–849. https://doi.org/10.1128/AEM.02966-14

van Summeren-Wesenhagen, P. V., & Marienhagen, J. (2013). Putting bugs to the blush: Metabolic engineering for phenylpropanoid-derived products in microorganisms. *Bioengineered*, *4*(6). https://doi.org/10.4161/bioe.23885

Verhoef, S., Ballerstedt, H., Volkers, R. J. M., De Winde, J. H., & Ruijssenaars, H. J. (2010). Comparative transcriptomics and proteomics of *p*-hydroxybenzoate producing *Pseudomonas putida* S12: Novel responses and implications for strain improvement. *Applied Microbiology and Biotechnology*, *87*(2), 679–690. https://doi.org/10.1007/s00253-010-2626-z

Verhoef, S., Wierckx, N., Westerhof, R. G. M., De Winde, J. H., & Ruijssenaars, H. J. (2009). Bioproduction of *p*-hydroxystyrene from glucose by the solvent-tolerant bacterium *Pseudomonas putida* S12 in a two-phase water-decanol fermentation. *Applied and Environmental Microbiology*, *75*(4), 931–936. https://doi.org/10.1128/AEM.02186-08

Verma, A. S., Agrahari, S., Rastogi, S., & Singh, A. (2011). Biotechnology in the Realm of History. *Journal of Pharmacy and Bioallied Sciences*, *3*(3), 321. https://doi.org/10.4103/0975-7406.84430

Virklund, A., Jensen, S. I., Nielsen, A. T., & Woodley, J. M. (2022). Combining genetic engineering and bioprocess concepts for improved phenylpropanoid production. *Biotechnology and Bioengineering*, *November*, 1–16. https://doi.org/10.1002/bit.28292

Volke, Daniel C., Friis, L., Wirth, N. T., Turlin, J., & Nikel, P. I. (2020). Synthetic control of plasmid replication enables target- and self-curing of vectors and expedites genome engineering of *Pseudomonas putida*. *Metabolic Engineering Communications*, *10*(January), e00126. https://doi.org/10.1016/j.mec.2020.e00126

Volke, Daniel C, Gurdo, N., Milanesi, R., & Nikel, P. I. (2023). Time-resolved, deuterium-based fluxomics uncovers the hierarchy and dynamics of sugar processing by *Pseudomonas putida*. *Metabolic Engineering*. https://doi.org/10.1016/j.ymben.2023.07.004

Volke, Daniel C, Wirth, N. T., & Nikel, P. I. (2021). Rapid Genome Engineering of *Pseudomonas* Assisted by Fluorescent Markers and Tractable Curing of Plasmids. *Bio-Protocol*, *11*(4), e3917. https://doi.org/10.21769/BioProtoc.3917

Volke, Daniel Christoph, Olavarría, K., & Nikel, P. I. (2021). Cofactor Specificity of Glucose-6-Phosphate Dehydrogenase Isozymes in *Pseudomonas putida* Reveals a General Principle Underlying Glycolytic Strategies in Bacteria. *MSystems*, *6*(2). https://doi.org/10.1128/msystems.00014-21

Volmer, J., Lindmeyer, M., Seipp, J., Schmid, A., & Bühler, B. (2019). Constitutively solvent-tolerant *Pseudomonas taiwanensis* VLB120ΔCΔ*ttgV* supports particularly high-styrene epoxidation activities when grown under glucose excess conditions. *Biotechnology and Bioengineering*, *116*(5), 1089–1101. https://doi.org/10.1002/bit.26924

Volmer, J., Neumann, C., Bühler, B., & Schmid, A. (2014). Engineering of *Pseudomonas taiwanensis* VLB120 for constitutive solvent tolerance and increased specific styrene epoxidation activity. *Applied and Environmental Microbiology*, *80*(20), 6539–6548. https://doi.org/10.1128/AEM.01940-14

Volmer, J., Schmid, A., & Bühler, B. (2017). The application of constitutively solvent-tolerant *P. taiwanensis* VLB120Δ*C*Δ*ttgV* for stereospecific epoxidation of toxic styrene alleviates carrier solvent use. *Biotechnology Journal*, *12*(7), 1–9. https://doi.org/10.1002/biot.201600558

Vrionis, H. A., Kropinski, A. M., & Daugulis, A. J. (2002). Enhancement of a two-phase partitioning bioreactor system by modification of the microbial catalyst: Demonstration of concept. *Biotechnology and Bioengineering*, *79*(6), 587–594. https://doi.org/10.1002/bit.10313

Waki, T., Mameda, R., Nakano, T., Yamada, S., Terashita, M., Ito, K., Tenma, N., Li, Y., Fujino, N., Uno, K., Yamashita, S., Aoki, Y., Denessiouk, K., Kawai, Y., Sugawara, S., Saito, K., Yonekura-Sakakibara, K., Morita, Y., Hoshino, A., … Nakayama, T. (2020). A conserved strategy of chalcone isomerase-like protein to rectify promiscuous chalcone synthase specificity. *Nature Communications*, *11*(1), 1–14. https://doi.org/10.1038/s41467-020-14558-9

Waki, T., Takahashi, S., & Nakayama, T. (2021). Managing enzyme promiscuity in plant specialized metabolism: A lesson from flavonoid biosynthesis: Mission of a “body double” protein clarified. *BioEssays*, *43*(3), 1–11. https://doi.org/10.1002/bies.202000164

Wang, Jia, Zhang, R., Chen, X., Sun, X., Yan, Y., Shen, X., & Yuan, Q. (2020). Biosynthesis of aromatic polyketides in microorganisms using type II polyketide synthases. *Microbial Cell Factories*, *19*(1). https://doi.org/10.1186/s12934-020-01367-4

Wang, Jian, Guleria, S., Koffas, M. A. G., & Yan, Y. (2016). Microbial production of value-added nutraceuticals. *Current Opinion in Biotechnology*, *37*, 97–104. https://doi.org/10.1016/j.copbio.2015.11.003

Wang, S., Fu, C., Bilal, M., Hu, H., Wang, W., & Zhang, X. (2018). Enhanced biosynthesis of arbutin by engineering shikimate pathway in *Pseudomonas chlororaphis* P3. *Microbial Cell Factories*, *17*(1), 174. https://doi.org/10.1186/s12934-018-1022-8

Wang, X., He, Q., Yang, Y., Wang, J., Haning, K., Hu, Y., Wu, B., He, M., Zhang, Y., Bao, J., Contreras, L. M., & Yang, S. (2018). Advances and prospects in metabolic engineering of *Zymomonas mobilis*. *Metabolic Engineering*, *50*(January), 57–73. https://doi.org/10.1016/j.ymben.2018.04.001

Wang, Y., Lin, X., Shao, Z., Shan, D., Li, G., & Irini, A. (2017). Comparison of Fenton, UV-Fenton and nano-Fe_3O_4 catalyzed UV-Fenton in degradation of phloroglucinol under neutral and alkaline conditions: Role of complexation of Fe^{3+} with hydroxyl group in phloroglucinol. *Chemical Engineering Journal*, *313*, 938–945. https://doi.org/10.1016/j.cej.2016.10.133

Wang, Z., Wen, Q., Harwood, C. S., Liang, B., & Yang, J. (2020). A disjointed pathway for malonate degradation by *Rhodopseudomonas palustris*. *Applied and Environmental Microbiology*, *86*(11). https://doi.org/10.1128/AEM.00631-20

Watson, D., Lindel, D. L., & Fall, R. (1983). *Pseudomonas aeruginosa* contains an inducible methylcitrate synthase. *Current Microbiology*, *8*(1), 17–21. https://doi.org/10.1007/BF01567308

Watson, J. L., Juergens, D., Bennett, N. R., Trippe, B. L., Yim, J., Eisenach, H. E., Ahern, W., Borst, A. J.,

Ragotte, R. J., Milles, L. F., Wicky, B. I. M., Hanikel, N., Pellock, S. J., Courbet, A., Sheffler, W., Wang, J., Venkatesh, P., Sappington, I., Torres, S. V., … Baker, D. (2023). De novo design of protein structure and function with RFdiffusion. *Nature*. https://doi.org/10.1038/s41586-023-06415-8

Weber, F. J., Ooijkaas, L. P., Schemen, R. M. W., Hartmans, S., & De Bont, J. A. M. (1993). Adaptation of *Pseudomonas putida* S12 to high concentrations of styrene and other organic solvents. *Applied and Environmental Microbiology*, *59*(10), 3502–3504. https://doi.org/10.1128/aem.59.10.3502-3504.1993

Wei, X., Luo, J., Pu, A., Liu, Q., Zhang, L., Wu, S., Long, Y., Leng, Y., Dong, Z., & Wan, X. (2022). From Biotechnology to Bioeconomy: A Review of Development Dynamics and Pathways. *Sustainability*, *14*(16), 10413. https://doi.org/10.3390/SU141610413

Weimer, A., Kohlstedt, M., Volke, D. C., Nikel, P. I., & Wittmann, C. (2020). Industrial biotechnology of *Pseudomonas putida*: advances and prospects. *Applied Microbiology and Biotechnology*. https://doi.org/https://doi.org/10.1007/s00253-020-10811-9

Weisser, P., Krämer, R., Sahm, H., & Sprenger, G. A. (1995). Functional Expression of the Glucose Transporter of *Zymomonas mobilis* Leads to Restoration of Glucose and Fructose Uptake in *Escherichia coli* Mutants and Provides Evidence for Its Facilitator Action. *Journal of Bacteriology*, *177*(11), 3351–3354.

Weissman, K. J., & Leadlay, P. F. (2005). Combinatorial biosynthesis of reduced polyketides. *Nature Reviews Microbiology*, *3*(12), 925–936. https://doi.org/10.1038/nrmicro1287

Wen, W., Alseekh, S., & Fernie, A. R. (2020). Conservation and diversification of flavonoid metabolism in the plant kingdom. *Current Opinion in Plant Biology*, *55*, 100–108. https://doi.org/10.1016/J.PBI.2020.04.004

Weng, J. K. (2014). The evolutionary paths towards complexity: a metabolic perspective. *New Phytologist*, *201*(4), 1141–1149. https://doi.org/10.1111/NPH.12416

Wery, J., Mendes Da Silva, D. I., & De Bont, J. A. M. (2000). A genetically modified solvent-tolerant bacterium for optimized production of a toxic fine chemical. *Applied Microbiology and Biotechnology*, *54*(2), 180–185. https://doi.org/10.1007/s002530000381

Whaley, S. G., Radka, C. D., Subramanian, C., Frank, M. W., & Rock, C. O. (2021). Malonyl-acyl carrier protein decarboxylase activity promotes fatty acid and cell envelope biosynthesis in Proteobacteria. *Journal of Biological Chemistry*, *297*(6), 101434. https://doi.org/10.1016/j.jbc.2021.101434

Wieland, W. (2020). *Gilgamesch-Epos und Gilgameschs Tod - Das älteste Epos der Menschheit* (3. Auflage). Epubli GmbH.

Wierckx, N. J. P., Ballerstedt, H., Bont, J. a M. De, & Wery, J. (2005). Engineering of Solvent-Tolerant *Pseudomonas putida* S12 for Bioproduction of Phenol from Glucose. *Applied and Environmental Microbiology*, *71*(12), 8221–8227. https://doi.org/10.1128/AEM.71.12.8221

Wierckx, N., Prieto, M. A., Pomposiello, P., de Lorenzo, V., O'Connor, K., & Blank, L. M. (2015). Plastic waste as a novel substrate for industrial biotechnology. *Microbial Biotechnology*, *8*(6), 900. https://doi.org/10.1111/1751-7915.12312

Williams, D. H., Stone, M. J., Hauck, P. R., & Rahman, S. K. (1989). Why are secondary metabolites (Natural Products) biosynthesized. *Journal of Natural Products*, *52*(6), 1189–1208. https://doi.org/10.1021/np50066a001

Winter, B., & Meys, R. (2022). Sugar-to-What? An Environmental Merit Order Curve for Biobased

Chemicals and Plastics. *ACS Sustainable Chemistry and Engineering*. https://doi.org/10.1021/acssuschemeng.2c03275

Wirth, N. T., Kozaeva, E., & Nikel, P. I. (2020). Accelerated genome engineering of *Pseudomonas putida* by I-*Sce*I—mediated recombination and CRISPR-Cas9 counterselection. *Microbial Biotechnology*, *13*(1), 233–249. https://doi.org/10.1111/1751-7915.13396

Witholt, B., de Smet, M. J., Kingma, J., van Beilen, J. B., Kok, M., Lageveen, R. G., & Eggink, G. (1990). Bioconversions of aliphatic compounds by *Pseudomonas oleovorans* in multiphase bioreactors: background and economic potential. *Trends in Biotechnology*, *8*(C), 46–52. https://doi.org/10.1016/0167-7799(90)90133-I

Wolf, S., Becker, J., Tsuge, Y., Kawaguchi, H., Kondo, A., Marienhagen, J., Bott, M., Wendisch, V. F., & Wittmann, C. (2021). Advances in metabolic engineering of *Corynebacterium glutamicum* to produce high-value active ingredients for food, feed, human health, and well-being. *Essays in Biochemistry*, *0*(April), 1–16. https://doi.org/10.1042/EBC20200134

Woodley, J. M. (2019). Accelerating the implementation of biocatalysis in industry. *Applied Microbiology and Biotechnology*, *103*(12), 4733–4739. https://doi.org/10.1007/S00253-019-09796-x

Wu, J., Zhou, L., Duan, X., Peng, H., Liu, S., Zhuang, Q., Pablo, C.-M. M., Fan, X., Ding, S., Dong, M., & Zhou, J. (2021). Applied evolution: Dual dynamic regulations-based approaches in engineering intracellular malonyl-CoA availability. *Metabolic Engineering*, *67*(August), 403–416. https://doi.org/10.1016/j.ymben.2021.08.004

Wu, S. B., Long, C., & Kennelly, E. J. (2014). Structural diversity and bioactivities of natural benzophenones. *Natural Product Reports*, *31*(9), 1158–1174. https://doi.org/10.1039/c4np00027g

Wubbolts, M. G., Hoven, J., Melgert, B., & Witholt, B. (1994). Efficient production of optically active styrene epoxides in two-liquid phase cultures. *Enzyme and Microbial Technology*, *16*(10), 887–894. https://doi.org/10.1016/0141-0229(94)90064-7

Wünschiers, R., Jahn, M., Jahn, D., Schomburg, I., Peifer, S., Heinzle, E., Burtscher, H., Garbe, J., Steen, A., Schobert, M., Oesterhelt, D., Wachtveitl, J., & Chan, A. (2013). Metabolism. In *Biochemical Pathways: An Atlas of Biochemistry and Molecular Biology: Second Edition* (pp. 37–209). John Wiley and Sons. https://doi.org/10.1002/9781118657072.CH3

Wylie, J. L., & Worobec, E. A. (1995). The OprB porin plays a central role in carbohydrate uptake in *Pseudomonas aeruginosa*. *Journal of Bacteriology*, *177*(11), 3021–3026. https://doi.org/10.1128/jb.177.11.3021-3026.1995

Wynands, B., Kofler, F., Sieberichs, A., Silva, N., & Wierckx, N. (2023). Engineering a *Pseudomonas taiwanensis* 4-coumarate platform for production of *para*-hydroxy aromatics with high yield and specificity. *Metabolic Engineering*, *78*, 115–127. https://doi.org/10.1016/j.ymben.2023.05.004

Wynands, B., Lenzen, C., Otto, M., Koch, F., Blank, L. M., & Wierckx, N. (2018). Metabolic engineering of Pseudomonas taiwanensis VLB120 with minimal genomic modifications for high-yield phenol production. *Metabolic Engineering*, *47*, 121–133. https://doi.org/10.1016/j.ymben.2018.03.011

Wynands, B., Otto, M., Runge, N., Preckel, S., Polen, T., Blank, L. M., & Wierckx, N. (2019). Streamlined *Pseudomonas taiwanensis* VLB120 Chassis Strains with Improved Bioprocess Features. *ACS Synthetic Biology*, *8*(9), 2036–2050. https://doi.org/10.1021/acssynbio.9b00108

Xu, P., Wang, W., Li, L., Bhan, N., Zhang, F., & Koffas, M. A. G. (2014). Design and kinetic analysis of a hybrid promoter-regulator system for malonyl-CoA sensing in *Escherichia coli*. *ACS Chemical*

Biology, *9*(2), 451–458. https://doi.org/10.1021/cb400623m

Yadav, A. N., Kour, D., Rana, K. L., Yadav, N., Singh, B., Chauhan, V. S., Rastegari, A. A., Hesham, A. E.-L. L., & Gupta, V. K. (2019). Metabolic Engineering to Synthetic Biology of Secondary Metabolites Production. In *New and Future Developments in Microbial Biotechnology and Bioengineering*. Elsevier B.V. https://doi.org/10.1016/b978-0-444-63504-4.00020-7

Yan, Qiang, Cordell, W. T., Jindra, M. A., Courtney, D. K., Kuckuk, M. K., Chen, X., & Pfleger, B. F. (2022). Metabolic engineering strategies to produce medium-chain oleochemicals via acyl-ACP:CoA transacylase activity. *Nature Communications*, *13*(1). https://doi.org/10.1038/s41467-022-29218-3

Yan, Qing, Liu, M., Kidarsa, T., Johnson, C. P., & Loper, J. E. (2021). Two pathway-specific transcriptional regulators, PltR and PltZ, coordinate autoinduction of pyoluteorin in *Pseudomonas protegens* Pf-5. *Microorganisms*, *9*(7). https://doi.org/10.3390/microorganisms9071489

Yan, Qing, Philmus, B., Chang, J. H., & Loper, J. E. (2017). Novel mechanism of metabolic co-regulation coordinates the biosynthesis of secondary metabolites in *Pseudomonas protegens*. *ELife*, *6*, 1–24. https://doi.org/10.7554/eLife.22835

Yang, D., Eun, H., & Prabowo, C. P. S. (2023). Metabolic Engineering and Synthetic Biology Approaches for the Heterologous Production of Aromatic Polyketides. *International Journal of Molecular Sciences*, *24*(10). https://doi.org/10.3390/ijms24108923

Yang, D., Eun, H., Prabowo, C. P. S., Cho, S., & Lee, S. Y. (2022). Metabolic and cellular engineering for the production of natural products. *Current Opinion in Biotechnology*, *77*, 102760. https://doi.org/10.1016/J.COPBIO.2022.102760

Yang, D., Kim, W. J., Yoo, S. M., Choi, J. H., Ha, S. H., Lee, M. H., & Lee, S. Y. (2018). Repurposing type III polyketide synthase as a malonyl-CoA biosensor for metabolic engineering in bacteria. *Proceedings of the National Academy of Sciences*, *115*(40), 9835–9844. https://doi.org/10.1073/pnas.1808567115

Yang, D., Park, S. Y., Park, Y. S., Eun, H., & Lee, S. Y. (2020). Metabolic Engineering of *Escherichia coli* for Natural Product Biosynthesis. *Trends in Biotechnology*, *38*(7), 745–765. https://doi.org/10.1016/j.tibtech.2019.11.007

Yang, F., & Cao, Y. (2012). Biosynthesis of phloroglucinol compounds in microorganisms - review. *Applied Microbiology and Biotechnology*, *93*(2), 487–495. https://doi.org/10.1007/s00253-011-3712-6

Yang, S., Fei, Q., Zhang, Y., Contreras, L. M., Utturkar, S. M., Brown, S. D., Himmel, M. E., & Zhang, M. (2016). *Zymomonas mobilis* as a model system for production of biofuels and biochemicals. *Microbial Biotechnology*, *9*(6), 699–717. https://doi.org/10.1111/1751-7915.12408

Yang, Y., Lin, Y., Li, L., Linhardt, R. J., & Yan, Y. (2015). Regulating malonyl-CoA metabolism via synthetic antisense RNAs for enhanced biosynthesis of natural products. *Metabolic Engineering*, *29*, 217–226. https://doi.org/10.1016/j.ymben.2015.03.018

Yi, J., Draths, K. M., Li, K., & Frost, J. W. (2003). Altered Glucose Transport and Shikimate Pathway Product Yields in *E. coli*. *Biotechnology Progress*, *19*(5), 1450–1459. https://doi.org/10.1021/bp0340584

Yonekura-Sakakibara, K., Higashi, Y., & Nakabayashi, R. (2019). The Origin and Evolution of Plant Flavonoid Metabolism. *Frontiers in Plant Science*, *10*(August), 1–16. https://doi.org/10.3389/fpls.2019.00943

Yu, D., Xu, F., Zeng, J., & Zhan, J. (2012). Type III polyketide synthases in natural product biosynthesis. *IUBMB Life*, *64*(4), 285–295. https://doi.org/10.1002/iub.1005

Yu, L. P., Wu, F. Q., & Chen, G. Q. (2019). Next-Generation Industrial Biotechnology-Transforming the Current Industrial Biotechnology into Competitive Processes. *Biotechnology Journal*, *14*(9). https://doi.org/10.1002/BIOT.201800437

Yu, T., Boob, A. G., Volk, M. J., Liu, X., Cui, H., & Zhao, H. (2023). Machine learning-enabled retrobiosynthesis of molecules. *Nature Catalysis*, *6*(2), 137–151. https://doi.org/10.1038/s41929-022-00909-w

Yuan, Z., Cang, S., Matsufuji, M., Nakata, K., Nagamatsu, Y., & Yoshimoto, A. (1998). High production of pyoluteorin and 2,4-diacetylphloroglucinol by *Pseudomonas fluorescens* S272 grown on ethanol as a sole carbon source. *Journal of Fermentation and Bioengineering*, *86*(6), 559–563. https://doi.org/10.1016/S0922-338X(99)80006-3

Żądło-Dobrowolska, A., Hammerer, L., Pavkov-Keller, T., Gruber, K., & Kroutil, W. (2020). Rational Engineered C-Acyltransferase Transforms Sterically Demanding Acyl Donors. *ACS Catalysis*, *10*(2), 1094–1101. https://doi.org/10.1021/acscatal.9b04617

Żądło-Dobrowolska, A., Schmidt, N. G., & Kroutil, W. (2019). Thioesters as Acyl Donors in Biocatalytic Friedel-Crafts-type Acylation Catalyzed by Acyltransferase from *Pseudomonas Protegens*. *ChemCatChem*, *11*(3), 1064–1068. https://doi.org/https://doi.org/10.1002/cctc.201801856

Zha, W., Rubin-Pitel, S. B., Shao, Z., & Zhao, H. (2009). Improving cellular malonyl-CoA level in *Escherichia coli* via metabolic engineering. *Metabolic Engineering*, *11*(3), 192–198. https://doi.org/10.1016/j.ymben.2009.01.005

Zha, W., Rubin-Pitel, S. B., & Zhao, H. (2008). Exploiting genetic diversity by directed evolution: Molecular breeding of type III polyketide synthases improves productivity. *Molecular BioSystems*, *4*(3), 246–248. https://doi.org/10.1039/b717705d

Zhang, B., Jin, W., Zhang, Y., Dai, Y., Li, H., Sun, Y., Wu, X., Luo, J., & Chen, Y. (2023). A Type I/Type III PKS Hybrid Generates Cinnamomycin A-D. *Organic Letters*, *25*, 16. https://doi.org/10.1021/acs.orglett.3c00293

Zhang, J., Yan, X., Huang, T., Liu, H., Liu, F., Yang, M., Yang, M. F., & Ma, L. (2022). Overexpressing 4-coumaroyl-CoA ligase and stilbene synthase fusion genes in red raspberry plants leads to resveratrol accumulation and improved resistance against *Botrytis cinerea*. *Journal of Plant Biochemistry and Biotechnology*, *3*. https://doi.org/10.1007/s13562-022-00784-3

Zhang, Q., Yu, S., Lyu, Y., Zeng, W., & Zhou, J. (2021). Systematically Engineered Fatty Acid Catabolite Pathway for the Production of (2*S*)-Naringenin in *Saccharomyces cerevisiae*. *ACS Synthetic Biology*, *10*(5), 1166–1175. https://doi.org/10.1021/acssynbio.1c00002

Zhang, W., Zhang, X., Feng, D., Liang, Y., Wu, Z., Du, S., Zhou, Y., Geng, C., Men, P., Fu, C., Huang, X., & Lu, X. (2023). Discovery of a Unique Flavonoid Biosynthesis Mechanism in Fungi by Genome Mining. *Angewandte Chemie*, *135*(12). https://doi.org/10.1002/ANGE.202215529

Zhang, X., & Shu, D. (2021). Current understanding on the Cambrian Explosion: questions and answers. *PalZ*, *95*(4), 641–660. https://doi.org/10.1007/S12542-021-00568-5

Zhao, Y., Wu, B. H., Liu, Z. N., Qiao, J., & Zhao, G. R. (2018). Combinatorial Optimization of Resveratrol Production in Engineered *E. coli*. *Journal of Agricultural and Food Chemistry*, *66*(51), 13444–13453. https://doi.org/10.1021/acs.jafc.8b05014

Zhou, S., Lama, S., Jiang, J., Sankaranarayanan, M., & Park, S. (2020). Use of acetate for the production of 3-hydroxypropionic acid by metabolically-engineered *Pseudomonas denitrificans*.

Bioresource Technology, *307*(March), 123194. https://doi.org/10.1016/j.biortech.2020.123194

Zhu, X., Tian, Y., Zhang, W., Zhang, T., Guang, C., & Mu, W. (2018). Recent progress on biological production of α-arbutin. *Applied Microbiology and Biotechnology*, *102*(19), 8145–8152. https://doi.org/10.1007/s00253-018-9241-9

Zimmerman, J. B., Anastas, P. T., Erythropel, H. C., & Leitner, W. (2020). Designing for a green chemistry future. *Science*, *367*(6476), 397–400. https://doi.org/10.1126/science.aay3060

Zobel, S., Benedetti, I., Eisenbach, L., De Lorenzo, V., Wierckx, N., & Blank, L. M. (2015). Tn7-Based Device for Calibrated Heterologous Gene Expression in *Pseudomonas putida*. *ACS Synthetic Biology*, *4*(12), 1341–1351. https://doi.org/10.1021/acssynbio.5b00058

Zobel, S., Kuepper, J., Ebert, B., Wierckx, N., & Blank, L. M. (2017). Metabolic response of *Pseudomonas putida* to increased NADH regeneration rates. *Engineering in Life Sciences*, *17*(1), 47–57. https://doi.org/10.1002/elsc.201600072

5. Appendices

Supporting information to article "A *Pseudomonas taiwanensis* malonyl-CoA platform strain for polyketide synthesis"

Tobias Schwanemann[a], Maike Otto[a], Benedikt Wynands[a], Jan Marienhagen[a,b] and Nick Wierckx[a‡]

[a]Institute of Bio- and Geosciences, IBG-1: Biotechnology, Forschungszentrum Jülich GmbH, 52425 Jülich, Germany
[b]Institute of Biotechnology, RWTH Aachen University, Worringer Weg 3, D-52074 Aachen, Germany

‡ corresponding author:

Nick Wierckx, Institute of Bio- and Geosciences, IBG-1: Biotechnology, Forschungszentrum Jülich, Wilhelm-Johnen-Straße, 52425 Jülich, Germany. e-mail: n.wierckx@fz-juelich.de

Table S1: Bacterial strains used in this study

Strains	Relevant characteristics	Reference
Escherichia coli		
HB101 pRK2013	HB101 with pRK2013	Ditta et al. (1980)
PIR2	*F⁻ Δlac169 rpoS(Am) robA1 creC510 hsdR514 endA recA1 uidA(ΔMluI)::pir*; host for *oriV(R6K)* plasmids	Thermo Fischer Scientific
DH5α	F⁻ *Φ80 lac*ZΔM15 Δ(*lac*ZYA-*arg*F)*U169 recA1 endA1 hsdR17*(r_k^-, m_k^+) *phoA supE44 thi-1 gyrA96 relA1* λ^-	Thermo Fischer Scientific
DH5α λ*pir*	λ*pir* lysogen of DH5α; host for *oriV(R6K)* plasmids	Víctor de Lorenzo lab
DH5α λ*pir* pTNS1	DH5α λ*pir* with pTNS1	Choi et al. (2005)
DH5α pSW-2	DH5α with pSW-2	Martínez-García & de Lorenzo (2011)
BL21 (DE3)	F– *ompT hsdS*$_B$ (r_B–, m_B–) *gal dcm* (DE3)	Thermo Fischer Scientific
Pseudomonas taiwanensis		
VLB120	Wild-type	Panke et al. (1998); MiKat#1
GRC1	Genome-reduced-chassis strain (deleted megaplasmid pSTY, four prophages, flagella apparatus and major biofilm-formation)	Wynands et al. (2019); MiKat#3
GRC2	Genome-reduced-chassis strain; Δprophage1/2::*ttgGHI*	Wynands et al. (2019); MiKat#4
GRC3	Genome-reduced-chassis strain; Δprophage1/2::*ttgVWGHI*	Wynands et al. (2019); MiKat#5
GRC3 Δ8pykA-tap (=GRC3 PHE)	Phenylalanine platform strain; GRC3 Δ*pobA*, Δ*hpd*, Δ*quiC*, Δ*quiC1*, Δ*quiC2*, Δ*phhAB*, Δ*katG*, ΔPVLB_10925, Δ*pykA*, *trpE*^{P290S}, *aroF-1*^{P148L}, *pheA*^{T310I}	Otto et al. (2019); MiKat#74
GRC3 PHE *attTn7::P$_{14g}$-his.AhSTS-Sc4CL^{A294G}-AtPAL2*	GRC3 PHE; with pinosylvin production module	This study; MiKat#182
GRC3 PHE Δ*phaCZC2*	Phenylalanine platform strain; deleted PHA cluster (PVLB_02155-65)	This study; MiKat#338
GRC3 PHE Δ*phaCZC2 attTn7::P$_{14g}$-his.AhSTS-Sc4CL^{A294G}-AtPAL2*	GRC3 PHE Δ*phaCZC2*; with pinosylvin production module	This study; MiKat#365
GRC3 PHE Δ*gcd*	Phenylalanine platform strain; deleted glucose dehydrogenase (PVLB_05240)	This study; MiKat#339
GRC3 PHE Δ*gcd attTn7::P$_{14g}$-his.AhSTS-Sc4CL^{A294G}-AtPAL2*	GRC3 PHE Δ*gcd*; with pinosylvin production module	This study; MiKat#366
GRC3 PHE Δ*tesB*	Phenylalanine platform strain; deleted type II thioesterase (PVLB_03305)	This study; MiKat#383
GRC3 PHE Δ*tesB attTn7::P$_{14g}$-his.AhSTS-Sc4CL^{A294G}-AtPAL2*	GRC3 PHE Δ*tesB*; with pinosylvin production module	This study; MiKat#388
GRC3 PHE ΔPVLB_02920	Phenylalanine platform strain; deleted putative regulator PVLB_02920	This study; MiKat#271
GRC3 PHE ΔPVLB_02920 *attTn7::P$_{14g}$-his.AhSTS-Sc4CL^{A294G}-AtPAL2*	GRC3 PHE ΔPVLB_02920; with pinosylvin production module	This study; MiKat#299
GRC3 PHE ΔPVLB_01730-01815	Phenylalanine platform strain; deleted putative secondary metabolite cluster	This study; MiKat#262
GRC3 PHE ΔPVLB_01730-01815 *attTn7::P$_{14g}$-his.AhSTS-Sc4CL^{A294G}-AtPAL2*	GRC3 PHE ΔPVLB_01730-01815; with pinosylvin production module	This study; MiKat#265
GRC3 PHE ΔP_{gltA}::P_{14a}*	Phenylalanine platform strain; exchanged promoter of citrate synthase	This study; MiKat#263

GRC3 PHE ΔP_{gltA}::P_{14a}* *attTn7*::P_{14g}-*his.AhSTS-Sc4CL*^{A294G}-*AtPAL2*	Phenylalanine platform strain; exchanged promoter of citrate synthase; with pinosylvin production module	This study; MiKat#266
GRC3 PHE Δ*prpC*	Phenylalanine platform strain; deleted methyl citrate synthase	This study; MiKat#314
GRC3 PHE Δ*prpC attTn7*::P_{14g}-*his.AhSTS-Sc4CL*^{A294G}-*AtPAL2*	Phenylalanine platform strain; deleted methyl citrate synthase; with pinosylvin production module	This study; MiKat#364
GRC3 PHE Δ*prpC* Δ*gltA*::*prpC*	Phenylalanine platform strain; deleted methyl citrate synthase in native locus and replaced citrate synthase	This study; MiKat#361
GRC3 PHE Δ*prpC* Δ*gltA*::*prpC attTn7*::P_{14g}-*his.AhSTS-Sc4CL*^{A294G}-*AtPAL2*	Phenylalanine platform strain; deleted methyl citrate synthase in native locus and replaced citrate synthase; with pinosylvin production module	This study; MiKat#367
GRC3 PHE Δ*prpC* ΔP_{gltA}::P_{14a}* Δ*gltA*::*prpC*	Phenylalanine platform strain; exchanged promoter of citrate synthase; deleted methyl citrate synthase in native locus and replaced citrate synthase	This study; MiKat#518
GRC3 PHE Δ*prpC* ΔP_{gltA}::P_{14a}* Δ*gltA*::*prpC attTn7*::P_{14g}-*his.AhSTS-Sc4CL*^{A294G}-*AtPAL2*	Phenylalanine platform strain; exchanged promoter of citrate synthase; deleted methyl citrate synthase in native locus and replaced citrate synthase; with pinosylvin production module	This study; MiKat#527
GRC3 PHE Δ*pycAB*	Phenylalanine platform strain; deleted pyruvate decarboxylase (PVLB_25325-30)	This study; MiKat#368
GRC3 PHE Δ*pycAB attTn7*::P_{14g}-*his.AhSTS-Sc4CL*^{A294G}-*AtPAL2*	Phenylalanine platform strain; deleted pyruvate decarboxylase (PVLB_25325-30); with pinosylvin production module	This study; MiKat#385
GRC3 PHE Δ*prpC* Δ*gltA*::*prpC* Δ*pycAB*	Phenylalanine platform strain; deleted methyl citrate synthase in native locus and replaced citrate synthase, deleted pyruvate decarboxylase (PVLB_25325-30)	This study; MiKat#370
GRC3 PHE Δ*prpC* Δ*gltA*::*prpC* Δ*pycAB attTn7*::P_{14g}-*his.AhSTS-Sc4CL*^{A294G}-*AtPAL2*	Phenylalanine platform strain; deleted methyl citrate synthase in native locus and replaced citrate synthase, deleted pyruvate decarboxylase (PVLB_25325-30); with pinosylvin production module	This study; MiKat#387
GRC3 PHE Δ*prpC* ΔP_{gltA}::P_{14a}* Δ*gltA*::*prpC* Δ*pycAB*	Phenylalanine platform strain; exchanged promoter of citrate synthase; deleted methyl citrate synthase in native locus and replaced citrate synthase, deleted pyruvate decarboxylase (PVLB_25325-30)	This study; MiKat#519
GRC3 PHE Δ*prpC* ΔP_{gltA}::P_{14a}* Δ*gltA*::*prpC* Δ*pycAB attTn7*::P_{14g}-*his.AhSTS-Sc4CL*^{A294G}-*AtPAL2*	Phenylalanine platform strain; exchanged promoter of citrate synthase; deleted methyl citrate synthase in native locus and replaced citrate synthase, deleted pyruvate decarboxylase (PVLB_25325-30); with pinosylvin production module	This study; MiKat#528
GRC3 Δ5	GRC3 derivative incapable of growing on 4-hydroxybenzoate, tyrosine and quinate (Δ*pobA*Δ*hpd*Δ*quiC*Δ*quiC1*Δ*quiC2*)	This study; MiKat#376
GRC3 Δ6	deleted *benABCD* in GRC3 Δ5	This study; MiKat#382
GRC3 Δ6 *attTn7*::*FRT-*P_{14f}-*SgRppA*	with 1,3,6,8-tetrahydroxynaphthalene synthase SgRppA for flaviolin synthesis without resistance marker	This study; MiKat#546

GRC3 Δ6 Δ*gcd attTn7*::*FRT-P*$_{14f}$*-SgRppA*	Deleted gcd in flaviolin producer	This study; MiKat#668
GRC3 Δ6 Δ*gcd* Δ*P*$_{gltA}$::*P*$_{14a}$* *attTn7*::*FRT-P*$_{14f}$*-SgRppA*	Exchanged promoter of citrate synthase in flaviolin producer	This study; MiKat#691
GRC3 Δ6 Δ*gcd* Δ*P*$_{gltA}$::*P*$_{14a}$* PVLB_23545-40::*P*$_{14f}$*-Cg_accBC-Cg_accD1 attTn7*::*FRT-P*$_{14f}$*-SgRppA*	Integration of ACC from *C. glutamicum* in flaviolin producer	This study; MiKat#801
GRC3 Δ6 Δ*gcd* Δ*P*$_{gltA}$::*P*$_{14a}$* PVLB_23545-40::*P*$_{14f}$*-Cg_accBC-Cg_accD1* ΔPVLB_18090 *attTn7*::*FRT-P*$_{14f}$*-SgRppA*	Deleted putative 3-oxoacyl-ACP synthase III in a flaviolin producer	This study; MiKat#813
GRC3 Δ6 Δ*gcd* Δ*P*$_{gltA}$::*P*$_{14a}$* PVLB_23545-40::P$_{14f}$*-Cg_accBC-Cg_accD1* ΔPVLB_18090 (=GRC3Δ6 MC-I)	Malonyl-CoA platform strain No.1 (GRC3Δ6MC I)	This study; MiKat#822
GRC3 Δ6 Δ*gcd* Δ*P*$_{gltA}$::P$_{14a}$* PVLB_23545-40::*P*$_{14f}$*-Cg_accBC-Cg_accD1* ΔPVLB_18090 Δ*pycAB attTn7*::*FRT-P*$_{14f}$*-SgRppA*	deleted pyruvate decarboxylase (PVLB_25325-30) in a flaviolin producer	This study; MiKat#852
GRC3 Δ6 Δ*gcd* Δ*P*$_{gltA}$::*P*$_{14a}$* PVLB_02480-85::*P*$_{EM7}$_PP3303 (*fabF-2*) *attTn7*::*FRT-P*$_{14f}$*-SgRppA*	Integrated cryptic long-chain 3-oxoacyl-ACP synthase II (FabF-2, PP_3303) from *P. putida* KT2440 in a flaviolin producer	This study; MiKat#912
GRC3 Δ6 Δ*gcd* Δ*P*$_{gltA}$::*P*$_{14a}$* PVLB_02480-85::*P*$_{EM7}$_PP3303 (*fabF-2*) Δ*fabF* (PVLB_07185) (=GRC3Δ6 MC-II) *attTn7*::*FRT-P*$_{14f}$*-SgRppA*	Deleted *fabF* (PVLB_07185) in a flaviolin producer with *fabF-2;* Platform strain No.2 flaviolin producer	This study; MiKat#912
GRC3 Δ6 Δ*gcd* Δ*P*$_{gltA}$::*P*$_{14a}$* PVLB_02480-85::*P*$_{EM7}$_PP3303 (*fabF-2*) Δ*fabF* (PVLB_07185) (=GRC3Δ6 MC-II)	Malonyl-CoA platform strain No.2 (GRC3Δ6MC II)	This study; MiKat#975
GRC3 Δ6 Δ*gcd* Δ*P*$_{gltA}$::*P*$_{14a}$* PVLB_02480-85::*P*$_{EM7}$_PP3303 (*fabF-2*) Δ*fabF* (PVLB_07185) PVLB_23545-40::*P*$_{14f}$*-Cg_accBC-Cg_accD1* (=GRC3Δ6 MC-III)	Malonyl-CoA platform strain No.2 with ACC from *C. glutamicum* (=> No.3) (GRC3Δ6MC III)	This study; MiKat#1058
GRC3 Δ6MC-II PVLB_23545-40::*P*$_{14f}$*-Cg_accBC-Cg_accD1* (=GRC3Δ6 MC-III) *attTn7*::*FRT-P*$_{14f}$*-SgRppA*	Malonyl-CoA platform strain No.3 flaviolin producer	This study; MiKat#1058
GRC3 Δ6MC-II *attTn7*::*P*$_{14g}$*-his.AhSTS-Sc4CL*^{A294G}*-AtPAL2*	Malonyl-CoA platform strain No.2 with pinosylvin production module	This study; MiKat#1003
GRC3 Δ6MC-III *attTn7*::*P*$_{14g}$*-his.AhSTS-Sc4CL*^{A294G}*-AtPAL2*	Malonyl-CoA platform strain No.3 with pinosylvin production module	This study; MiKat#1024
GRC3 Δ6MC-III *attTn7*::*P*$_{14g}$*-his.AhSTS-Sc4CL*^{A294G}*-StsTAL*	Malonyl-CoA platform strain No.3 with resveratrol production module	This study; MiKat#1127
GRC3 Δ6MC-III *aroF-1*^{P148L}	Malonyl-CoA platform strain No.3 aroF-1 mutant	This study; MiKat#1151
GRC3 Δ6MC-III *aroF-1*^{P148L} *attTn7*::*P*$_{14g}$*-his.AhSTS-Sc4CL*^{A294G}*-AtPAL2*	Malonyl-CoA platform strain No.3 aroF-1 mutant; with pinosylvin production module	This study; MiKat#1628
GRC3 Δ6MC-III *aroF-1*^{P148L} *attTn7*::*P*$_{14g}$*-his.AhSTS-Sc4CL*^{A294G}*-StsTAL*	Malonyl-CoA platform strain No.3 aroF-1 mutant with resveratrol production module	This study; MiKat#1629

Table S2: Plasmids used in this study

Plasmid	Relevant characteristics	HiFi assembly note	Reference & No.
pTNS1	Amp^R, *oriV(R6K)*, TnSABC+D operon	-	Choi et al. (2005)
pBBFLP	plasmid for antibiotic markers excision in *P. putida* strains; Tc^R, *oriV*(pBBR1) *oriT*(RK2) mob^+ λP_R::FLP λ(cI857) *sacB tet*	-	De Las Heras et al. (2008)
pEMG	Km^R, *oriV(R6K)*, *oriT*, *traJ*, *lacZα*-MCS flanked by two I-SceI restriction sites	-	Martínez-García & de Lorenzo (2011)
pGNW2	Derivative of vector pEMG carrying P_{14g}→*msfGFP*	-	Wirth et al. (2020) plasmid #19
pSNW2	Derivative of vector pEMG carrying P_{14g}-BCD2→*msfGFP*	-	Volke et al. (2020, 2021) plasmid #142
pSW-2	Gm^R, *oriV(RK2), oriT, xylS, Pm→ I-SceI*	-	Martínez-García & de Lorenzo (2011)
pSEVA6213S	Gm^R, *oriV(RK2)*, P_{EM7}→*I-SceI*;	-	Wirth et al. (2020)
pGNW2-fabD(Ts) W258Q	Genomic exchange of $TGG_{772-774}$ -> CAG (W258Q) (temperature sensitive) in *fabD* (PVLB_07170)	Fragment BW682/BW683 from pGNW2; Fragment TS029/TS030 and TS031/TS032 from VLB120 genome	This study Plasmid #59, #84
pEMG-Ex-P_{gltA}-P_{14a}	Exchange native promoter region of *gltA* (PVLB_16320) P_{gltA} by P_{14a}-BCD2 (P_{14a}*)	Cut pEMG with EcoRI and XbaI; Fragment TS042/TS043 and TS046/TS047 from VLB120 genome, Fragment TS044/TS045 from pBG14a	This study Plasmid #80
pGNW2-KO-prpC	Deletion vector for *prpC* (PVLB_08385)	Fragment BW682/BW683 from pGNW2; Fragment TS091/TS092 and TS093/TS094 from VLB120 genome	This study Plasmid #90
pEMG-KO-gltA	Deletion vector for *gltA* (PVLB_16320)	Cut pEMG with EcoRI and XbaI; Fragment TS042/TS097 and TS098/TS099 from VLB120 genome	This study Plasmid #91
pSNW2-KO-gltA-$apra^R$	Deletion vector for *gltA* (leave 99bp) and exchange with apramycin resistance	Cut pSNW2 with EcoRI and XbaI; Fragment TS042/TS097 and TS189/TS099 from VLB120 genome, Fragment TS187/TS188 from pQT8	This study Plasmid #190
pEMG-Ex-gltA-prpC	Exchange of *gltA* (leave 99bp) with *prpC*	Cut pEMG with EcoRI and XbaI; Fragment TS042/TS097 and TS101/TS099 and TS102/TS103 from VLB120 genome	This study Plasmid #92
pEMG-Ex-gltA-prpC with P_{14a}	Exchange of P_{gltA} by P_{14a}* and exchange of *gltA* (leave 99bp) with prpC	Cut pEMG with EcoRI and XbaI; Fragment TS101/TS099 and TS102/TS103 from VLB120 genome, TS042/TS097 from VLB-genome with P_{GltA}::P_{14a}*	This study Plasmid #93
pEMG-KO-phaCZCII	Deletion vector for *phaCZC2* (PVLB_02155-65)		Nies et al. (2020)
pEMG-KO-tesB	Deletion vector for *tesB* (PVLB_03305)		Nies et al. (2020)
pEMGg-aroF-1^{P148L}	Genomic exchange of CCG_{442} -> CTG (P148L) in *aroF-1* (PVLB_08330)		Wynands et al. (2018)

pGNW-KO-pycAB	Deletion vector for *pycAB* (PVLB_25325-25330)	Fragment BW682/BW683 from pGNW2; Fragment TS135/TS136 and TS137/TS138 from VLB120 genome	This study Plasmid #135
pGNW-KO_FabF	Deletion vector for aa residues 1-386 of *fabF* (PVLB_07185) with insertion of unique barcode with stop codon in all reading frames	Fragment BW682/BW683 from pGNW2; Fragment TS163/TS164 and TS165/TS166 from VLB120 genome	This study Plasmid #141
pSNW2-KO_PVLB_16225	Deletion vector for *fabB* (PVLB_16225)	Fragment BW682/BW683 from pSNW2; Fragment TS254/TS255 and TS256/TS257 from GRC3 genome	This study Plasmid #289
pSNW2-KO-oprF	Deletion vector for *oprF* (PVLB_07655)	Cut pSNW2 with EcoRI and XbaI; Fragment TS204/TS205 and TS206/TS207 from VLB120 genome	This study Plasmid #193
pSNW2-KO-PVLB17265 (fabH2)	Deletion vector for PVLB_17265 (*fabH2*)	Cut pSNW2 with EcoRI and XbaI; Fragment TS232/TS217 and TS218/TS235 from GRC3 genome	This study Plasmid #196
pSNW2-KO_PVLB18090 (fabH)	Deletion vector for PVLB_18090 (*fabH*)	Cut pSNW2 with EcoRI and XbaI; Fragment TS210/TS211 and TS212/TS213 from VLB120 genome	This study Plasmid #195
pSNW2-attTn7recycling VLB120	Deletion of marker-free insert at Tn7-site for wt sequence	Cut pSNW2 with EcoRI and XbaI; Fragment TS239/TS240 from VLB120 genome	This study Plasmid #228
pSEVA412S-benABCD	Deletion vector for PVLB_12215-12230 (*benABCD*)		Otto et al. (2020)
pEMG-PVLB_02480/85-P_{em7}-msfgfp	Integration of *msfgfp* at landing pad PVLB_02480/85 with P_{EM7}		Lechtenberg et al., manuscript in preparation
pEMG-PVLB_02480/85-P_{em7}-fabF2	Integration of *fabF2* (PP_3303) from *P. putida* KT2440 at landing pad PVLB_02480/85 with P_{EM7}	Fragment TS-019/BW463 from plasmid pEMG-PVLB_02480/85-Pem7-msfgfp and TS251/TS252 from *P. putida* KT2440	This study Plasmid #277
pEMG-PVLB_23545-40-P_{14f}-tyrA^{fbr}	Integration at landing pad PVLB_23545/40 (homologue to PP_0340-PP_0341) with P_{14f}		Lechtenberg, Wynands; personal communication
pEMG-PVLB_23545-40-P_{14f}-CgaccBC-accD1	Integration of *accBC-accD1* genes from *C. glutamicum* at landing pad PVLB_23545-23540 with P_{14f}	Fragment BW-463/TS-019 from pEMG-PVLB_23545-P14f-tyrA(fbr), Fragment TS036/TS250 from pEKEx3_accBC_accD1	This study Plasmid #249
pBT'Tmcs	Derivative of pBT'mcs, Km^R, Ori/IHF, expression vector, constitutive *Ptac* promoter, with RBS, no terminator		Koopman et al. (2010)
pBNTmcs(t)	Km^R, oriV(pBBR1) expression vector containing the salicylate-inducible *nagR/pNagAa* promotor		Verhoef et al. (2010)
pEKEx3_accBC_accD1	$spec^R$; pEKEx3 derivative containing *accBC* and *accD1* genes from *C. glutamicum*		Milke et al. (2019)
pBT'T-CgaccBC-accD1	Expression vector for *accBC-D1* from *C. glutamicum*	Cut pBT'Tmcs' with EcoRI, Fragment TS034/TS035 from pEKEx3_accBC_accD1	This study Plasmid #78

pBNT-FabD	Salicylate inducible expression vector for *fabD* (PVLB_07170)	Cut pBNT'Tmcs' with EcoRI, Fragment TS224/TS225 from VLB120 genome	This study Plasmid #203
pBNT-FabD W258Q	Salicylate inducible expression vector for $fabD^{W258Q}$ (PVLB_07170)	Cut pBNT'Tmcs' with EcoRI, Fragment TS224/TS225 from pGNW-fabD(Ts) W258Q	This study Plasmid #204
pBNT-sigX	Salicylate inducible expression vector for *sigX* (PVLB_07650)	Cut pBNT'Tmcs' with EcoRI, Fragment TS222/TS223 from VLB120 genome	This study Plasmid #205
pBG14g	Tn7 delivery vector; Km^R Gm^R, oriV(R6K), Tn7L, and Tn7R flanks, BCD2-*msfgfp* fusion, synthetic promoter variants		Zobel et al. (2015)
pBG14g-PstrSTS-Sc4CL^{A294G}-AtPAL2	Pinosylvin synthesis module with STS from *P. strobus*		Otto (2019) Plasmid #90
pBG14g-PstrSTS*-Sc4CL^{A294G}-AtPAL2	Pinosylvin synthesis module with STS from *P. strobus* (codon optimized for *E. coli*)		Otto (2019) Plasmid #89
pBG14g-AhSTS-Sc4CL^{A294G}-AtPAL2	Pinosylvin synthesis module with STS from *A. hypogaea* (UniProt: Q9SLV5; GeneBank: AXN70034.1; UniProt: P45724)		Otto (2019) Plasmid #54
pBG14g-his.AhSTS-Sc4CL^{A294G}-AtPAL2	Pinosylvin synthesis module with his-tag	Fragment TS015/TS001 and TS016/TS004 from pBG14g-ahSTS-4CL-atPAL	This study Plasmid #52
pBG14g-his.AhSTS.opt-Sc4CL^{A294G}-AtPAL2	Pinosylvin synthesis module with his-tag (codon optimized)	Fragment TS001/TS002 and TS003/TS004 from pBG14g-ahSTS-4CL-atPAL; gBlock opt.AhSTS from synthesis	This study Plasmid #53
pBG14f_Kan_FRT_StsTAL	Plasmid containing tyrosine ammonia lyase from *Streptomyces sp*. NRRL F-4489 (UniProt: A0A0X3WEK2)		Wynands et al., manuscript in preparation, Plasmid #279
pBG14g-his.AhSTS-Sc4CL^{A294G}-stsTAL	Resveratrol synthesis module with his-tag	Fragment TS-275/TS-276 from pBG14g-his.AhSTS-Sc4CL^{A294G}-AtPAL2 (plasmid #52), TS277/TS278 from pBG14f_Kan_FRT_StsTAL (Wynands, manuscript in preparation)	This study Plasmid #343
pBG14f_FRT_Kan	Km^R flanked by FRT sites, *oriV(R6K)*, *oriT*, mini-Tn7 transposon delivery vector, P_{14f}*(BCD2)→msfgfp*		Ackermann et al. (2021)
pBG14f_Km_FRT_SgRppA.opt	Recyclable flaviolin production module (1,3,6,8-tetrahydroxynaphthalene synthase) (UniProt: Q54240)	Fragment TS-106/TS-019 from pBG14f-Kan-FRT, gBlock SgRppA.opt from synthesis	This study Plasmid #207
pBG14f_Km_FRT_his.AhSTS-Sc4CL^{A294G}-AtPAL2	Pinosylvin synthesis module with recyclable KmR	Fragment TS-106/TS-019 from pBG14f-Kan-FRT, Fragment TS020/TS238 from pBG14g-his.ahSTS-4CL-atPAL (plasmid #52)	This study Plasmid #229

Table S3: Oligonucleotides used in this study

Shown are their name, sequence, and description. Oligonucleotides used for diagnostic PCRs and sequencings are not included.

Primer No.	Description	Sequence
BW_463	pBG42 amplification fwd primer	gaattcgagctcggtaccc
BW_682	pGNW or pEMG BB amplification fwd	tctagagtcgacctgcag
BW_683	pGNW or pEMG BB amplification rev	gaattcagattaccctgttatcc
TS-001	BB pBG14ffg_fwd with overhang atPAL	tatctgctaaagaattcgagctcggtac
TS-002	BB pBG14ffg_rev with overhang opt.His-tag	tgatgatgcgagctgcccattagaaaacctccttagcatg
TS-015	BB pBG14ffg_rev with overhang His-tag	tgatggtgatggctgctgcccattagaaaacctccttagcatg
TS-016	AhSTS fwd with His6tag overhang	atgggcagcagccatcaccatcatcaccacagccaggatccaatggtgtccgtgtccggcatc
TS-019	rev on BCD2 for BB amplification	attagaaaacctccttagcatg
TS-020	fwd on BCD2 for Insert amplification	atgctaaggaggttttctaatg
TS-029	fwd TS1 fabD W258Q	taacagggtaatctgaattcgaaggacgccgttcgcct
TS-030	rev TS1 fabD W258Q	cgcactcgacctggcgtaccggctggtacaac
TS-031	fwd TS2 fabD W258Q	ggtacgccaggtcgagtgcgtgcagac
TS-032	rev TS2 fabD W258Q	gcctgcaggtcgactctagacgttgttgaccaagatagccg
TS-034	fwd Cg accBCD1 in pBT	acaggaaacaggaggtaccgaatatgtcagtcgagactagg
TS-035	rev Cg accBCD2 in pBT	atgctcctctagactcgaggttattacagtggcatgttgcc
TS-036	fwd Cg accBCD1 in pMO_RiboJ-bcd	tgctaaggaggttttctaatgtcagtcgagactagg
TS-037	rev Cg accBCD1 in pMO_RiboJ-bcd	gcctgcaggtcgactctagaggcttacagtggcatgttgcc
TS-042	fwd TS1 GltA promoter exchange	agtatagggataacagggtaatctggcgccatccagtcatagag
TS-043	rev TS1 GltA promoter exchange	gtcaacctagttagctaccccgtcacgttgtc
TS-044	fwd Insert promoter 14a	tgacggggtagctaactaggttgacatggatataatg
TS-045	rev Insert promoter 14a	ttttttgtcagccattagaaaacctccttagc
TS-046	fwd TS2 GltA promoter exchange	aggttttctaatggctgacaaaaaagcgcag
TS-047	rev TS2 GltA promoter exchange	aagcttgcatgcctgcaggtcgacttcatgtgcaggaagtttttc
TS-050	fwd TS1 mega-operon	taacagggtaatctgaattccgtcgaactgagcgaagcaggac
TS-051	rev TS1 mega operon	caacactatcccaagcgccggcgatccg
TS-052	fwd TS2 mega operon	cggcgcttgggatagtgttgactttccgccc
TS-053	rev TS2 mega operon	gcctgcaggtcgactctagagcgcgagaaactgtcgcaatc
TS-067	fwd TS1 PVLB_02920 - TetR	taacagggtaatctgaattcaaccagttatccacagcatcgcgcg
TS-068	rev TS1 PVLB_02920 - TetR	agtgagctgatcggctggctgcagcggc
TS-069	fwd TS2 PVLB_02920 - TetR	agccagccgatcagctcactcggctgag

TS-070	rev TS2 PVLB_02920 - TetR	gcctgcaggtcgactctagatcagctttccgtcatctcc
TS-091	fwd TS1 PVLB_08385 - PrpC	taacagggtaatctgaattcctggatgacgtgttgacc
TS-092	rev TS1 PVLB_08385 - PrpC	tcttccacgaggtttttctcctttcttgaaattg
TS-093	fwd TS2 PVLB_08385 - PrpC	gagaaaaacctcgtggaagacgccgggg
TS-094	rev TS2 PVLB_08385 - PrpC	gcctgcaggtcgactctagacgacgatctccggcaggc
TS-097	rev TS1 GltA	gcggacgtcgattacatcag
TS-098	fwd TS2 GltA	ctgatgtaatcgacgtccgctaagcccctggccgaacg
TS-099	rev TS2 GltA	tgcatgcctgcaggtcgactggtatgtgggcagagtcgtg
TS-101	fwd TS2 GltA-PrpC exchange	gaccagcgctgataagcccctggccgaacg
TS-102	fwd PrpC Insert PVLB_08385 with native RBS	tggtcctgatgtaatcgacgtccgctaacaatttcaagaaaggagaaaaaccatggc
TS-103	rev PrpC Insert PVLB_08385	ggccaggggcttatcagcgctggtcgatcgg
TS-106	fwd BB pBGxx amplification	taaagaattcgagctcggtaccc
TS-109	rev on pBGxx BB to insert	tgcccgtcgtattaaagagg
TS-135	fwd TS1 pycAB (PVLB_25325-25330)	taacagggtaatctgaattccttacggacccttcaccg
TS-136	rev TS1 pycAB (PVLB_25325-25330)	gaagactccagatacgccctcatctacaag
TS-137	fwd TS2 pycAB (PVLB_25325-25330)	agggcgtatctggagtcttcccaaagccgtag
TS-138	rev TS2 pycAB (PVLB_25325-25330)	gcctgcaggtcgactctagactgggcgcggttgaccac
TS-163	fwd TS1 fabF (PVLB_07185)	taacagggtaatctgaattccgctactgtgccggtgaac
TS-164	rev TS1 fabF (PVLB_07185)	cgttagcccaatggcaggattaagtactctccttttctaataacagagtttcttg
TS-165	fwd TS2 fabF (PVLB_07185) with barcode	taatcctgccattgggctaacgaaatggcgaataactaactgaattcatgaatatcgacgttgtactgtccaactc
TS-166	rev TS2 fabF (PVLB_07185)	gcctgcaggtcgactctagatgcaccgggattgccagc
TS-169	CsR counter selection for KO and Ex GltA (PVLB_16320)	gcgcgggtgatcttcgactcgcacg
TS-170	CsR counter selection for KO and Ex GltA (PVLB_16320)	aaaccgtgcgagtcgaagatcaccc
TS-171	CsR counter selection for KO FabF (PVLB_07185)	gcgcgtggcgacagcatacccatac
TS-172	CsR counter selection for KO FabF (PVLB_07185)	aaacgtatgggtatgctgtcgccac
TS-173	CsR counter selection for Point mutation FabD W258Q (PVLB_07170)	gcgcgacgcactcgacccagcgtac
TS-174	CsR counter selection for Point mutation FabD W258Q (PVLB_07170)	aaacgtacgctgggtcgagtgcgtc
TS-187	fwd Ins Apra in GltA KO	ctgatgtaatcgacgtccgctaatttacactttatgcttccggctc
TS-188	rev Ins Apra in GltA KO	ttcggccaggggcttatcagccaatcgactggcg
TS-189	fwd TS2 KO GltA-Apra	ctgataagcccctggccgaacg
TS-204	fwd TS1 OprF (PVLB_07655)	agggataacagggtaatctgaattcgtgatgctgaaggtgctg

TS-205	rev TS1 OprF (PVLB_07655)	aaaccaattaccgttaaatccccatctg
TS-206	fwd TS2 OprF (PVLB_07655)	gatttaacggtaattggtttgacgtttcatg
TS-207	rev TS2 OprF (PVLB_07655)	tgcatgcctgcaggtcgactctagaggtagtcaacggcatcac
TS-210	fwd TS1 PVLB_18090 (FabH1)	agggataacagggtaatctgcagatcgactttaccggc
TS-211	rev TS1 PVLB_18090 (FabH1)	aggaacgacctgagtcttgggctgacgg
TS-212	fwd TS2 PVLB_18090 (FabH1)	ccaagactcaggtcgttcctctggtcaaag
TS-213	rev TS2 PVLB_18090 (FabH1)	tgcatgcctgcaggtcgactcaccgggagtctggttcaag
TS-216	fwd TS1 PVLB_17265 (FabH2)	agggataacagggtaatctggcaagcgcgggtcagccg
TS-217	rev TS1 PVLB_17265 (FabH2)	ttgggaagcctaagcgctgccagtaggttactcttcg
TS-218	fwd TS2 PVLB_17265 (FabH2)	gcagcgcttaggcttcccaataaataacagctcaataccaccgtc
TS-219	rev TS2 PVLB_17265 (FabH2)	tgcatgcctgcaggtcgactccgtgccgacggcggtgt
TS-222	fwd sigX in pBNT	acaggaaacaggaggtaccgaattcatgcgttatgacccccgc
TS-223	rev sigX in pBNT	atgctcctctagactcgaggctaagtttcactcaacccggc
TS-224	fwd fabD (W258Q) in pBNT	acaggaaacaggaggtaccgaattcatgtctgcatccctcgcattcgtctttcc
TS-225	rev fabD (W258Q) in pBNT	atgctcctctagactcgaggtcaggccagcgccgcacg
TS-235	rev new TS2 PVLB_17265 (FabH2)	tgcatgcctgcaggtcgactagaagcactttaccctcg
TS-238	rev on pBGxx BB to insert	ccgggtaccgagctcgaattc
TS-250	rev CgaccBC-D1 cloning in landing pad PVLB_23545	cgggtaccgagctcgaattcttacagtggcatgttgcc
TS-251	fwd fabF2 from KT2440 (PP_3303)	tgctaaggaggttttctaatgactcacaacgttaatcaaaagcg
TS-252	rev fabF2 from KT2440 (PP_3303)	cgggtaccgagctcgaattctcatacgttggcctcccag
TS-254	fwd TS1 PVLB_16225 (FabB)	agggataacagggtaatctggaagacctgctgcgctgc
TS-255	rev TS1 PVLB_16225 (FabB)	cagcgtcttagcgaataacccttagaaattgtcagtg
TS-256	fwd TS2 PVLB_16225 (FabB)	ggttattcgctaagacgctgatgcggtaattg
TS-257	rev TS2 PVLB_16225 (FabB)	atccccgggtaccgagctcggccattgcgcaatcatcc
TS-275	rev on gene spacer in pBG	cctcctttcggtacccgcatag
TS-276	fwd on mcs of pBG	agaattcgagctcggtacc
TS-277	fwd StsTAL with overhangs	atgcgggtaccgaaaggaggtctatatgccgagcctggactcc
TS-278	rev StsTAL with overhangs	gggtaccgagctcgaattctttaggccgcacccgtcaa

Table S4: Synthetic DNA fragments.
Overhangs for cloning are indicated by small letters, capital letters represent coding sequences.

Name	Sequence (5' → 3')	Note
AhSTS.opt	ATGGGCAGCTCGCATCATCACCACCATCACAGCCAAGACCCGATGGTGTCTGTCA GCGGTATCCGTAAAGTCCAGCGTGCGGAGGGTCCGGCAACCGTGCTCGCCATCG GCACCGCGAACCCACCGAACTGCGTGGACCAGAGCACTTACGCTGACTACTACTT CCGCGTCACTAACAGCGAACATATGACCGATCTGAAGAAGAAGTTCCAGCGCATC TGCGAGCGCACCCAGATCAAGAACCGCCACATGTATCTGACCGAAGAGATCCTGA AAGAGAACCCGAACATGTGCGCTTACAAGGCCCCATCCCTCGACGCCCGCGAAGA TATGATGATCCGTGAGGTCCCGCGTGTTGGCAAGGAAGCCGCTACCAAGGCCATT AAAGAGTGGGGCCAGCCTATGTCGAAAATCACCCACCTGATCTTCTGCACCACCA GTGGCGTGGCACTGCCGGGTGTGGACTACGAACTGATTGTACTGCTGGGTCTGGA CCCAAGCGTGAAGCGTTACATGATGTATCACCAGGGCTGCTTCGCCGGCGGTACC GTTCTGCGCCTCGCCAAGGATCTGGCAGAGAACAACAAAGACGCCCGTGTGCTGA TCGTCTGCTCGGAGAACACGAGCGTTACCTTCCGTGGTCCTTCCGAGACCGACATG GACTCCCTGGTCGGCCAGGCCCTGTTTGCCGATGGCGCTGCTGCTATCATCATCGG CTCGGACCCGGTCCCAGAAGTCGAAAACCCGCTGTTCGAGATCGTCTCGACCGAC CAGCAGCTGGTTCCGAACTCCCACGGTGCCATCGGTGGTCTGCTGCGGGAAGTCG GTTTGACCTTCTACCTGAACAAGTCCGTGCCTGACATCATCTCCCAGAACATCAAC GATGCACTGAGCAAGGCGTTCGACCCACTGGGTATCAGCGACTACAATAGCATCT TCTGGATCGCGCATCCGGGTGGCCGTGCAATCCTGGACCAGGTCGAGGAAAAAG TGAACCTGAAGCCTGAAAAGATGAAGGCTACGCGTGATGTGCTGTCCAACTACGG TAATATGTCCAGCGCCTGCGTCTTCTTCATCATGGACCTGATGCGTAAGAAATCGC TGGAAGCCGGCCTGAAGACCACGGGCGAAGGCCTGGATTGGGGCGTACTGTTCG GTTTCGGTCCTGGTCTGACCATCGAAACTGTTGTGCTGCGCTCCATGGCCATCTAA	codon-optimized and his-tagged stilbene synthase *AhSTS* (UniProt: Q9SLV5) from *Arachis hypogaea*
StsTAL	ATGCCGAGCCTGGACTCCATCGTTGAGGCCGCGAGCTGGACTGCCAAGTTGGGCC CCCTCACTGACGCGGACGTCGCTCGCATGGATCGCTCGGGGGCCACCGTTGATGC CTACCTGGCTGAGGGTCGTCCTGTATATGGTCTGACGCAGGGCTTCGGCCCGCTG GTTACCTATAGCGCTACCTCGGAGATGGAGCAAGGCGCGAGCCTGATCAGCCATC TGGGCACTGCGCAGGGGCGTCCTATCGACCCCGATGCGTCGCGCCTGGTCTTCTG GCTGCGCCTCAACAGTATGCGTAAGGGCTTCAGCGCAGTCTCGACCGAGTTTTGG CAACGTCTGGCTGACCTGTGGAACGCCGGCTTTACTCCTGTAATCCCCCGCGACGG CACTGTGAGTGCAAGCGGTGACTTGCAGCCCTTGGCTCACGTGGCGCTGGCCTGC GCCGGTCATGGCGAAGCCTGGGTGCGCGATGAACAGGATCGTTGGACCCGTCGC CCAGCAGCTGAAGCACTGGCTGGTCTGGGTGCTGAACCGCTGGTGTGGCCCGTCC GCGAGGCGCTGGCATTCGTAAACGGCACCGGTGTAGGCTTGGCCGTCGCCATCTT GAACCAGCGCTCCGCTGTGCGTCTGGTGCGTGCTGTGGCGACTCTGACCGCACGT TTGACCGACCTGTTGGGCGGCAATGCCGAACACTACGATGAAGGTGTGGGTCAA GCCCGTAATCAGCTGGGCCAGTTGGAAGTAGCGCGCTGGATCCGCGCCGAAATCC CTGCCGGTCATCGGCGTGATGAGCGTCGGCCCCTGCAAGAGCCGTATAGTCTGCG CTGCGCCCCGCAGGTACTGGGCGCAGTCCTGGACCAACTGACCACTGCCGGTGAG ATCCTCCTGCGCGAGGCCAACGGTTGTACCGACAATCCCTTGACCTACGAGGACC GCGTTCTCCACGCGGGTAACTTCCATGCCATGCCCGTTGGCTTCGCGAGCGAGCA GACGGGGCTGGCCATGCACATGGCCGCGTACCTCGCCGAACGTCAGTTGGGGCT GGTGGTGAATCCGACGACCAACGGCGACCTGCCGATCATGCTGACCCCACGCGCT GGGCGTGGTTGTGGCCTGGCTGGTGTACAAATTAGCGCGACCAGCTTTATCAGTC	codon-optimized tyrosine ammonia lyase *StsTAL* (Uniprot: A0A0X3WEK2) from *Streptomyces sp.* NRRL F-4489

	GCATCCGCCAACTGGTGACCCCGGCCTCGCTGACCACCCTCCCGACGAACGGCTG GAACCAGGACCATGTGCCAATGGCTCTCAATGGTGCAAACGGCGTCGGCGAAGC GTTGGAGCTGGGCTGGTTGGCAGTAGGTAGTCTGGCCTTGGCGGCTGCCCAATTG GCCGTCATGACTGGCAAAGCTGAGAGTGCCACCGGTGTCTGGGCGGAGCTGGCC CGCATTAGCCCGGCACTCGACGCAGACCGCCCCATGGCTGGCGAAGTCCGTGCCG CTGCGGAACTGTTCCGCGATCACGCTGAACGCCAGTTGACGGGTGCGGCCTAA	
SgRppA	tgctaaggaggttttctaATGGCCACGCTGTGCCGTCCTGCCATTGCCGTCCCGGAACAT GTGATCACCATGCAGCAGACCCTCGATCTGGCGCGCGAAACCCACGCTGGCCACC CGCAGCGGGACCTGGTCCTGCGCCTGATCCAGAACACCGGCGTCCAGACCCGCCA CTTGGTGCAACCGATCGAGAAAACCCTGGCCCATCCCGGCTTCGAAGTGCGTAAC CAAGTGTACGAGGCGGAGGCCAAAACGCGTGTGCCGGAGGTTGTACGTCGGGCT TTGGCGAACGCGGAAACGGAACCGAGCGAAATCGACCTGATCGTCTACGTGTCGT GCACCGGCTTCATGATGCCGTCGCTGACCGCCTGGATCATCAATTCCATGGGCTTT CGCCCCGAGACCCGTCAGCTGCCTATCGCTCAGCTGGGCTGCGCAGCCGGTGGCG CTGCGATCAACCGCGCCCACGATTTCTGTGTCGCATATCCGGATAGCAACGTCTTG ATCGTCAGCTGTGAGTTCTGCTCCCTGTGCTACCAGCCTACCGATATCGGTGTCGG CTCCCTGCTGAGTAACGGCCTGTTCGGCGACGCACTGAGCGCGGCAGTGGTGCGT GGTCAGGGCGGGACCGGTATGCGCCTGGAGCGCAATGGCAGTCACCTCGTTCCC GACACCGAGGACTGGATCTCCTACGCCGTCCGCGATACCGGGTTCCACTTCCAGCT GGACAAGCGCGTGCCCGGCACCATGGAAATGCTGGCCCCCGTCCTCCTGGATCTG GTGGATCTGCACGGTTGGAGCGTGCCGAACATGGACTTCTTCATCGTACACGCGG GCGGCCCACGCATCCTGGACGATCTGTGCCACTTCCTCGACCTGCCCCCGGAGATG TTCCGGTATAGCCGCGCCACCCTGACTGAGCGGGGCAACATCGCCTCGTCCGTGG TGTTTGATGCCCTGGCACGCCTGTTCGACGATGGCGGGGCCGCCGAGTCGGCCCA GGGCCTGATCGCTGGCTTCGGCCCTGGCATCACCGCCGAGGTAGCCGTTGGCTCC TGGGCAAAGGAGGGGCTGGGCGCAGATGTGGGTCGCGACCTGGATGAGTTGGA GCTGACCGCGGGCGTCGCCCTGTCCGGCTAAagaattcgagctcggta	codon-optimized 1,3,6,8-tetrahydroxynaphthalene synthase *SgRppA* (UniProt: Q54240) from *Streptomyces griseus*

Supplement S5: Calibration Growth Profiler

The following function was used to convert green values into an OD_{600} equivalent:

$$OD_{600}\ \text{equivalent} = a * (gValue - gBlank)^b + c * (gValue - gBlank)^d + e * (gValue - gBlank)^f$$

with a = 0.0305, b = 1, c = $8 * 10^{-8}$, d = 3.8, e = $1.77 * 10^{-13}$, f = 6.7 and gBlank = 18.787. Abbreviations: gValue, green value; gBlank, green value of reference medium. The calibration was performed for the *P. taiwanensis* VLB120 wild type in half-deepwell microtiter plates (CR1496d, EnzyScreen) sealed with sandwich covers (CR1296c, EnzyScreen).

Sample Name 929 i

RT:

8.933

Compound Name:

flaviolin 310nm

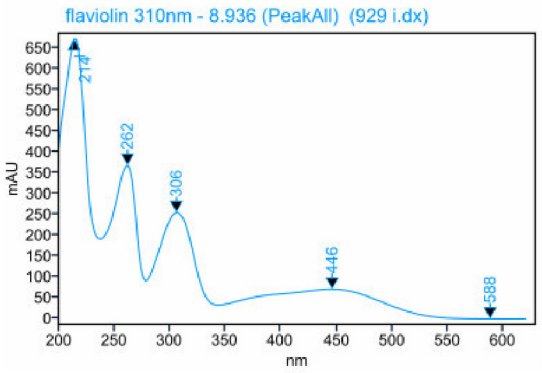

Figure S6: Flaviolin UV spectrum.

UV spectrum of flaviolin peak in HPLC from supernatant at retention 8.933 min. Relative quantification by peak area occurred at 310 nm. Sample derives from supernatant of strain GRC3Δ6 MC-II *attTn7*::*FRT-P*$_{14f}$-*SgRppA* (strain #929). Reference spectrum for comparison is published by Gross et al. (2006)

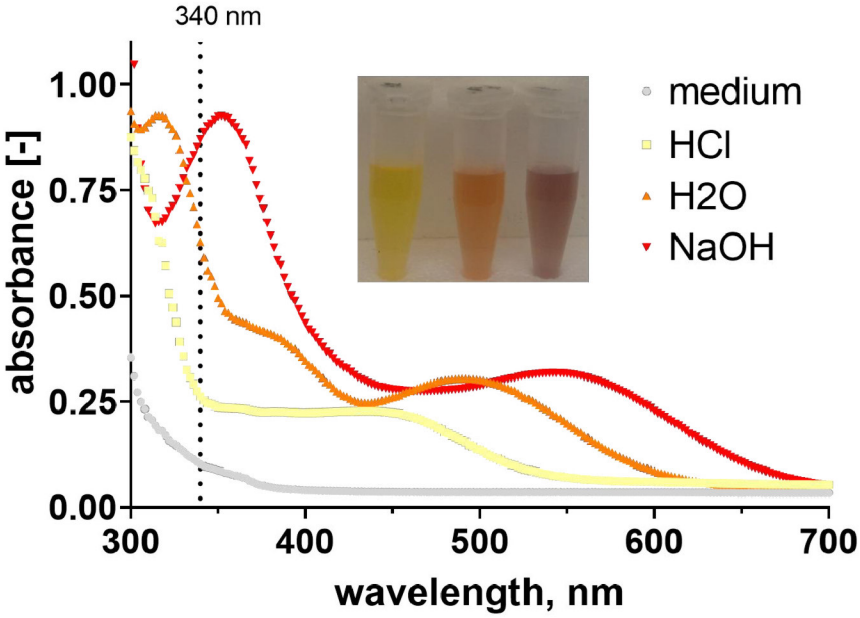

Figure S7:

Absorbance spectrum and picture of culture supernatant with secreted flaviolin. Addition of 50 µL 1 M HCl for acidification, 50 µL H_2O for unmodified at pH 7 or 50 µL 1 M NaOH for basic conditions in 950 µL supernatant and mineral salts medium with 1-fold buffer as control. Absorption at 340 nm is indicated.

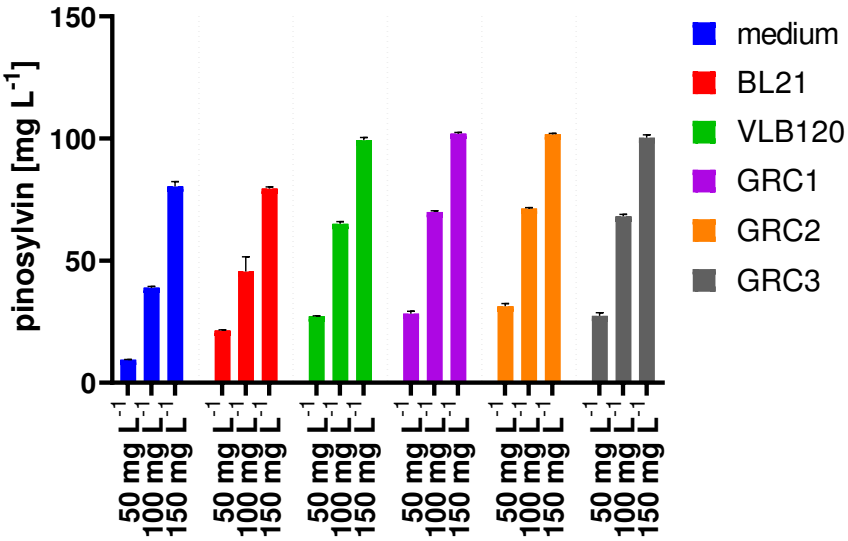

Figure S8:
Remaining pinosylvin in culture supernatant after 4 days of cultivation. Initially applied pinosylvin concentrations are indicated at the x-axis. Error bars represent the standard deviation (n=3).

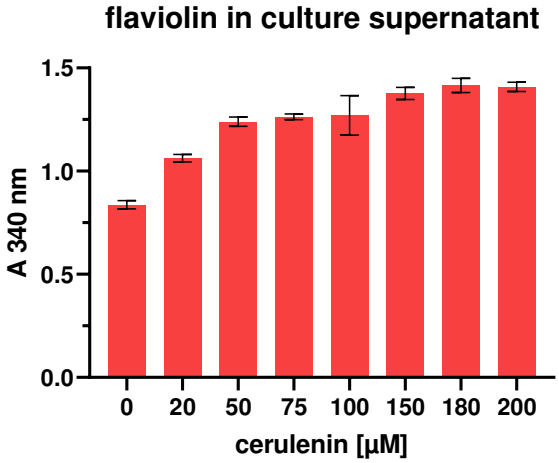

Figure S9:
Absorbance at 340 nm of culture supernatants of flaviolin producer GRC3 Δ6 *attTn7*::*FRT-P*$_{14f}$-*SgRppA* pSenFapRPseudoTermV1 with different concentrations of cerulenin (x-axis). Measured in plate reader in 96 well plate. Error bars represent standard deviation (n=3).

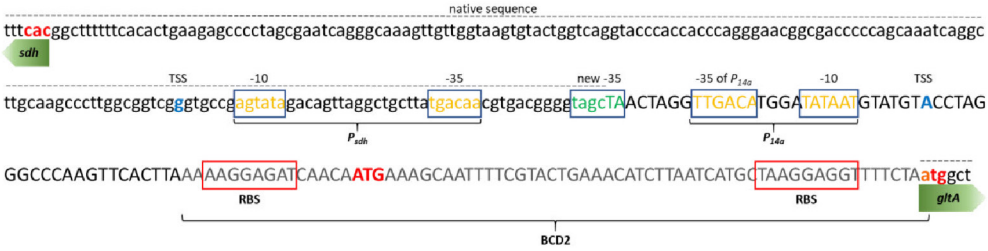

Figure S10: Design of promoter P_{14a}*

Intergenic sequence of *P. taiwanensis* VLB120 position 3568779 – 3568956 bp between succinate dehydrogenase (*sdh*, PVLB_16315) and type II citrate synthase (*gltA*, PVLB_16320) with exchanged promoter region of *gltA* with synthetic promoter P_{14a}*. Sequence predictions are based on σ70 promoter prediction tool SAPPHIRE (P_{sdh}, P-value 2.408E-5; P_{14a}*, P-value 5.0064E-4). Native sequence, small letters and dashed line; synthetic promoter sequence with bicistronic design 2 (BCD2), capital letters; translation start codon, red and bold; RBS, ribosome binding site; -10, Pribnow box; -35, consensus sequence for promoter; TSS, putative transcription start site.

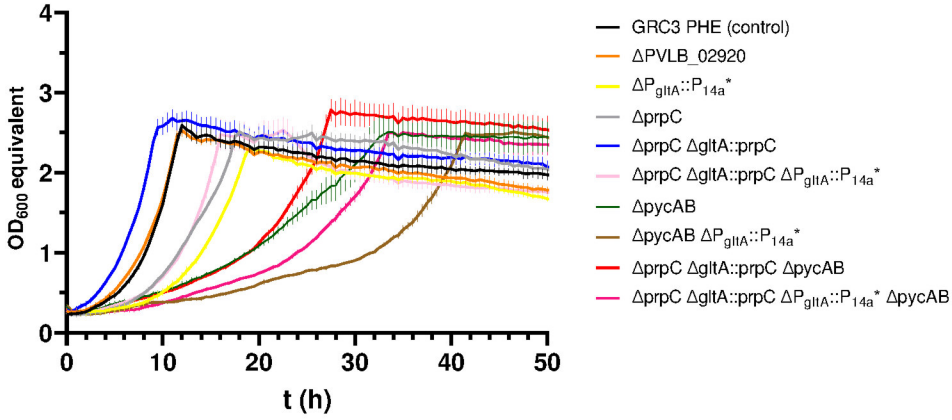

Figure S11:

Separate growth experiment of GRC3 PHE pinosylvin producing strains with modifications of the acetyl-CoA node in Growth Profiler in 96-square well plate at 30°C, 224rpm, 50 mm amplitude. Error bars represent the standard deviation of four replicates.

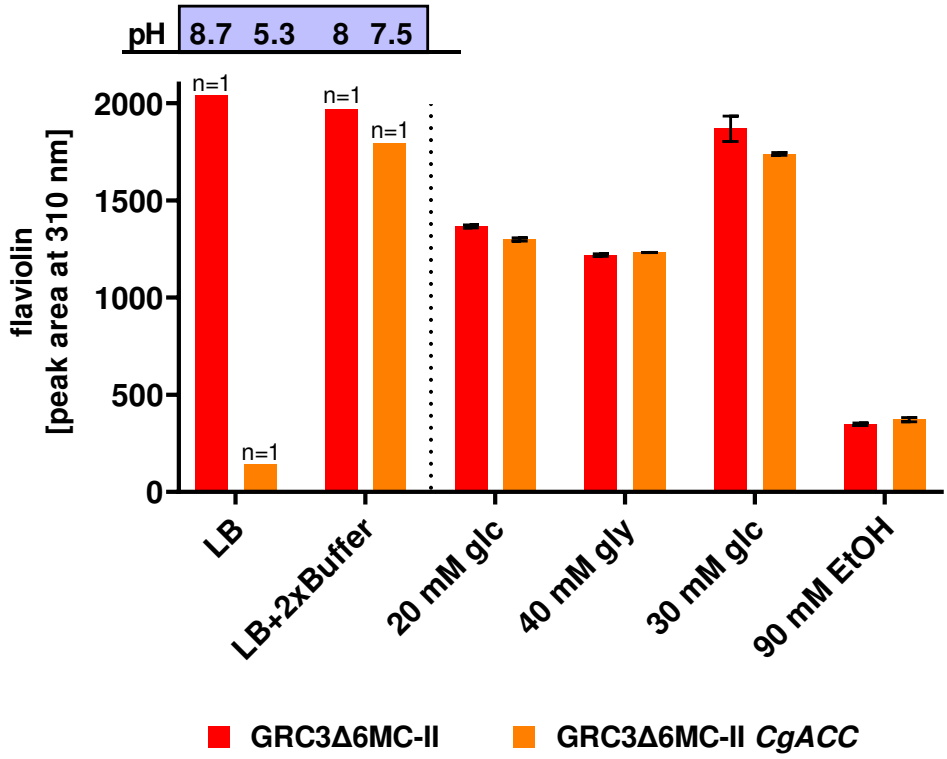

Figure S12:
Flaviolin titers in supernatant and pH of LB seed culture (n=1) of GRC3Δ6 MC-II and GRC3Δ6 MC-II *CgACC* (MC-III) flaviolin producers without and with additional 2x buffer (left; cell pellets appeared dark of GRC3Δ6 MC-II *CgACC* in LB) and comparison of flaviolin titers from different carbon sources in 3x buffered MSM (right). Error bars represent the standard deviation (n=3). Abbreviations: glc, glucose; gly, glycerol, EtOH, ethanol

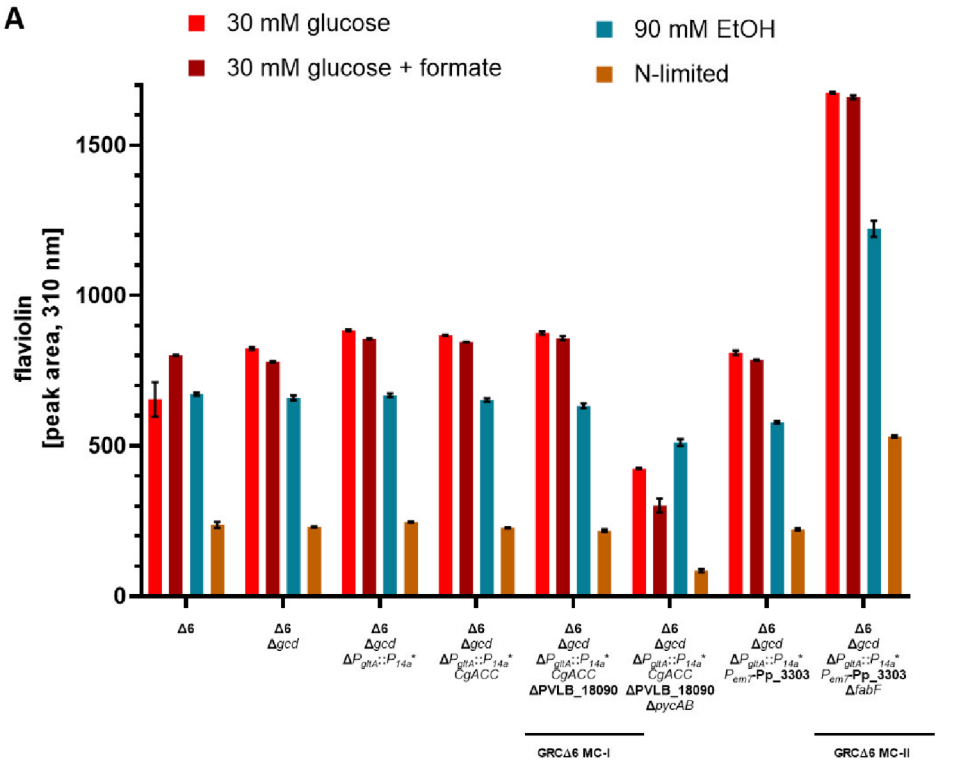
A
30 mM glucose
30 mM glucose + formate
90 mM EtOH
N-limited
flaviolin [peak area, 310 nm]
1500
1000
500
0
Δ6
Δ6 Δgcd
Δ6 Δgcd ΔP_gltA::P_14a* CgACC
Δ6 Δgcd ΔP_gltA::P_14a* CgACC ΔPVLB_18090
Δ6 Δgcd ΔP_gltA::P_14a* CgACC ΔPVLB_18090 ΔpycAB
Δ6 Δgcd ΔP_gltA::P_14a* P_emi7-Pp_3303
Δ6 Δgcd ΔP_gltA::P_14a* P_emi7-Pp_3303 ΔfabF
GRCΔ6 MC-I
GRCΔ6 MC-II

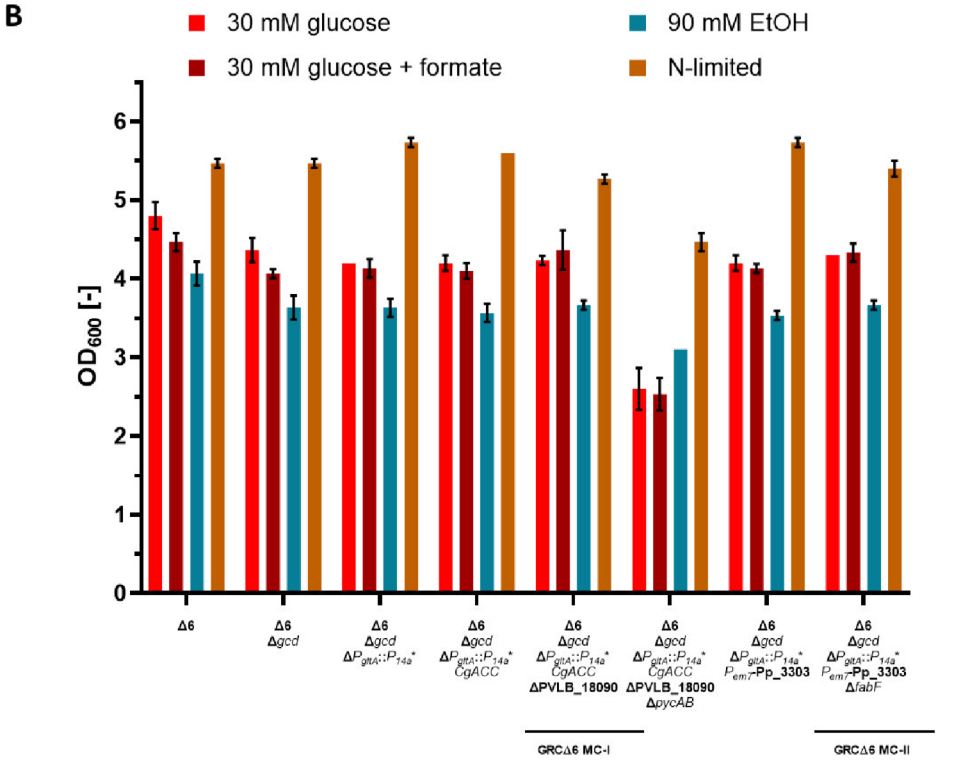
B
30 mM glucose
30 mM glucose + formate
90 mM EtOH
N-limited
OD600 [-]
6
5
4
3
2
1
0
Δ6
Δ6 Δgcd
Δ6 Δgcd ΔP_gltA::P_14a*
Δ6 Δgcd ΔP_gltA::P_14a* CgACC
Δ6 Δgcd ΔP_gltA::P_14a* CgACC ΔPVLB_18090
Δ6 Δgcd ΔP_gltA::P_14a* CgACC ΔPVLB_18090 ΔpycAB
Δ6 Δgcd ΔP_gltA::P_14a* P_emi7-Pp_3303
Δ6 Δgcd ΔP_gltA::P_14a* P_emi7-Pp_3303 ΔfabF
GRCΔ6 MC-I
GRCΔ6 MC-II

Figure S13:

Flaviolin titers in supernatant (A) and OD_{600} (B) of different flaviolin producer strains based on aromatics catabolism deficient GRC3Δ6 with additional indicated modifications. Made in 3-fold buffered MSM with 30 mM glucose (glc.), or with additional 10 mM formate, or 90 mM ethanol or $1/6^{th}$ of ammonium sulfate for nitrogen limiting conditions (C/N ~6) in 1.5 mL System Duetz cultures (30°C, 300 rpm, 50 mm amplitude). Samples were taken after 91 h, 92.5 h, 93h and 93.5 h, respectively to ensure full growth and THN oxidation to flaviolin. Error bars represent the standard deviation (n=3). Abbreviation: EtOH, ethanol; GRC3Δ6 MC-I, genotype of malonyl-CoA platform strain 1; GRC3Δ6 MC-II, genotype of malonyl-CoA platform strain 2.

Supplement S14: Genetic modifications without positive effect on product titers

- pinosylvin production with AhSTS outperformed PstrSTS or PstrSTS* in GRC3 PHE
- Deletion of secondary metabolite operon PVLB_01730-PVLB_01815 did not increase pinosylvin production in GRC3 PHE platform strain.
- The putative TetR-type regulator PVLB_02920 shares similarities to FabR of *P. fluorescens* WH6 (73%aa identity) and some to DesT from *P. aeruginosa* PAO1 (72%aa identity) which are likely involved in regulation of fatty acid biosynthesis. Deletion of fabR-like regulator encoded by PVLB_02920 in GRC3 PHE background did not increase pinosylvin synthesis.
- Deletion of *glnB* in GRC3Δ6 MC-II flaviolin producer did not increase flaviolin production.
- Plasmid expression of *sigX*, *fabD* or $fabD^{W258Q}$ for flaviolin synthesis in strain GRC3 Δ6 Δ*gcd* ΔP_{gltA}::P_{14a}*-BCD PVLB_23545-40::P_{14f}-*Cg_accBC_accD1 attTn7*::FRT-P_{14f}-*SgRppA* (MiKat#801) did not increase flaviolin production.

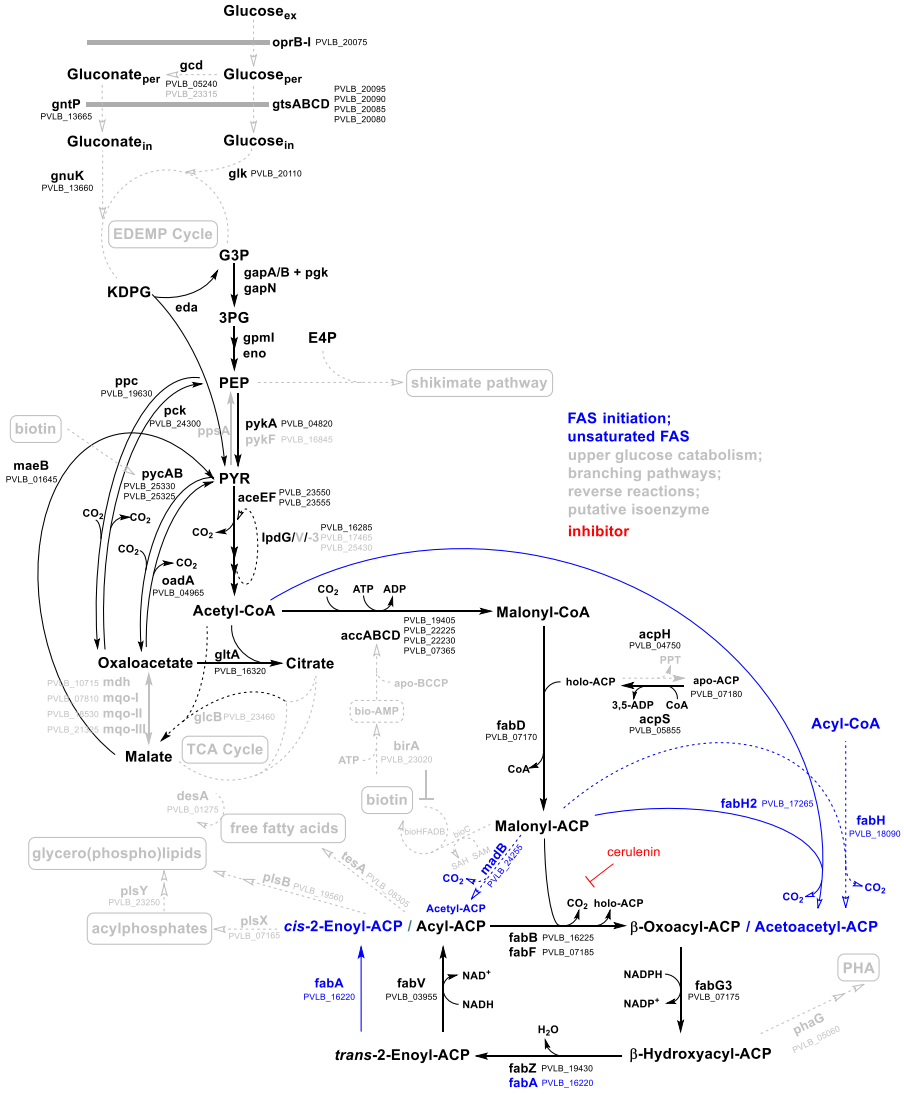

putative fatty acid biosynthesis (FAS) genes:
accA, acetyl-CoA carboxylase subunit alpha
accB, acetyl-CoA carboxylase biotin carboxyl carrier protein (BCCP)
accC, acetyl-CoA carboxylase biotin carboxylase
accD, acetyl-CoA carboxylase subunit beta
fabD, malonyl-CoA:ACP transacylase
fabB, 3-oxoacyl-ACP synthase **I**
fabF, 3-oxoacyl-ACP synthase II
fabH, 3-oxoacyl-ACP synthase III
fabH2, 3-oxoacyl-ACP synthase III
madB, malonyl-ACP decarboxylase
fabG3, 3-oxoacyl-ACP reductase
fabZ, 3-hydroxyacyl-ACP dehydratase
fabA, 3-hydroxyacyl-ACP dehydratase / *trans*-2-decenoyl-ACP isomerase (bifunctional)
fabV, *trans*-2-enoyl-ACP reductase

putative pathway-associated genes / branching pathways:
acpP, (PVLB_07180) acyl carrier protein
acpS, (PVLB_05855) 4'-phosphopantetheinyl transferase (ACP synthase)
acpH, (PVLB_04750) acyl carrier protein phosphodiesterase (ACP hydrolase)
birA, (PVLB_23020) bifunctional biotin-BCCP ligase / biotin operon repressor
phaG, (PVLB_05060) (R)-3-hydroxydecanoyl-ACP:CoA transacylase
tesA, (PVLB_08305) arylesterase
desA, (PVLB_01275) fatty acid desaturase
plsB, (PVLB_19560) glycerol-3-phosphate acyltransferase
plsX, (PVLB_01765) phosphate acyltransferase
plsY, (PVLB_23250) glycerol-3-phosphate acyltransferase

further FAS homologs in VLB120:
FabG, PVLB_06480 3-oxoacyl-ACP reductase
FabG2, PVLB_06885 3-oxoacyl-ACP reductase
FabG4, PVLB_22120 3-oxoacyl-ACP reductase

putative FAS regulatory genes:
PVLB_02920 TetR transcriptional regulator
psrA, PVLB_07930 TetR transcriptional regulator
Anr, PVLB_16605 Crp/FNR transcriptional regulator

putative secondary metabolite operon:
PVLB_01730 3-oxoacyl-ACP synthase
FabG1, PVLB_01735 3-oxoacyl-ACP reductase
PVLB_01745 3-oxoacyl-ACP synthase
PVLB_01795 acyl carrier protein
PVLB_01800 acyl carrier protein

Figure S15: Proposed fatty acid biosynthesis in *P. taiwanensis* VLB120.

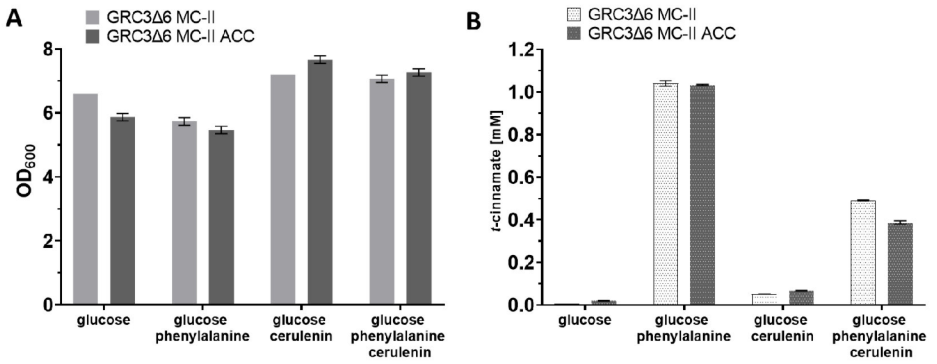

Figure S16:
Biomass in OD_{600} (A) and cinnamate titer (B) after bioconversion towards pinosylvin with supplemented phenylalanine and/or cerulenin after 21 h. Error bars represent the standard deviation (n=3); for some OD_{600} values the error bar is too small to be displayed.

Supplement S17: Evaluation of platform strain GRC3Δ6 MC-III by stilbenoid synthesis

Biotransformation experiments with GRC3Δ6 MC-III revealed that higher pinosylvin titers can be obtained when phenylalanine is supplemented. To close the loop of the *de novo* stilbenoid synthesis and to reduce the metabolic burden, only one point mutation, namely *aroF-1*^{P148L} (Wynands et al., 2018) was introduced into GRC3Δ6 MC-III to moderately increase the flux into the shikimate pathway.

The strains were grown in minimal medium with 30 mM glucose with and without supplementation of 0.5 mM of the respective phenylpropanoid or aromatic amino acid. Under these conditions, *de novo* synthesis of 12.3 ± 4.9 mg L^{-1} (0.06 mM) pinosylvin and 3.8 ± 0.8 mg L^{-1} (0.017 mM) resveratrol was achieved using the GRC3Δ6 MC-III strain (Supplementary S15, Supplementary S16). *De novo* formation of pinosylvin was higher than resveratrol, but this was likely due to the different precursor supply provided by different PAL/TAL activities.

With cinnamate or phenylalanine supplementation the pinosylvin titers were not further increased but the overall high variance in pinosylvin titers may hide potential tendencies which were previously observable in high biomass biotransformation. This clonal variability remained also in a separate experiment (data not shown), indicating a genetic instability. The *p*-coumarate titers of *aroF-1*^{P148L} mutant were not higher than from parental GRC3Δ6 MC-III, but these titers were anyway one order of magnitude lower than that of cinnamate, likely due to a higher Km value of StsTAL (Cui et al., 2020) than AtPAL2 (Cochrane et al., 2004). The supplementation of tyrosine reduced resveratrol titers below 1 mg L^{-1}. Here, it has to be considered that the used strain is also able to form some *de novo*-synthesized *p*-coumarate through StsTAL activity.

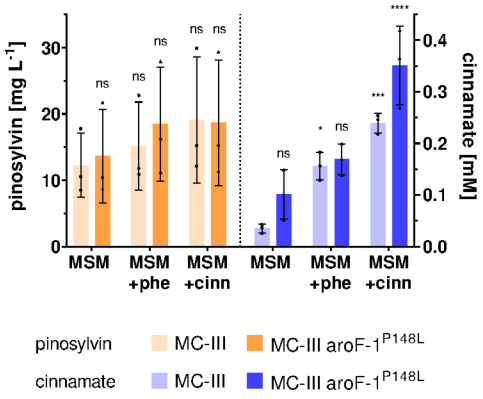

Figure S17: Titers of pinosylvin and cinnamate in *de novo* production experiments and with supplementation of phenylalanine (0.5 mM) or cinnamate (0.5 mM). Cultivation was performed in MSM 30 mM glucose with 3x buffer in 1.5 mL square-well System Duetz plate, initial OD_{600} was 0.2, sampled after 24 h. Individual pinosylvin titers are indicated by a triangle. Error bars represent the standard deviation (n=3) and * indicates $p<0.05$ confidence interval (***, $p\leq0.001$; ****, $p\leq0.0001$) of two-way ANOVA analysis. Abbreviation: ns, not significant, MSM, mineral salt medium; phe, phenylalanine; cinn, cinnamate.

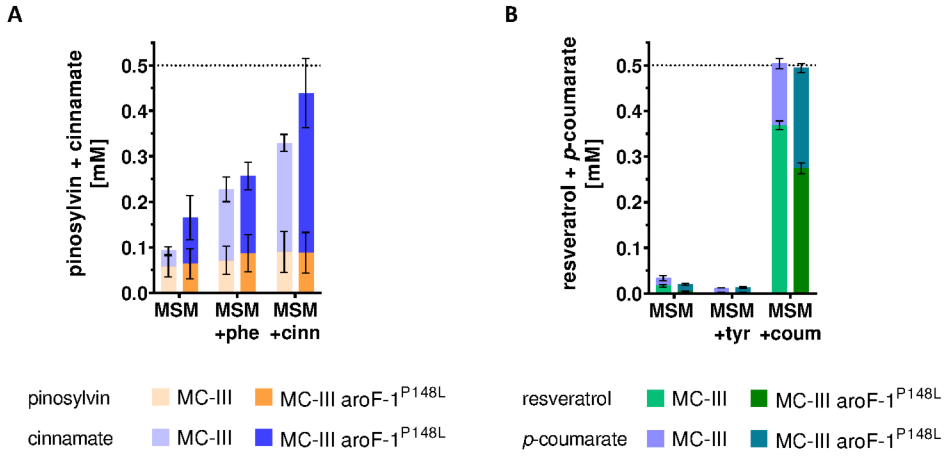

Figure S18:
Stacked pinosylvin and cinnamate titers in mM from *de novo* production experiments and with supplementation of phenylalanine (0.5 mM) or cinnamate (0.5 mM) (A); and stacked titers of resveratrol and *p*-coumarate from *de novo* synthesis and supplemented approaches with tyrosine (0.5

mM) or *p*-coumarate (0.5 mM) (B). Experimental conditions: MSM with initial OD_{600} of 0.2 in 1.5 mL System Duetz cultures at 30°C, 300 rpm, 50 mm amplitude, sampling after 24 h. Error bars represent the standard deviation (n=3)

Table S19: Different bioconversions in shake flasks and 24 square well plates with indicated substrate, precursor, product titers after approx. 25 h

Strain basis	Tn7-site	Substrate	Supplemented precursor	Initial OD	OD	Remaining phenylpropanoid precursor	Titer [mg L^{-1}] Stilbene / phenylpropanoid	comment
GRC3Δ6	*P_{14g}-his.AhSTS-Sc4CL^{A294G}-AtPAL2*	30 mM glc	2 mM cinnamate	0.2	4.1	1.38 mM	9.9 ± 0.42 pinosylvin	
GRC3Δ6MC-I		30 mM glc	2 mM cinnamate	0.2	3.93	1.49 mM	1.4 ± 0.7 pinosylvin	
GRC3Δ6MC-II		30 mM glc	none	0.2	4.2		9.3 ± 0.13 pinosylvin 0.01 mM *t*-cinnamate	
GRC3Δ6MC-II		30 mM glc	2 mM cinnamate	0.2	4.1	1.65 mM	8.5 ± 0.9 pinosylvin	
			2 mM phenylalanine	0.2	3.37	1.06 mM	7.1 ± 0.8 pinosylvin	
		60 mM glc	2 mM cinnamate	0.2	6.23	1.26 mM	22.3 ± 0.44 pinosylvin	After 47h
			2 mM phenylalanine	0.2	4.43	0.74 mM	8.43 ± 0.5 pinosylvin	After 47h
		30 mM glc	2 mM coumarate	0.2	4.27	1.56 mM *p*-coumarate	65.7 ± 3.9 Resveratrol 5.4 ± 0.3 Pinosylvin 0.16 mM *t*-cinnamate	
GRC3Δ6MC-II *Cg_ACC*		30 mM glc	2 mM cinnamate	0.2	3.87	1.73 mM	16.2 ± 1 pinosylvin	
GRC3Δ6MC-II *trpE^{P290S}*		30 mM glc	none	1	4		7.1 ± 0.22 pinosylvin 1.593 ± 0.004 mM cinnamate	
GRC3Δ6MC-II *trpE^{P290S}*		30 mM glc	none	0.2	4		7.4 ± 0.3 pinosylvin 1.6 ± 0.01 mM cinnamate	
		60 mM glc	none	0.2	5.43		11.6 ± 0.4 pinosylvin 2.26 ± 0.03 cinnamate	After 47h
GRC3Δ6MC-III		30 mM glc	none	1%			12.3 ± 4.9 pinosylvin 0.035 ± 0.01 cinnamate	Figure S15
GRC3Δ6MC-III *aroF-1^{P148L}*		30 mM glc	none	1%			13.6 ± 7 pinosylvin 0.1 ± 0.05 cinnamate	Figure S15
GRC3Δ6MC-III		30 mM glc	0.5 mM cinnamate	1%			19.1 ± 9.5 pinosylvin 0.24 ± 0.02 cinnamate	Figure S15
GRC3Δ6MC-III *aroF-1^{P148L}*		30 mM glc	0.5 mM cinnamate	1%			18.7 ± 9.5 pinosylvin 0.35 ± 0.08 cinnamate	Figure S15
GRC3Δ6MC-III		30 mM glc	0.5 mM phenylalanine	1%			15.2 ± 6.6 pinosylvin 0.156 ± 0.03 cinnamate	Figure S15
GRC3Δ6MC-III *aroF-1^{P148L}*		30 mM glc	0.5 mM phenylalanine	1%			18.5 ± 8.6 pinosylvin 0.17 ± 0.03 cinnamate	Figure S15
GRC3Δ6MC-III	*P_{14g}-his.AhSTS-Sc4CL^{A294G}-StsTAL*	30 mM glc	none	1%			3.8 ± 0.7 resveratrol 0.015 mM coumarate	Figure S15
GRC3Δ6MC-III *aroF-1^{P148L}*		30 mM glc	none	1%			1 resveratrol 0.015 mM coumarate	Figure S15
GRC3Δ6MC-III		30 mM glc	0.5 mM coumarate	1%			84 ± 2.2 resveratrol 0.135 ± 0.011 mM coumarate	Figure S15
GRC3Δ6MC-III *aroF-1^{P148L}*		30 mM glc	0.5 mM coumarate	1%			62.5 ± 2.6 resveratrol 0.22 ± 0.01 mM coumarate	Figure S15
GRC3Δ6MC-III		30 mM glc	0.5 mM tyrosine	1%			0.53 ± 0.12 resveratrol 0.01 mM coumarate	Figure S15
GRC3Δ6MC-III *aroF-1^{P148L}*		30 mM glc	0.5 mM tyrosine	1%			0.43 ± 0.07 resveratrol 0.01 mM coumarate	Figure S15

Supporting information to article “Engineered passive glucose uptake in *Pseudomonas taiwanensis* VLB120 for increased resource efficiency in bioproduction”

Tobias Schwanemann[a], Nicolas Krink[b], Pablo Nikel[b], Benedikt Wynands[a] and Nick Wierckx[a‡]

[a] Institute of Bio- and Geosciences, IBG-1: Biotechnology, Forschungszentrum Jülich GmbH, 52425 Jülich, Germany
[b] *The Novo Nordisk Foundation Center for Biosustainability, Technical University of Denmark, Kongens Lyngby, Denmark*

‡ corresponding author:

Nick Wierckx, Institute of Bio- and Geosciences, IBG-1: Biotechnology, Forschungszentrum Jülich, Wilhelm-Johnen-Straße, 52425 Jülich, Germany. e-mail: n.wierckx@fz-juelich.de

Table S1: Bacterial strains used in this study

Strains	Relevant characteristics	Reference and strain No.
Escherichia coli		
HB101 pRK2013	HB101 with pRK2013	Ditta et al. (1980)
PIR2	*F⁻ Δlac169 rpoS(Am) robA1 creC510 hsdR514 endA recA1 uidA(ΔMluI)::pir*; host for *oriV(R6K)* plasmids	Thermo Fischer Scientific
DH5α λ*pir*	λ*pir* lysogen of DH5α; host for *oriV(R6K)* plasmids	Víctor de Lorenzo lab
DH5α λ*pir* pTNS1	DH5α λ*pir* with pTNS1	Choi et al. (2005)
DH5α pSW-2	DH5α with pSW-2	Martínez-García & de Lorenzo (2011)
Pseudomonas taiwanensis		
GRC3	Genome-reduced-chassis strain; Δprophage1/2::*ttgVWGHI*	Wynands et al. (2019); MiKat #5
GRC3 PVLB_06360/65::P_{gts}-*Zm_glf*	GRC3 with additional Glf_{Zm}	This study; MiKat #1709
GRC3 Δ*gtsABCD*::*Zm_glf*	GRC3 with exchanged glucose transporter GtsABCD by Glf_{Zm}	This study; MiKat #1706
GRC3 Δ*gcd*	GRC3 with deleted glucose dehydrogenase (PVLB_05240)	This study; MiKat #684
GRC3 Δ*gcd* PVLB_06360/65::P_{gts}-*Zm_glf*	GRC3 Δgcd with additional Glf_{Zm}	This study; MiKat #1710
GRC3 Δ*gcd* Δ*gtsABCD*::*Zm_glf*	GRC3 Δgcd with exchanged glucose transporter GtsABCD by Glf_{Zm}	This study; MiKat #1707
GRC3Δ6 MC-III	Malonyl-CoA platform strain No. 3	(Schwanemann, Otto, et al., 2023); MiKat #1009
GRC3Δ6 MC-III PVLB_06360/65::P_{gts}-Zm_glf	GRC3Δ6 MC-III with additional Glf_{Zm}	This study; MiKat #1654
GRC3Δ6 MC-III Δ*gtsABCD*::*Zm_glf*	GRC3Δ6 MC-III with exchanged glucose transporter GtsABCD by Glf_{Zm} (GRC3Δ6 MC-IV)	This study; MiKat #1618
GRC3Δ6 MC-III *attTn7*::*FRT-P14f-his.AhSTS-Sc4CL*^{A294G}	Malonyl-CoA platform strain No. 3 with stilbene module	This study; MiKat #1722
GRC3Δ6 MC-III PVLB_06360/65::P_{gts}-*Zm_glf attTn7*::*FRT-P14f-his.AhSTS-Sc4CL*^{A294G}	GRC3Δ6 MC-III with additional Glf_{Zm} with stilbene module	This study; MiKat #1813
GRC3Δ6 MC-III Δ*gtsABCD*::*Zm_glf attTn7*::*FRT-P14f-his.AhSTS-Sc4CL*^{A294G}	GRC3Δ6 MC-III with exchanged glucose transporter gtsABCD by glf (GRC3Δ6 MC-IV) with stilbene module	This study; MiKat #1724

GRC3 Δ8-tap-ΔpykA (GRC3 PHE)	Phenylalanine platform strain	(Otto et al., 2019); MiKat #74
GRC3 PHE *attTn7*::*P14f-AtPAL2*	Cinnamate producer based on GRC3 PHE, Gm^R	(Otto et al., 2019); MiKat #384
GRC3 PHE *attTn7*::*FRT-P14f-AtPAL2*	Cinnamate producer based on GRC3 PHE, without antibiotic resistance	This study, MiKat #1746
GRC3 PHE PVLB_06360/65::P_{gts}-*Zm_glf*	GRC3 PHE with additional Glf_{Zm}	This study; MiKat #1711
GRC3 PHE PVLB_06360/65::P_{gts}-*Zm_glf attTn7*::*P14f-AtPAL2*	With cinnamate production module, Gm^R	This study, MiKat #1720
GRC3 PHE PVLB_06360/65::P_{gts}-*Zm_glf attTn7*::*FRT-P14f-AtPAL2*	With cinnamate production module, without antibiotic resistance	This study, MiKat #1748
GRC3 PHE Δ*gtsABCD*::*Zm_glf*	GRC3 PHE with exchanged glucose transporter GtsABCD by Glf_{Zm}	This study; MiKat #1708
GRC3 PHE Δ*gtsABCD*::*Zm_glf attTn7*::*P14f-AtPAL2*	With cinnamate production module, Gm^R	This study; MiKat #1719
GRC3 PHE Δ*gtsABCD*::*Zm_glf attTn7*::*FRT-P14f-AtPAL2*	With cinnamate production module, without antibiotic resistance	This study, MiKat #1747
GRC3 PHE Δ*gcd*	Phenylalanine platform strain with deleted *gcd* (PVLB_05240)	(Schwanemann, Otto, et al., 2023); MiKat#339
GRC3 PHE Δ*gcd attTn7*::*P14f-AtPAL2*	With cinnamate production module, Gm^R	This study, MiKat #2298
GRC3 PHE Δ*gcd* PVLB_06360/65::P_{gts}-*Zm_glf*	GRC3 PHE Δ*gcd* with additional Glf_{Zm}	This study; MiKat #2150
GRC3 PHE Δ*gcd* PVLB_06360/65::P_{gts}-*Zm_glf attTn7*::*P14f-AtPAL2*	With cinnamate production module, Gm^R	This study, MiKat #2299
GRC3 PHE Δ*gcd* Δ*gtsABCD*::*Zm_glf*	GRC3 PHE Δ*gcd* with exchanged glucose transporter GtsABCD by Glf_{Zm}	This study; MiKat #2204
GRC3 PHE Δ*gcd* Δ*gtsABCD*::*Zm_glf attTn7*::*P14f-AtPAL2*	With cinnamate production module, Gm^R	This study, MiKat #2300

Table S2: Plasmids used in this study

Plasmid	Relevant characteristics	HiFi assembly note	Reference & No.
pTNS1	Amp^R, *oriV(R6K)*, TnSABC+D operon	-	Choi et al. (2005)
pBBFLP	plasmid for antibiotic markers excision in *P. putida* strains; Tc^R, *oriV*(pBBR1) *oriT*(RK2) mob^+ λP_R::FLP λ(cI857) *sacB tet*	-	De Las Heras et al. (2008)
pEMG	Km^R, *oriV(R6K)*, *oriT*, *traJ*, *lacZα*-MCS flanked by two I-SceI restriction sites	-	Martínez-García & de Lorenzo (2011)
pSNW2	Km^R, *oriV(R6K)*, *oriT*, *traJ*, *lacZα*-MCS flanked by two I-SceI restriction sites, P_{14g}-BCD2→*msfGFP*	-	Volke et al. (2020, 2021) plasmid #142
pSW-2	Gm^R, *oriV(RK2), oriT, xylS, Pm→ I-SceI*	-	Martínez-García & de Lorenzo (2011)
pSEVA6213S	Gm^R, *oriV(RK2)*, P_{EM7}→*I-SceI*;	-	Wirth et al. (2020)
pEMG-gcd	Deletion vector for glucose dehydrogenase gcd (PVLB_05240)	-	Wynands unpublished, Plasmid #290
pSNW2-Ex-Pro-J23108-PP3303-LP_02480	Exchange vector for P_{EM7} in GRC3Δ6 MC-III by P_{J23108} and BCD10	Fragment TS-280/TS281 from pSNW2; Fragments TS-310/ TS-311 and TS-304/TS-305 from GRC3Δ6 MC-II genome; Fragment TS-309/TS-307 from pSEVA62J23108-BCD10-GFP	Plasmid #515
pSNW2-Ex-gtsABCD-glf KT2440	Exchange vector for glucose transporter gtsABCD with Zm_glf in *P. putida* KT2440	Fragment TS-280/TS281 from pSNW2; Fragments TS-282/TS-283 and TS-286/TS-287 from KT2440-genome; Fragment TS-284/TS-285 from *glf*-template	plasmid #511
pSNW2-Ex-gtsABCD-glf VLB120	Exchange vector for glucose transporter gtsABCD with Zm_glf in *P. taiwanensis* VLB120	Fragment TS-280/TS281 from pSNW2; Fragments TS-288/TS-289 and TS-290/TS-291 from VLB120-genome; Fragment TS-284/TS-285 from *glf*-template	plasmid #512
pSNW2-LP_PVLB06360-65-Pgts-Zm_glf for VLB120	Insertion of Zm_glf into landing pad PVLB_06360/65 in VLB120 with P_{gts} promoter	Fragment TS-280/TS281 from pSNW2; Fragments TS-337/TS-338 and TS-343/TS-344 from VLB120-genome; Fragment TS-339/TS-340 from MC-III Δ*gtsABCD*::*glf* genome; Fragment TS-341/TS-342 from GRC3Δ6 MC-III genome	plasmid #513

pSNW2-LP_PP1738-Pgts-Zm_glf for KT2440	Insertion of Zm_glf into landing pad PP_1738 in KT2440 with P_{gts} promoter	Fragment TS-280/TS281 from pSNW2; Fragments TS-329/TS-330 and TS-335/TS-336 from VLB120-genome; Fragment TS-331/TS-332 from SEM11Δ2-glf genome; Fragment TS-333/TS-334 from GRC3Δ6 MC-III genome	plasmid #514
pBG14f-AtPAL2	cinnamate synthesis module for Tn7 integration	-	(Otto et al., 2019)
pBG14f_FRT_Kan	Km^R flanked by FRT sites, *oriV(R6K)*, *oriT*, mini-Tn7 transposon delivery vector, P_{14f}*(BCD2)→msfgfp*	-	Ackermann et al. (2021)
pBG14f_Km_FRT_AtPAL2	Recyclable cinnamate production module for Tn7 integration	Fragment TS-106/TS-019 from pBG14f-Kan-FRT,	Lechtenberg unpublished, Plasmid #368
pBG14f_Km_FRT_his.AhSTS-Sc4CL^{A294G}	Recyclable stilbene synthesis module with his-tag for Tn7 integration	Fragment TS-368/TS-369 from pBG14f_Km_FRT_his.AhSTS-Sc4CL^{A294G}-AtPAL2 (plasmid#229)	This study Plasmid #537

Table S3: Oligonucleotides used in this study

Shown are their name, sequence, and description. Oligonucleotides used for diagnostic PCRs and sequencings are not included.

Primer No.	Description	Sequence
TS-280	pSNW2 fwd	agtcgacctgcaggcatg
TS-281	pSNW2 rev	acagattaccctgttatccctatactg
TS-282	fwd TS1 gtsA KT2440	gggataacagggtaatctgttgggcgcggttgctgttg
TS-283	rev TS1 gtsA KT2440	tgactactttcagaactcatcggagcacctttcttgttgttatgc
TS-284	fwd glf	atgagttctgaaagtagtcaggg
TS-285	rew glf	ttacttctgggagcgccac
TS-286	fwd TS2 gtsD in KT2440	tgtggcgctcccagaagtaaaggacaacgtggctcacttc
TS-287	rev TS2 gtsD in KT2440	tgcatgcctgcaggtcgactgaagtcgcaagggaagctg
TS-288	fwd TS1 gtsA PVLB_20095	gggataacagggtaatctgtcgacctcaaccaggtgttg
TS-289	rev TS1 gtsA PVLB_20095	tgactactttcagaactcatgagagcacctttttcttgttg
TS-290	fwd TS2 gtsD PVLB_20080	tgtggcgctcccagaagtaaaggacaacgtggcccgct
TS-291	rev TS2 gtsD PVLB_20080	tgcatgcctgcaggtcgactacgggaagctgttgaagtcctc
TS-304	fwd TS2 ex prom of 3303 in KT2440	aggatcgtttctaatgactcacaacgttaatcaaaag
TS-305	rev TS2 ex prom of 3303 in KT2440	aagcttgcatgcctgcaggtcgacttcgaagccatagcgtatg
TS-307	rev J23108 cloning	gttgtgagtcattagaaacgatcctccgcatg
TS-309	fwd J23108 cloning in VLB landing pad	atcgctgaataatctagggcggcggatttg
TS-310	fwd TS1 ex prom 3303 in LP VLB120	gtatagggataacagggtaatctgtatgaagaaagacccgcgtg
TS-311	rev TS1 ex prom 3303 in LP VLB120	ccgccgccctagattattcagcgatcagccag
TS-329	fwd flank1 landing Pad PP_1738	gggataacagggtaatctgtagctggtgggcgatgacag
TS-330	rev flank1 landing Pad PP_1738	gatagaggtccaaatgccaccgcagcgg
TS-331	fwd insert Pgts-Zm_glf (for KT2440)	gtggcatttggacctctatcacgcctac
TS-332	rev insert Pgts-Zm_glf (for KT2440)	gctcgaattcgtagacgagtcaacggcc
TS-333	fwd insert terminator in landing pad	actcgtctacgaattcgagctcggtacc
TS-334	rev insert terminator in landing pad	gcaagtacgctatctgacgtccttggac
TS-335	fwd flank2 landing Pad PP_1738	acgtcagatagcgtacttgctatctgcaac
TS-336	rev flank2 landing Pad PP_1738	tgcatgcctgcaggtcgacttgctcaatttctgaaagctg
TS-337	fwd flank1 landing Pad PVLB_06360-65	gggataacagggtaatctgttggtgggcgacgacagttg
TS-338	rev flank1 landing Pad PVLB_06360-65	cggccccacgcgacaaagaccaccgcac
TS-339	fwd insert Pgts-Zm_glf (for VLB)	gtctttgtcgcgtggggccgattgactg
TS-340	rev insert Pgts-Zm_glf (for VLB)	gctcgaattcgtagacgtttcaacgtcccttg
TS-341	fwd insert terminator in landing pad	aaacgtctacgaattcgagctcggtacc
TS-342	rev insert terminator in landing pad	acatctggggtatctgacgtccttggac
TS-343	fwd flank2 landing Pad PVLB_06360-65	acgtcagataccccagatgttatggcgatg
TS-344	rev flank2 landing Pad PVLB_06360-65	tgcatgcctgcaggtcgactttcaacccttgcgcatctc
TS-368	fwd FRT-Km-14f-stilbene module	gcgttaataaagaattcgagctcggtac
TS-369	rev FRT-Km-14f-stilbene module	ctcgaattctttattaacgcggttcacg

Table S4 Coding DNA fragments

Name	Sequence (5′ → 3′)	Note
Glf_{Zm}	ATGAGTTCTGAAAGTAGTCAGGGTCTAGTCACGCGACTAGCCCTAATCGCTGCTATAGGCGGCTTGCTTTTC GGTTACGATTCAGCGGTTATCGCTGCAATCGGTACACCGGTTGATATCCATTTTATTGCCCCTCGTCACCTGT CTGCTACGGCTGCGGCTTCCCTTTCTGGGATGGTCGTTGTTGCTGTTTTGGTCGGTTGTGTTACCGGTTCTTT GCTGTCTGGCTGGATTGGTATTCGCTTCGGTCGTCGCGGCGGATTGTTGATGAGTTCCATTTGTTTCGTCGC CGCCGGTTTTGGTGCTGCGTTAACCGAAAAATTATTTGGAACCGGTGGTTCGGCTTTACAAATTTTTTGCTTT TTCCGGTTTCTTGCCGGTTTAGGTATCGGTGTCGTTTCAACCTTGACCCCAACCTATATTGCTGAAATTGCTC CGCCAGACAAACGTGGTCAGATGGTTTCTGGTCAGCAGATGGCCATTGTGACGGGTGCTTTAACCGGTTAT ATCTTTACCTGGTTACTGGCTCATTTCGGTTCTATCGATTGGGTTAATGCCAGTGGTTGGTGCTGGTCTCCG GCTTCAGAAGGCCTGATCGGTATTGCCTTCTTATTGCTGCTGTTAACCGCACCGGATACGCCGCATTGGTTG GTGATGAAGGGACGTCATTCCGAGGCTAGCAAAATCCTTGCTCGTCTGGAACCGCAAGCCGATCCTAATCT GACGATTCAAAAGATTAAAGCTGGCTTTGATAAAGCCATGGACAAAAGCAGCGCAGGTTTGTTTGCTTTTG GTATCACCGTTGTTTTTGCCGGGGTATCCGTTGCTGCCTTCCAGCAGTTGGTCGGTATTAACGCCGTGCTGT ATTATGCACCGCAGATGTTCCAGAATTTAGGTTTTGGAGCTGATACGGCATTATTGCAGACCATCTCTATCG GTGTTGTGAACTTCATCTTCACCATGATTGCTTCCCGTGTTGTTGACCGCTTCGGCCGTAAACCTCTGCTTAT TTGGGGTGCTCTCGGTATGGCTGCAATGATGGCTGTTTTAGGCTGCTGTTTCTGGTTCAAAGTCGGTGGTG TTTTGCCTTTGGCTTCTGTGCTTCTTTATATTGCAGTCTTTGGCATGTCATGGGGCCCTGTCTGCTGGGTTGT TCTGTCAGAAATGTTCCCGAGTTCCATCAAGGGCGCAGCTATGCCTATCGCTGTTACCGGACAATGGTTAGC TAATATCTTGGTTAACTTCCTGTTTAAGGTTGCTGATGGTTCTCCAGCATTGAATCAGACTTTCAACCACGGT TTCTCCTATCTCGTTTTCGCAGCATTAAGTATCTTAGGTGGCTTGATTGTTGCTCGCTTCGTGCCGGAAACCA AAGGTCGGAGCCTGGATGAAATCGAGGAGATGTGGCGCTCCCAGAAGTAA	Coding sequence for glucose facilitator protein (UniProt P21906) from *Zymomonas mobilis*

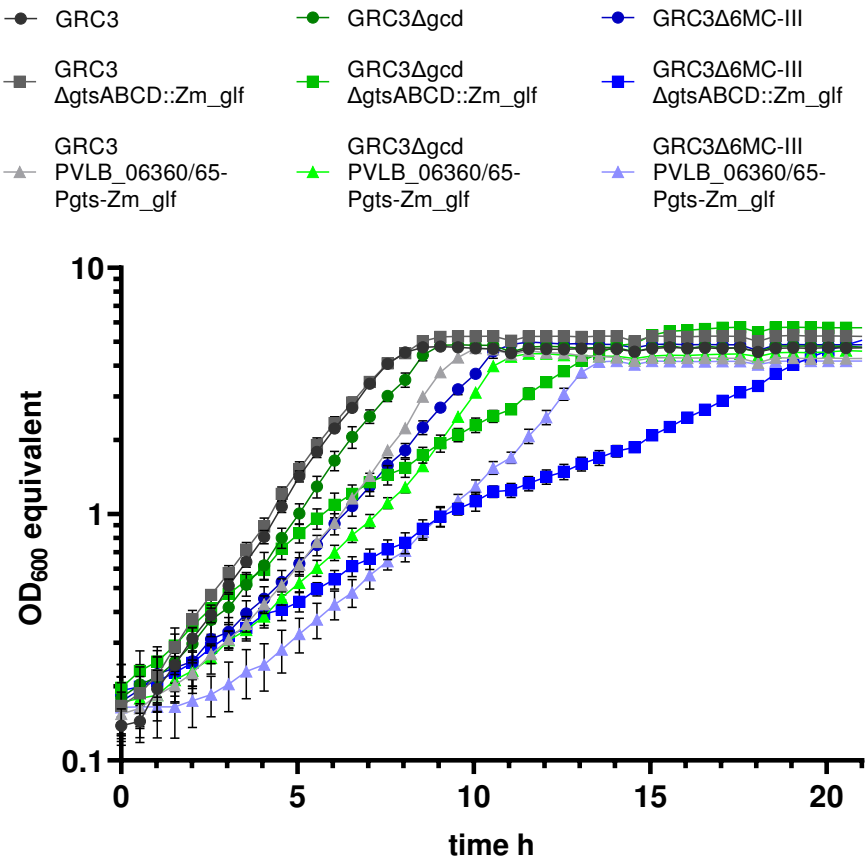

Figure S5:
Growth of *P. taiwanensis* VLB120 GRC3, GRC3Δgcd and GRC3Δ6MC-III with either replaced glucose transporter gene *gtsABCD* by Zm_glf or with Zm_glf expression from landing pad PVLB_06360/65. Grown in Growth Profiler with 20 mM glucose and 3-fold buffered MSM for 25 h with inoculation to OD_{600} 0.1 from adaption cultures. Error bars represent the standard deviation (n=4). Conversion to 'OD_{600} equivalent' by equation OD_{600} = a*(gvalue-gblanc)^b + c*(gvalue-gblanc)^d + e*(gvalue-gblank)^f (a, 0.0267; b, 1.01; c, 0.00000399; d, 3.18, e, 0.00000000000004; f, 0.01).

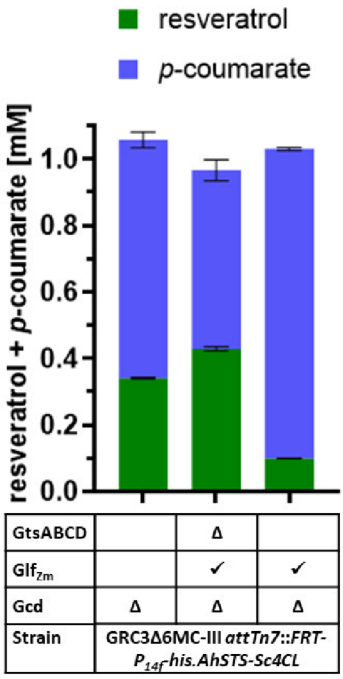

Figure S6:
Stacked concentrations of *p*-coumarate and resveratrol of GRC3Δ6MC-III with stilbene module (*attTn7*::*FRT-P$_{14f}$-his.AhSTS-AtPAL2*) with either replaced glucose transporter gene *gtsABCD* by *Zm_glf* or with *Zm_glf* expression from landing pad PVLB_06360/65. Grown in 24-square deep well plate with 30 mM (5.4 g L^{-1}) glucose, 3-fold buffered MSM and 1 mM *p*-coumarate for 24 h. Error bars represent the standard deviation (n=3). Same data as Figure 2-12 in the main article.

Supporting information to article "Production of (hydroxy)benzoate-derived polyketides by engineered *Pseudomonas* with *in situ* extraction"

Tobias Schwanemann[a], Esther A. Urban[a], Christian Eberlein[b], Jochem Gätgens[a], Daniela Rago[c], Nicolas Krink[c], Pablo I. Nikel[c], Hermann J. Heipieper[b], Benedikt Wynands[a] and Nick Wierckx[a]‡

[a] Institute of Bio- and Geosciences, IBG-1: Biotechnology, Forschungszentrum Jülich GmbH, Germany
[b] Department of Environmental Biotechnology, Helmholtz-Centre for Environmental Research - UFZ, 04318 Leipzig, Germany
[c] The Novo Nordisk Foundation Center for Biosustainability, Technical University of Denmark, Kongens Lyngby, Denmark

‡ corresponding author:

Nick Wierckx, Institute of Bio- and Geosciences, IBG-1: Biotechnology, Forschungszentrum Jülich, Wilhelm-Johnen-Straße, 52425 Jülich, Germany. e-mail: n.wierckx@fz-juelich.de

Table S1 Microbial strains used in this study

Strains	Relevant characteristics	Reference
Escherichia coli		
HB101 pRK2013	HB101 with pRK2013, Km^R	(Ditta et al., 1980)
PIR2	*F⁻ Δlac169 rpoS(Am) robA1 creC510 hsdR514 endA recA1 uidA(ΔMluI)::pir*; host for *oriV(R6K)* plasmids	Thermo Fischer Scientific
DH5α	F⁻ *Φ80 lacZ*ΔM15 Δ(*lacZYA-argF*)*U169 recA1 endA1 hsdR17*(r_k^-, m_k^+) *phoA supE44 thi-1 gyrA96 relA1* λ^-	Thermo Fischer Scientific
DH5α λ*pir*	λ*pir* lysogen of DH5α; host for *oriV(R6K)* plasmids	Víctor de Lorenzo lab
DH5α λ*pir* pTNS1	DH5α λ*pir* with pTNS1, Amp^R	(K. H. Choi et al., 2005)
***Bacillus subtilis* substrain 168**	Wildtype, DSM-23778	MiKat#1044
***Streptomyces venezuelae* NRRL B-65442**	Wildtype, DSM 112328	MiKat#1046
***Corynebacterium glutamicum* ATCC 13032**	Wildtype, DSM 20300	MiKat#1045
***Saccharomyces cerevisiae* S288C**	DSM 1333; MATalpha SUC2 mal mel gal2 CUP1 flo1 flo8-1 hap1	ATCC 204508, MiKat#537
***Pseudomonas putida* KT2440**	*P. putida* mt-2 derivative, cured from the TOL plasmid pWW0	(Bagdasarian et al., 1981), MiKat#30
Pseudomonas taiwanensis		
VLB120	Wild-type	(Panke et al., 1998), MiKat#1
GRC3	Genome-reduced-chassis strain; Δprophage1/2::*ttgVWGHI*	(Wynands et al., 2019) MiKat#5
GRC3Δ6	GRC3 derivative incapable of growing on 4-hydroxybenzoate, tyrosine, quinate and benzoate (Δ6=Δ*pobA*Δ*hpd*Δ*quiC*Δ*quiC1*Δ*quiC2*Δ*benABCD*)	(Schwanemann, Otto, et al., 2023) MiKat#382
GRC3Δ6 MC-II	Malonyl-CoA platform strain No. 2 (Δ6 Δ*gcd* ΔP_{gltA}::P_{14a}* PVLB_02480-85::P_{EM7}_PP3303 (*fabF-2*) Δ*fabF* (PVLB_07185))	(Schwanemann, Otto, et al., 2023) MiKat#975
GRC3Δ6MC-II *attTn7*::*FRT-*P_{14f}*-SgRppA*	Flaviolin production strain	(Schwanemann, Otto, et al., 2023) MiKat#912
GRC3Δ6 MC-III	Malonyl-CoA platform strain No. 3 (GRC3Δ6 MC-II PVLB_23545-40::P_{14f}-*Cg_accBC-Cg_accD1*)	(Schwanemann, Otto, et al., 2023) MiKat#1058
GRC3Δ6 MC-III *attTn7*::*FRT-*P_{14f}*-phdBCDE-sc4CL-atPAL*	Malonyl-CoA platform strain No.3 with benzoate synthesis module	This study, MiKat#1679
GRC3Δ6 MC-III *attTn7*::P_{14f}*-LaCH-II*	Gm^R, Malonyl-CoA platform strain No.3 with 3-hydroxybenzoate synthesis module	This study, MiKat#1680
GRC3Δ6 MC-III *attTn7*::P_{14g}*-menF-pchB*	Gm^R, Malonyl-CoA platform strain No.3 with 2-hydroxybenzoate synthesis module	This study, MiKat#1681

Table S2 Plasmids used in this study

Plasmid	Relevant characteristics	HiFi assembly note	Reference & plasmid map
pBT'Tmcs	Km^R, derivative of pBT'mcs, Ori/IHF, expression vector, P_{tac} (constitutive in *Pseudomonas*), with RBS, no terminator		(Koopman et al., 2010), P-map #66
pBT'T-HaBPS-RpBZL	Expression vector for a combination of a benzophenone synthase and a benzoate-CoA ligase	Cut pBT'Tmcs' #66 with EcoRI; Fragment TS143/TS144 from pRsetB-HaBPS; Fragment TS141/TS142 from pCT-topo-RpBZL	This study, P-map #120
pBT'T-HaBPS-PxBCLm	Expression vector for a combination of a benzophenone synthase and a benzoate-CoA ligase	Cut pBT'Tmcs' #66 with EcoRI; Fragment TS143/TS144 from pRsetB-HaBPS; Fragment TS131/TS132 from *Paraburkholderia xenovorans* LB400 (DSM 17367) genome	This study, P-map #121

pBT'T-HaBPS-Ta3HBCL	Expression vector for a combination of a benzophenone synthase and a benzoate-CoA ligase	Cut pBT'Tmcs' #66 with EcoRI; Fragment TS143/TS144 from pRsetB-HaBPS; Synthetic DNA fragment Ta3HBCL	This study, P-map #122
pBT'T-HsBPS-RpBZL	Expression vector for a combination of a benzophenone synthase and a benzoate-CoA ligase	Cut pBT'Tmcs' #66 with EcoRI; Fragment TS151/TS152 from pRsetB-HsBPS; Fragment TS141/TS142 from pCT-topo-RpBZL	This study, P-map #126
pBT'T-HsBPS-PxBCLm	Expression vector for a combination of a benzophenone synthase and a benzoate-CoA ligase	Cut pBT'Tmcs' #66 with EcoRI; Fragment TS151/TS152 from pRsetB-HsBPS; Fragment TS131/TS132 from *Paraburkholderia xenovorans* LB400 (DSM 17367) genome	This study, P-map #127
pBT'T-HsBPS-Ta3HBCL	Expression vector for a combination of a benzophenone synthase and a benzoate-CoA ligase	Cut pBT'Tmcs' #66 with EcoRI; Fragment TS151/TS152 from pRsetB-HsBPS; synthetic DNA fragment Ta3HBCL	This study, P-map #128
pBT'T-GmBPS-RpBZL	Expression vector for a combination of a benzophenone synthase and a benzoate-CoA ligase	Cut pBT'Tmcs' #66 with EcoRI; Synthetic DNA fragment GmBPS; Fragment TS141/TS142 from pCT-topo-RpBZL	This study, P-map #123
pBT'T-GmBPS-PxBCLm	Expression vector for a combination of a benzophenone synthase and a benzoate-CoA ligase	Cut pBT'Tmcs' #66 with EcoRI; Synthetic DNA fragment GmBPS; Fragment TS131/TS132 from *Paraburkholderia xenovorans* LB400 (DSM 17367) genome	This study, P-map #124
pBT'T-GmBPS-TaHBCL	Expression vector for a combination of a benzophenone synthase and a benzoate-CoA ligase	Cut pBT'Tmcs' #66 with EcoRI; Synthetic DNA fragment GmBPS; Synthetic DNA fragment Ta3HBCL	This study, P-map #125
pBT'T-ScCHS-RpBZL	Expression vector for a combination of a chalcone synthase and a benzoate-CoA ligase	Cut pBT'Tmcs' #66 with EcoRI; Synthetic DNA fragment ScCHS; Fragment TS141/TS142 from pCT-topo-RpBZL	This study, P-map #129
pBT'T-ScCHS-PxBCLm	Expression vector for a combination of a chalcone synthase and a benzoate-CoA ligase	Cut pBT'Tmcs' #66 with EcoRI; Synthetic DNA fragment ScCHS; Fragment TS131/TS132 from *Paraburkholderia xenovorans* LB400 (DSM 17367) genome	This study, P-map #130
pBT'T-ScCHS-Ta3HBCL	Expression vector for a combination of a chalcone synthase and a benzoate-CoA ligase	Cut pBT'Tmcs' #66 with EcoRI; Synthetic DNA fragment ScCHS; Synthetic DNA fragment Ta3HBCL	This study, P-map #131
pBT'T-SaBIS1-RpBZL	Expression vector for a combination of a biphenyl synthase and a benzoate-CoA ligase	Cut pBT'Tmcs' #66 with EcoRI; Fragment TS156/TS157 from pRsetB-SaBIS; Fragment TS141/TS142 from pCT-topo-RpBZL	This study, P-map #132
pBT'T-SaBIS1-PxBCLm	Expression vector for a combination of a biphenyl synthase and a benzoate-CoA ligase	Cut pBT'Tmcs' #66 with EcoRI; Fragment TS156/TS157 from pRsetB-SaBIS; Fragment TS131/TS132 from *Paraburkholderia xenovorans* LB400 (DSM 17367) genome	This study, P-map #133
pBT'T-SaBIS1-Ta3HBCL	Expression vector for a combination of a biphenyl synthase and a benzoate-CoA ligase	Cut pBT'Tmcs' #66 with EcoRI; Fragment TS156/TS157 from pRsetB-SaBIS; synthetic DNA fragment Ta3HBCL	This study, P-map #134
pBT'T-MdBIS1-RpBZL	Expression vector for a combination of a biphenyl synthase and a benzoate-CoA ligase; MdBIS1 equals triple mutant SaBIS1$^{P11H\ S97P\ P389T}$	BB fragment TS198/TS199, fragment TS200/TS201 and TS202/TS203 from pBT'T-SaBIS1-RpBZL #132;	This study, P-map #188
pBT'T-PcBIS1-RpBZL	Expression vector for a combination of a biphenyl synthase and a benzoate-CoA ligase	Fragment TS177/TS178 from pBT'T-HaBPS-RpBZL #120; Synthetic DNA fragment PcBIS1;	This study, P-map #206
pBT'T-GmBPS-sdgA	Expression vector for a combination of a benzophenone synthase and a benzoate-CoA ligase	Fragment TS226/TS227 from pBT'T-GmBPS-RpBZL #124; Synthetic DNA fragment sdgA;	This study, P-map #223
pBT'T-SaBIS1-sdgA	Expression vector for a combination of a biphenyl synthase and a benzoate-CoA ligase	Fragment TS226/TS227 from pBT'T-SaBIS1-RpBZL #132; Synthetic DNA fragment sdgA;	This study, P-map #224

pBT'T-MdBIS1-sdgA	Expression vector for a combination of a biphenyl synthase and a benzoate-CoA ligase; MdBIS1 equals triple mutant SaBIS1$^{P11H\ S97P\ P389T}$	Fragment TS226/TS227 from pBT'T-MdBIS1-RpBZL #188; Synthetic DNA fragment sdgA;	This study, P-map #225
pBT'T-PcBIS1-sdgA	Expression vector for a combination of a biphenyl synthase and a benzoate-CoA ligase	Cut pBT'Tmcs' #66 with EcoRI; Synthetic DNA fragment PcBIS1; Synthetic DNA fragment sdgA	This study, P-map #226
pBTrc'T-mcs'Km	Km^R, derivative of pBT'Tmcs with cytosine insertion in promoter (P_{tac} -> P_{trc})	Fragment TS-259/TS260 from plasmid pBT'Tmcs' #66	This study, P-map#308
pBTrc'T-HsBPS-RpBZL		Fragment TS-259/TS260 from pBT'T-HsBPS-RpBZL #126	This study, P-map#309
pBTrc'T-MdBIS1-RpBZL		Fragment TS-259/TS260 from pBT'T-MdBIS1-RpBZL #188	This study, P-map#310
pBTrc'T-PcBIS1-sdgA		Fragment TS-259/TS260 from pBT'T-PcBIS1-sdgA #226	This study, P-map#311
pTNS1	Amp^R, *oriV(R6K)*, TnSABC+D operon		(K. H. Choi et al., 2005)
pBBFLP	plasmid for antibiotic markers excision in *P. putida* strains; Tc^R, *oriV*(pBBR1) *oriT*(RK2) mob^+ λP_R::FLP λ(cI857) *sacB tet*		(De Las Heras et al., 2008)
pBG14f_FRT_Kan	Km^R flanked by FRT sites, *oriV(R6K)*, *oriT*, mini-Tn7 transposon delivery vector, P_{14f}*(BCD2)→msfgfp*		(Ackermann et al., 2021), P-map#113
pBG14f_kan_FRT-phdBCDE-sc4CL-atPAL	mini-Tn7 transposon vector (with FRT sites, to flip out Km^R after insertion) for integration of benzoate synthesis module: phenylpropanoid degradation operon from *Corynebacterium glutamicum*, 4-cinnamate::CoA-ligase mutant A294G from *Streptomyces coelicolor* and phenylalanine ammonia lyase 2 (PAL2) from *Arabidopsis thaliana* (codon-optimized for *P. taiwanensis* VLB120)	Fragment TS-106/TS019 from pBG14f-Kan-FRT; Fragment TS020/TS238 from pBG14g-CgPhdBCDE-Sc4CL-atPAL (P-map #68) (Otto et al., 2020)	This study, P-map #236
pBG14xx	Tn7 delivery vector; Km^R Gm^R, oriV(R6K), Tn7L, and Tn7R flanks, BCD2-*msfgfp* fusion, synthetic promoter variants		(Zobel et al., 2015), P-map#10-16
pBG14d/f/g-LaCH-II	mini-Tn7 transposon vector for integration of 3-hydroxybenzoate synthesis module LaCH-II (WP_052685672.1), codon optimized for VLB120	Fragment TS-106/TS-019 from pBG14d/f/g; Synthetic DNA fragment LaCH-II from *Lentzea aerocolonigenes*	This study, P-map #109
pBG14g-menF-pchB	mini-Tn7 transposon vector for integration of 2-hydroxybenzoate synthesis module menF (UniProt: P38051) and pchB (UniProt: Q51507)		This study, P-map #273 Wynands unpublished
pBG14f_kan_FRT-HsBPS-RpBZL	mini-Tn7 transposon vector (with FRT sites, to flip out Km^R after insertion) for integration of benzophenone synthesis module	Fragment TS106/TS019 from pBG14f-Kan-FRT; Fragment TS370/TS371 from pBT'T-HsBPS-RpBZL (#126)	This study, P-map#537
pBG14f_kan_FRT-PcBIS1-sdgA	mini-Tn7 transposon vector (with FRT sites, to flip out Km^R after insertion) for integration of 4-hydroxycoumarin synthesis module	Fragment TS106/TS019 from pBG14f-Kan-FRT; Fragment TS372/TS373 from pBT'T-PcBIS1-sdgA (#226)	This study, P-map#538

Table S3 Oligonucleotides used in this study

The listed oligonucleotides were used as PCR primers in cloning procedures. Shown are their name, sequence, and description.

Primer No.	Description	Sequence
TS-019	rev on BCD2 for BB amplification	attagaaaacctccttagcatg
TS-020	fwd on BCD2 for Insert amplification	atgctaaggaggttttctaatg
TS-106	fwd BB pBGxx amplification	taaagaattcgagctcggtaccc
TS-131	fwd PxBCL$_M$ cloning in pBT	gcggccgcgaaaggaggtctatatggaagctctgctggaaaaagcggcg
TS-132	rev PxBCL$_M$ cloning in pBT	atgctcctctagactcgaggaattcattatgactgttcgcgcagtttgaagc
TS-141	fwd RpBZL cloning in pBT	gcggccgcgaaaggaggtctatatgaatgcagccgcggtcacgcc
TS-142	rev RpBZL cloning in pBT	atgctcctctagactcgaggaattcattagcccaacacaccttcgcgcagc
TS-143	fwd HaBPS cloning in pBT	acaggaaacaggaggtaccgaatatggccccggcgatggag
TS-144	rev HaBPS cloning in pBT	agacctcctttcgcggccgctcactggagaattgggacactctgg
TS-151	fwd HsBPS cloning in pBT	acaggaaacaggaggtaccgaatatggcccctgcaatggag
TS-152	rev HsBPS or HpaBPS cloning in pBT	agacctcctttcgcggccgctcactggaggatggggac
TS-156	fwd SaBIS1 cloning in pBT	acaggaaacaggaggtaccgattatggcgcctttggttaag
TS-157	rev SaBIS1 cloning in pBT	agacctcctttcgcggccgcttagcatggaatagattcactac
TS-177	fwd BB repair pBT'T-xxBPS/BIS-Ta3HBCL	gcggccgcgaaaggaggtc
TS-178	rev BB repair pBT'T-xxBPS/BIS-Ta3HBCL	catattcggtacctcctgtttcctgtgtg
TS-179	fwd Ins repair pBT'T-GmBPS-Ta3HBCL	aacaggaggtaccgaatatggccccggcgatggacagc
TS-180	rev Ins repair pBT'T-GmBPS-Ta3HBCL	agacctcctttcgcggccgcttacgcaatcgggacgctacgg
TS-181	fwd Ins repair pBT'T-SaBIS-Ta3HBCL	aacaggaggtaccgaatatggcgcctttggttaagaatc
TS-182	rev Ins repair pBT'T-SaBIS-Ta3HBCL	agacctcctttcgcggccgcttagcatggaatagattcactac
TS-198	for pBT'T-SaBIS1 P11H S97P P389T -RpBZL	tgaatctattacctgctaagcggccgcgaaa
TS-199	for pBT'T-SaBIS1 P11H S97P P389T -RpBZL	tggcatgttggtgctctccatgattcttaaccaaaggcg
TS-200	for pBT'T-SaBIS1 P11H S97P P389T -RpBZL	tggagagcaccaacatgccaaaatcctag
TS-201	for pBT'T-SaBIS1 P11H S97P P389T -RpBZL	ggacctccggattcaacatgtcttggcg
TS-202	for pBT'T-SaBIS1 P11H S97P P389T -RpBZL	catgttgaatccggaggtcccaaagctaggg
TS-203	for pBT'T-SaBIS1 P11H S97P P389T -RpBZL	cttagcaggtaatagattcactacgcagtacg
TS-226	fwd BB amplification for ligase exchange	attcctcgagtctagagg
TS-227	rev binding intergene for ligase exchange	atagacctcctttcgcgg
TS-238	rev on pBGxx BB to insert	ccgggtaccgagctcgaattc
TS-259	fwd Ptac to Ptrc	ccctgttgacaattaatcatccggctcgtataatgtgtg
TS-260	rev Ptac to Ptrc	atgattaattgtcaacaggg
TS-370	fwd HsBPS cloning in pBG14x	tgctaaggaggttttctaatggcccctgcaatggagtac
TS-371	rev RpBZL cloning in pBG14x	taccgagctcgaattctttatcattagcccaacacaccttc
TS-372	fwd PcBIS1 cloning in pBG14x	tgctaaggaggttttctaatggcgccgctggtcaaaaac
TS-373	rev sdgA cloning in pBG14x	taccgagctcgaattctttatcatacggcctccacgctg

Table S4 Synthetic and coding DNA fragments

Used coding sequences and ordered synthetic DNA fragments. Coding sequence in capital letters, overhangs for cloning in small letters in synthetic DNA fragments.

Name	Sequence (5' → 3')	Note
RpBZL	ATGAATGCAGCCGCGGTCACGCCGCCACCCGAGAAGTTTAATTTTGCCGAGCACCTGCTGCAGACCAATCG CGTGCGGCCGGACAAGACGGCGTTCGTCGACGACATCTCGTCGCTGAGCTTCGCGCAACTCGAAGCTCAG ACGCGTCAGCTCGCCGCCGCCTTACGCGCGATCGGGGTGAAACGCGAAGAGCGCGTGCTGCTGCTGATGC TCGACGGCACGGATTGGCCGGTGGCGTTTCTCGGCGCAATCTACGCCGGCATCGTGCCGGTCGCGGTCAAT ACGCTGCTGACGGCGGACGACTACGCCTACATGCTCGAGCATTCGCGGGCTCAGGCCGTGCTGGTCAGCG GCGCGCTGCACCCGGTGCTCAAGGCAGCGCTGACCAAGAGCGATCACGAGGTGCAGCGAGTGATCGTTTC GCGCCCAGCGGCTCCGCTGGAGCCGGGCGAGGTCGACTTCGCTGAGTTCGTCGGCGCACATGCGCCGCTT GAGAAGCCTGCCGCTACGCAAGCGGACGATCCGGCGTTCTGGCTGTATTCGTCGGGTTCTACCGGGCGGC CGAAGGGCGTGGTGCACACTCACGCCAATCCGTACTGGACCTCGGAGCTGTACGGCCGCAACACGCTGCA TCTGCGCGAAGACGACGTCTGCTTTTCGGCGGCCAAACTGTTTTTCGCTTACGGCCTCGGCAACGCGCTGAC GTTTCCGATGACGGTCGGCGCGACCACGCTGCTGATGGGCGAGCGACCGACGCCGGACGCGGTGTTCAAG CGCTGGCTCGGCGGCGTCGGCGGTGTGAAACCGACCGTGTTCTACGGCGCGCCCACCGGCTACGCCGGCA TGTTGGCCGCGCCGAACCTGCCGTCGCGAGACCAGGTGGCGTTGCGGCTCGCGTCGTCGGCGGGCGAAGC ACTGCCGGCGGAGATTGGGCAGCGCTTCCAGCGCCATTTCGGCCTCGACATCGTCGATGGCATCGGCTCGA CCGAGATGCTGCACATCTTTCTGTCGAACCTGCCAGACCGGGTGCGCTACGGCACCACCGGATGGCCGGTG CCGGGCTATCAGATCGAGCTGCGCGGCGACGGCGGCGGACCGGTCGCCGACGGAGAGCCGGGCGATCTC TACATTCACGGCCCGTCATCGGCGACGATGTATTGGGGCAACCGGGCCAAGAGCCGCGACACCTTCCAGG GCGGCTGGACCAAGAGCGGCGACAAATACGTCCGCAACGACGACGGCTCCTACACCTATGCGGGCCGCAC CGACGACATGCTGAAGGTCAGCGGCATCTATGTCAGCCCGTTCGAGATCGAAGCGACGCTGGTGCAGCAT CCCGGTGTGCTCGAAGCCGCAGTGGTCGGGGTCGCCGACGAACACGGCCTGACCAAACCGAAGGCCTATG TGGTGCCGCGGCCCGGCCAGACCCTGTCGGAGACCGAGCTGAAGACCTTCATCAAGGATCGACTGGCGCC GTACAAATATCCGCGCAGCACGGTGTTCGTCGCCGAATTGCCGAAGACGGCGACCGGCAAGATTCAGCGC TTCAAGCTGCGCGAAGGTGTGTTGGGCTGA	Benzoate-CoA ligase (UniProt Q93TK0) from *Rhodopseudomonas palustris*
$PxBCL_M$	ATGGAAGCTCTGCTGGAAAAAGCGGCGAATCCGCCCGCCGCGACGGTCGAAGCGCCGCCCGCGCTATTCA ATTTCGCGGCCTATCTGTTTCGACTGAACGAAACGCGCGCCGGCAAGACCGCCTATATCGACGACACCGGC AGCACCACCTACGGCGAACTCGAAGAACGCGCGCGGCGTTTCGCCAGCGCGCTGCGTACGCTCGGCGTGC ATCCCGAAGAGCGAATTCTGCTCGTGATGCTCGACACCGTTGCGCTGCCGGTCGCCTTTCTCGGCGCACTCT ATGCGGGCGTCGTGCCGGTCGTCGCGAATACGCTGCTCACACCTGCCGACTACGTGTACATGCTCACGCAC AGCCACGCGCGCGCCGTGATCGCCTCCGGTGCGCTAGTGCAGAACGTGACGCAGGCGCTGGAGTCAGCCG AACATGACGGCTGTCAGCTGATCGTCTCACAGCCCCGCGAAAGCGAGCCGCGCCTCGCGCCTTTGTTCGAA GAACTGATCGATGCCGCCGCACCCGCCGCCAAAGCCGCCGCAACCGGATGTGACGATATCGCCTTCTGGCT GTATTCGTCGGGTTCGACCGGCAAGCCGAAGGGCACCGTCCACACGCATGCGAATCTGTACTGGACCGCC GAACTGTATGCGAAGCCGATTCTCGGCATCGCCGAAAACGACGTGGTGTTCTCCGCGGCCAAGCTGTTCTT CGCGTACGGTCTCGGCAATGGACTGACGTTCCCGCTCTCGGTCGGCGCGACTGCGATCCTGATGGCCGAGC GCCCCACCGCCGACGCGATTTTCGCGCGCCTCGTCGAACATCGGCCCACTGTGTTCTACGGCGTGCCCACG CTCTACGCGAACATGCTCGTGTCGCCCAACCTGCCCGCGCGCGCCGATGTCGCGATACGCATCTGCACGTC GGCGGGAGAGGCGTTGCCGCGTGAAATCGGCGAGCGCTTCACCGCGCACTTCGGCTGCGAGATTCTCGAC GGCATCGGCTCGACGGAAATGCTGCATATCTTCCTGTCGAATCGCGCGGGCGCGGTCGAATACGGCACCA CCGGCCGACCGGTACCCGGCTACGAAATCGAATTGCGCGACGAAGCCGGCCATGCGGTGCCCGACGGCGA AGTCGGCGACCTGTATATCAAGGGACCCAGCGCCGCCGTGATGTACTGGAATAACCGTGAGAAGTCGCGC GCCACCTTTCTCGGCGAATGGATCCGCAGCGGCGACAAGTACTGCCGGCTGCCCAACGGCTGCTATGTCTA TGCGGGCCGCAGCGACGACATGCTGAAAGTCAGCGGCCAGTATGTCTCGCCTGTCGAAGTGGAAATGGTG CTGGTGCAGCACGACGCGGTGCTCGAAGCGGCAGTGGTCGGCGTCGATCATGGCGGCCTCGTCAAGACGC GCGCGTTCGTGGTTTTGAAGCGTGAATTCGCGCCGTCTGAGATACTCGCGGAGGAGTTGAAGGCATTCGT GAAAGACCGCCTCGCGCCGCATAAATATCCGCGCGATATCGTATTCGTCGACGATCTGCCGAAAACCGCCA CCGGCAAAATTCAACGCTTCAAACTGCGCGAACAGTCATAA	Benzoate-CoA ligase (UniProt Q13WK3) from *Paraburkholderia xenovorans* LB400

Ta3HBCL (VLB120 codon optimized)	gcggccgcgaaaggaggtctatATGTCGGAGCAGCTCCAGCCTCAACAGAGCATGAACGCCGCCGACGAAATTAT CGGCCGTCCATTGGCCCAGGGTCTGGGCGAACAGACCGCTATGCTGTGCGCAGAGCGCAGCATTACCTAC CGCGAGCTGGACGCAGCGACCAACCGCCACGGGAACGCGCTGCGCGCACATGGCGTAGGTAAGGGCGAC CGTGTCCTGTTCCTCATGGACGACTCGCCGGAACTGGTCGCTGCCTACCTGGGCACCTTGCGTATCGGTGCC GTGGCCGTTGCACTGAACGTCCGGCTGGCGCCGCGGGACGTCCTCTACGTGATCCAGGATAGCGCCTGCC GCCTGCTGTACATCGACGCCGAGTTCCTGCACCTGTACCAGCAAATCGCCGGTGAGCTGGAGCAACCACCG CAAGTCGTGGTACGCGGCGATGAGGCGCCAGCTCCCGCCATCATTGCGTTCAAGCACTTCCTGGACGGTCA GGCGGCGACCCTGGAATCCGTTCAGGTGGCGCCGGACGATGTTGCGTATTGGCTCTACTCGTCCGGCACCA CCGGCCGTCCTAAGGCGGTCATGCACGCCCATCGCTCGGTCCTCATCGCGGATCGCCTGGAGCGCGAGTAC TTCGGTATCAAGCCGGGTGACCGCGTATTCACCACCAGCAAGATGTTCTTCGGCTGGTCGCTGGGGCATTC GCTTATGGGTGGCCTTCAGTGCGGTGCCACCGTCATCGTCGCACCGGGTTGGCCCGATGCGGAACGCGTCA TGGCCACCGCTGCACGACATCGCCCTACCATCCTGTTCAGTACTCCAGTGATGTACCGCAACTTGCTCCGTG AAGGCGCAGGTGAGAGCGCCGCCATGCGTGATATCCGACACTTCGTGTCCGCCGGCGAGAAGCTGCCAGA GAACATCGGCCAGCAGTGGCTGGACACCTTCGGCATCCCGATCACGGAAGGCATCGGCGCCAGCGAAACC GTGTTCCTGTTCTTGTGCGCCCGGCCTGACGCCTACCGTATCGGCTCGTGTGGTAAGCGGGTGCCATGGGC AGAAGTTCGCCTGCTGGACGAACTGGGCAACGAAATCACCACCCCGGATACCCCCGGCCTGATCGCCATCC GTATGGCAAGCCAGTTTGTGGGCTACTGGAAGTTGCCCGAAACCACCGAAAAGGCGTTGCGTGATGGCTG GTACTACCCCGGCGACATGTTTAGTTTCGACGCCGACGGGTTCTGGTATCACAACGGCCGAGCCGACGACA TGCTGAAGATCTCGGGCCAGTGGGTTAGCCCAGGTGAGATCGAATCCTGCGCCTCGGCCGTGCCAGGCAT CGCAGAGGCGGTAGTGGTCGCGGTGCCGAACGATGATGGCCTCACGCGCCTCACGCTGTTCATCGTCCCTG AAGATCCAAGCGCCAGCCAACAGAAGCTGTCGGAGGCCTGGATGACTACCTTGCGTGGCACCCTGAGTATT TACAAGTGCCCGCGAACCATCCAATTCCTCGAAGAGTTGCCGCGCACCGCCACGGGCAAGGTGCAGAAGT ATCGCCTGCGTGATATGCTTCAGGCAACCCTCTGAattcctcgagtctagaggagcat	codon-optimized 4-hydroxy/ 3-hydroxy benzoate CoA ligase (UniProt Q9AIS8) from *Thaurea aromatica* K172
sdgA (VLB120 codon optimized)	ggccgcgaaaggaggtctatATGACGCGTGAAGGTTTCGTCCCATGGCCCAAGGAGGCGGCCGACCGTTACCGC GAAGCCGGCTACTGGCGTGGGCGTCCTCTGGGCTCCTACCTGCATGAGTGGGCCGAGACCTACGGCGACA CTGTGGCCGTCGTGGACGGCGACACTCGCTTGACCTATCGCCAGCTGGTAGACCGGGCAGATGGGCTGGC ATGTCGTTTGCTGGACAGTGGCCTGAACCCAGGCGATGCCATGCTGGTCCAACTGCCGAACGGTTGGGAG TTCGTGACCCTGACGCTGGCCTGCCTGCGTGCGGGCATCGCACCAGTCATGGCCATGCCGGCGCACCGCGG CCACGAATTGCGTTACCTCGCGGCCCATGCAGAGGTGACCAGCATCGCAGTGCCAGACCGCCTGGGCGAC TTCGACCACCAGGCGTTGGGTCGTGAGGTCGCCGAAGACACCCCGAGCGTCGGTCTGCTGCTGGTCGCAG GTGGCACCGTAGGCACTGACGCAACCGACCTGCGTGCACTGGCCGAGCCGGCTGACGATCCGGTGACCGC ACGTGCTCGTCTGGACCGCATCGCGCCAGACTCGGGCGACATTGCAGTCTTCTTGCTGTCGGGTGGCACCA CCGGCCTCCCGAAGCTCATCACCCGCACCCACGATGATTACGAGTATAACGCGCGCCGCAGCGCCGAAGTT TGCGGCTTGGACTCGGACTCCGTATACCTGGTCGCACTGCCGGCCGGTCATAACTTTCCCCTGGCGTGCCCA GGCATCCTCGGCACCCTGATGAACGGTGGCCGTGTGGTGCTCGCTCGCACCCCCGAGCCTGGTAAGGTCTT GCCCCTCATGGCAGCCGAGGGCGTGACGGCAACTGCTGCCGTGCCGGCAGTTGTTCAACGTTGGATTGAC GCGGTAGCCAGCGGTCGTCACCCGGCACCACCTGCGCTCCGTCTGTTGCAGGTTGGTGGCGCACGTCTCGC ACCGGAAGTGGCACGCCGGGCCGAACCAGTGCTCGGTGGGACCCTGCAACAGGTGTTCGGCATGGCAGA GGGCCTGCTGAACTACACCCGTCCGGATGACCCCGACGACATCAAGATCGAGACCCAAGGCCGCCCAATGT GCCCGGACGACGAAATCCTGGTTGTGGATGCGAGCGATAATCCGGTGCCACCGGGTGAAATGGGTGCCCT GCTGACCCGTGGCCCTTACACCCCGCGCGGTTACTATCGCGCTGCCGAACATAACGCCCGTGCGTTTACGCC AGATGGCTGGTATCGGACCGGCGACGTGGTTCGTCTGCACCCAAGCGGCAACTTGGTGGTGGAAGGGCGC GATAAGGACCTGATCAACCGCGGCGGCGAAAAGATCAGCGCTGAAGAGGTGGAAAACCTGATTTATCGCC TGCCAGGCGTAGCCCGTGTCGCCGCAGTCGCGAAAGCTGACCCGGACCTGGGTGAACGCGTGTGCGCCGT CGTAGTGGTCGAACCAGGCACCCAGTTGTCCTTGGAGAGTGTCCGTGCAGCCCTGACCGCCATGCAGGTG GCCCGCTACAAGCTCCCGGAAGACCTCCTGGTGGTGGACGAACTCCCTCTCACCAAAGTGGGCAAGATCGA CAAGAAGCGCCTGCGGGACGTAGTTCGGGGCAAGGCCGACAGCGTGGAGGCCGTATGAattcctcgagtctag aggag	Codon optimized 2-hydroxybenzoate-CoA ligase (UniProt Q7X279) from *Streptomyces* sp. WA46

HaBPS	ATGGCCCCGGCGATGGAGTACTCAACCCAGAACGGCCAGGGGGAGGGAAAGAAGAGAGCTAGTGTCCTC GCTATTGGAACAACCAACCCGGAACATTTCATCTTGCAGGAGGACTACCCCGACTTCTACTTCAGGAACACC AACAGCGAGCACATGACCGAGCTCAAGGAGAAATTTAAACGTATCTGTGTTAAGTCTCATATTAGGAAGAG GCACTTCTACCTAACCGAGGAGATTCTCAAGGAGAACCAGGGGATCGCCACCTATGGCGCGGGCTCCCTTG ACGCCCGCCAGAGGATCCTCGAGACCGAGGTCCCGAAGCTGGGTCAGGAGGCGGCCCTCAAAGCCATCGC GGAGTGGGGCCAGCCCATCTCCAAGATAACACACGTGGTGTTCGCGACGACCTCCGGGTTCATGATGCCC GGGGCAGACTACGTCATCACCCGCCTCCTCGGCCTCAACCGCACCGTCAGGCGCGTCATGCTCTACAACCA GGGCTGCTTCGCTGGGGGCACGGCCCTCCGTGTCGCCAAGGACCTCGCGGAGAACAACGAGGGCGCGCG CGTGCTCGTCGTGTGCGCGGAGAACACCGCCATGACTTTCCACGCCCCCAACGAGTCCCACCTAGACGTGA TCGTGGGGCAAGCCATGTTCTCAGATGGCGCGGCTGCTCTGATCATCGGGGCATGCCCTGACGTTGCTTCT GGGGAGCGCGCAGTGTTCAATATCCTGTCGGCGAGCCAGACGATCGTGCCGGGCTCCGACGGGGCGATA ACGGCGCACTTCTACGAGATGGGGATGAGCTACTTCCTTAAGGAGGACGTCATCCCTCTCTTCCGTGATAA CATCGCCGCCGTCATGGAGGAGGCCTTCTCTCCGCTTGGGGTCTCCGACTGGAACTCCCTCTTCTACTCCAT CCACCCCGGTGGCCGAGGGATCATCGACGGCGTCGCCGGGAACCTTGGGATCAAGGACGAGAACCTTGTG GCGACCAGGCACGTCCTCGGCGAGTACGGGAACATGGGGTCAGCCTGCGTGATGTTCATCCTTGACGAGC TTAGGAAGAGCTCCAAGGTCAACGGGAAGCCCACCACCGGCGACGGCAAGGAGTTCGGCTGCCTCATCGG CCTCGGCCCTGGCCTCACCGTGGAAGCCGTCGTCCTCCAGAGTGTCCCAATTCTCCAGTGA	2,4,6-Trihydroxybenzophenone synthase (UniProt Q8SAS8) from *Hypericum androsaemum*
HsBPS	ATGGCCCCTGCAATGGAGTACTCAACCCAGAACGGCCAGGGGGAGGGAAAGAAGAGGGCCAGTGTCCTC GCCATTGGAACGACCAACCCGGAGCACTTCATCTTGCAGGAGGACTACCCGGACTTCTACTTCAGGAACAC CAACAGCGAGCACATGACCGATCTCAAGGAGAAATTCAAGCGCATCTGTGTAAAGTCTCATATTAGGAAGA GGCACTTCTACCTGACCGAGGAGATCCTCAAGGAGAACCAGGGCATCGCCACCTACGGCGCGGGCTCCCT GGACGCCCGCCAGAGGATCCTTGAGACTGAGGTCCCCAAGCTAGGCCAAGAGGCGGCCCTCAAGGCCATC GCGGAGTGGGGCCAGCCCATCTCCAAGATCACCCACGTGGTGTTTGCGACCACCTCCGGGTTCATGATGCC CGGCGCAGACTACGCCATCACCCGCCTCCTCGGCCTCAACCGCACTGTTAGGCGCGTGATGCTCTACAACCA GGGCTGCTTTGCCGGGGGCACGGCCCTCCGAGTCGCCAAGGACCTCGCAGAGAACAACGAAGGCGCGCG GGTCCTCGTCGTGTGCGCGGAGAACACCGCCATGACTTTCCACGCTCCCAACGAGTCCCACCTCGACGTGA TCGTGGGGCAGGCCATGTTCTCAGATGGTGCTGCCGCTCTGATCATCGGGGCAGGCCCTGACGTTGCCGCG GGGGAGCGCGCAGTGTTCAATATCCTATCGGCGAGCCAGACGATCGTGCCGGGCTCCGACGGGGCGATAA CGGCGCACTTCTACGAGATGGGGATGAGCTACTTCCTTAAGGAGGACGTCATCCCTCTCTTCAGGGACAAC ATCGCCGCCGTCATGGAGGAGGCCTTCTCCCCGCTTGGGGTCTCCGACTGGAACTCCCTCTTCTACTCCATC CACCCCGGCGGCCGCGGTATCATCGACGGAGTCGCCGGGAACCTCGGGATCAAGGACGAGAACCTCGTGG CCACCAGGCACGTCCTCGGCGAGTACGGGAACATGGGGTCAGCGTGCGTCATGTTCATCCTGGACGAGCT CAGGAAGAGCTCCAAGCTCAGCGGGAAGCCCACCACCGGCGACGGCAAAGAGTTCGGCTGCCTCATCGGC CTCGGCCCCGGCCTCACCGTGGAGGCCGTTGTCCTCCAGAGTGTCCCCATCCTCCAGTGA	2,4,6-Trihydroxybenzophenone synthase (UniProt K4HQC0) from *Hypericum sampsonii*
GmBPS (VLB120 codon optimized)	acaggaaacaggaggtaccgaatATGGCCCCGGCGATGGACAGCGCGCAGAATGGCCACCAGTCGCGTGGCAGT GCCAACGTGCTGGCTATCGGCACCGCGAACCCGCCGAATGTCATCCTCCAAGAAGACTACCCCGATTTCTAC TTCAAGGTGACCAACTCGGAGCATCTGACCGACCTGAAGGAAAAGTTCAAGCGTATCTGCGTGAAGAGCA AGACCCGTAAGCGCCACTTTTATCTGACGGAACAGATCCTGAAGGAAAACCCCGGTATTGCTACCTACGGC GCAGGCTCCTTGGACAGCCGGCAAAAAATTCTGGAGACCGAGATCCCCAAGCTGGGGAAGGAAGCCGCA ATGGTGGCAATCCAGGAGTGGGGCCAGCCGGTGAGCAAAATCACCCATGTCGTGTTTGCGACCACGAGCG GCTTCATGATGCCAGGCGCCGATTACTCCATCACTCGGCTGTTGGGCCTCAACCCTAACGTGCGCCGCGTCA TGATTTACAACCAAGGTTGCTTCGCAGGCGGCACCGCACTGCGCGTAGCCAAAGACCTGGCGGAGAACAA TAAGGGGGCGCGTGTCCTGGTCGTCTGCGCTGAGAACACGGCCATGACCTTCCACGGCCCAAATGAAAAC CACTTGGACGTGCTGGTGGGCCAGGCCATGTTCAGCGATGGCGCAGCCGCCCTGATTATTGGCGCCAACCC AAACCTCCCCGAAGAACGCCCTGTGTACGAGATGGTCGCCGCCCACCAGACCATCGTGCCCGAAAGCGAC GGCGCAATCGTGGCCCACTTTTACGAGATGGGTATGAGCTACTTCCTGAAGGAAAACGTGATCCCGCTGTT CGGCAACAACATCGAGGCGTGCATGGAGGCGGCATTTAAGGAGTATGGTATCTCGGACTGGAACAGCCTG TTCTACAGCGTGCATCCCGGCGGTCGCGCCATCGTTGATGGCATCGCCGAGAAACTGGGTCTGGACGAAG AGAATCTGAAGGCCACCCGTCATGTGTTGTCGGAATACGGCAACATGGGCTCCGCCTGCGTGATCTTTATC CTGGATGAACTGCGCAAAAAATCGAAAGAGGAGAAGAAGCTGACCACCGGCGACGGCAAGGAATGGGGT TGCCTCATCGGCCTGGGCCCAGGCTTGACTGTGGAAACGGTGGTTCTCCGTAGCGTCCCGATTGCGTAAgcg gccgcgaaaggaggtctat	Codon-optimized 2,4,6-Trihydroxybenzophenone synthase (UniProt L7NCQ3) from *Garcinia mangostana*

ScCHS (old annotation ScBPS)	acaggaaacaggaggtaccgaatATGGTGGCCGTGAAGGAGTTCTCGCGTCCAGAACGTGCCGACGGCCTGGCGT CCGTTCTGGCCATCGGCACCGCCACCCCGCCGAACTGCGTGGACCAGAGCACCTACCCGGACCTGTACTTC CGCATCACCAACTCGGAACACATGGTGGCCCTGAAGGAAAAGTTCCAGCGCATCTGCGACAAGTCGTCGAT CAAGAAGCGCCACCTGTACCTGACCGAAGACATCCTGAAGCAGAACCCGTCGCTGCTGGAACCGATGGCCT CGTCGTTCGACGCCCGCCAGGAAATCCTGGTGTCGGAAGTGCCGAAGCTGGGCCAGGAAGCCTCGGAAAA CGCCATCTCGGAATGGGGCCAGCCGAAGTCGTCGATCACCCACCTGCTGTTCTGCACCTCGTCGGGCATCG AAATGCCGGGTGCCGACTACCAGGTGGCCCGTCTGCTGGGCCTGTCGCCGTCGGTGAAGCGCCTGATGTTC TACCAGCAGGGCTGCTTCGCCGGTGGCACCGTGCTGCGCGTGGCCAAGGACATCGCCGAAAACAACAAGG GCGCCCGCGTGCTGCTGGTGTGCTCGGAAATCACCGCCATCTTCTACCGCGGCCCGAACGAAGACTACCTG GACGGTCTGGTGGGCATGGCCCTGTTCGCCGATGGTGCAGCCGCTGTGATCGTGGGCTCGGACCCGATTC CCGGCGTGGAAACCCCGTCGTTCGAACTGGTGTCGGCCGCCCAGACCATCGTGCCGGACTCGCACGGCGC CATCAAGGGCCACGTGCGCGAAGCCGGCCTGGTGCTGCACCTGCACAAGGACATTCCGGGTCTGATTTCG AAGAACATCGACAAGTGCCTGGAAGACGCCTTCCGCCCGCTGGGCATCTCGGACTGGAACTCGATCTTCTG GGTGGTGCACCCTGGCGGCACCGCCATCCTGGACCAGCTGGAACAGAAGTTCTCGCTGGACCCGGAACGT CTGCGCCCGACCCGCAACGTGCTGTCGGAATACGGCAACATGTCGTCGGTCTGCGTGTTCTTCATCCTGAAC GAGATCCGCAAGTCGTCGATCAAGAACGGCAAGAGCACGACCGGTGACGGCCAGCAATGGGGTGTGCTG TTCGGCCTGGGTCCCGGCATCACCGTGGAAACCATCGTGCTGAAGTCGGTGGCCATCAACCAGAACTAAgc ggccgcgaaaggaggtctat	Codon-optimized putative chalcone synthase (UniProt A0A5J6EFZ9) from *Swertia chirayita*
SaBIS1	ATGGCGCCTTTGGTTAAGAATCATGGAGAGCCTCAACATGCCAAAATCCTAGCCATTGGCACTGCAAATCC ACCAAACGTCTACTACCAAAAAGACTATCCTGATTTCTTGTTTCGAGTCACCAAAAATGAGCACAGGACAGA TTTAAGAGAGAAGTTTGATCGCATTTGTGAGAAATCAAGAACAAGGAAGCGTTACTTGCATCTAACAGAGG AGATTCTAAAGGCTAACCCAAGCATATATACCTATGGTGCCCCATCACTCGATGTGCGCCAAGACATGTTGA ATTCTGAGGTCCCAAAGCTAGGGCAACAAGCAGCACTGAAAGCCATCAAAGAGTGGGGCCAACCCATCTC AAAGATCACCCACCTCATCTTTTGCACAGCTTCATGTGTTGACATGCCAGGTGCCGACTTCCAATTGGTCAA GCTCCTCGGCCTTAACCCATCTGTCACTAGAACCATGATCTACGAAGCTGGTTGCTATGCTGGTGCAACTGT CCTCCGCCTAGCCAAGGACTTCGCAGAGAACAACGAGGGTGCACGCGTCCTTGTGGTGTGCGCTGAGATC ACGACCGTGTTCTTCCACGGACTCACTGACACCCACTTGGACATACTGGTGGGCCAGGCTCTTTTTGCTGAC GGAGCATCTGCTGTGATAGTTGGGGCCAATCCAGAGCCTAAAATTGAGAGGCCACTATTTGAAATCGTGGC ATGCAGGCAGACAATCATACCGAACTCAGAGCATGGTGTGGTGGCCAACATTCGTGAAATGGGGTTTACTT ATTATTTATCAGGAGAAGTCCCCAAATTTGTTGGTGGAAATGTTGTGGATTTTCTGACTAAAACTTTTGAAA AAGTTGACGGAAAGAATAAGGACTGGAACTCCTTGTTTTTCAGTGTGCACCCTGGTGGACCCGCCATTGTA GACCAGGTGGAGGAGCAACTGGGTTTGAAGGAAGGGAAGCTTAGGGCAACAAGGCATGTGTTGAGTGAG TATGGCAACATGGGAGCTCCATCTGTGCACTTTATTTTGGATGATATGAGAAAGAAGTCGATTGAGGAAGG CAAATCCACAACTGGCGAAGGTTTGGAATGGGGTGTCGTGATTGGAATCGGACCAGGACTCACTGTTGAG ACAGCCGTACTGCGTAGTGAATCTATTCCATGCTAA	3,5-dihydroxybiphenyl synthase (UniProt Q27Z07) from *Sorbus aucuparia*
MdBIS1 (*SaBIS1*$^{P11H S97P P389T}$)	ATGGCGCCTTTGGTTAAGAATCATGGAGAGCACCAACATGCCAAAATCCTAGCCATTGGCACTGCAAATCC ACCAAACGTCTACTACCAAAAAGACTATCCTGATTTCTTGTTTCGAGTCACCAAAAATGAGCACAGGACAGA TTTAAGAGAGAAGTTTGATCGCATTTGTGAGAAATCAAGAACAAGGAAGCGTTACTTGCATCTAACAGAGG AGATTCTAAAGGCTAACCCAAGCATATATACCTATGGTGCCCCATCACTCGATGTGCGCCAAGACATGTTGA ATCCGGAGGTCCCAAAGCTAGGGCAACAAGCAGCACTGAAAGCCATCAAAGAGTGGGGCCAACCCATCTC AAAGATCACCCACCTCATCTTTTGCACAGCTTCATGTGTTGACATGCCAGGTGCCGACTTCCAATTGGTCAA GCTCCTCGGCCTTAACCCATCTGTCACTAGAACCATGATCTACGAAGCTGGTTGCTATGCTGGTGCAACTGT CCTCCGCCTAGCCAAGGACTTCGCAGAGAACAACGAGGGTGCACGCGTCCTTGTGGTGTGCGCTGAGATC ACGACCGTGTTCTTCCACGGACTCACTGACACCCACTTGGACATACTGGTGGGCCAGGCTCTTTTTGCTGAC GGAGCATCTGCTGTGATAGTTGGGGCCAATCCAGAGCCTAAAATTGAGAGGCCACTATTTGAAATCGTGGC ATGCAGGCAGACAATCATACCGAACTCAGAGCATGGTGTGGTGGCCAACATTCGTGAAATGGGGTTTACTT ATTATTTATCAGGAGAAGTCCCCAAATTTGTTGGTGGAAATGTTGTGGATTTTCTGACTAAAACTTTTGAAA AAGTTGACGGAAAGAATAAGGACTGGAACTCCTTGTTTTTCAGTGTGCACCCTGGTGGACCCGCCATTGTA GACCAGGTGGAGGAGCAACTGGGTTTGAAGGAAGGGAAGCTTAGGGCAACAAGGCATGTGTTGAGTGAG TATGGCAACATGGGAGCTCCATCTGTGCACTTTATTTTGGATGATATGAGAAAGAAGTCGATTGAGGAAGG CAAATCCACAACTGGCGAAGGTTTGGAATGGGGTGTCGTGATTGGAATCGGACCAGGACTCACTGTTGAG ACAGCCGTACTGCGTAGTGAATCTATTACCTGCTAA	3,5-dihydroxybiphenyl synthase (AFX71921) from *Malus domestica*

PcBIS1 (VLB120 codon optimized)	aacaggaggtaccgaatATGGCGCCGCTGGTCAAAAACCATGTGGAGCCACCGCACGCGAAGATCCTGGCGATC GGCACGGCCAATCCACCGAACGTCTACTACCAGAAGGACTACCCGGACTTCCTGTTCCGCGTCACCAAGAA TGAGCACCGCACCGATCTGCGCGAAAAGTTTGACCGCATCTGCGAAAAGAGCCGCACGCGCAAGCGCTAT CTGTATCTGACTGAAGAGATCCTGAACGCCAATCCGTCGATCTACACCTACGGCGCTCCAAGCCTGGACGT GCGCCAAGACATGCTGAATCCGGAGGTCCCGAAGCTGGGCCAGCAAGCGGCATTGAAGGCTATCAAGGA GTGGGGTCAGCCGATCAGTAAAATCACGCATCTCATCTTTTGCACCGCCAGCTGCGTCGATATGCCAGGTG CGGATTTCCAGCTCGTGAAACTGCTGGGCCTGAACCCGTCCGTGACCCGGACTATGATCTATGAGGCCGGC TGCTATGCGGGCGCTACCGTGCTGCGCCTGGCAAAGGACTTCGCCGAGAACAACGAAGACGCGCGTGTCC TGGTTGTGTGCGCCGAGATCACGACCGTCTTCTTCCACGGGCTGACCGACACCCATCTGGACATCCTGGTG GGCCAAGCGCTGTTCGCGGACGGTGCGAGCGCGGTCATCGTCGGTGCCAACCCGGAACCGGAGATCGAA CGTCCGCTCTTTGAGATTGTCGCCTGCCGCCAAACCATCATCCCAAACAGCGAACACGGTGTGGTGGCTAA TATCCGCGAAATGGGCTTCAACTACTACCTGAGCGGCGACGTCCCGAAGTTCGTTGGCGGCTCCGTGGTGG ACTTTCTGACGAAGACCTTCGAGAAGGTGGACGGCAAGAACAAGGATTGGAACAGCCTCTTCCTGTCCGTG CACCCTGGGGGCCCCGCGATTGTTGACCAGGTGGAGGAGCAGCTCGGCCTGAAAGAAGGTAAGCTGCGT GCCACCCGGCACGTCCTGAGCGAGTACGGGAACATGGGTGCACCCTCCGTGCACTTTATTCTGGACGAAAT GCGCAACAAAAGCATCGGCGAGGGGAAGGCAACCACCGGCGAAGGCCTCGAATGGGGCGTCGTCATCGG CATCGGCCCAGGGCTGACCGTCGAGACGGCCGTTCTGCGGAGCGAAAGCATCCCTTGCTGAgcggccgcgaaa ggaggtct	Codon-optimized 3,5-dihydroxybiphenyl synthase (ANT48448) from *Pyrus communis*
PqsD (VLB120 codon optimized)	gaaacaggaggtaccgaatATGGGTAATCCGATCCTGGCAGGGCTGGGCTTCAGCCTGCCGAAGCGCCAGGTGA GTAACCACGATCTGGTGGGTCGTATCAACACCTCGGACGAGTTCATCGTGGAACGCACCGGCGTCCGCACC CGGTATCATGTGGAGCCAGAACAGGCAGTGAGTGCACTGATGGTGCCGGCTGCACGTCAGGCCATCGAAG CTGCCGGCCTGCTCCCTGAGGACATTGATCTGTTGCTGGTGAACACCCTGTCGCCGGATCATCATGACCCGA GCCAGGCCTGTCTGATCCAACCGCTCCTGGGCCTGCGGCACATCCCTGTGCTGGACATCCGTGCACAGTGC AGTGGCCTGCTGTACGGCCTGCAAATGGCCCGTGGTCAGATTCTGGCAGGTCTCGCCCGTCACGTGCTGGT CGTATGTGGCGAGGTGCTCTCGAAACGCATGGACTGTAGCGACCGCGGCCGGAATCTGTCGATCCTGTTG GGTGATGGTGCAGGTGCTGTGGTGGTCAGCGCAGGTGAGAGCCTGGAGGATGGTCTGCTGGATTTGCGG TTGGGGGCGGACGGCAACTACTTCGATCTGCTGATGACTGCTGCACCAGGCAGCGCAAGCCCAACCTTCCT CGACGAAAACGTTCTGCGGGAGGGCGGTGGTGAGTTCCTGATGCGTGGCCGTCCCATGTTCGAGCATGCC TCGCAAACTCTGGTCCGTATCGCAGGCGAGATGCTGGCCGCCCATGAGTTGACCCTCGACGACATCGACCA CGTCATTTGTCACCAGCCAAATCTGCGCATCCTGGACGCGGTGCAGGAACAGCTGGGCATCCCGCAGCATA AATTTGCCGTAACCGTGGACCGTCTGGGCAATATGGCAAGCGCGAGCACGCCCGTGACCTTGGCGATGTTC TGGCCGGACATCCAGCCGGGTCAGCGTGTGTTGGTGCTCACCTACGGTAGCGGTGCAACTTGGGGTGCAG CCCTGTACCGCAAGCCCGAAGAAGTTAATCGTCCGTGCTGAgcggccgcgaaaggaggtct	Codon-optimized 4-hydroxycoumarin synthase / Anthraniloyl-CoA anthraniloyltransferase (UniProt P20582) from *Pseudomonas aeruginosa*
LaCH-II (VLB120 codon optimized)	atgctaaggaggtttttctaATGACCCAGGCCCAGCAGACCGTCAACCTGCCCAGCTCGGTGTTCACCGGCCTCACG GAAGTGTCCGACGTCGCTGCCACCGGCAACGTCCTCGGTGTGATCAATTACACCACCGAGTGCACCGGTCC CCGCGTGGAAAACGGCCTGCTGACCCTGGACCTGCATATGGCCTCGGACCTGGGCGAGGCGTTCGCCGAA GTGTGGACCACCAGCCGTCCAGCGGAGACCGGTGAACATCACGGCGTGGTGTACGCCCACGATGGCGAAT ACCTGCTGGTCGCCGGTCGCATCGCGCCGACCGGCCGCTATACTGAAGACACCCGCGCGGCTTATGTGGCG GCACTGGACCTGATGGATACCCTGGGCTACAAGAACTGCTTTCGCATGTGGAACTTCATCAACGACATCAA TGCCGATAACACCGAAGGCTTAGAAATCTACCGCGATTTCTGCAAGGGCCGCGCCGAGGCGTTCGAACTCT TCCACTTCGGGGACAAGGAGGTGCCGAGCGCGACCGGGATCGGCAGCCAGGGCGGTGGCATTGCGTTCT ACTTCCTGGCCTCGCGCTCCGCCGCGCTGACCAGCGTGGAAAACTCGAAGCAGATGGCCGCGTACCACTAC CCGCGTCAGTACGGTCCGCGTCCACCGAAGTTCGCCCGTGCCACGTACCTGGCCAGCACCCACACGGACCG TCGCAGCGGCCAAGTCTACGTCGCCGGTACGGCAAGTATCCGCGGCCACGAAACGCTGCACGACGGCGAC ATCGTGGCCCAGGTCAAACTGAGCCTGGACAACATCGAGCACCTGATTAGCGACGAGAACCTCGCCGACTA CGAGATCACCCAGGGCAACAGCCTGCTGAACCTGGATAACATCAAGGTGTACGTTCGCCACCGTAGTGACA TCCCCGTGGTCCGCCGTATGTGCGAGGAACGCTTTAGTCCGAACGCCCGCGTGCAATACCTGAACGTGGAC GTGTGCCGTGCCGACCTGCTGGTAGAGATTGAGGGCATTGTGGCATGAtaaagaattcgagctcggta	Codon-optimized chorismate lyase (WP_052685672.1) for 3-Hydroxybenzoate synthesis from *Lentzea aerocolonigenes* Supplementary of Grüninger et al. (2019)

menF	ATGCAATCACTTACTACGGCGCTGGAAAATCTACTGCGCCATTTGTCGCAAGAGATTCCGGCGACACCCGG CATTCGGGTTATCGATATTCCTTTCCCTCTCAAAGACGCTTTTGATGCCTTGAGCTGGCTGGCCAGTCAGCA AACATACCCGCAATTCTACTGGCAACAACGTAATGGTGATGAAGAAGCTGTCGTCCTGGGCGCGATTACCC GTTTTACGTCGTTGGACCAGGCACAACGTTTTCTTCGCCAGCACCCGGAACACGCCGACTTACGCATTTGGG GGCTGAATGCTTTTGACCCGTCGCAGGGCAATTTACTTTTACCCCGCCTGGAATGGCGACGCTGTGGCGGT AAAGCCACGCTGCGGCTGACGCTATTCAGCGAAAGCTCCCTTCAGCACGATGCGATTCAGGCAAAAGAATT TATCGCCACACTGGTGAGTATCAAGCCCTTGCCTGGGTTACATTTAACCACCACGCGAGAACAACACTGGCC GGACAAAACGGGCTGGACGCAATTAATCGAACTGGCAACGAAAACCATCGCCGAAGGTGAGCTCGACAAA GTGGTGCTCGCTCGGGCAACTGACCTGCATTTCGCAAGTCCGGTCAACGCGGCGGCGATGATGGCTGCCA GTCGTCGACTGAATCTGAATTGCTACCATTTTTACATGGCCTTTGATGGCGAAAATGCTTTTCTTGGCTCTTC ACCGGAACGGTTATGGCGGCGGCGTGACAAAGCGCTGCGTACTGAAGCGCTGGCGGGAACAGTAGCAAA TAATCCTGATGATAAGCAGGCGCAGCAGTTAGGAGAGTGGCTGATGGCGGATGATAAAAACCAGCGCGA GAACATGCTGGTGGTGGAAGATATCTGTCAACGATTACAGGCCGATACCCAGACGCTGGATGTTTTACCGC CGCAGGTACTGCGTCTGCGTAAAGTGCAGCATCTTCGCCGCTGTATCTGGACTTCACTCAACAAAGCGGAT GATGTGATCTGTTTACATCAGTTGCAGCCAACGGCAGCAGTTGCTGGCTTACCGCGCGATCTGGCGCGACA GTTTATCGCCCGTCACGAACCGTTCACCCGAGAATGGTACGCCGGTTCTGCGGGCTATCTCTCATTACAACA AAGCGAATTCTGCGTTTCCCTGCGCTCAGCAAAAATTAGCGGCAATGTCGTGCGATTATATGCTGGCGCGG GCATTGTCCGTGGTTCCGACCCCGAGCAAGAGTGGCAGGAAATCGACAACAAAGCGGCAGGGCTGCGTAC TTTATTACAAATGGAATAG	Isochorismate synthase (UniProt: P38051) from *Escherichia coli* K-12
pchB	ATGAAAACTCCCGAAGACTGCACCGGCCTGGCGGACATCCGCGAGGCCATCGACCGGATCGACCTGGATA TCGTCCAGGCCCTCGGCCGCCGCATGGACTACGTCAAGGCGGCGTCGCGCTTCAAGGCCAGCGAGGCGGC GATTCCGGCGCCCGAGCGGGTCGCCGCGATGCTCCCCGAGCGCGCCCGCTGGGCCGAGGAAAACGGACTC GACGCGCCCTTCGTCGAGGGACTGTTCGCGCAGATCATCCACTGGTACATCGCCGAGCAGATCAAGTACTG GCGCCAGACACGGGGTGCCGCATGA	isochorismate pyruvate lyase (UniProt: Q51507) from *Pseudomonas aeruginosa*

Supplement S5: 2,4,6-TriHBP stability, toxicity and pH dependent partitioning

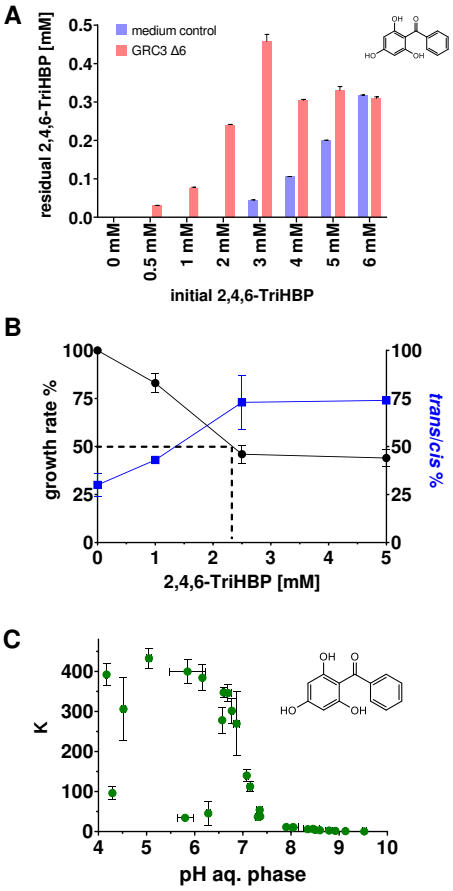

Figure S5 A) Remaining 2,4,6-TriHBP concentration after 66.5 h from medium control and grown cultures of *P. taiwanensis* VLB120 GRC3Δ6 in MSM with 20 mM glucose with 0-6 mM supplemented 2,4,6-TriHBP in 96-square-well plate Growth Profiler cultivation with initial OD_{600} 0.2. **B:** Relative growth rate from OD_{560} and *trans/cis* ratio of membrane phospholipids of *P. taiwanensis* VLB120 wildtype grown in MSM with 10 mM succinate in dependence to added 2,4,6-TriHBP. Error bars representing the standard deviation of the mean (n_{bio}=2, n_{tech}=3). Dashed line represents the concentration of IC_{50}. **C:** Plot of the partitioning coefficient of a 2,4,6-TriHBP aquatic solution (170 mg L^{-1}) containing 36 mM phosphate buffer with 1-octanol in 1:1 mixtures in dependence of the pH in equilibrium (pH 4.17 to 9.52). The pH was adjusted with 0.1 M HCl_{aq} and $NaOH_{aq}$ at 25°C. Error bars represent the standard deviations of the pH and logK (n=3, if not indicated differently).

Supplement S6: GC-ToF MS identification of polyketides

See file „Supplementary GC-ToF MS Results.xlsx" for detailed GC-ToF MS results for compounds identification from gene combination experiment with supplemented cerulenin. Identified compounds include polyketide 2,4,6-trihydroxybenzophenone, 3,5-dihydroxybiphenyl, 2,3',4,6-Tetrahydroxybenzophenone, supplemented precursors and by-products (including phenylpropanoids).

Table S6

Summary of GC-ToF MS results to verify benzoate-derived polyketide formation from biotransformation experiment with cerulenin (see Figure 2-14A, B, C; see file „Supplementary GC-ToF MS Results.xlsx").

Sample name	Strain	PKS III	Ligase	Precursor	Aim of detection	Results / detected compounds
1D_B_TS_Pool_1_s10/100	solution of precursors + some reference compounds				2,4,6-TriHBP, 3,5-dihydroxybiphenyl, phenylpropanoids, precursors	all compounds identified
1D_B_TS_3HBCer_397x4_s10/100	MiKat#397	HsBPS	RpBZL	3HB	2,3',4,6-TetraHBP, precursor, byproduct	3 different derivates (MeOX & TMS groups) of TetraHBP were found; cerulenin, 3-hydroxybenzoate, 3-hydroxycinnamate
1D_B_TS_3HBCer_406x4_s10/100	MiKat#406	SaBIS1	RpBZL	3HB	2,3',5-trihydroxybiphenyl, precursor, byproduct	no biphenyl with an extra OH-group, cerulenin, 3-hydroxybenzoate
1D_B_TS_BenzCer_394x1_s10/100	MiKat#394	HaBPS	RpBZL	Benzoate	2,4,6-TriHBP, precursor, byproduct	3 TMS derivate of TriHBP was found; cerulenin, benzoate, cinnamate
1D_B_TS_BenzCer_406iix4_s10/100	MiKat#406	SaBIS1	RpBZL	Benzoate	2,5-dihydroxybiphenyl, precursor, byproduct	cerulenin, 3,5-dihydroxybiphenyl
1D_B_TS_TriHBP_Pi_0.25x_s10/100	2,4,6-TriHBP solution in 0.25-fold buffer				2,4,6-TriHBP, degradation compounds	no small size degradation products detected
1D_B_TS_TriHBP_Pi_3x_s10/100	2,4,6-TriHBP solution in 3-fold buffer				2,4,6-TriHBP, degradation compounds	no small size degradation products detected; large phosphate signal
1D_B_Alkane_s10_02	control for Retention Index					
1D_B_QC CS-Mix_02	control for GC split					

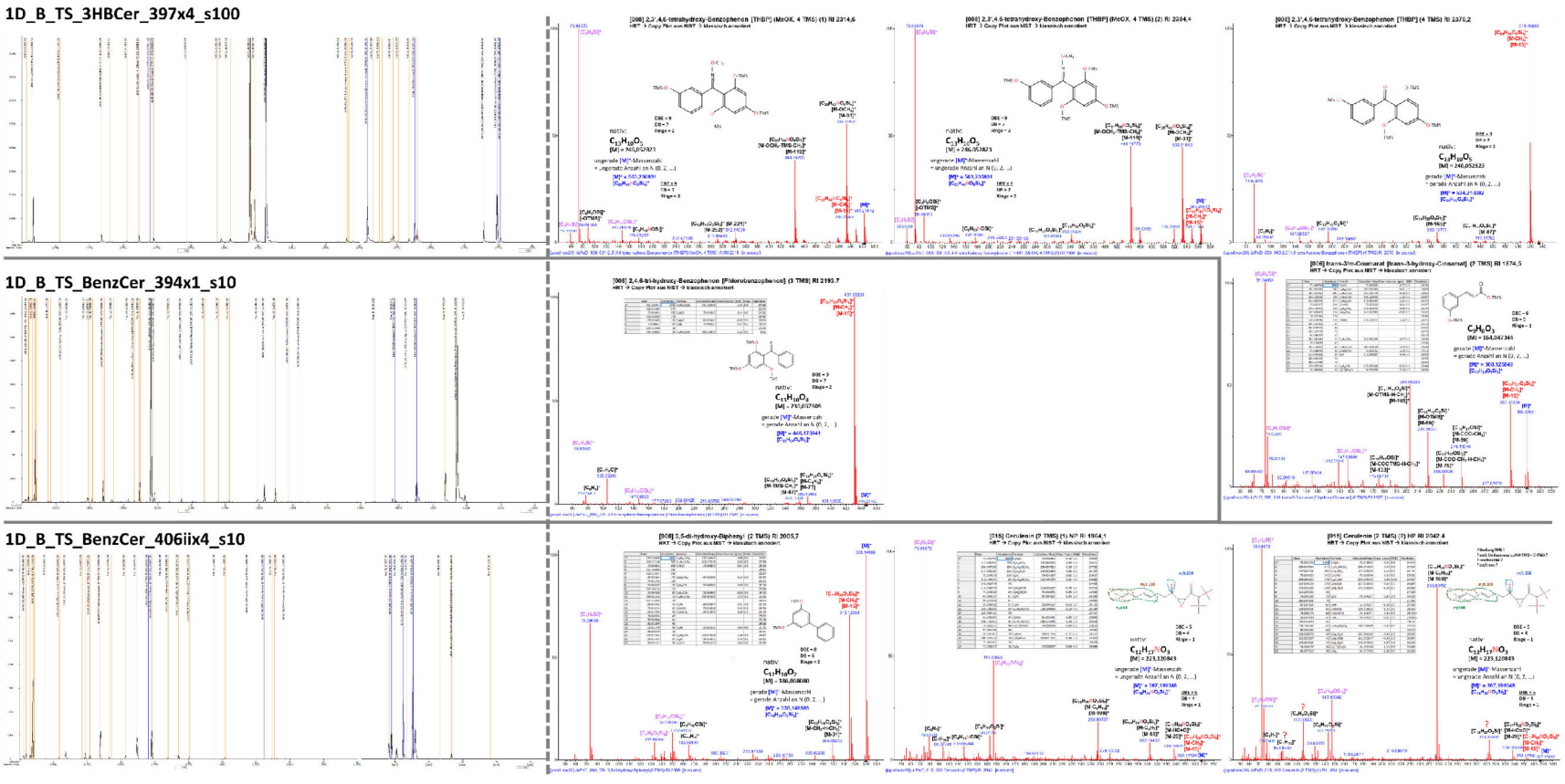

Figure S6: Sample composition analysis by GC-ToF MS. Chromatogram with given retention index and annotation if possible (left) and selected fragmentation patterns of MeOX and TMS derivatized compounds from selected samples for 2,3',4,6-TetraHBP synthesis (1D_B_TS_3HBCer_397x4_s100), for 2,4,6-TriHBP synthesis (1D_B_TS_BenzCer_394x1_s10) and for 3,5-dihydroxybiphenyl synthesis (1D_B_TS_BenzCer_406iix4_s10) are shown (right).

Supplement S7: LC-MS/MS identification of fluorine-products

See file "Supplementary mutasynthesis MS-Results.xlsx" for detailed data of all samples and replicates.

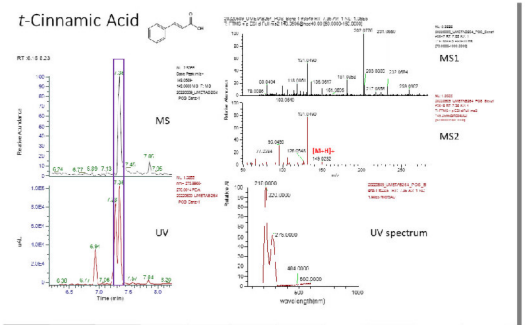

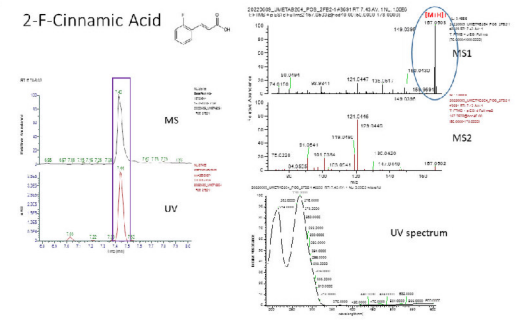

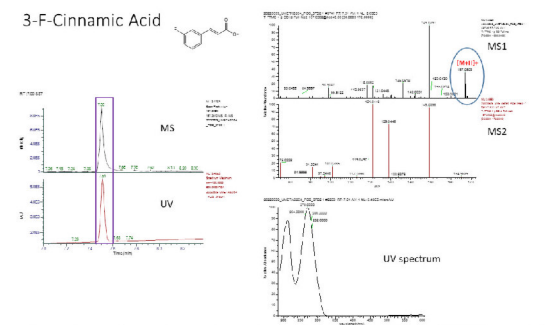

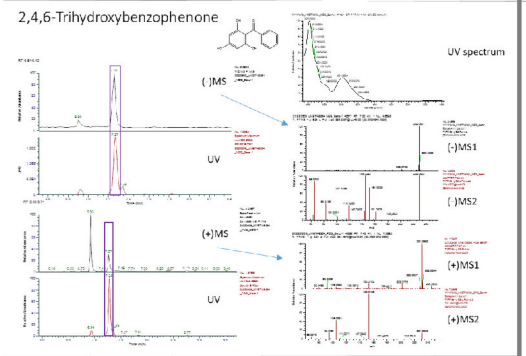

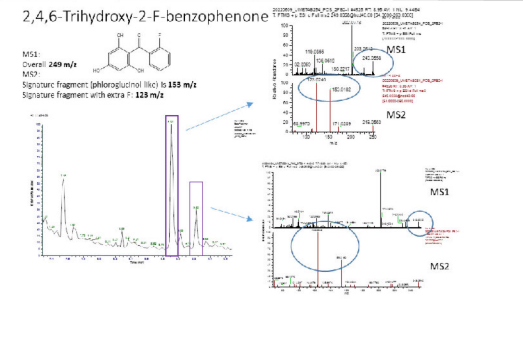

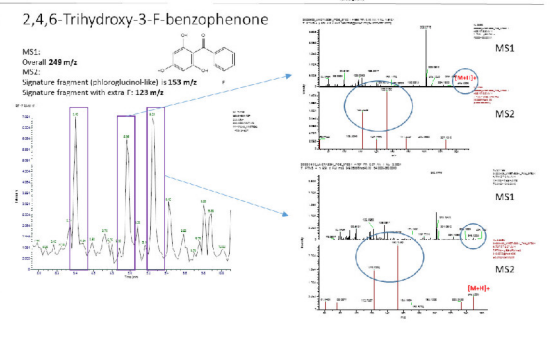

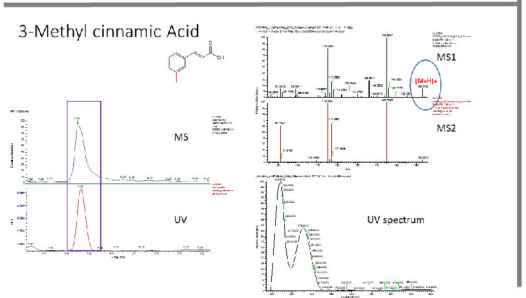

[redacted]

Supplement S8: 2,4,6-TriHBP radical polymerization hypothesis

2,4,6-TriHBP was not stable under cultivation conditions in mineral salt medium and was converted to a red colored conversion product. With GC-ToF MS no major degradation product or modified 2,4,6-TriHBP could be detected. Nevertheless, GC-ToF MS is biased by volatile and derivatized molecules with limited molecular weight. Experiments showed that 2,4,6-TriHBP is stable at low pH and only converted in buffered solutions at pH 6 and higher. Beside pH the presence of trace elements in the buffered solution increased conversion and iron was identified as one promising candidate that influences the conversion. Based on these findings the formation of benzoyl-phlorotannin is proposed via oxidative phenol coupling based on radical-radical coupling (Figure S8) (Phang et al., 2023). Here, 2,4,6-TriHBP is present in its anionic form and a metal catalyst is reduced by one electron from the anion. Alternatively, the electron is transferred from H_2O, forming a reactive oxygen species and the radical behavior in transferred to the previously charged 2,4,6-TriHBP. The formed radical of 2,4,6-TriHBP are the coupled with each other to form carbon-carbon or C-O-C bonds. Thus, oligomers and subsequent a polymer is formed like in phlorotannin formation by phloroglucinol. In order to balance the equation the reduced metal has to be oxidized.

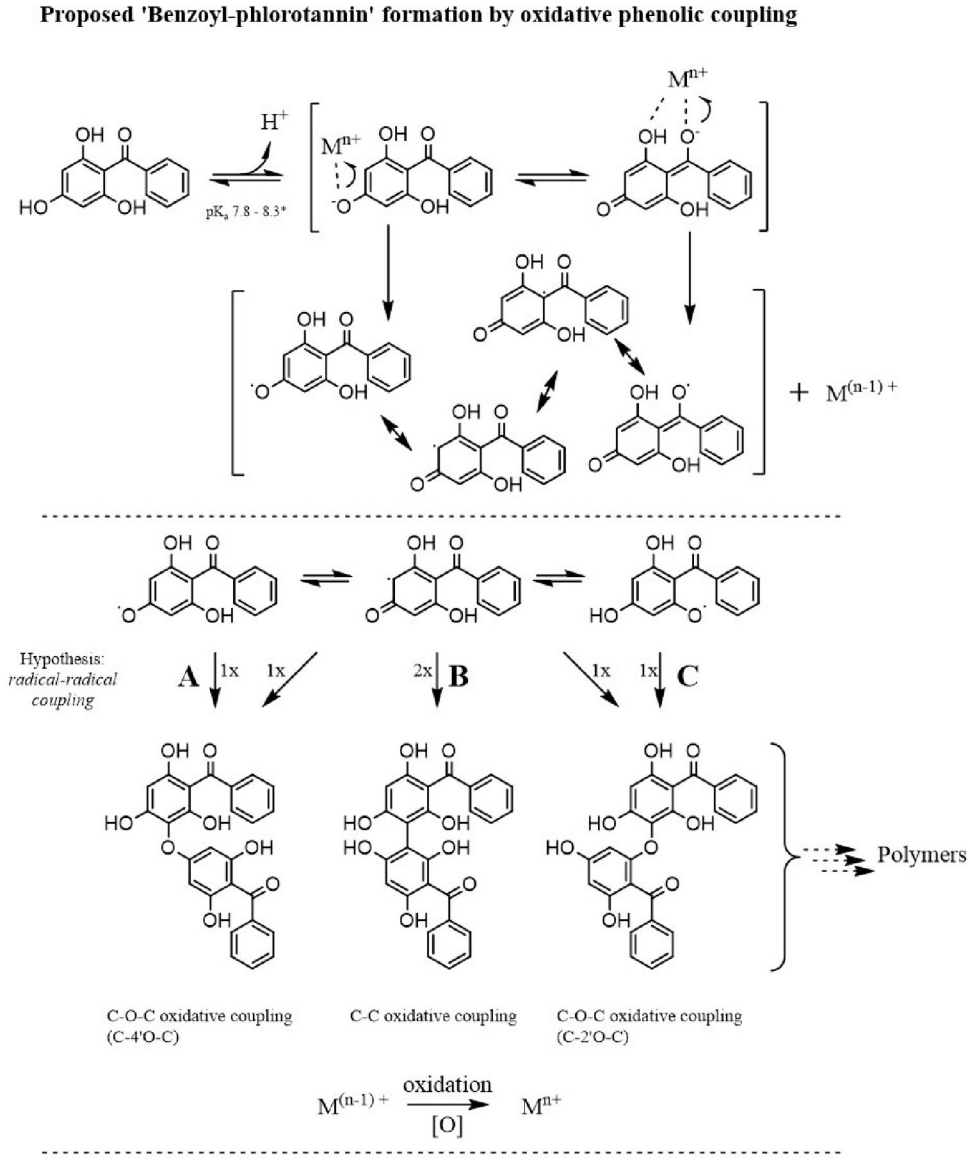

Figure S8: Scheme of proposed benzoyl-phlorotannin formation from 2,4,6-TriHBP at moderate or elevated pH with a metal ion or reactive oxygen species as catalyst.

Table S9 Solvents properties from public databases

Table S9: Solvents and their properties from public databases or suppliers. Abbreviation: n.a., not available

Solvent	CAS number	Density ($g \cdot L^{-1}$)	Solubility ($g \cdot L^{-1}$)	Boiling point (°C)	$LogP_{OW}$ value	Flashpoint (°C)	Price (€·100 mL) (July 2023)	Health Score
1-Octanol	111-87-5	826 (25°C) [a]	0.054 (25°C) [a]	195 [a]	3 [a]	81 [a]	10-20 [d]	2[c]
1-Decanol	112-30-1	840 (25°C) [a]	0.037 (25°C) [a]	230 [a]	4.6 [a]	82 [a]	5 [d]	2[c]
1-Nonanol	143-08-8	827 (20°C) [a]	0.14 (25°C) [a]	213 [a]	4.3 [a]	74 [a]	9 [d]	2[c]
2-Undecanone	112-12-9	826 (20°C) [a]	0.02 (25°C) [a]	231 [a]	4.1 [a]	89 [a]	18 [d]	2[c]
Methyl decanoate	110-42-9	873 (20°C) [a]	$4.4 \cdot 10^{-3}$ (20°C) [a]	224 [a]	4.7 [a]	110 [b]	10 [d]	1[c]
Ethyl decanoate	110-38-3	863 (20°C) [a]	$1.59 \cdot 10^{-5}$ (25°C) [a]	241 [a]	4.6 [a]	102 [b]	11[b,d]	1[c]
Butyl octanoate	589-75-3	858 [f]	$3.52 \cdot 10^{-2}$ (25°C) [a]	240 [a]	4.4 [a]	99 [e]	124 [d]	n. a.
Isobutyl octanoate	5461-06-3	860 [d]	$4.06 \cdot 10^{-3}$ (25°C) [e]	231 [a]	4.4 [a]	94 [e]	90 [d]	n. a.
Dioctyl ether	629-82-3	820 [a]	0.1 [b]	286 [e]	6.9 [a]	110 [b]	53-81 [b,d]	n. a.
2-Butyloctanoic acid	27610-92-0	887 [b]	$6.75 \cdot 10^{-3}$ (25°C) [e]	230 [b]	4.3 [a]	113 [b]	310 [b]	n. a.
2-Hexyldecanoic acid	25354-97-6	874 [b]	0.5 (20°C) [b]	268 [b]	6.4 [a]	113 [b]	120 [b]	n. a.
Hexadecane	544-76-3	770 (25°C)	$2.1 \cdot 10^{-8}$ (25°C)	287 [a]	8.3 [a]	135 [a]	11-25 [d]	n. a.
Ethyl oleate	111-62-6	870 (25°C) [b]	$5.8 \cdot 10^{-7}$ (25°C) [b]	217 [b]	8 [a]	113 [a]	11 [b]	n.a.

Sources: a: PubChem; b: Sigma Aldrich; c: European Chemicals Agency (ECHA); d: TCI; e: ChemSpider f: Springer Materials

Supplement S10 Solvent screening: partitioning in solvents

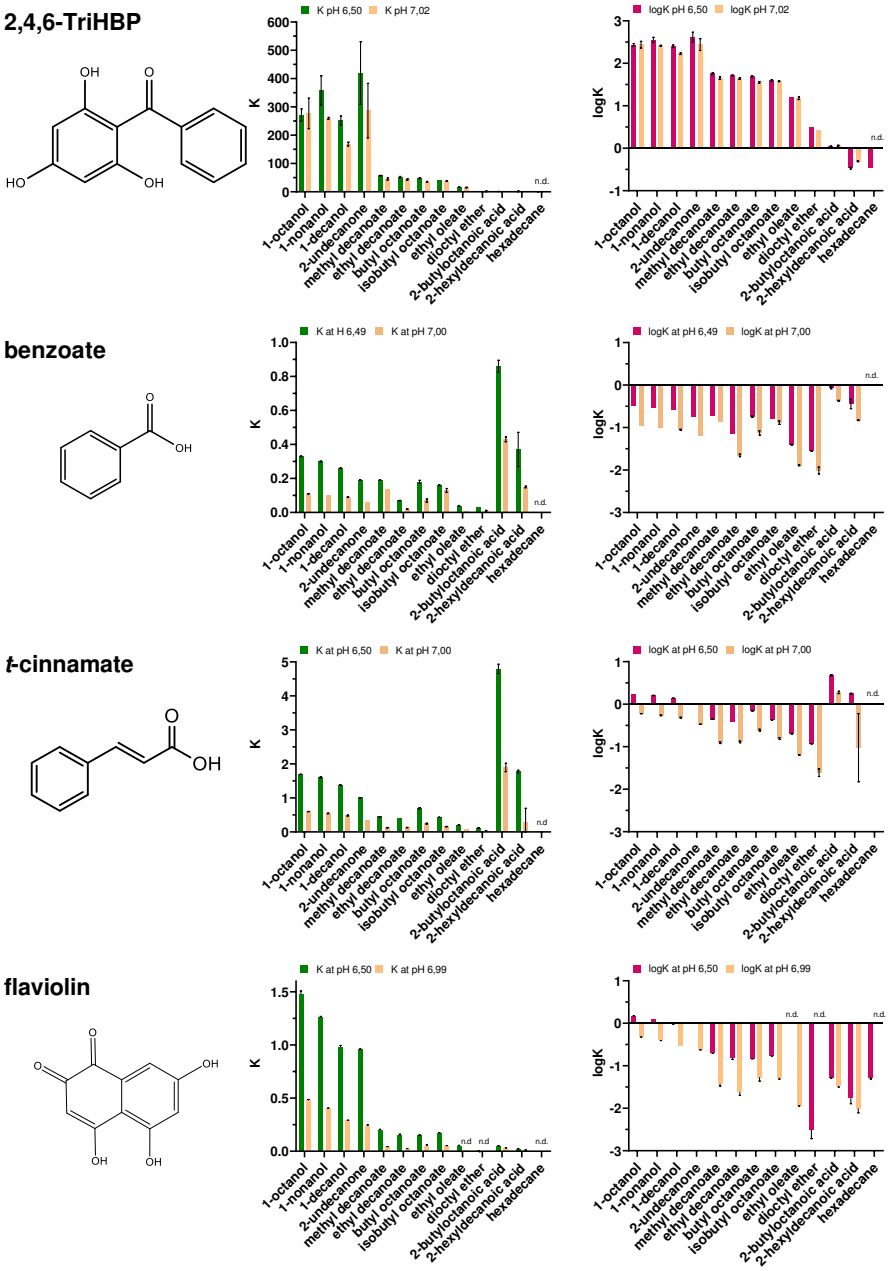

Figure S10: Partitioning coefficient (K) and logK of 2,4,6-TriHBP, benzoate, cinnamate and flaviolin in different phosphate buffer solvent mixtures at pH 6.5 and 7. Flaviolin originates from culture supernatant of strain GRC3Δ6MC-II *attTn7*::*FRT-P*$_{14f}$-*SgRppA* (Schwanemann, Otto, et al., 2023). Error bars represent the standard deviation of n=3.

Table S11 Solvent screening: Table partitioning in solvents

Table of partitioning coefficient (K), logarithmic partitioning coefficient logK (~logP), extraction efficiency and separation factors at pH 7 of 2,4,6-TriHBP, benzoate, cinnamate and flaviolin with all tested solvents, except hexadecane due to failed measurements in HPLC. Flaviolin originates from culture supernatant of strain GRC3Δ6MC-II *attTn7*::*FRT-P*$_{14f}$-*SgRppA* (Schwanemann, Otto, et al., 2023). Errors represent the standard deviation of n=3. Abbreviation: SD, standard deviation; ND, not determined

solvent extraction pH 7	K TriHBP	SD K	logK TriHBP	SD logK	efficiency %	SD efficiency %	K benzoate	SD K	logK benzoate	SD logK	K cinnamate	SD K	logK cinnamate	SD logK	separation factor $K_{(TriHBP)}/K_{(benzoate)}$	separation factor $K_{(TriHBP)}/K_{(cinnamate)}$	K flaviolin	SD K	logK flaviolin	SD logK
1-octanol	276,7	53,9	2,44	0,08	99,63	0,07	0,11	0,001	-0,94	0,003	0,60	0,004	-0,22	0,003	2421	461	0,48	0,01	-0,32	0,01
1-nonanol	259,6	3,3	2,41	0,01	99,62	0,00	0,10	0,000	-1,01	0,002	0,54	0,010	-0,26	0,008	2640	477	0,4	0,01	-0,40	0,01
1-decanol	168,7	6,6	2,23	0,02	99,41	0,02	0,09	0,001	-1,05	0,005	0,48	0,014	-0,32	0,012	1898	351	0,29	0,00	-0,53	0,00
2-undecanone	287,0	96,1	2,44	0,14	99,63	0,11	0,06	0,000	-1,20	0,002	0,34	0,001	-0,47	0,001	4524	851	0,24	0,01	-0,62	0,01
methyl decanoate	44,9	3,5	1,65	0,03	97,81	0,17	0,14	0,000	-0,87	0,001	0,12	0,006	-0,90	0,022	330	360	0,04	0,00	-1,43	0,05
ethyl decanoate	43,5	2,2	1,64	0,02	97,75	0,12	0,02	0,001	-1,66	0,029	0,13	0,006	-0,89	0,020	1970	336	0,02	0,00	-1,62	0,08
butyl octanoate	35,3	1,5	1,55	0,02	97,24	0,11	0,07	0,009	-1,13	0,051	0,24	0,012	-0,61	0,022	473	144	0,05	0,01	-1,27	0,09
isobutyl octanoate	37,9	1,3	1,58	0,01	97,42	0,09	0,13	0,011	-0,88	0,038	0,16	0,007	-0,81	0,020	289	243	0,05	0,00	-1,28	0,03
dioctyl ether	1,8	1,5	0,42	0,00	72,52	0,05	0,01	0,002	-2,01	0,084	0,02	0,005	-1,61	0,091	179	71	ND	ND	ND	ND
2-butyloctanoic acid	1,2	0,03	0,06	0,01	53,50	0,73	0,43	0,014	-0,37	0,014	1,90	0,124	0,28	0,028	3	1	0,03	0,001	-1,48	0,02
2-hexyldecanoic acid	0,5	0,01	-0,31	0,01	33,03	0,41	0,15	0,005	-0,83	0,015	0,28	0,416	-1,02	0,803	3	2	0,01	0,002	-2,01	0,10
ethyl oleate	15,1	1,1	1,18	0,03	93,76	0,40	0,01	0,000	-1,89	0,012	0,06	0,001	-1,19	0,008	1169	235	0,01	0,00	-1,94	0,00

Supplement S12 Solvent screening: Phase separation and interphase formation

Emulsion/interphase formation of *P. taiwanensis* strain GRC3Δ6MC-II in triple buffered MSM (OD_{600} 10; 10.8) with 20 mM glucose after shaking with different solvents. Images were taken after shaking at 1400 rpm for 13 h, after shaking and centrifuging at 5000 g or 4000 g for the indicated time. Culture and solvent were mixed in a 2:1 ratio. Solvents were ranked according interphase formation from 1-5, where 5 represents the desired property of no interphase formation.

Solvent:MSM (1:2)	octanol	nonanol	decanol	2-undecanone	methyl decanoate	ethyl decanoate	butyl decanoate	isobutyl decanoate	dioctyl ether	2-butyl-octanoic acid	2-hexyl-decanoic acid	hexadecane	ethyl oleate
OD_{600} 10, Before centrifugation													
OD_{600} 10, 1 min, 5000 g													
OD_{600} 10, 5 min, 5000 g													
Rating 1-5 (poor to good)	1	1	2	4	3	3	3	4	3	4	5	3	3
Comment	Cells stay resolved, Large interphase	Cells stay resolved, Large interphase	Cells stay resolved, Large interphase, Good in separate exp.	Good pellet forming, Clear org. phase	Large interphase	Large interphase	Large interphase	Moderate interphase, Clear org. phase	Good pellet forming, Large interphase but less dense	Cells stay resolved, Clear org. phase	Good pellet forming, Clear org. phase	Good pellet forming	Large interphase
Separate experiment: OD_{600} 10.8, 6.5 min, 4000g													

Supplement S13 Solvent screening: Biocompatibility of solvents

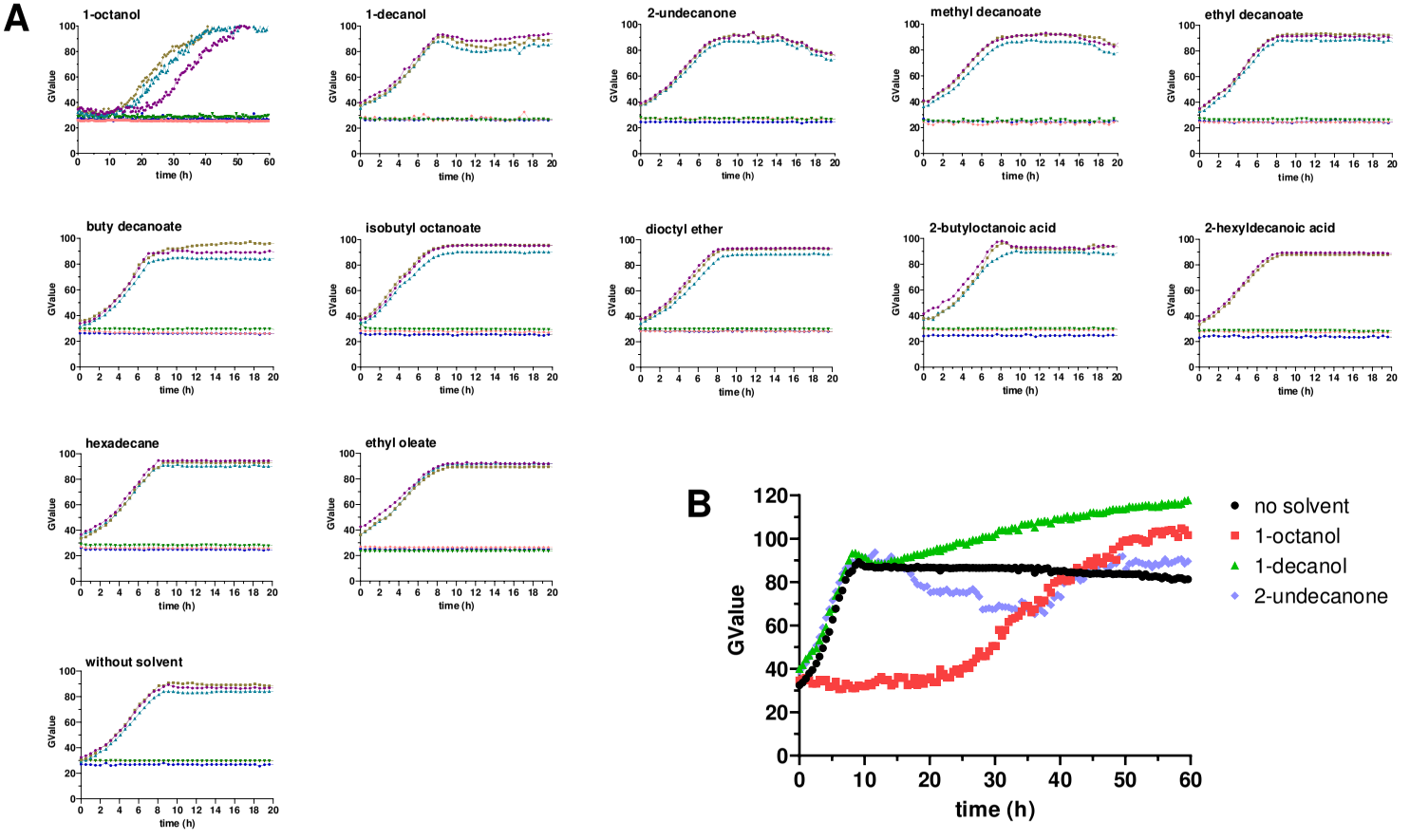

Figure S13: Growth of *P. taiwanensis* GRC3Δ6MC-II in MSM 3x buffered, 20 mM glucose and respective non-inoculated medium control in presence of a second layer of organic solvent (10 %) (A). Representative growth curves for single cultures that were not affected by the solvent, those that serve as additional carbon source and with strong inhibiting effect are separately displayed (B). Cultivation was done in transparent glas vial system in Growth Profiler with 500 µL medium and 50 µL solvent. Three individual replicates are displayed in A. X-axis scale of 1-octanol cultivation varies from the others. Adaption culture was performed in MSM 3x buffered, 20 mM glucose with 1 mM octanol.

Table S14 Solvent screening: Catabolism of solvents by *P. taiwanensis* VLB120

Table S14: Cell density of *P. taiwanensis* GRC3Δ6MC-II cultures cultivated in 3x buffered MSM with organic solvents as sole carbon source. Adaption culture was done with additional 0.5 mM octanol in MSM with 20 mM glucose. The main cultures were inoculated to an OD_{600} of 0.2 and were cultivated at a solvent level of 16.7 % (v/v) for 100 h in System Duetz. Cultivation was performed in duplicates. ‚+' indicates cell growth; ‚o' symbolizes minor cell growth and ‚-' signals no cell growth. The respective classification of growth capability was additionally expressed in a ranking from 1 to 5 where 1 represents the undesired property of growth and 5 represents no growth with the solvent as sole carbon source.

solvent	octanol		nonanol		decanol		2-undecanone		methyl decanoate		ethyl decanoate		butyl octanoate		isobutyl octanoate		dioctyl ether		2-butyloctanoic acid		2-hexyldecanoic acid		hexadecane		ethyl oleate		no solvent no carbon	
replicate	I	II			I	II	I	II	I	II	I	II	I	II	I	II	I	II	I	II	I	II	I	II	I	II	I	II
OD_{600}	3.5	0	5.5	0.9	3.25	5.2	0.1	0.1	0.35	0.85	0.65	0.45	0.25	0.4	1.75	1.7	0.15	0.2	0.15	0.15	0.3	0.35	0.4	0.05	0.6	0.75		0.1
Growth indication	+	-	+	+	+	+	-	-	o	+	o	o	-	o	+	+	-	-	-	-	-	-	o	-	o	o		-
Rating (1-5) used to unused	1		1		1		5		3		3		4		2		5		5		5		5		3		-	

Supplement S15 biphasic production with solvents

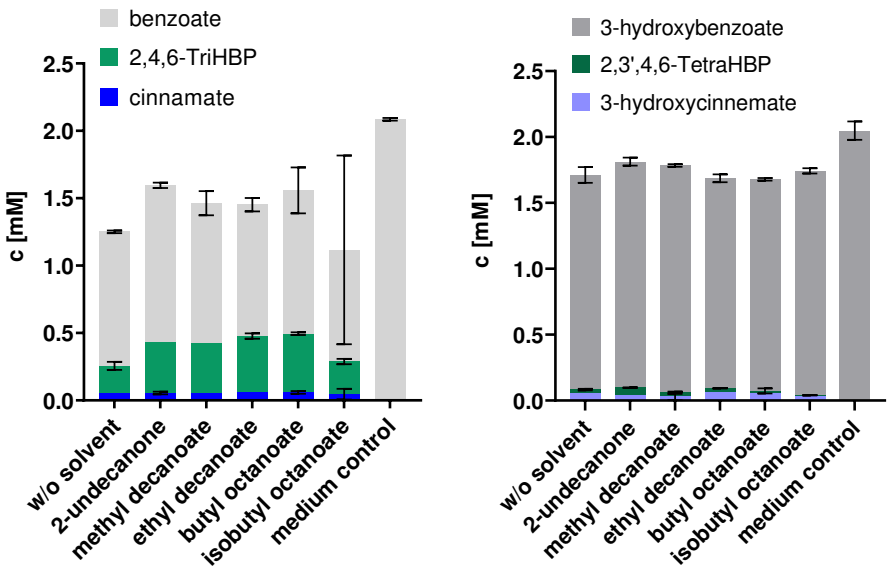

Figure S15: Stacked titers of supplemented precursor, by-product formation and benzophenone product from bioconversion with different solvents. Production of 2,4,6-TriHBP in A, and production of 2,3',4,6-TetraHBP in B. Error bars represent the standard deviation (n=3).

Supplement S16 growth during biphasic production with solvents

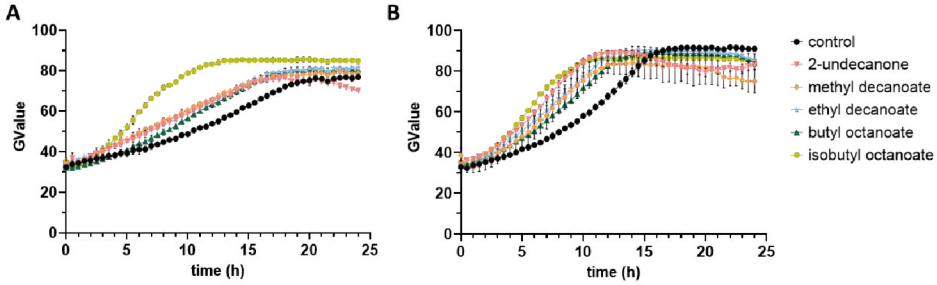

Figure S16: Growth of production strains in presence of no solvent (control) or different solvents and benzoate for 2,4,6-TriHBP production in A and with 3-hydroxybenzoate for 2,3',4,6-TetraHBP synthesis in B. Error bars represent the standard deviation (n=3).

Supplement S17 Back-extraction of 2,4,6-TriHBP from 2-undecanone

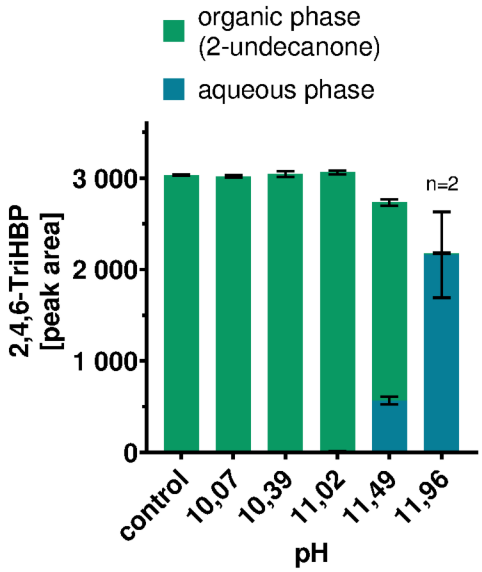

Figure S17: Distribution of 2,4,6-TriHBP between the 2-undecanone and alkaline phase at different pH. The peak area of 2,4,6-TriHBP in 2-undecanone (green) after extraction and 2,4,6-TriHBP in NaOH solution which was acidified after extraction (turquoise) in dependence to the pH value of the aquatic phase. NaOH solution and 2-undecanone were mixed in a 1:1 ratio. Measurement was performed by HPLC. Error bars represent the standard deviation (n=3, or n=2 when indicated).

Supplement S18 Flaviolin production with organic solvent layer

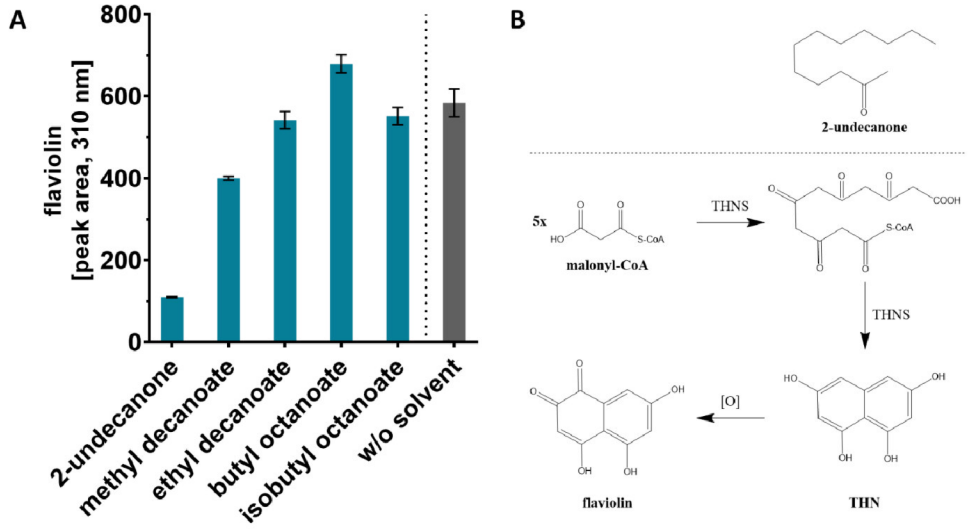

Figure S18: Titers of flaviolin (A) by GRC3Δ6MC-II *attTn7*::*FRT-P*$_{14f}$-*SgRppA* in MSM and with solvent layers. Error bars represent the standard deviation (n=3). Schematic biosynthesis of flaviolin (B) by 1,3,6,8-tetrahydroxynaphthalene synthase (THNS) and spontaneous oxidation and structure of 2-undecanone to illustrate structural similarities to polyketide intermediate.

Supplement S19 Tolerance of different microorganisms against 2-undecanone

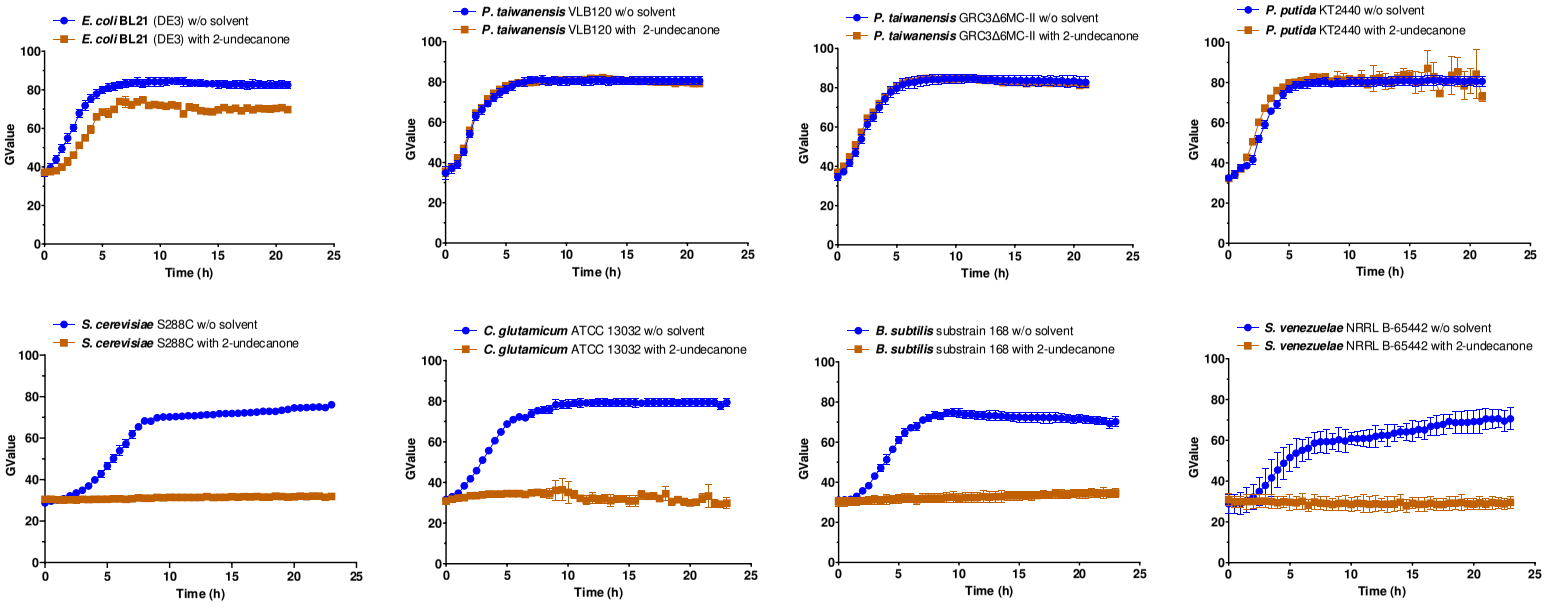

Figure S19: Growth of different organisms in presence of 2-undecanone. *E. coli* BL21 (DE3), *P. taiwanensis* VLB120, GRC3Δ6MC-II, *P. putida* KT2440, *S. cerevisiae* S288C, *C. glutamicum* ATCC 13032, *B. subtilis* substrain 168 and *S. venezuelae* NRRL B-65442 were cultivated on complex media without added 2-undecanone and in presence of 10 % (v/v) 2-undecanone in the Growth Profiler. Error bars represent the standard deviation (n=3).

Supporting information IV: MaCoA Quantification from quenched samples (protocol)

The following protocol was developed by T. Schwanemann during an external research stay at the Systems Environmental Microbiology (SEM) group at the Novo Nordisk Foundation Center for Biosustainability at the Technical University of Denmark (DTU Biosustain), Lyngby, Denmark.

Quantification of intracellular MaCoA in strains of *Pseudomonas* (Version 2022-June)

In order to compare intracellular malonyl-CoA levels between different strains a MaCoA omics approach is developed based on quenching of the metabolism and subsequent LC-MS analysis of extracts for CoA esters.

First, a LC MS method for malonyl-CoA quantification had to be developed by Angelika Semmler from the analytics department at CfB.

Four separate quenching experiments were made with different strains with different sampling volumes and procedures. Most samples had the MaCoA signal within the noise of the LC-MS method, especially because the linear range of MaCoA in the developed LC-MS method was much smaller than for any other CoA ester. Finally, the sampling procedure with quenching was adjusted to end in the following protocol:

Related references for quenching protocols:

(Krink-Koutsoubelis et al., 2018) https://pubs.acs.org/doi/10.1021/acssynbio.7b00466
(Gläser et al., 2020) https://microbialcellfactories.biomedcentral.com/articles/10.1186/s12934-020-01413-1
(Peyraud et al., 2009) https://www.pnas.org/doi/full/10.1073/pnas.0810932106

Material

- vacuum filtration device
- nitrocellulose filter paper (0.45 µm; 47 mm diameter)
- tweezers
- pre-cooled Petri dishes with 60 mm diameter (store in freezer)
- Quenching solution (-80°C): acetonitrile/methanol/water/1M formic acid-Solution (8:8:3:1) (results in quenching solution with 50mM formic acid); make aliquots of 1 mL in pre-annotated tubes
- bucket with dry ice
- pre-cooled tips and annotated tubes (store in freezer)
- optional: size exclusion filters (Da-filter)
- optional: stock solution of CoA-ester of interest to be able to make some samples with spiked-in compound for error evaluation in sampling procedure and analytic
- Photometer for OD_{600}

Sampling and processing

1. Preparation: place filter paper on vacuum burette by tweezers (tip: make a small "dog-ear" somewhere to facilitate later removal into quenching solution); annotated cuvettes for OD measurement (with dilution if needed (e.g. 1:1)); aliquots with quenching solution in dry ice; pre-cooled petri dish with quenching solution on dry ice (close lid);

2. Take sample corresponding to culture OD 1 in exponential phase -> transfer 4 mL sample broth (corresponding to total OD 4 (3-10)) on filter paper and filter via Filterbürette (time critical step)

3. lay filter paper with biomass film into 2 mL of cool quenching solution in a small Petri dish (liquid after thawing from -80°C) (time critical step, be fast until this step; work on dry ice)

4. optional: spike 13C-labeled internal standard

5. incubate the filter in petri dish on dry ice for 3-5 min

6. measure OD of culture

7. rinse filter paper in petri dish and transfer liquid into tube again (cooled tips)

8. Rinse petri dish & filter with 2 mL of fresh quenching solution several times and add that to the sample tube (cooled tips); use a separate tube here that is later combined

9. Incubate for 1 h at -20°C or in dry ice

10. centrifuge ice cold quenching solution at 17 000 g for 20 min at -9°C

11. Optional: Supernatant centrifugation through size exclusion filter (Da-filter) for protein clearance

12. transfer all supernatant to pre-cooled tubes and combine the previously separate tubes in 15 mL falcon tube and store at -80°C (cooled tips)

13. lyophilize sample solution at -120°C

14. resolve in 50-100 µL (less if possible) cold water or ammonium buffer at low pH (0-4°C), centrifuge 5 min at 17000 g at cold temperature (1-4°C)

15. transfer into vials with inlays (do not freeze anymore) and use for analysis

Analytics

16. prepare MaCoA standards for calibration (stock is 10 mM in H_2O) range 0.1 µM - 10 µM

Supporting information V: Production modules constructed in this work

Table: Production modules constructed, used or considered in this thesis with respective plasmid and strain numbers.

Product	Donor plasmid	Donor Strain	Plasmid map #	Comment
Flaviolin	pBG14f_kan_FRT_SgRppA.opt	535	207	KmR recyclable
Cinnamate	pBG14f-atPAL	542	-----	Phe specific (Otto et al. 2019)
	pBG14f-FRT-atPAL	1143	368	KmR recyclable
Benzoate	pBG14f-phdBCDE-4CL-PAL	231	68	(Otto et al. 2020)
	pBG14f_kan_FRT-phdBCDE-sc4CL-atPAL	709	236	KmR recyclable
3-Hydroxybenzoate (3HB)	pBG14d/f/g-LaCH-II	322-324	109	3 promoter versions
2-Hydroxybenzoate (salicylate; 2HB)	pBG14g-Irp9	501	194	weak activity; better use menF-pchB (Wynands unpublished)
	pBG14g-menF-pchB	810	273	production of 2HB (Wynands unpublished)
2,3-dihydroxybenzoate	pBG14f Kan-FRT-menF-entBA	818	272	production of 2,3-DHB (Wynands unpublished)
2,5-dihydroxybenzoate	pBG14g-LaCHII-sal	921	340	production of 2,5-DHB (Wynands unpublished)
4-Hydroxybenzoate (4HB)	pBG14g-PrUbiC	803	266	Best performance like SpCH-IV (Wynands unpublished)
	pBG14g-SmCH-IV	811	267	A tested CH-IV (Wynands unpublished)
	pBG14g-SpCH-IV	812	268	Best performance like PrUbiC (Wynands unpublished)
	pBG42-ubiC^{fbr}	156	56	A tested fbr. UbiC (Wynands unpublished)
Coumarate	pBG14f_Kan_FRT_StsTAL	882	279	Tyr specific TAL; KmR recyclable
	pBG14f_Kan_FRT_RpcTAL	1569	502	Fbr & tyr specific TAL; KmR recyclable
Pinosylvin	pBG14g-ahSTS-sc4CL-atPAL	91	54	Unsure sequencing; Not used
	pBG14g-his.ahSTS-sc4CL-atPAL	174	52	His.Pino (used)
	pBG14g-his.opt.ahSTS.opt-sc4CL-atPAL	176	53	Codon optimized STS
	pBG14f_kan_FRT-his.ahSTS-sc4CL-atPAL	692	229	KmR recyclable; his.Pino
	pBG14g psSTS/*-sc4CL-atPAL	89/90	----	Pinus strobus STS (*E.coli opt.) slower than AhSTS
Resveratrol	pBG14g-his.ahSTS-sc4CL-stsTAL	1060	343	Tyr specific TAL
Stilbene (Pinosylvin/Resveratrol)	pBG14f_kan_FRT-his.ahSTS-sc4CL	1670	536	Biotransformation module; KmR recyclable
Raspberry ketone	pBG14f_Kan_FRT_RiRZS_RpBAS_Sc4CL (A294G)	1959	600	Biotransform. module; KmR recyclable (Wynands unpublished)
x-Hxdroxybenzophenones (2,4,6-TriHBP/ 2,3',4,6-TetraHBP	pBT'T-HsBPS-RpBZL	346	126	Plasmid-based, best gene combi
	pBTrc'T-HsBPS-RpBZL	990	309	Plasmid-based, Ptrc promoter
	pBG14f_kan_FRT-HsBPS-RpBZL	1671	537	biotransformation module; KmR recyclable
3,5-Dihydroxybiphenyl	pBT'T-MdBIS1-RpBZL	487	188	Plasmid-based, best gene combi
	pBTrc'T-MdBIS1-RpBZL	991	310	Plasmid-based, Ptrc promoter
4-Hydroxycoumarin	pBT'T-PcBIS1-sdgA	655	226	Plasmid-based, best gene combi
	pBTrc'T-PcBIS1-sdgA	992	311	Plasmid-based, Ptrc promoter
	pBG14f_kan_FRT-PcBIS1-sdgA	1672	538	biotransformation module; KmR recycable
Phloroglucinol	pBG14d/f/g-phlD-phlE	308-310	105	3 promoter versions with transporter (unpublished)
2,4-Diacetylphloroglucinol (DAPG)	pBG14d/f/g-phlD-phlACB-phlE	311-313	106	3 promoter versions with transporter (unpublished)

Danksagung

Herzlichst möchte ich mich bei meinem Doktorvater Prof. Dr. Nick Wierckx bedanken. Als ich dich während meines Studiums anschrieb, dass ich eine Idee hätte aus der ich ein eigenes Projekt für meine Doktorarbeit machen möchte, hast du dich zeitig mit mir getroffen und interessiert zugehört. Deine erste Reaktion war nicht: „Naja, da solltest du nochmal drüber nachdenken.“, sondern „Klingt super. Wie kann man dafür noch Förderung bekommen? Und bisher ist noch kein Student mit einem eigenen Projekt an mich getreten.“. Von da an hast du mich unterstützt und mir auch alternative Doktorarbeiten angeboten, falls eine Förderung ausbliebe. Über all die Jahre habe ich mich gefreut als dein erster Düsseldorfer PhD-Student von dir betreut zu sein. Ich habe mich immer in den richtigen Händen gefühlt und habe wissenschaftlich viel gelernt. Ich weiß deine Unterstützung zu würdigen, als ich beispielsweise einen zusätzlichen Forschungsaufenthalt im Ausland anstrebte und erleben durfte. Herzlichen Dank für deine Unterstützung!

Des Weiteren möchte ich mich bei Prof. Dr. Julia Frunzke als meine Mentorin und Übernahme der Zweitbetreuung bedanken.

Ein besonderer Dank gilt Dr. Benedikt Wynands, der über den gesamten Zeitraum im IBG-1 des Forschungszentrum Jülich ein offenes Ohr hatte und stetig den Wissenschaftler in mir geschliffen hat. Die wissenschaftlichen Auseinandersetzungen und Diskussionen waren stets eine Freude und hoffentlich eine beidseitige Bereicherung.

Ebenso herzlichen Dank all meinen Kollegen der Gruppe „Mikrobielle Katalyse“, die oftmals von mir als Kätzchen in Mails bezeichnet wurden. Dank euch hatte ich eine wunderbare Zeit in den Laboren und auch Büros. Ich habe uns immer als eine harmonische und gegenseitig unterstützende Gruppe empfunden und ich freue mich mit euch zusammengearbeitet zu haben und auch freundschaftlich verbunden zu sein. *‚miau‘*

Herzlichen Dank auch an Esther Urban, die ich während ihrer Abschlussarbeit begleiten durfte. Es hat mir stets Freude gemacht mich mit dir auszutauschen und du trägt einen nicht unerheblichen Teil des Erfolgs der Zwei-phasen Kultivierung bei. Ich denke wir konnten beide voneinander lernen und ich hoffe du bleibst weiterhin neugierig und aufmerksam.

Ohne Dr. Martin Zimmermann als Ansprechpartner während des Studiums an der RWTH Aachen hätte ich diese Dissertation wohl in dieser Form nicht gemacht. Dir konnte ich als erstes im Vertrauen von meiner ersten Projektidee erzählen, um einen ersten Eindruck zu bekommen, ob die Erarbeitung eines eigenen Dissertationsthemas überhaupt realistisch war. Aus dieser Idee und deiner Beratung entstand diese Arbeit.

Herzlichen Dank an Prof. Dr. Pablo Ivan Nikel und Dr. Nicolas Krink. Es hat mir eine Freude gemacht mit euch im *Center for Biosustainability* in Lyngby zu forschen und ich hoffe unsere gemeinsamen Kollaborationen werden weiterhin so erfolgversprechend sein wie bisher.

Die Deutsche Bundesstiftung Umwelt (DBU) hat in meinem Vorhaben die gesellschaftliche Relevanz und das Potential für den Umweltschutz erkannt. Dank der persönlichen Förderung der DBU konnte meine Idee aufblühen und ich konnte mich selbstbestimmt in dieses wissenschaftliche Thema eingraben, sodass diese Arbeit und weitere Publikationen daraus hervorgehen konnten und werden. Herzlichen Dank für dieses Vertrauen, die Förderung und die Vielfältigkeit des Umweltschutzes.

Besonders danken möchte ich meinen Eltern Gerhild und Ulf und meiner Schwester Esther. Ihr habt mir vieles im Leben ermöglicht, mir aber dennoch alle Freiheit gelassen meinen eigenen Weg zu wählen. Als ich entschied was ich Studieren werde, wo und auch, dass ich länger brauchen möchte durch zusätzliche Semester für einen Studierendenwettbewerb, Auslandsemester und ein Industrie-Praktikum, konnte ich mich immer auf euch verlassen.

Meine Freunde, egal ob aus dem Studium und vom Sport, mussten sich nicht selten meine Begeisterung ertragen für diese oder jene biologische Besonderheit, einen Trick im Cyr Wheel oder kreatives Getränk. Meist freut ihr euch einfach für mich, für was ich mich begeistern kann. Ich kann mich Glücklich schätzen euch bei mir haben zu dürfen. Eure Herzlichkeit und Unterstützungsbereitschaft suchen seines Gleichen.

In all meiner Studienzeit und anschließenden Promotionszeit hatte ich einen besonderen Menschen an meiner Seite, meine Frau Viola. Dich bei mir zu haben ist das Beste. Du bist meine Stütze, mein Lächeln und mein Navigator, um auf Kurs zu bleiben und Krisen zu bestreiten. Dein Vertrauen und deine Unterstützung sind endlos. Mit dir kann ich mich fallen lassen.

Scientific Curriculum Vitae

Personal data

Name: Tobias Philipp Schwanemann
Born: August, 1994 in Hannover, Germany

Education

02/2020- 10/2023	PhD student in Forschungszentrum Jülich, Institute of Bio- and Geoscience (IBG-1): Biotechnology, Jülich, Germany Topic: "Strain- and process engineering for polyketides production with *Pseudomonas taiwanensis* VLB120 in two-phase cultivations"
04/2017-09/2019	Master of Science program: Molecular and Applied Biotechnology RWTH Aachen University, Aachen, Germany Overall grade: 1.3 (very good) Thesis topic: "Artificial Production of Pinosylvin by Rationally Engineered Strains of *Pseudomonas taiwanensis* VLB120" grade: 1.3 (very good)
01-05/2017	Exchange studies at Aalto University Schools of Chemical Engineering, Espoo, Finland (ERASMUS+)
10/2013-12/2016	Bachelor of Science program: Molecular and Applied Biotechnology RWTH Aachen University, Aachen, Germany Overall grade: 2.1 (good) Thesis topic: "A Biosensor-based High Throughput Screening approach Applicable on a Developed *Pseudomonas taiwanensis* Mutant Library for Enhanced production of *p*-Hydroxybenzoic Acid" grade: 1.1 (very good)
06/2013	Abitur (higher education entrance qualification), Gymnasium Lehrte, Germany

Work experience

since 10/2019	Scientific employee and doctoral candidate at the Forschungszentrum Jülich IBG-1: Biotechnology, Jülich, Germany
02-06/2022	Guest researcher in the Systems Environmental Microbiology (SEM) group at the Novo Nordisk Foundation Center for Biosustainability at the Technical University of Denmark (DTU Biosustain), Lyngby, Denmark
04-07/2019	Research Assistant at Forschungszentrum Jülich IBG-1: Biotechnology, Jülich, Germany
08-10/2018	Student Research Assistant at the Institute of Applied Microbiology (iAMB), RWTH Aachen University, Aachen Germany
07-11/2017	Industry internship at Production Department of c-LEcta GmbH, Leipzig, Germany
10/2015-03/2016	Student Research Assistant at the Institute of Biotechnology, RWTH Aachen University, Aachen Germany

Extracurricular activities

2015	Vice world champion in Cyr Wheel (wheel gymnastics), Lignano, Italy
2013	Participant at 8th Aerobic European Championships, Arques, France

Awards and Grants

2020-2023	PhD scholarship of Deutsche Bundesstiftung Umwelt (DBU) to execute the self-made PhD project (Funding 20019/638-32)
2022	DAAD scholarship „Forschungsstipendien für Doktorandinnen und Doktoranden“, 2021/22 (Funding 57556281), Lyngby, Denmark
2017/2018	Dean’s List Award for excellent academic performances during the Master of Science studies in Molecular and Applied Biotechnology
2017	ERASMUS+ scholarship for exchange semester, Espoo, Finland
2015	iGEM student competition Team Aachen, Gold medal and winner of “Manufacturing Track”, Boston, USA

Publications

Journal articles

Schwanemann, T., Urban, E., Eberlein, C., Gätgens, J., Rago, D., Krink, N., Nikel, P.I., Heipieper, H.J., Wynands, B., & Wierckx, N. (2023). Production of (hydroxy)benzoate-derived polyketides by engineered *Pseudomonas* with *in situ* extraction. *Bioresource Technology*, *388*(129741), 0–11. https://doi.org/10.1016/j.biortech.2023.129741

Schwanemann, T., Otto, M., Wynands, B., Marienhagen, J., & Wierckx, N. (2023). A *Pseudomonas taiwanensis* malonyl-CoA platform strain for polyketide synthesis. *Metabolic Engineering*, *77*(February), 219–230. https://doi.org/10.1016/j.ymben.2023.04.001

Schwanemann, T., Otto, M., Wierckx, N., & Wynands, B. (2020). *Pseudomonas* as Versatile Aromatics Cell Factory. *Biotechnology Journal*, *1900569*, 1900569. https://doi.org/10.1002/biot.201900569

Poster presentations

Schwanemann, T., Urban, E., Eberlein, C., Gätgens, J., Rago, D., Krink, N., Nikel, P.I., Heipieper, H.J., Wynands, B., & Wierckx, N. (2023). Production of (hydroxy)benzoate-derived polyketides by engineered *Pseudomonas* with *in situ* extraction. (Sept. 17-21, 2023), ECCE&ECAB 2023, Berlin, Germany

Schwanemann, T., Urban, E., Wynands, B., & Wierckx, N; "Solvent Selection for Enhanced Heterologous Polyketide Production - Imposing on Tolerance-Traits for ISPR”, (June 16, 2022) Innovation for Biomanufacturing - Next Generation Cell-Factories and Bioprocess Development, DTU, Lyngby, Denmark

Schwanemann, T., Otto, M., Wynands, B., & Wierckx, N; “Heterologous Production of the Polyphenol Pinosylvin with *Pseudomonas taiwanensis* VLB120”, (March 9, 2020) 6th joint conference of DGHM & VAAM, Leipzig, Germany

Oral presentations

Schwanemann, T., Otto, M., Wynands, B., Marienhagen, J., & Wierckx, N; “Construction of a Pseudomonas malonyl-CoA platform strain”, (September 21, 2022) GASB6 - 6th annual conference on synthetic biology, Würzburg, Germany

Schwanemann, T., Cardenas Espinosa, M.J., Gätgens, J., Eberlein, C., Heipieper, H.J., & Wierckx, N; “Benzoic acid-derived polyketides - Heterologous benzoic acid-derived polyketide biosynthesis with *Pseudomonas*”, (September 7, 2021) ECNP - 4th European Conference on Natural by DECHEMA, online.

Schwanemann, T., Otto, M., & Wierckx, N; “Artificial production of Pinosylvin by rationally engineered strain of *Pseudomonas taiwanensis* VLB120”, (November 7-8, 2019) 2nd Pseudomonas Grassroots Meeting, University of Leiden, the Netherlands

Eidesstattliche Erklärung

Hiermit versichere ich an Eides Statt, dass die Dissertation von mir selbständig und ohne unzulässige fremde Hilfe unter Beachtung der „Grundsätze zur Sicherung guter wissenschaftlicher Praxis an der Heinrich-Heine-Universität Düsseldorf“ erstellt worden ist. Die Dissertation wurde in der vorgelegten oder in ähnlicher Form noch bei keiner anderen Institution eingereicht. Ich habe bisher keine erfolglosen Promotionsversuche unternommen.

Tobias Schwanemann

Band / Volume 263
9th Georgian-German School and Workshop in Basic Science
September 12 – 16, 2022 | Kutaisi, Tbilisi | Georgia
A. Kacharava, E. Portius, N. J. Shah, H. Ströher (2022)
ISBN: 978-3-95806-664-9

Band / Volume 264
Self-assembly of Au-Fe_3O_4 dumbbell nanoparticles
N. Nandakumaran (2022), xiv, 234 pp
ISBN: 978-3-95806-666-3

Band / Volume 265
Time-resolved and three-dimensional characterisation of magnetic states in nanoscale materials in the transmission electron microscope
T. Weßels (2023), xx, 211 pp
ISBN: 978-3-95806-685-4

Band / Volume 266
Dissecting iron and heme regulatory networks and adaptation to heme stress in *Corynebacterium glutamicum*
A. Krüger (2023), IV, 274 pp
ISBN: 978-3-95806-686-1

Band / Volume 267
Morphological and functional characterization of layer 5 neurons in rat medial prefrontal cortex, their synaptic microcircuitry and serotonin modulation
R. Rama (2023), 116 pp
ISBN: 978-3-95806-688-5

Band / Volume 268
Magnetic and transport studies of the parent and Fe doped Hexagonal-Mn_3Ge Weyl semimetal
V. Rai (2023), xviii, 156 pp
ISBN: 978-3-95806-695-3

Band / Volume 269
The complex inositol metabolism of *Corynebacterium glutamicum* and its application for the production of rare inositols
P. Ramp (2023), VI, 161 pp
ISBN: 978-3-95806-699-1

Band / Volume 270
Spin- and orbital-dependent band structure of unconventional topological semimetals
K. Hagiwara (2023), v, 115 pp
ISBN: 978-3-95806-701-1

Band / Volume 271
Neutron scattering
Experimental Manuals of the JCNS Laboratory Course held at Forschungszentrum Jülich and at the Heinz-Maier-Leibnitz Zentrum Garching
edited by T. Brückel, S. Förster, K. Friese, M. Kruteva, M. Zobel and R. Zorn
(2023), ca 150 pp
ISBN: 978-3-95806-705-9

Band / Volume 272
Ab-initio investigation of the interplay between the hyperfine interaction and complex magnetism at the nanoscale
S. R. S. Shehada (2023), ix, xi, 119 pp
ISBN: 978-3-95806-718-9

Band / Volume 273
Analysis of the signal transduction cascade tuning the 2-oxoglutarate dehydrogenase activity in *Corynebacterium glutamicum*
L. Sundermeyer (2023), VI, 119 pp
ISBN: 978-3-95806-722-6

Band / Volume 274
Multicellular defense against phage infection in *Streptomyces* – impact of secondary metabolites and mycelial development
L. Kever (2023), iv, 246 pp
ISBN: 978-3-95806-724-0

Band / Volume 275
Investigation of the electronic band structure of 2D transition metal dichalcogenides via angle-resolved photoemission spectroscopy
B. Parashar (2023), xvii, 156 pp
ISBN: 978-3-95806-725-7

Band / Volume 276
Strain- and process engineering for polyketides production with *Pseudomonas taiwanensis* VLB120 in two-phase cultivations
T. P. Schwanemann (2023), 230 pp
ISBN: 978-3-95806-726-4

Schlüsseltechnologien / Key Technologies
Band / Volume 276
ISBN 978-3-95806-726-4

Mitglied der Helmholtz-Gemeinschaft

JÜLICH
Forschungszentrum